



## Integration of Synthesis and Operational Design of Batch Processes

Papaoikonomou, Eirini

*Publication date:*  
2006

*Document Version*  
Publisher's PDF, also known as Version of record

[Link back to DTU Orbit](#)

*Citation (APA):*  
Papaoikonomou, E. (2006). *Integration of Synthesis and Operational Design of Batch Processes*. Technical University of Denmark.

---

### General rights

Copyright and moral rights for the publications made accessible in the public portal are retained by the authors and/or other copyright owners and it is a condition of accessing publications that users recognise and abide by the legal requirements associated with these rights.

- Users may download and print one copy of any publication from the public portal for the purpose of private study or research.
- You may not further distribute the material or use it for any profit-making activity or commercial gain
- You may freely distribute the URL identifying the publication in the public portal

If you believe that this document breaches copyright please contact us providing details, and we will remove access to the work immediately and investigate your claim.

---

# Integration of Synthesis and Operational Design of Batch Processes

---

Ph.D. Thesis

Irene Papaeconomou  
CAPEC

Department of Chemical Engineering  
Technical University of Denmark

2005

Copyright ©Irene Papaeconomou, 2005

ISBN 87-91435-25-0

Printed by Book Partner, Nørhaven Digital, Copenhagen, Denmark

# Preface

This thesis is submitted as partial fulfillment of the requirements for the Ph.D.-degree at Danmarks Tekniske Universitet (Technical University of Denmark). The work has been carried out at Institut for Kemiteknik (Department of Chemical Engineering) from June 2000 to April 2004 under the supervision of Professor Sten Bay Jørgensen and Professor Rafiqul Gani. The work was funded partially from Syngenta and was financed partly by the Danish Energy Authority under contract ENS 1273/00-0026 and mainly by the Research and Training Network Knowledge-driven Batch Production (BatchPro) project under the European Commission contract HPRN-CT-2000-00039.

I would first like to express my gratitude to Professor Sten Bay Jørgensen and Professor Rafiqul Gani for their constructive supervision and guidance. If it wasn't for Professor Rafiqul Gani, I might never have been writing these lines, since he was the one who trusted me after the completion of my master thesis and gave me the opportunity to work on this Ph.D project. Professor Sten Bay Jørgensen provided his support and insights all the way through and for that I sincerely thank him.

Also, a special thank must go to Joan Cordiner for believing in my work and inviting me to carry out the necessary external research in Syngenta. I was very happy that during my stay in Grangemouth, Scotland, she regarded me as a colleague, but also as a friend. The feelings are mutual.

I would like to extend my thanks to various coworkers that throughout the years have offered their help with the computational tools I used, when various modifications, bug fixings and improvements needed to be implemented. Dr. Martin Hostrup and Boris Russel took up the job in the beginning and Loic d'Anterroches and Dr. Jorge Marrero Morejon took over in the end. Of course, I would like to thank all the coworkers that contributed to a great working environment. Particularly, thanks go to Dr. Dennis Bonné and Dr. Mario Richard Eden for the numerous fun hours of discussions in the offices of DTU.

Last, but definitely not least, I would like to thank my family and friends for enduring me through my Ph.D writing moods. I am grateful to my parents for always believing in me and not becoming an obstacle in my way, even if that meant losing me to Denmark. And above all, I would like to thank my husband for his understanding, his empathy and his support. I couldn't have done it without you.

Frederiksberg, August 2005

Irene Papaeconomou



# Abstract

This thesis describes the development of a methodology that targets the synthesis problem for batch processes and additionally handles the operational design for batch reaction, distillation and crystallization. The lack of available synthesis approaches has led to the use of simple and conservative routes that have proved to work in the laboratory, but can significantly profit from optimization even at the synthesis level.

Rule-based algorithms are developed that work at two communicating levels. Given the reaction sets that lead from raw materials to product and the purity and yield specifications for the latter, the upper level algorithm identifies and places the necessary separation tasks in the generated batch route. The most feasible separation technique is also identified for the separation task by exploiting the relationship between physio-chemical properties and separation process principles. The developed algorithm provides also initial estimates for the intermediate objectives of each task in the batch route.

At the lower level, three algorithms are developed with the intention of providing a feasible and near optimum batch operations model for several batch processes. Motivation is found in the recognition of the fact that even when rigorous optimization is performed, the resources needed to determine the optimum batch operations model depend strongly on the initial estimate. Therefore, there is a need for a simple and fast way to provide feasible, near optimum solutions that could eventually be used for further optimization.

Based on thermodynamic insights and knowledge gained from available simple models, the developed algorithms generate a sequence of operations that satisfy all path and terminal constraints, while trying to do so in minimum time. For batch reaction, the algorithm attempts to maximize the selectivity of desired reactions over competing reactions, while remaining physically feasible. Selectivity is promoted through changes in operating temperature, as determined from kinetically and/or thermodynamically derived knowledge of the temperature sensitivity of competing reactions. For batch distillation, reflux ratio profiles are determined taking into consideration that operating at the largest driving force makes the separation easier and faster. The driving force approach is also used to identify when a reflux ratio becomes infeasible, determining in that way the end of the corresponding operation. For batch crystallization, phase diagrams are used to identify the feasibility of the precipitation of a specified solid, the necessary batch operation and the operating conditions that will achieve the maximum amount of precipitating solid.

The lower level algorithms generate batch operations models that satisfy the intermediate objectives for the task, set by the synthesis algorithm. Once

the algorithms are applied, information of the existing state of the mixture is returned to the upper level synthesis algorithm. After that more detailed calculations can be made for the remaining tasks in the batch route.

Various computational tools are necessary for applying the algorithms developed and verifying the batch operation models generated. The ICAS computational package is used in this thesis and attention is drawn to the particular features of the ICAS package tools employed in the various steps of the algorithms. The algorithms developed have been tested in a series of application examples, where the batch operation models were generated for various batch processes. The application of the algorithms on an integrated example for both the synthesis and operational design of batch processes have also been performed.

# Resumé på dansk

Denne afhandling beskriver udviklingen af en metodik rettet mod syntese problemet ved batch processer og som endvidere håndterer operationelt design for batch reaktion, destillation og krystallisering. Manglen på tilgængelige syntese metoder har ført til anvendelsen af simple og konservative ruter der har vist sig at virke i laboratoriet, men som kan profitere signifikant af optimering selv på syntese niveau.

Regel-baserede algoritmer, som virker på to kommunikerende niveauer, er udviklet. Givet reaktions sættene der leder fra råmaterialer til produkt, samt renheds- og udbyttespecifikationer for sidstnævnte, identificerer og placerer det øvre niveau algoritme de nødvendige separationsopgaver i den genererede batch rute. Den mest gennemførlige separationsteknik for separationensopgaven, er identificeret ved at udnytte relationen mellem fysisk-kemiske egenskaber og separationsprocessens principper. Den udviklede algoritme giver også indledende estimater for de mellemliggende mål for hver opgave i batch ruten.

På det nedre niveau er tre algoritmer udviklet med hensigt på, at tilvejebringe en gennemførlig og nær optimal batch operations model for flere batch processer. Motivationen er fundet i erkendelsen af det faktum, at selv når rigoristisk optimering udføres, er de nødvendige resurser til at fastslå den optimale batch operations model kraftigt afhængige af det indledende estimat. Derfor er der et behov for en simpel og hurtig måde at tilvejebringe gennemførlige, nær optimale løsninger der endeligt kan bruges til yderligere optimering.

Baseret på termodynamisk indsigt og viden opnået fra tilgængelige simple modeller, genererer de udviklede algoritmer en sekvens af operationer der tilfredsstiller alle mellemliggende og endelige betingelser, samtidig søges dette gjort på minimal tid. For batch reaktion, forsøger algoritmen at maksimere selektiviteten af ønskede reaktioner frem for konkurrerende reaktioner, samtidig med at disse vedbliver fysisk gennemførlige. Selektivitet er fremmet ved ændringer i operations temperatur som bestemt ved kinetisk og/eller termodynamisk kendskab til temperatur sensitivitet af konkurrerende reaktioner. For batch destillation, fastslås reflux forholds profiler under hensyntagen til, at drift ved den største drivende kraft gør separationen lettere og hurtigere. Den drivende krafts diagram anvendes også til identifikation af når et reflux forhold bliver ugennemførligt, hvorved slutningen af den tilsvarende operation bestemmes. For batch krystallisering, anvendes fase diagrammer til identifikation af gennemførligheden af udfældningen af et specificeret fast stof, den nødvendige batch operation og de driftsbetingelser der vil opnå den maksimale mængde af udfældet fast stof.

Algoritmerne på det nedre niveau genererer batch operations modeller der



tilfredsstiller de mellemliggende mål for opgaven, fastlagt af syntese algoritmen. Så snart algoritmerne er anvendt, returneres information om blandingens eksisterende tilstand til syntesealgoritmen på det øvre niveau. Derefter kan mere detaljerede beregninger udføres for den resterende opgave i batch ruten.

Forskellige computer værktøjer er nødvendige for anvendelsen af de udviklede algoritmer og for verifikationen af de genererede batch operations modeller. ICAS computer pakken er anvendt i denne afhandling og opmærksomheden henledes på de bestemte faciliteter i ICAS pakken anvendt i de forskellige trin i algoritmen. De udviklede algoritmer er blevet testet i en række eksempler, hvor batch operations modeller blev genereret for forskellige batch processer. Anvendelsen af algoritmerne på et integreret eksempel på både syntesen og det operationelle design af batch processer er også blevet udført.

# Contents

<b>Preface</b>	<b>iii</b>
<b>Abstract</b>	<b>v</b>
<b>Resumé på dansk</b>	<b>vii</b>
<b>1 INTRODUCTION</b>	<b>1</b>
<b>2 STATE-OF-THE-ART</b>	<b>7</b>
2.1 Introduction to Batch Processing . . . . .	7
2.2 Batch Process Synthesis . . . . .	8
2.3 Batch Process Unit (Task) Optimization . . . . .	9
2.3.1 Batch Reaction . . . . .	10
2.3.2 Batch Distillation . . . . .	12
2.3.3 Batch Crystallization . . . . .	13
2.4 Batch Process Control . . . . .	15
2.4.1 Single and multi- variable control layers . . . . .	15
2.4.2 Iterative Learning Control . . . . .	16
2.4.3 Model Predictive Control . . . . .	16
2.5 Batch Process Plant Design . . . . .	17
2.6 Batch Process Scheduling and Planning . . . . .	18
2.6.1 Optimization-based Approaches . . . . .	19
2.6.2 Heuristic Solution Methods . . . . .	24
2.7 Concluding remarks . . . . .	29
2.8 Thesis objective . . . . .	31
<b>3 METHODOLOGY</b>	<b>33</b>
3.1 Introduction . . . . .	33
3.2 Task: Batch Reaction . . . . .	34
3.2.1 Introduction . . . . .	34
3.2.2 Theoretical background . . . . .	35
3.2.3 Batch Reaction Algorithm . . . . .	37
3.3 Task: Batch Distillation . . . . .	57
3.3.1 Introduction . . . . .	57
3.3.2 Theoretical Background . . . . .	58
3.3.3 Batch Distillation Algorithm . . . . .	63
3.4 Task: Batch Crystallization . . . . .	77
3.4.1 Introduction . . . . .	77
3.4.2 Theoretical Background . . . . .	77
3.4.3 Batch Crystallization Algorithm . . . . .	83

3.5	Synthesis of Batch Processes . . . . .	97
3.5.1	Introduction . . . . .	97
3.5.2	Theoretical Background . . . . .	98
3.5.3	Batch Processes Synthesis Algorithm . . . . .	99
<b>4</b>	<b>COMPUTATIONAL TOOLS</b>	<b>111</b>
4.1	Introduction . . . . .	111
4.1.1	ICAS - Integrated Computer Aided System . . . . .	111
4.1.2	The CAPEC Database and reaction database . . . . .	112
4.1.3	ProPred: Property prediction . . . . .	113
4.1.4	Utility toolbox . . . . .	113
4.1.5	PDS: Process Design Studio . . . . .	113
4.1.6	CAPSS . . . . .	114
4.1.7	BRIC and Dynamic simulator . . . . .	114
4.2	Batch Reaction Algorithm Tools . . . . .	115
4.3	Batch Distillation Algorithm Tools . . . . .	116
4.4	Batch Crystallization Algorithm Tools . . . . .	117
4.5	Batch Synthesis Algorithm Tools . . . . .	118
<b>5</b>	<b>APPLICATION EXAMPLES</b>	<b>121</b>
5.1	Introduction . . . . .	121
5.2	Operational modelling of a liquid phase reaction . . . . .	121
5.3	Operational modelling of two-phase reaction system . . . . .	128
5.4	Separation of ternary non-azeotropic system by batch distillation	134
5.5	Separation of binary azeotropic system by batch distillation . .	140
5.6	Separation of ternary electrolyte systems by batch crystallization	143
5.6.1	Separation of Type I ternary system . . . . .	143
5.6.2	Separation of Type II ternary system . . . . .	146
5.7	Separation of quaternary electrolyte system by batch crystalliza- tion . . . . .	149
5.8	Generation of batch route (integrated example) . . . . .	155
<b>6</b>	<b>CONCLUSIONS</b>	<b>165</b>
6.1	Achievements . . . . .	165
6.2	Future Work . . . . .	170

## Appendices

<b>A</b>	<b>Batch Reaction: Promoting reaction system selectivity through temperature change</b>	<b>173</b>
<b>B</b>	<b>Batch Distillation: Deciding on an intermediate cut</b>	<b>177</b>
<b>C</b>	<b>Property - separation technique relationship</b>	<b>181</b>

---

<b>D</b>	<b>Calculation of operational costs for case study 5.2</b>	<b>185</b>
<b>E</b>	<b>Column geometric specifications for case study 5.4</b>	<b>187</b>
<b>F</b>	<b>Property lists for case study 5.8</b>	<b>189</b>
	<b>List of definitions</b>	<b>197</b>
	<b>Nomenclature</b>	<b>199</b>
	<b>References</b>	<b>203</b>



# List of Figures

2.1	Schematic of a multiproduct batch plant . . . . .	20
2.2	Schematic of a sequential multipurpose batch plant . . . . .	21
2.3	Schematic of a non-sequential multipurpose batch plant . . . . .	22
3.1	Block diagram of the methodology for the synthesis of batch processes as well as the generation of the batch operations model for each task . . . . .	34
3.2	Block diagram of the algorithm A1a for operation model generation for a reaction task (one-phase reactor) . . . . .	53
3.3	Block diagram of the algorithm A1b for operation model generation for a reaction task (two-phase reactor) . . . . .	55
3.4	Schematic of a Simple Distillation Operation . . . . .	58
3.5	Schematic of a Batch Distillation Column . . . . .	60
3.6	McCabe-Thiele method for the calculation of bottom composition $x_B$ . . . . .	62
3.7	Driving force $F_{Di}$ as a function of composition $x_i$ . . . . .	64
3.8	Data flow between levels 1 and 2 of the Batch Distillation Algorithm (for identification and generation of separation sequences and their operational model) . . . . .	69
3.9	Block diagram of the algorithm A2 for the generation of a sequence of separation tasks based on batch distillation as well as the generation of the operational model for each separation task . . . . .	72
3.10	xy-diagram for a binary pair forming a minimum boiling azeotrope . . . . .	74
3.11	Sequence of products for a ternary system with a minimum boiling azeotrope present . . . . .	76
3.12	Cartesian and triangular coordinates in an equilateral plot . . . . .	78
3.13	Construction lines and material balances represented in an equilateral plot . . . . .	78
3.14	3D representation of a phase diagram in the tetrahedral space model [(Takano, 2000)] . . . . .	79
3.15	2D representation of a phase diagram in a Jänecke projection [(Takano, 2000)] . . . . .	79
3.16	A typical phase diagram for a Type I system . . . . .	82
3.17	A typical phase diagram for a Type II system . . . . .	82
3.18	Solid-liquid phase diagram for a ternary system with evaporation axis . . . . .	84
3.19	Selection of operating temperature for the crystallization based on slurry density . . . . .	90

3.20 Ternary solid-liquid diagram for a Type I system, where alternate precipitation of solids is necessary to achieve specified product recovery . . . . .	91
3.21 Block diagram of the algorithm A3 for the generation of a sequence of separation tasks based on batch crystallization as well as the generation of the operational design for each separation task . . . . .	96
3.22 Block diagram of the algorithm S for the generation of a batch route (sequence of reaction and separation tasks) together with the batch operations model for each task . . . . .	107
4.1 Use of computational tools in the batch reaction algorithms A1a-b	115
4.2 Use of computational tools in the batch distillation algorithm A2	116
4.3 Use of computational tools in the batch crystallization algorithm A3 . . . . .	118
4.4 Use of computational tools in the batch synthesis algorithm S .	119
5.1 Selectivity $S_{12}$ versus $x_{R_2}$ for the generated operational sequences	125
5.2 Reactor temperature versus $x_{R_2}$ for the generated operational sequences . . . . .	127
5.3 Total operating costs for the generated operational sequences .	128
5.4 Reactor temperature profile for the generated operational sequence in the two-phase batch reactor . . . . .	131
5.5 Reactor pressure profile for the generated operational sequence in the two-phase batch reactor . . . . .	132
5.6 Driving force diagram for benzene - MCB separation . . . . .	135
5.7 Driving force diagram for MCB - o-DCB separation . . . . .	135
5.8 Distillate composition over time for benzene - MCB - o-DCB separation . . . . .	138
5.9 Reboiler composition over time for benzene - MCB - o-DCB separation . . . . .	138
5.10 Reflux ratio profile for benzene - MCB - o-DCB separation . .	139
5.11 Condenser and reboiler temperature profile for benzene - MCB - o-DCB separation . . . . .	139
5.12 Distillate accumulate in various tanks as function of time for benzene - MCB - o-DCB separation . . . . .	139
5.13 Driving force diagram for MeOH - MeAc separation . . . . .	141
5.14 Reboiler composition over time for MeOH - MeAc separation .	142
5.15 Condenser temperature profile for MeOH - MeAc separation . .	142
5.16 Generated operational path for the type I system illustrated on the ternary phase diagram . . . . .	145
5.17 Generated operational path for the type II system illustrated on the ternary phase diagram . . . . .	147
5.18 Solvent-free ternary phase diagram at $T=0^\circ\text{C}$ . . . . .	151
5.19 Solvent-free ternary phase diagram at $T=25^\circ\text{C}$ . . . . .	151

---

5.20	Solvent-free ternary phase diagram at $T=35\text{ }^{\circ}\text{C}$ . . . . .	151
5.21	Solvent-free ternary phase diagram at $T=50\text{ }^{\circ}\text{C}$ . . . . .	151
5.22	Solvent-free ternary phase diagram at $T=75\text{ }^{\circ}\text{C}$ . . . . .	151
5.23	Solvent-free ternary phase diagram at $T=100\text{ }^{\circ}\text{C}$ . . . . .	151
5.24	Generated operational path for the quaternary system illustrated on the ternary solvent-free phase diagram . . . . .	154
5.25	Suggested batch route for the adapted example (Allgor <i>et al.</i> , 1996) . . . . .	155
5.26	Suggested batch route for the case study from the Synthesis al- gorithm . . . . .	160
C.1	List of important pure component properties . . . . .	182
C.2	Property - separation techniques relationship . . . . .	183
C.3	Property - separation techniques relationship, continued . . . .	184
E.1	Flooding reflux ratio value for example's column geometric spec- ifications . . . . .	188





# List of Tables

2.1	Abbreviations used in chapter 2 and their corresponding explanations . . . . .	30
5.1	Reaction rate constants for the set of reactions in the one-phase batch reactor . . . . .	122
5.2	Feasibility check of the isothermal and adiabatic operations . .	124
5.3	Generated family of alternative operational sequences for application example 5.2 . . . . .	126
5.4	Reaction rate constants for the set of reactions in the two-phase batch reactor . . . . .	129
5.5	Generated sequence of sub-tasks for the two-phase reactor . . .	131
5.6	Comparison of generated operational sequence for the two-phase reactor . . . . .	132
5.7	Duration and feasibility check for the constant heating operations for the two-phase reactor . . . . .	133
5.8	Batch recipe for obtaining first pure product benzene in example 5.4 . . . . .	136
5.9	Batch recipe for obtaining second pure product MCB in example 5.4 . . . . .	137
5.10	Accumulated results for the separation of benzene - MCB - o-DCB mixture . . . . .	138
5.11	Comparison of suggested reflux ratio profile with constant reflux ratio operation (for product benzene) in example 5.4 . . . . .	140
5.12	Batch recipe for removing the minimum boiling azeotrope in example 5.5 . . . . .	142
5.13	Operational sequence for the batch crystallizer for the separation of the type I ternary system . . . . .	146
5.14	Operational sequence for the batch crystallizer for the type II ternary system . . . . .	148
5.15	Operational sequence for the batch crystallizer for the separation of the quaternary electrolyte system . . . . .	153
5.16	Comparison of the reactant mixtures after succeeding reaction tasks based on the property of vapour pressure . . . . .	157
5.17	Comparison of the reactant mixtures after succeeding reaction tasks based on the property of boiling point . . . . .	157
5.18	Comparison of the reactant mixtures resulting after succeeding reaction tasks in terms of separation boundaries . . . . .	158
5.19	Holdup and temperature of the reactor effluent, for the first reaction task . . . . .	158

---

5.20	Intermediate product from the first batch distillation column . . . . .	159
5.21	Intermediate product mixture from the second batch reaction task . . . . .	161
5.22	Final product obtained as distillate from the second batch distillation column . . . . .	161
D.1	Operational costs for the generated alternative sequences of sub-tasks based on heating and cooling . . . . .	186
E.1	Column geometry . . . . .	187
F.1	Property lists for the mixture after the 1 <sup>st</sup> reaction task . . . . .	190
F.2	Property lists for the mixture after the 1 <sup>st</sup> reaction task, continued . . . . .	191
F.3	Property lists for the mixture after the 1 <sup>st</sup> reaction task, continued . . . . .	192
F.4	Property lists for the mixture after the 2 <sup>nd</sup> reaction task . . . . .	193
F.5	Property lists for the mixture after the 2 <sup>nd</sup> reaction task, continued . . . . .	194
F.6	Property lists for the mixture after the 2 <sup>nd</sup> reaction task, continued . . . . .	195

# List of Rules

## Algorithm A1

Rule A1.1	Selection of first sub-task	42
Rule A1.2	Sub-task end (selectivity violation)	43
Rule A1.3	Identification of final sub-task	44
Rule A1.4	Subsequent sub-task identification (selectivity violation)	44
Rule A1.5	Subsequent sub-task design (selectivity violation)	45
Rule A1.6	Subsequent/final sub-task design (selectivity violation)	45
Rule A1.7	Sub-task end ( $T_{up}$ violation)	46
Rule A1.8	Subsequent sub-task identification ( $T_{up}$ violation)	46
Rule A1.9	Sub-task end ( $T_{low}$ violation)	46
Rule A1.10	Subsequent sub-task identification ( $T_{low}$ violation)	46
Rule A1.11	Sub-task end ( $P_{up}$ violation)	48
Rule A1.12	Subsequent sub-task identification ( $P_{up}$ violation)	48
Rule A1.13	Subsequent sub-task identification ( $P_{up}$ and $T$ violation)	48
Rule A1.14	Subsequent sub-task identification ( $P_{up} - \Delta P$ violation)	48
Rule A1.15	Subsequent sub-task identification ( $P_{low}$ violation)	49
Rule A1.16	Subsequent sub-task identification ( $T_{up}$ violation)	49
Rule A1.17	Subsequent sub-task identification ( $T_{up}$ and $P$ violation)	49
Rule A1.18	Subsequent sub-task identification ( $T_{up} - \Delta T$ violation)	49
Rule A1.19	Subsequent sub-task identification ( $T_{low}$ violation)	49
Rule A1.20	Sub-task end ( $P_{low}$ violation)	50
Rule A1.21	Subsequent sub-task identification ( $P_{low}$ violation)	50
Rule A1.22	Subsequent sub-task identification ( $P_{low}$ and $T$ violation)	50
Rule A1.23	Subsequent sub-task identification ( $P_{low} + \Delta P$ violation)	50
Rule A1.24	Subsequent sub-task identification ( $P_{up}$ violation)	50
Rule A1.25	Subsequent sub-task identification ( $T_{low}$ violation)	51
Rule A1.26	Subsequent sub-task identification ( $T_{low}$ and $P$ violation)	51
Rule A1.27	Subsequent sub-task identification ( $T_{low} + \Delta T$ violation)	51
Rule A1.28	Subsequent sub-task identification ( $T_{up}$ violation)	51

## Algorithm A2

Rule A2.1	Separation task $k$ identification	66
Rule A2.2	Separation task identification (intermediate cut removal)	66
Rule A2.3	Subsequent separation task identification	67
Rule A2.4	Separation task identification (min. boil. azeotrope)	67
Rule A2.5	Subsequent separation task identification (after azeotrope removal)	67
Rule A2.6	Subsequent separation task identification (after azeotrope removal)	67
Rule A2.7	First sub-task design ( $V$ )	68
Rule A2.8	Sub-task design ( $R$ vs $V$ )	69

Rule A2.9	Sub-task end	69
Rule A2.10	Final sub-task identification	70
Rule A2.11	Operations model generation end for separation task $k$	70
Rule A2.12	Complete batch operations model generation end	70
<b>Algorithm A3</b>		
Rule A3.1	Single solid precipitation feasibility check	84
Rule A3.2	Task identification (identity of solid to precipitate)	85
Rule A3.3	Task identification (hydrate involved)	85
Rule A3.4	Task identification (identity of solid to precipitate)	85
Rule A3.5	Task identification (hydrate involved)	85
Rule A3.6	Task identification (multicomponent system)	86
Rule A3.7	Sub-task identification (evaporation)	86
Rule A3.8	Sub-task design (evaporation)	86
Rule A3.9	Sub-task identification (further evaporation)	87
Rule A3.10	Sub-task identification (dilution)	87
Rule A3.11	Sub-task design (dilution)	87
Rule A3.12	Sub-task identification (evaporation, hydrate involved)	88
Rule A3.13	Sub-task identification (dilution, hydrate involved)	88
Rule A3.14	Sub-task identification (evaporation, multicomponent system)	88
Rule A3.15	Sub-task identification (dilution, multicomponent system)	88
Rule A3.16	Sub-task design (multicomponent system)	89
Rule A3.17	Sub-task design (temperature)	89
<b>Algorithm S</b>		
Rule S.1	Initial sequence of tasks identification	101
Rule S.2	Number of separation tasks identification	101
Rule S.3	Separation technique identification	102
Rule S.4	Separation batch operations model identification	102
Rule S.5	Sep. task prior to 1 <sup>st</sup> reaction task identification (raw materials)	102
Rule S.6	No separation task prior to 1 <sup>st</sup> reaction task (impurities and reaction)	102
Rule S.7	No separation task prior to 1 <sup>st</sup> reaction task (impurities and separation)	102
Rule S.8	Sep. task prior to 1 <sup>st</sup> reaction task identification (impurities and reaction)	102
Rule S.9	Sep. task prior to 1 <sup>st</sup> reaction task identification (impurities and separation)	103
Rule S.10	Sep. task identification between two consecutive reaction tasks	103
Rule S.11	Sep. task identification between two consecutive reaction tasks (feasibility/easiness of separation)	103
Rule S.12	Sep. task identification between two consecutive reaction tasks (byproduct-final product separation boundary)	104

---

Rule S.13	Sep. task identification between two consecutive reaction tasks (reaction kinetics)	104
Rule S.14	Total recovery expression	105
Rule S.15	Purity specification of intermediate separation tasks	105
Rule S.16	(Initial) intermediate task recovery specification	105
Rule S.17	Final separation task identification	105



# INTRODUCTION

Through history, batch technologies have been used to process natural resources and produce a series of products, such as food, wine and beer, medicine, paints, etc. The shift from batch to continuous operation took place when the need of mass production appeared and especially with the rise of petrochemical industries, continuous processes started dominating large-scale industry. However, the observed increase in the production of high-added-value, low-volume specialty chemicals, fine chemicals, pharmaceuticals and biochemicals has created a growing interest in batch processing technologies. A variety of problems in batch processing have attracted a lot of attention and research. However, there is the lasting problem of the synthesis of batch processes, which can be outlined as follows: Given the identity of the raw materials and the product specifications, identify and sequence the necessary tasks, such as reaction, separation or a combination thereof, that need to be performed in order to produce and purify the desired products.

This thesis makes an effort to solve the batch synthesis problem and generate this sequence of batch processes, which is called the batch route. In addition to the identity and sequence of the tasks, the conditions of operation for each task need to be determined (operational design), in order for the generated batch route to be complete. The operational design for each batch process considered entails the identification of a sequence of sub-tasks necessary to achieve a set of intermediate objectives for each task. This sequence of sub-tasks is called the batch operations model.

## Background and Motivation

Batch processing covers a very wide area of problems. A particular problem that has received little attention is the identification of the tasks that need to be performed in order to reach a specified objective and the possible variations in the specified task performances. Decisions related to the extent one task should be allowed to progress and under which operating conditions, have a significant impact on the tasks that follow. This is because the state and properties of the material transferred to the next task depends on the extent of advancement of the preceding task.

The majority of batch processes are frequently scaled up from the laboratory to the full size plant without much process optimization to reduce the time to



market. Consequently, the batch route employed is the simple and conservative route used in the laboratory to produce the specified product. The research carried out that refers to batch processes synthesis addresses usually a different problem, that of the design of a batch plant, where batch sizes and equipment are determined for profit maximization. Moreover, in existing methodologies for planning and scheduling, the batch routes are neither determined nor optimized, but assumed as given data. The processing times for each task in the sequence are also assumed to be known in advance.

There is a need, therefore, for a systematic methodology that will be able to generate the sequence of reaction and separation tasks that can produce and obtain the specified products of a desired purity and recovery, in minimum time and/or cost. At the same time, the terminal objectives for each task in the sequence in terms of recovery and purity need to be specified. As mentioned already, the extent of advancement of one task as well as its presence has an effect to the tasks that follow, so it is important to make sure that the intermediate task objectives can be satisfied. This implies that a feasible and preferably optimum batch operations model can be determined and applied for each task in the batch route.

The determination of the optimum operating profile for batch reactors, batch distillation columns or crystallizers have been the subject of research in numerous papers. A large number of papers have appeared that applied Pontryagin's Maximum Principle (Pontryagin et al., 1962) to search for optimal solutions, subject to certain objectives. For this reason, rigorous models of the batch process considered are used, that are complicated even when short-cut models are derived. Furthermore, even when rigorous models are used an initial estimation for the operating profile usually needs to be available and the realization of the optimal solution depends on the initial input provided.

Hence, there is a need for a simple, easy and fast way to generate a sequence of sub-tasks that satisfies all path and terminal objectives for the batch processes mentioned above. Since the optimal solution has to satisfy physical feasibility, it is most desirable that the generated solution is feasible. In order to serve as a good initial point for further optimization, the generated solution also needs to be close to the optimum. Determining a near optimal solution in a systematic, but simple way can be challenging, since shifting from one operation to another can be difficult because of the abundance of options. It is, therefore, essential to limit these options by screening out the infeasible alternatives and significant to be able to choose the best alternative by exploiting all the available knowledge.

### **Hypothesis**

The hypothesis adopted as a basis for further work in this thesis is as follows:

#### Fundamental Hypothesis:

One can rise above the limitations of the simple models used to describe the nature of batch processes by taking advantage of the embedded thermodynamic and process insights. Both the batch process synthesis problem and

the batch operations model generation problem can be solved in a feasible and near-optimal manner, once these insights are identified, understood and applied.

This hypothesis can be split up into a batch process synthesis hypothesis and a batch operations model generation hypothesis.

#### Batch Process Synthesis Hypothesis:

The relationship between physical and chemical properties and separation process principles can be used to identify the most feasible and easy separation technique for a given separation. The combination of these thermodynamic insights as well as the insights provided by analysis of reaction kinetics allow the identification and the positioning of the necessary separation tasks in the batch route.

#### Batch Operations Model Generation Hypothesis:

i) Batch Reaction: When more than one reaction is taking place and undesired reactions are present, then the selectivity of the desired reaction over the unwanted reaction can be promoted with appropriate heating or cooling. The decision is based on the activation energies or the endothermicity/exothermicity of the desired reaction and the unwanted one.

ii) Batch Distillation: The driving force, which is the difference in chemical/physical properties between two co-existing phases (vapour and liquid), can be used to identify the minimum reflux ratio for any given composition. Any selected constant reflux ratio becomes at some point infeasible as the distillation progresses; that point can also be identified on the driving force diagram.

iii) Batch Crystallization: Solid-liquid equilibrium diagrams can be used to identify and illustrate feasible operations, operating conditions and operational paths for a given separation. The feasibility of the precipitation of a specific solid can also be identified over a range of temperatures and the best temperature can be selected.

### **Methodology**

The objective of this Ph.D. project is to propose a methodology for providing feasible (and near optimal) solutions for the synthesis and operational design of batch processes based on thermodynamic and process insights. The developed methodology handles the complete synthesis of batch processes at two levels. The upper level of the methodology is comprised of the synthesis algorithm where the actual batch route is generated. The sequence of reaction and separation tasks is generated from that algorithm and together with that the intermediate objectives for each task in the sequence are determined. These objectives are the recovery and purity of the specified product of each task. Initially, estimates for the intermediate objectives are suggested, which are later calculated in more detail, after additional input from the lower level is provided.

In the synthesis algorithm the composition of the outflow of a batch reactor (for each reaction set) is analyzed and the most feasible subsequent separation technique is identified, according to the largest property ratio that separation technique is related to. Mixture analysis (identification of separation boundaries) is used to determine whether a separation task is needed prior to a reaction task. In the case where multiple reaction sets are needed to obtain the final product, the necessity of intermediate separation tasks is determined, if a byproduct or an inert component form a separation boundary with the specified final product and jeopardize either the product's purity or recovery. The identity of the most feasible separation technique is also identified for each intermediate separation task. The presence of an intermediate separation task might also be decided based on whether the succeeding reaction tasks are aided when waste is removed in advance and reaction rates are increased because of lower reaction volumes.

The decision related to the extent one task should be allowed to progress in terms of specified product recovery is considered at this stage, taking into account the influence the preceding task has on the succeeding ones. The small progress of a reaction task can be important, for example, to the separation task that follows, if any unconverted raw material is separated together with the specified product risking its purity. Likewise, a separation task that does not separate a sufficient amount of intermediate product can endanger the overall recovery of the final product.

The lower level comprises a total of three algorithms which tackle the operational design problem for batch reaction and separation, and as specific separation methods, batch distillation and crystallization, when the objective is to satisfy some previously specified intermediate or final task objectives. The batch operations model for each reaction and separation task is developed through the generation of a sequence of sub-tasks giving the heating, temperature or reflux ratio profiles. In this thesis, the sub-tasks are defined as operations where the manipulated variables remain constant during the sub-task period, let that variable be temperature, heating/cooling rate, reflux ratio, etc. So, a sub-task can be reacting at a specific temperature, operating at a constant reflux ratio, heating or cooling with a specific constant rate while reactions take place, evaporation or precipitation at a certain temperature and so on.

The three lower level algorithms share the following characteristics, namely the existence of a number of path and terminal constraints that need to be satisfied and the usage of manipulated variables to ensure feasible operation. All the developed algorithms are governed by rule sets which are developed based on process and thermodynamic insights. With the help of these rules, operational issues related to sub-task "start" and sub-task "end" are addressed, as the imminent violation of a constraint is identified, thereby detecting the end of a particular sub-task, and the next sub-task that will be able to maintain the operation feasible is determined, and so forth, until the specified end objectives for the overall task are met. A sub-task "end" could be identified if the tem-

perature or pressure or selectivity constraint is close to violation or if a reflux ratio becomes infeasible for the corresponding still composition. The actual constraints are never met, because slack variables are introduced to keep away from them. The next sub-task is decided so as to counteract the imminent violation. So, for example, cooling will be chosen if the upper temperature constraint is hit, vapour release is an option when pressure approaches the maximum limit and operating at a higher reflux ratio is the obvious choice when a reflux ratio becomes infeasible, according to the developed rules.

The algorithm for batch reaction provides the batch operations model for the case of one-phase (liquid) and two-phase (vapour and liquid) reactors, where multiple reactions take place in the liquid phase and a specific amount of product needs to be produced, while constraints on the operating temperature and pressure are present. The terminal objective is the product recovery and the minimization of operating time and/or costs. The reactions are categorized in terms of desired and unwanted/competing reactions and afterward it is determined if heating or cooling promotes the desired over the competing reactions. The operating profile is found such that selectivity is maximized or remains above a constraint. The algorithm for batch distillation handles the operational design of multicomponent batch distillation columns, for zeotropic and azeotropic mixtures. The separation taking place is considered to occur as a split between two components or as the removal of an azeotrope. In both cases, the vapour liquid equilibrium data for the binary pair between which either the split happens or the azeotrope forms can be used to generate a reflux ratio profile necessary to obtain the specified product, in terms of purity and recovery, in minimum time. In that way, the separation of a multicomponent mixture into its components can be seen as a sequence of binary splits that can in turn be handled with the driving force approach. The algorithm for batch crystallization provides the operational path for the separation of ternary and quaternary electrolyte systems. The objective is the product recovery for one or more solids and constraints are considered for the operating temperature of the crystallizer. The solid-liquid equilibrium diagram and the information it contains are used to identify the precipitating solid, the temperature at which the most solid is recovered and the amount of solvent that needs to be removed or added, in order to avoid cocrystallization issues and thus infeasible operation. A specified recovery for one solid might need to be achieved after alternate precipitation of two solids and the necessary number of precipitations can be determined in advance based on the phase diagram.

The two levels of the methodology are in communication with each other. The initial estimates of the intermediate objectives for each task determined by the upper level synthesis algorithm are provided to the lower level algorithms as part of their given data. The batch operations model is generated, where for the developed batch separation algorithms the flexibility of batch processes and the ability of obtaining more than one high purity product from a batch separation unit are considered. Afterward, the current state of the mixture through the production path is returned to the upper level synthesis algorithm

and more detailed calculations are allowed to be made for the remaining tasks in the sequence.

### **Thesis Outline**

The thesis is divided into six chapters. Chapter 2 covers the theoretical background in different aspects of batch processing together with selected state-of-the-art methods reported in the open literature. In chapter 3, the methodology for the synthesis of batch processes is given along with the four rule-based algorithms that together provide the batch route and the operational design of each task in the sequence. The computational tools used in the individual algorithms in this thesis are presented in chapter 4. The application of the different algorithms in several case studies is illustrated in chapter 5. Finally, conclusions are drawn in chapter 6, where also essential future work is discussed.

# STATE-OF-THE-ART

## 2.1 Introduction to Batch Processing

Batch processing is widely practiced in industry, however the study thereof has not received much attention and has not advanced nearly as much as for continuous processes. Explicit differences between the two processing types can partially explain the limited attention. In a continuous plant there will usually be a requirement for a single product, while a batch plant will normally be multiproduct and therefore have to be constructed to allow high flexibility. Batch processes have to be handled by models that can describe the behavior of the system over a range of conditions that may vary widely from the beginning to the end of the batch. Batch models with such a wide application range are only available to a limited extent. On the other hand, continuous processes can be handled by models that only need to make predictions at or close to steady state operating conditions. With respect to integrated approaches for batch processes, and especially computer-aided approaches, there has not been nearly the same advancement as for continuous processes. This is due to the fact that only simple models with a too limited application range describe the nature of the systems typically handled in batch processes. However, one can overcome the limitations of the simple models by taking advantage of the thermodynamic and process insights that are embedded in them. Recognizing, understanding and using these insights can allow one to provide feasible and near-optimal solutions to the batch operations model generation problem and the batch process synthesis problem.

There are many issues one could consider regarding the design and operation of batch processes and batch chemical plants. Extensive reviews on the representative batch processing problems have been provided by Rippin (1983a), (1983b) and (1993). In the following sections, some of the important batch processing areas and problems are defined and their current status is given.

For a single product line, the problem of batch process synthesis is the one that arises first, in the sense that the problem of identifying the sequence of tasks needed to obtain a product is fundamental. Once the necessary sequence is determined, the next step is the generation of the optimal operating profile for each processing task in the sequence. The study and the optimization of the individual batch units have also attracted significant research interest and

appeared regularly in the literature. After the generation of the open-loop optimal operating profile for each batch process unit, the problem of tracking the optimal profile and rejecting any disturbances present concerns the numerous papers that cover the area of control of batch processes. The problem of batch control is important both for the single product line, since reproducibility from one run to the other is essential, but also for the multiple product lines, because achieving the product objectives at the same finite operating time is important for the solution of the scheduling and planning problem. Once the entire batch plant is considered, the interactions of the various tasks in the batch production path are accounted for in the batch process plant design problem, where the goal is to satisfy certain product objectives and minimize a specified cost function for the plant. The batch process plant design problem is closely connected to the scheduling and planning problem, especially in the case where intermediate storage needs to be decided and designed. Lastly, having solved the problems of synthesis, optimization and control of each single product line, and when multiple product lines are considered, then the problem of scheduling and planning of batch processes for various types of plants, multiproduct or multipurpose, needs to be addressed. Significant research effort has been dedicated to that. These are the areas of batch processing that will be reviewed in the following sections.

## 2.2 Batch Process Synthesis

The general case of the batch process synthesis problem is concerned with establishing the processing tasks and their order for converting raw materials into a given set of final products, determining the operating policy for each task. Several papers refer to the synthesis of batch processes, but the sequence of tasks needed to produce a specified product is considered known for the various problems considered.

Birewar and Grossmann (1990) proposed a methodology based on MINLP models and addressed the structural design problem of multiproduct batch plants for deciding which tasks to merge in what units and in what units to use parallel equipment and the sizing of these units while simultaneously accounting for the production scheduling. There are major trade-offs when assigning and merging tasks, if each task has its own unit there are high capital costs, less efficient utilization of equipment, but the smallest cycle times, while if tasks are merged together, there are fewer batches and less idle time, but the large equipment has high capital cost and the cycle times are increased. The objective was to take into account the various economic trade-offs and determine the assignment of processing tasks to the processing units (also the new superunits) and the number of parallel equipment for each unit and their sizes, while accounting for the scheduling, so as to minimize the investment costs. When design and scheduling are considered simultaneously, significant

economic savings can be achieved.

Iribarren *et al.* (1994) took advantage of the flexibility of batch designs and the ability of merging agreeable tasks in single units to suggest a heuristic procedure that reduces the number of alternatives to be searched to find a good design. Initially, both batch and continuous designs are considered for a known flowsheet where each task is assigned to one unit and at further steps of the search progressively more compact batch designs are investigated. Heuristics are developed to identify the best mergings and combinations of continuous units and merged batch units are also considered. The alternative designs are evaluated according to the best total annualized capital cost. Each alternative design is the optimized in terms of the process decision variables, with the assumption that no batch size constraints are present and unlimited free intermediate storage is available.

Charalambides *et al.* (1995) assumed the structure of the processing network to be known and concentrated on determining the operating policies for the various tasks. The network considered included one reaction, one mixing and one distillation task with recycle, at its periodic steady state. The optimal cooling water profile for the reactor and the reflux ratio profile for the distillation were found solving a multistage optimal control problem, where a control vector parameterization approach is utilized to reduce the problem to a finite dimensional nonlinear programming problem. The objective is the maximization of the total net revenue. However, the discretization of the operating time for the reaction and the distillation tasks were performed *a priori* and the optimal cooling water flowrate and reflux ratio profiles were given in a piecewise constant fashion.

In general, various researchers have considered the case of merging tasks in one piece of equipment, regarded parallel units for a task and determined whether intermediate storage is needed and where it should be placed. However, the problem of the generation of the sequence of the actual reaction and separation tasks has not been addressed, but it has been considered to be already solved.

## 2.3 Batch Process Unit (Task) Optimization

The study and the optimization of individual batch units have appeared extensively in the literature. That includes developing and solving models for batch systems and determining profiles of operating variables for optimal batch performance (such as temperature, addition rate of a reactant in a batch reactor or reflux rate in a batch distillation, etc.). These are generically called the optimal batch operations model.

The complete solution of the batch operations model problem lies in answering two specific sub-problems. First, the optimal batch operations model needs to be determined as a sequence of batch operations performed in the same vessel, such as charging, heating, reacting in a specific way, evaporating or adding



solvent and so on, where the main issue is to achieve feasible operation, that is no constraints violation, and furthermore to satisfy several objectives for the specified product(s), such as purity and yield. The second sub-problem deals with deciding how to track the operating profile that the optimal batch operations model corresponds to. The closed-loop control problem of batch processes is discussed later on as a different area of batch processing.

### 2.3.1 Batch Reaction

In optimizing the performance of the individual batch reactor, it has been most popular to study the effect of a temperature profile on the course of a batch reaction and to a lesser extent the effect of the addition rate of one of the reactants. The usual objective of the optimization is either the maximum conversion at a given time or the minimum time for a required conversion. The optimization of the performance for a batch reactor is also closely connected with the control of the reactor, since tracking, for example, a specified temperature profile is connected to the manipulation of a cooling or heating agent that will control the reactor temperature.

Several papers have appeared in the sixties and the seventies that applied Pontryagin's Maximum Principle (Pontryagin et al., 1962) to search for optimal solutions, subject to certain objectives and for a number of different reaction schemes (summarized in Rippin's review (1983a)). Later, Cuthrell and Biegler (1989) applied Successive Quadratic Programming (SQP) to solve the optimization problem and obtained optimal feed rate profiles for a biochemical reactor.

Garcia *et al.* (1995) proposed an approach using a physical process model and a non-linear programming (NLP) formulation for the solution of the optimal control problem. They solved the problem by the generalized reduced gradient procedure coupled with the golden search method, for the search of the total batch time. The objective was to maximize the yield of the product and different cases are considered, where a) a temperature profile was found for fixed feed rate and operation time, b) a feed rate profile was produced for isothermal operation and fixed operation time, c) a temperature and a feed rate profile were calculated for fixed final batch time, d) temperature and feed rate profiles were simultaneously optimized with the operation time and e) additionally to d) the total amount of the reactant added was optimized. Lower and upper bounds for the temperature and flow rate were considered as well as possible constraints on the heating and cooling rates. The effect of the latter together with the effect of purity constraints upon the temperature and feed rate profiles were examined. However, the approach did not account for the exothermicity of the reactions and the energy balances on the reactor and its jacket.

A review of the operation of batch and semi-batch reactors was given by Bonvin (1998). The issues of interest to industry were listed and the industrial needs were compared with the research solutions proposed by academia. The characteristics of discontinuous reactors and the challenges they pose to the

monitoring, control and optimization of the reactors were discussed. The major modelling aspects for batch reactors were summarized, as well as state and parameter estimation methods. Control of batch reactors was described in terms of tracking a profile and rejecting disturbances, and the different kinds of operation related to thermal control were listed. The optimization strategies for batch and semi-batch reactors were classified in three categories, one-time optimization, run-to-run optimization and on-line optimization.

Luus (1999) suggested an approach, the objective of which is to maximize the yield of a desired product in a batch reactor, using iterative dynamic programming (IDP) in multi-pass fashion. The optimal temperature profile and the optimal isothermal temperature were found for a specified final time and used as benchmarks. Additionally, the optimal flow rates of heating and cooling fluids were determined. The effect of the heat transfer coefficient was found to be quite important, but inaccurate modelling of it can be corrected while running the reactor. If an error in the heat transfer term is detected, then the actual state can be used as an initial condition for the remaining time (stages) while the optimization is repeated. Even though the resulting control policy is open loop in nature, as long as the optimization can be carried out within a single or few sample periods, the parameters can be updated over the course of the reaction and the optimization problem can be solved repeatedly making the control, in essence, feedback in nature. Results showed that the optimal control policy achieves a yield larger than what can be expected from the best isothermal operation.

Maximizing the yield of a single second order reaction taking place in isothermal conditions, by manipulating the inlet flow rate of one of the reactant was considered by Ubrich *et al.* (1999). Once the kinetic parameters of the reaction were determined, using coupled spectroscopic and calorimetric methods, an optimization of the reaction system was performed numerically and verified experimentally. The feed rate profile was constructed with certain safety considerations in mind. Apart from the lower and upper bounds on the flow rate, constraints on the amount of heat produced that is related to the reactor's cooling capacity were imposed as well. Most importantly, limitations to the feed rate in the case of cooling failure were also imposed, with that flowrate calculated in connection to a maximum allowed temperature attained because of the residual non converted reactants. Results showed that a variable and optimized feed rate enables a given conversion to be achieved in a significantly shorter time than with a constant input.

As earlier mentioned, a lot of papers have appeared that search for the optimal solution for batch reaction. However, a common point is that rigorous models are used for the optimization that require a good initial point for the optimal solution to be realized. This initial point can be hard or time consuming to find, but it is essential since a bad initial point can actually lead to sub-optimal solutions.

### 2.3.2 Batch Distillation

Batch distillation is an important and very widely used unit in the batch processing industry. On the dynamic optimization of batch distillation columns, extensive research has been carried out by several investigators. The control variable that is mainly used is the reflux ratio  $R$ , which is very important since it affects both the rate and the concentration of the distillate  $D$ . The optimum reflux policy is typically found for two kinds of problems. The first problem is called the maximum-distillate problem, where the objective is to maximize the distillate amount of a specified concentration in a prescribed length of time. The other problem is called the minimum-time problem, where the objective is to minimize the distillation time needed to collect a fixed distillate amount with a specific concentration. Alternatively, the maximization of the profit per unit time of operation, which combines both of the two first objectives, is another problem that has been addressed.

The time-optimal problem for tray and packed columns was solved by Christensen and Jørgensen (1987) using Pontryagin's maximum principle and the model equations were discretized in time using the method of orthogonal collocation, according to efficient numerical algorithms from Hansen and Jørgensen (1986). The effect of a recycled waste cut was considered for binary batch distillation. It was advantageous, particularly for difficult separations, to use recycling since it meant significant time savings for both tray and packed columns. The difference in the optimal control profiles of a conventional batch distillation without recycling and the one with recycling is that the large increase in the reflux at the end of the conventional distillation is avoided and an overall lowering of the reflux is noticed. A measure of the degree of difficulty of separation in a given tray column was also proposed, in order to predict whether recycling would be advantageous.

Diwekar *et al.* (1987) solved the maximum distillate problem using Pontryagin's maximum principle to obtain the optimal reflux rate policy for multi-component batch distillation columns. A short-cut method to simulate the column was developed, which was based on the assumptions of zero holdup, constant molar overflow and constant relative volatility. The Hamiltonian was maximized using the method of the steepest ascent of Hamiltonian by using an iterative procedure to find the optimal reflux rate policy. However, the convergence to the maximum strongly depends on the initial values for the reflux rate vector, the Hamiltonian and the Lagrange multiplier. The short-cut method developed was used in Diwekar and Madhavan (1989) to solve the optimization problem, where the objective was to maximize profit. The problem was extended from single to multiple fraction batch distillation columns and was solved for both constant and variable reflux. The short-cut method was later compared with rigorous models in Diwekar and Madhavan (1991), where tuning parameters for the model were introduced to take into account nonidealities and the holdup effect. For the case of nonidealities, the tuning parameter was the value of  $\phi$  in the Underwood equation. The incorporation

of the holdup effect was accounted for with a lumped dynamic model for the top of the column.

Mujtaba and Macchietto (1996) presented a general formulation for the simultaneous design and operation of multicomponent batch distillation columns utilizing dynamic models of the column in the form of a generic system of differential and algebraic equations (DAEs). Single and multiple duties were considered, since in multiproduct plants the distillation columns can be used to separate different feed mixtures alternately. The design variable that was optimized was the number of plates  $N$  and the operation variables that were optimized were usually two for each task, typically the purity of a product and an amount (or recovery) of it. The control variables used were the reflux ratios and the switching times and the objective was to maximize a profit function. The objective function used gave better results compared to that of Logsdon *et al.* (1990). However, it should be noted that the specific sequence of tasks and choice of main and off-cut products was given *a priori* and so was the number of control intervals for each task.

Kim (1999) used a dynamic model for the optimal design of multiproduct batch distillation columns, where liquid holdup in a still, a reflux drum and trays was included. Successive quadratic programming was applied to obtain the optimal reflux ratio, when the objective was the maximization of the profit per unit time. The initial operation condition for the dynamic model was obtained from a rigorous simulation with total reflux after an iterative procedure was implemented to find the liquid composition in the trays. The reflux ratio profile was found either as constant or as a combination of constant and exponential reflux profile. However, the sequence of main and off-specification products was given in advance and for each product there was only one constant value for the reflux ratio, while for the exponential variation of the reflux ratio, two variables were found for each product. The dynamic model was compared with the quasi-steady model of Farhat *et al.* (1990) and the combination of constant/exponential reflux ratio profile was found to be an improvement.

The papers focusing on the optimization of batch distillation are numerous. However, the models used are mainly complicated and need an initial reflux ratio profile to be given as starting point for the optimal solution to be found. Additionally, when multicomponent mixtures are handled the order of main products and waste cut-off products seem to be given in advance. Furthermore, the models used consider constant relative volatility.

### 2.3.3 Batch Crystallization

Batch crystallization is often associated with evaporation strategies and cooling profiles that control the nucleation and growth rates and the crystal size distribution of the formed crystals. However, the systems involved in these cases are mainly single solute systems in a solvent. On the other hand, the separation of multicomponent mixtures in their constituents is usual for the case of electrolyte solutions and fractional crystallization is used for that purpose. There

are also cases where for the separation of multicomponent mixtures traditional distillation can not be used, if for example the desired product decomposes at its boiling point, and then fractional crystallization becomes very attractive. Additionally, fractional crystallization can be attractive over traditional batch distillation, since the former is less expensive than the latter. An investigation of the progress in the study of fractional crystallization follows next.

A benchmark paper on the design of fractional crystallization processes was presented by Fitch (1970). Graphical methods are used to represent the system, its equilibria, and the results of various process manipulations, since material balances can be represented and calculated on the phase diagram. The representation and separation of various types of systems with three and four component solutions are illustrated through examples, where basic operations as heating/cooling affect the separation. The purpose of the paper was to give a systematic approach for the engineer that is faced with a fractional crystallization problem.

Cisternas and Rudd (1993) presented a procedure for identifying alternative process designs for fractional crystallization from solution that minimize the rates of evaporation, dilution and recycle. The process designs are derived for the cases where the crystallizations are operated at hot and cold points of multiple saturation. The order of the salts in the phase diagram needs to be specific, in order to facilitate and systematize the identification of the designs. The systems illustrated are ternary and quaternary solutions, which form anhydrous and hydrated single salts, and anhydrous and hydrated, congruently or incongruently soluble, double salts.

Dye and Ng (1995) considered the different operations that affect the separation of two- and three-solute mixtures. Guidelines were presented for obtaining one solute by isothermal evaporation or dilution and then using stream mixing or heating/cooling to overcome a multiple saturation point/curve and recover another pure solute. The operation at three different temperatures for obtaining all three solutes in a quaternary mixture was also considered. The authors formulated design equations and identified constraints on the design variables, but chose the values for the design variables. The effect of the changes in the design variables on the recycle flows was discussed.

From the same laboratory, Cesar and Ng (1999) presented a systematic method for improving the recovery of the desirable product in an existing fractional crystallization process. Solid-liquid-phase behaviors and techniques relevant to product recovery were discussed. Retrofit targets were identified through an analysis of the phase diagram of the mixture under consideration. Conceptual design techniques consisting of heat and mass balances, heuristics, and short-cut unit models were used to determine the necessary changes in flow sheet structure and equipment design in order to meet the retrofit objective.

For fractional crystallization, phase diagrams have been used to identify the operational paths for obtaining one or more solutes from a mixture. However, no systematic procedure for choosing the operating temperature has been provided. Furthermore, in some cases operation is chosen to take place on invariant

points, which might prove infeasible.

## 2.4 Batch Process Control

The control problem of batch processes is a non-linear and time varying problem that is of a difficult nature (Jørgensen *et al.*, 2004). Despite that fact, various approaches to the problem have been suggested by different researchers. The recommended methods are using either first engineering principle models or empirically based models. One of the methods that uses first engineering principle models is based on on-line optimization, where the optimal batch operations model is periodically updated during the batch execution at previously chosen sampling times, in order to optimize some performance measure. However, since detailed first principles models are not so often available for industrial applications, empirically based models have been suggested by a bigger number of research groups. The actual implementation of the optimal batch operations model, which is given as setpoint trajectories, can be done by a set of controllers that change the manipulated variables in order for the controlled variables to follow the prescribed trajectories. This is called Closed Loop Optimizing Control and various forms of it are investigated below.

### 2.4.1 Single and multi- variable control layers

Using on-line optimization techniques, Eaton and Rawlings (1990) presented a method that used nonlinear models to solve feedback control problems for multivariable chemical processes, without linearization. Their method handled multiple inputs and outputs without pairing. The optimal control policy was found using a simultaneous optimization and model solution approach. The differential equations were approximated by a set of algebraic equations using orthogonal collocation on finite elements and then solved simultaneously with the other constraints with successive quadratic programming. The important process model parameters were updated with the feedback from the measurements and the optimal profile was then recomputed.

Palanki *et al.* (1993) studied singular optimal control problems, where the objective was not to keep the system at a set point but rather to maximize the product of interest at the end of the batch cycle. Thus, the role of the control was to optimize a performance index at the final time of operation. The synthesis of optimal state feedback laws, which guarantee optimality at a fixed final time, was studied for both time-invariant and time-varying systems.

An empirical based model approach was presented by Srinivasan *et al.* (2003a) and (2003b). They suggested a framework that uses measurements rather than a model of the process for implementing the optimal solution. They determined a sequence of approximate input trajectories using approximate models and subsequently used batch plant measurements to refine the input trajectories through tracking the Necessary Conditions of Optimality (NCO). The sequence

of input trajectories and the switching times between them were established in order to satisfy the terminal constraints or were adapted to take advantage of compromises in the system. The optimal solution proposed treated the path and terminal objectives independently. In the second paper, optimization under uncertainty was handled using feedback control based on measurements. The concept of solution model was then introduced by Srinivasan and Bonvin (2004) and the procedure for obtaining it consisted of dissecting the input profiles based on the effect of uncertainty and linking their elements to the different parts of the NCO.

### 2.4.2 Iterative Learning Control

Since batch processes are repetitive in nature and achieving the same product qualities and performance is highly desirable, learning control in an iterative manner becomes very appealing. Iterative Learning Control (ILC) is a technique for improving the response and tracking performance of processes that follow the same operating profile over and over, starting basically from the same initial conditions each time. The learning control algorithm is executed off-line at the end of each batch, where the motivation is to learn from the errors of the previous batch and compute modifications in the input trajectories, in order to reach the desired performance level.

Moore *et al.* (1992) considered Iterative Learning Control (ILC) for the case of linear time-invariant (LTI) plants and controllers. They gave the development of general convergence conditions for LTI learning controllers, proposed a learning control system based on parameter estimation for use with unknown LTI plants and developed a one-step learning controller with “memory” for finite horizon problems. They finally described a time-varying learning control technique that can be applied to a class of nonlinear systems.

### 2.4.3 Model Predictive Control

Model Predictive Control (MPC) is built on model-based predictions of future process behavior and provides an optimal actuator sequence, which will bring the process to a desired operation point within a given time horizon. The current control action is obtained by solving, at each sampling instant, a finite horizon open-loop optimal control problem, using the current state of the plant as the initial state. The optimal sequence is found according to an objective, which can be the minimization of the deviation from a given batch operations model, the minimization of costs or the maximization of production rate and so forth. An important advantage of this type of control is its ability to cope with hard constraints on controls and states.

The discussion of linear model predictive control based on a nominally stabilizing, infinite horizon, linear quadratic regulator was taken by Muske and Rawlings (1993). They presented a MPC formulation that addresses the plant stability and the state-space formulation was used as the model plant. The

output feedback was performed with the use of linear quadratic filtering theory and target tracking in the controller was obtained by using results from standard linear quadratic regulatory theory.

A review of the model predictive control problem was presented by Morari and Lee (1999). The difficulties in modelling, sensing, non-linear state estimation, fault detection/diagnosis, etc. were indicated as the limits in the performance and applicability of MPC and a need for further research in these areas with connection to MPC is clear. Mayne *et al.* (2000) focused on model predictive control of constrained systems, both linear and nonlinear, in their review of the subject. They dealt with stability and optimality and provided a concise characterization of most of the model predictive controllers, in terms of terminal state, terminal cost, terminal constraint set and terminal cost and constraint set.

When ILC is applied between batches as the only control scheme, no corrective actions are offered during the operation of a single batch. However, the batch duration is often long in chemical plants and therefore handling intrabatch disturbances might give significant benefit, if iterative learning and multivariable control are combined. This combination was investigated by Lee *et al.* (2000) and Bonné and Jørgensen (2004). Merging ILC and MPC offers the learning capabilities of the ILC in a MPC framework. Such a merger provides a MPC framework which asymptotically rejects the effect of batchwise persistent disturbances including the effects of model bias introduced by the linear process approximation.

## 2.5 Batch Process Plant Design

Task performance and how the extent of one task is affecting the downstream tasks is discussed for the design of batch processes by Salomone *et al.* (1994). Their work is directed at the optimization of a single product plant modelled with posynomial expressions, where dynamic simulation provides the parameters for the analytical posynomial expressions from the input-output response of the stages involved. A posynomial expression is one that relates, for example, the batch size  $B$  and the operation time  $T_j$  for an equipment  $j$  as such:  $T_j = T_j^0 + T_j^1(B)^{a_j}$ , where  $T_j^0$  and  $T_j^1$  are positive constants and  $a_j$  can be either positive or negative and not necessarily an integer number. Their interest is in optimizing process decision variables that trade off the cost of different process stages, such as the conversion of a reactor, the composition of a recycle, etc. Treating process items where time can both be independent of the batch size and proportional to the batch size, the results obtained from the optimization include the optimal values for the decision variables, the batch sizes and times and the equipment sizes.

The problem of batch process development was introduced by Allgor *et al.* (1996) where they attempted to identify a set of decisions variables that can



be used for further optimization. The need of tools that can facilitate the simultaneous investigation of processing tradeoffs at the unit and the process level was pointed out. They discussed how the operating policy of a task can affect the downstream tasks and showed in an example that modifying the operating policy of a reaction task in a way that it is not the optimal for the unit, can actually optimize the overall task network. The insights to modify the operating policy were provided from process modelling technology, and the study of the reaction mechanism, especially the reaction rate expressions and constants.

A process systems methodology for incorporating environmental concerns in the optimal design and scheduling of batch/semi-continuous processes was presented by Stefanis *et al.* (1997). The Minimum Environmental Impact (MEI) methodology, which embeds principles from Life Cycle Analysis (LCA), was extended to batch processes. The proposed methodology involved three main steps: i) the definition of an expanded batch plant boundary, ii) the aggregated environmental impact assessment and iii) the incorporation of environmental impact criteria in batch plant design/scheduling. The input wastes and the waste generation sources within the plant were identified and the output emissions were linked to input waste generation and all quantified in a global waste vector. A general multi-objective formulation was considered for the design of multipurpose batch plants, where environmental criteria were used together with cost as distinct design objectives. Examples from the dairy industry were presented to demonstrate that zero discharge might not necessarily be the best environmental policy and that more environmentally friendly batch designs and schedules can frequently derive from increased input waste generation.

## 2.6 Batch Process Scheduling and Planning

The batch chemical plants are very flexible compared to continuous plants, because of their capability to manufacture multiple products by sharing the same process resources. Products can be produced either in sequence or simultaneously, but it is resource constraints, storage limitations and production demands that make the scheduling of batch plants a fertile area of interest. The combinatorial nature of scheduling problems makes them very complex, since their solution requires many discrete decisions. According to computational complexity theory, in effect all industrial scheduling problems are NP (Non-deterministic Polynomial time)-complete problems. Given the nature of scheduling problems, there are three strategies for approaching their solution (Applequist *et al.*, 1997):

*Strategy 1 - Change the problem to be solved to make it easier.* A very popular strategy that involves loosening the constraints, parameters and objective function of the problem until a given scheduling algorithm can solve the problem. Depending on the extent of the modifications, this strategy will always work. However, modifications to a problem with a feasible solution also can

result in substantial economic and performance penalties.

*Strategy 2 - Use an exact algorithm which may require unreasonable computational time.* The execution time of an exact algorithm is in the worst case exponential to the size of the considered problem. This means that for large scheduling problems the time required is unacceptably long. Thus, the exact methods are usually paired with methods using Strategy 1 or Strategy 3.

*Strategy 3 - Use a heuristic algorithm which may obtain a poor answer.* Heuristic solution methods will always have a reasonable execution time, but they also run the risk of providing poor solutions or even fail to find a feasible solution. Since failure in the solution of the scheduling problem is not an acceptable option for practical applications, the necessity to combine Strategy 3 with the other strategies arises.

The combination of the available strategies implies a trade-off between execution time and feasibility/solution quality. The appropriate trade-off needs to be found for the individual application that will secure a high quality solution in reasonable time. The available methods for the solution of scheduling problems can be classified according to the strategies discussed above as: i) exact or optimization-based approaches which find an optimal or near-optimal solution, along with a measure of its quality, and ii) heuristic solution methods which seek an adequate solution with a reasonable computational effort.

### 2.6.1 Optimization-based Approaches

Scheduling problems require solutions where many discrete decisions need to be taken, such as sequencing the production tasks, assigning the right equipment to accomplish a task, deciding on the utilization of storage tanks, etc. Each decision is assigned a variable and the constraints of the operations are then expressed as equalities or inequalities in terms of these variables. The goal is to maximize the performance of the plant in the form of an objective function.

The optimization-based approaches treat scheduling and planning problems as Linear programs (LP), Mixed-Integer Linear Programs (MILP) or Mixed-Integer Nonlinear Programs (MINLP). The optimization-based approaches for scheduling are used for two kinds of operations: a) traditional campaign operations and, b) a general and flexible operational mode. For the *campaign-based operation* two subclasses of operations can be identified: the multiproduct plant (multiple products in a sequence of single product campaigns) and the multipurpose plant (each campaign involves one or more production lines and products).

#### 2.6.1.1 Multiproduct Plant

For the multiproduct plant, as shown in figure 2.1, all the products follow the same production path. Suhami and Mah (1981) modelled the scheduling of batch processing of materials as a flowshop scheduling problem with no intermediate storage, for which the objective is to minimize the makespan, where

makespan is the difference between the latest finishing time among all tasks and the earliest starting time of all tasks, for all the products scheduled. They used a branch and bound procedure for the no intermediate storage (NIS) serial flowshop, where once the resulting solution was not probable to be better than the current solution, the search branches were fathomed. A heuristic rule is used to obtain an initial solution which serves as an upper bound to the optimum. Ku and Karimi (1988) studied the scheduling of  $N$  products in an  $M$ -unit serial multiproduct batch process, under the minimum makespan criterion, with various storage policies. They developed an optimal MILP formulation and proposed a heuristic strategy to reduce the number of binary variables by assigning products to specific neighborhoods of a sequence.

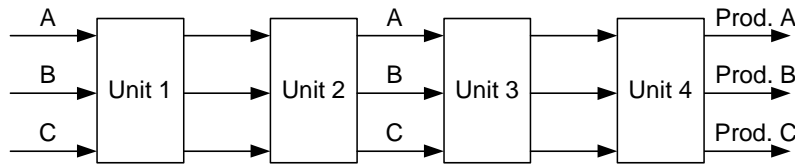


Figure 2.1: Schematic of a multiproduct batch plant

Kim *et al.* (1996) suggested optimal strategies, where the objective function is the minimization of the makespan. These strategies are formulated as MINLP for serial multiproduct batch processes for various storage policies, such as unlimited intermediate storage (UIS), NIS, finite intermediate storage (FIS), zero wait (ZW), and mixed intermediate storage (MIS). The formulations are based on completion time algorithms with nonzero transfer time, sequence-dependent setup times in processing units and the storage setup times.

Ha *et al.* (2000) presented various intermediate storage tank operation strategies in the production scheduling of multiproduct plants, addressing for the first time constraints in the storable time and possible product constraints in intermediate storage. An MILP model is proposed, for which the objective is to minimize the makespan. The completion times of products on each unit are determined and the optimal number of intermediate storage tanks and their location is also decided, for the NIS and ZW storage policies.

#### 2.6.1.2 Multipurpose Plant

For the multipurpose plant, all products do not follow the same production path. However, if a specific direction in the plant floor can be recognized, then the plant is a sequential plant, as shown in figure 2.2. All remaining cases are non-sequential multipurpose plants, illustrated in figure 2.3. Mauderli and Rippin (1979) suggested a partly heuristic procedure that generates dominant (efficient) single or multi-product campaigns using an LP screening method to reject the nondominant campaigns. Solving a multi-time period MILP prob-

lem, the production time is allocated to selected dominant campaigns, in order to produce any desired mix of products in an optimal fashion.

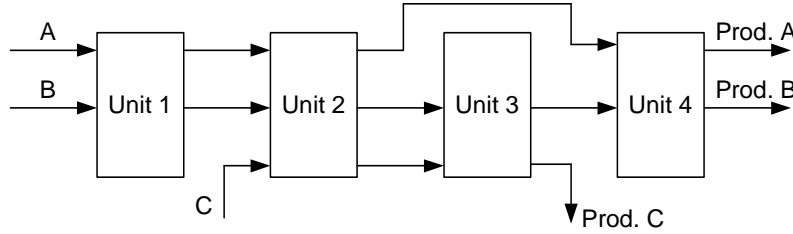


Figure 2.2: Schematic of a sequential multipurpose batch plant

Suhami and Mah (1982) proposed a strategy for the optimal design of a multipurpose batch plant. The problem is formulated as an MINLP and it is solved using a generalized reduced gradient code. The proposed strategy generates feasible sequences and nonredundant horizon constraints, and with the help of a set of rules the optimal or near optimal configurations are selected, based on rigorous and heuristic considerations. For plants with up to 10 unit types and up to 7 products, the procedure yields designs very close to the optimum. Wellons and Reklaitis (1991a) presented an MINLP formulation to generate the best single product campaigns. A further MILP procedure generates multiple parallel lines with the highest production rate and selects among the dominant campaigns the ones that maximize net profit. Both the single and the multiple product campaign problems are solved via Benders decomposition (Benders, 1962). The changeover and the start-up time for each campaign are accounted for, while no intermediate storage vessels are included in their formulations. Mauderli's campaigns (Mauderli and Rippin, 1979) compare quite well with those obtained from Wellons and Reklaitis (1991b).

Voudouris and Grossmann (1996) proposed an MILP formulation for the integrated scheduling and design of sequential multipurpose batch plants under a MIS policy. A periodic scheduling approach based on an aggregation scheme is derived, which allows the problem to be solved in the product space rather than that of individual batches. A reduction scheme is proposed that yields a significant decrease of the binary dimensionality of the problem. Two cases of problems are considered, namely one where all potential production paths are given and a second where the actual production path is an optimization variable. In both cases the equipment sizes are determined, where the objective is the maximization of the profitability of the plant. The potential existence of intermediate storage in the production paths is also considered.

Kim *et al.* (2000) presented an MILP mathematical model for the optimal scheduling of non-sequential multipurpose batch processes that have one unit per processing stage, under finite intermediate storage policy. The objective is to determine the optimal sequence of products in each unit, in order to

minimize makespan. For the non-sequential multipurpose plant, this product sequence is different for each unit. In their scheduling problem formulation, the starting and finishing time of a task in each unit are represented with two coordinates. One is based on products identity, and the other is based on the given operation sequences. The variables used in the two coordinates are matched into one with binary variables and logical constraints, based on the availability of the next unit and the availability of storage. The formulation of this problem as an MILP guarantees the optimality of the solutions.

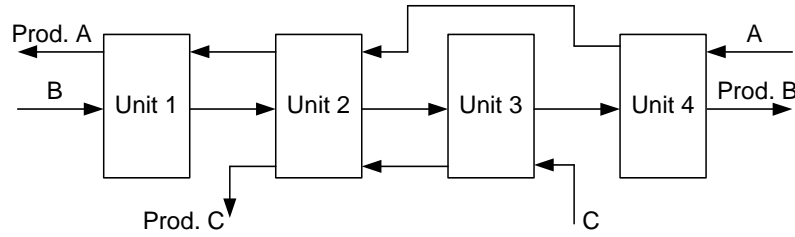


Figure 2.3: Schematic of a non-sequential multipurpose batch plant

### 2.6.1.3 General Multipurpose Operation Plant

In the general multipurpose operation plant, the equipment and resource utilization profiles exhibit no regular pattern over time. The multipurpose plant is operated with no defined production lines and production occurs in an aperiodic fashion, since the restrictions on campaign and cyclic operation are relaxed (Reklaitis, 1995). The key challenge for these batch plants is to represent in a detailed fashion the operation of the plant over time. This is done by discretizing time in some fashion. The most common mode of time discretization is the so-called uniform time discretization, where uniform time intervals are used. Sargent and coworkers (Kondili *et al.*, 1993; Shah *et al.*, 1993) applied first this type of models in multipurpose plants.

Kondili *et al.* (1993) formulated an MILP for the short-term scheduling problem of multipurpose plants. The MILP formulation is based on a uniform time discretization model (UDM) and also on the representation of the recipe used to manufacture each product as a simple state-task network (STN). The novel feature of this representation is that both the individual batch operations are expressed as task nodes and the feedstocks, intermediate and final products are included explicitly as state nodes. The objective is to maximize a profit function that takes into account the value of products and material, capital and operating costs. Variable product demands and deliveries over the time horizon are taken into account. Furthermore, limited availability of the raw materials, both at the start and during the time horizon of interest, can be accommodated, but only at the interval boundaries. The possible variation of utility costs and their availability over time, as well as flexible equipment allocation, variable

batchsizes and MIS policies involving both dedicated and multipurpose storage vessels are taken into account. The formulation may result in MILPs involving large numbers of binary variables. Shah *et al.* (1993) described various aggregation techniques for the efficient solution of these problems, in order to reduce the amount of computation required without compromising the optimality of the solution obtained. They combined reformulation of some of the UDM constraints, use of a more compact linear programming relaxation of the MILP, and reduction of the non-integrality of the solutions of relaxed LPs through *a posteriori* solution analysis.

Barbosa-Povoa and Macchietto (1993) proposed an MILP formulation for the optimal selection of both equipment units and the network of connections for multipurpose batch plants. There are two different design objectives, namely the maximization of the plant profit and the minimization of the capital costs (units, piping), when given production requirements for a variety of products need to be satisfied. A special novelty of the formulation is the superstructure used, the maximal state-task network, which further considers the suitability of the plant units for the tasks, the transfer information between the units themselves and the storage vessels and the suitability of the storage vessels for the state nodes of the network. The formulation presented provides the possibility of generating directly the optimal connectivity between process units, sizing and costing of all transfer lines, and the optimal storage policies, and associated vessel sizes, if any, for stable intermediates without the need for *a priori* assumptions.

Mockus and Reklaitis (1997a) presented an MILP formulation using state-task network representation, in order to handle a wide range of short-term scheduling problems of multipurpose plants. Capacity constraints, limited availability of utilities and manpower, and cleaning of equipment are considered in the formulation. The scheduling horizon for the problem is divided in non-uniform time intervals based on Zentner's NUCM (Non-Uniform Continuous time Modelling) formulation (Zentner *et al.*, 1992), but variable batch sizes and changeovers are considered. The resulting model can be simplified via exact linearization to yield a mixed integer bilinear program (MIBLP) in which the only nonlinearity arises in the objective function as a product of continuous variables. The model is solved using the Outer Approximation method (Duran and Grossmann, 1986) modified for nonconvexities. The same authors extended their model and formulated the problem as an MINLP, using the Bayesian heuristic (BH) approach to solve the resulting model (Mockus and Reklaitis, 1997b). Their results show that combining the NUDM formulation with the BH global optimization method is a very efficient method for the solution of batch scheduling problems.

Ierapetritou and Floudas (1998) proposed a novel continuous-time formulation for the short-term scheduling of batch plants. The proposed formulation results in an MILP problem that is smaller in size both in terms of continuous variables and constraints but primarily in terms of binary variables. The novel elements of the proposed formulation compared to previous approaches

are (i) the decoupling of the unit events from the task events, which also results in small integrality gaps, (ii) the time sequencing constraints, and (iii) its linearity. The STN representation provides information to reduce the number of constraints and with the resulting formulation better objective values can be easily accomplished, since the models are easier to solve to optimality, in significantly less CPU time.

## 2.6.2 Heuristic Solution Methods

The heuristic approaches can be sub-divided in four families (Applequist *et al.*, 1997):

- Rule-based methods, which provide solutions based on experience and empirical observations.
- Constraint-guided heuristics, where schedules are found that satisfy the problem constraints, such as due dates, production levels, etc.
- Randomized searches, such as simulated annealing and genetic algorithms, where the solution is repeatedly changed at random and favorable changes are kept.
- Simulation-based approaches, where each trial simulation of a schedule is evaluated and then rejected, modified or accepted.

### 2.6.2.1 Rule-based Approaches

An extensive review of intelligent systems in process engineering was presented by Stephanopoulos and Han (1996). The use of rule-based intelligent systems in scheduling and planning problems was discussed among others. Kuriyan and Reklaitis (1989) addressed the problem of the minimization of makespan for the network flowshop scheduling problem. They proposed decomposing the problem into two components: sequence generation and sequence evaluation. They analyzed various sequencing algorithms, such as local-search procedures, best-fit heuristic sequencing and bottleneck-sequencing. Several dispatching rules were examined, such as longest processing time first or shortest processing time first. A simple list-scheduling strategy is used in the sequence evaluation procedure to determine unit assignments.

Kudva *et al.* (1994) presented a heuristic algorithm for the scheduling of batch or semicontinuous multiproduct plants. They used rules that take into consideration the priority of the orders. They addressed problems involving multiple identical units for each stage, intermediate product draw-offs, raw-material feeds to any stage, finite intermediate storage inserted between all stages, and order-deadlines.

Kim and Lee (1997) proposed a rule-based reactive rescheduling system for multipurpose batch plants, in order to cope with unexpected process events,

such as sudden changes of ordered set of products, preemptive valuable products and process faults or emergency situations. The developed method consists of an on-line monitoring module that continuously monitors the production status for deviations in the scheduled starting and ending times of a processing task. Once a deviation from the initial schedule is detected, a delay index, used to measure the effects of the unexpected events on the remaining scheduled operations, is calculated. Evaluation of the delay index helps to determine whether the rescheduling module must be activated. The rescheduling module determines next the appropriate actions to minimize the effect of the deviation on the remaining initial schedule by selecting several heuristic dispatching rules. There are three categories of rules used, rules of simple shifting for some tasks, rules for re-allocation and rules for re-sequencing.

Rules are easy to use, but do not guarantee optimal solutions. Therefore, rule-based approaches are usually employed in connection with a different methodology, such as constraint-guided searches.

#### 2.6.2.2 Constraint-guided Approaches

Steffen and Greene (1986) described a heuristic approach to developing scheduling systems for a multipurpose batch plant consisting of parallel processing units. They adopted a hierarchical approach, derived from research in artificial intelligence (AI), where all the objectives are set as constraints. The constraints consider incompatibilities between products placing limitations on the product sequences of a given processor, product to processor preferences, material and labor limitations and desired safety stock in the product storage. The total set of constraints then defines the set of feasible schedules, which is rated by heuristics. For each level of the hierarchy, namely production planning, loading and sequencing, a sub-set of the problem constraints actually apply, and create a search space. If the problem becomes overly constrained, constraints are heuristically relaxed. The limitation of the approach is that any new requirements need to be added in the form of constraints. The authors expressed as a major limitation the increase of the execution time following as a consequence with the addition of new constraints for evaluation.

Goldman and Boddy (1997) developed a constraint-based scheduler, the Honeywell Batch Scheduler. This scheduler uses a scheduling technique called constraint envelope scheduling, which employs a partial order representation of schedules. The scheduler draws on a number of databases, such as orders database, recipes database and plant database, in order to generate a schedule. Advanced search techniques are used to rapidly find answers to scheduling problems, using the batch domain model of the scheduler and a constraint engine to check solutions for consistency. If no answer is possible, then the scheduler identifies the constraints that must be relaxed.

Das *et al.* (1998) investigated a simple but typical batch production scheduling problem for a multipurpose multistage batch plant. They used the commer-



cially available ILOG scheduler software package, where the two major resource constraints of the considered problem, the equipment items and the feed material constraints, were considered. The ILOG system defined scheduling rule was used to provide the event based constrained logic programming solutions. The provided solutions are not optimized, as for example some equipment items might remain idle during a cycle. However, no mathematical model is required, and the solutions can be generated within very modest computation time, but require considerable preprocessing of the input data.

Huang and Chung (2000) proposed a general constraint model to solve scheduling problem for pipeless batch plants, in order to meet consumer demands by generating feasible production schedules. A general constraint model based on constraint satisfaction techniques (CST) is presented. In this model, constraints on resource allocation, activity precedence, time bound and safety issues are considered. The search algorithm used in the scheduling system was also presented, as well as the computer system, BPS (Batch Processing Scheduler), which was used to solve the scheduling problem. CST does not require an elaborate mathematical model, only the problem to be stated in terms of its constraints. The main advantage of CST is that rather than searching the entire space for a solution, it exploits the constraints themselves to reduce the search space.

### 2.6.2.3 Randomized search Approaches

Simulated annealing (SA) is a randomized search procedure for optimization that provides asymptotically optimal solutions to combinatorial optimization problems, but can actually find good suboptimal solutions with reasonable computational effort. Ku and Karimi (1991) developed a simulated annealing method for solving scheduling problems for the serial multiproduct batch process with unlimited intermediate storage. The goal was to determine a production sequence for a given set of products so as to minimize the total production time. The Metropolis SA algorithm was compared with the best heuristic method, the Idle Matrix Search (IMS), and two so-called control algorithms, one with random sequences and the other with uphill moves. Results showed that for different size problems, SA almost always gives the best solution, and in other cases, it gives nearly the best solution. Its only drawback is the large computational effort required, but the simplicity of the algorithm and the near-optimal nature of its solutions far outweigh this drawback.

Tandon *et al.* (1995) used a simulation annealing method for the solution of the problem of scheduling multiple products with the objective of minimizing tardiness. The batch plant considered consists of numerous serial stages with unrelated parallel units at each stage. In the implementation of the SA, sequence-dependent clean-up times, varying processing rates for different products on different units, and constraints on feasible product-to-unit assignments are considered. The solutions obtained are compared with solutions obtained by the heuristic improvement method (HIM), (Musier and Evans, 1989), for

similar computational effort, and solutions obtained by a list scheduling algorithm. The SA method is found superior in all cases, except for small problems of product dependent unit dependent (PDUD) networks.

Raaymakers and Hoogeveen (2000) proposed a simulated annealing algorithm for the scheduling of multipurpose batch process industries with no-wait restrictions and overlapping operations present. They characterized these problems as multiprocessor, no-wait job shop scheduling problems with overlapping operations. The SA algorithm proposed obtained near-optimal solutions with respect to makespan. It was shown that the no-wait restrictions require several adaptations of the neighborhood structure used by simulated annealing. In particular, a procedure was required that ensured feasibility of the schedule after each move. The performance of the algorithm was evaluated against several simple heuristic dispatching rules. SA consistently gave better results within acceptable computation time.

A genetic algorithm (GA) is a heuristic search which maintains a population of many different solutions of a problem. The heuristic solution is reached by improving the overall quality of the population by combination or random crossover over several generations until a stopping criterion is met. Jain and ElMaraghy (1994) proposed a new approach based on genetic algorithms for the scheduling of multiproduct multi-machine flexible manufacturing systems (FMS). They used a set of six different dispatching rules, such as shortest imminent task processing time (SI) or first come first served (FCFS), and three different performance measures, such as mean flow time or average machine utilization. Based on these dispatching rules and performance measures, the GA determined the best routing to be used. Additionally, six different batch splitting policies were considered for splitting batches based on the process plan of the various parts, which provided the demand, machine requirement and the processing times. The best dispatching rule varied according to the performance measure used, but the results showed that the proposed batch-splitting policies improve the performance of the manufacturing system.

Cheng *et al.* (1996) discussed various encoding techniques for the genetic algorithms used to solve the job-shop scheduling problem (JSP). Nine representation schemes for the job-shop scheduling problem are examined and classified into two basic encoding approaches, the direct and the indirect approach. An example of the direct approach is the operation-based representation, while priority rule-based representation is an example of the indirect approach. A technique for repairing an illegal chromosome to a legal one is also mentioned, the partially mapped crossover (PMX) operator, which can produce a representation of a feasible schedule from an infeasible offspring.

Jung *et al.* (1998) developed a genetic algorithm for effectively solving large-size scheduling problems for multiproduct batch processes. The objective was the minimization of makespan and different intermediate storage policies (UIS and ZW) were examined to test the performance of the GA. The reproduction operator for the GA was based on a decimal string and a sigmoid fitness func-

tion, while for the crossover operator, PMX and order crossover (OX) operators were used in turn. The results obtained were compared to those of Rapid Access Extensive Search (RAES) and SA. GA was found superior for both small and large-size problems and for both storage policies examined.

Shaw *et al.* (1999) formulated multiobjective genetic algorithms (MOGAs) to allow individual treatment of several objectives simultaneously, and by doing so they extended the standard evolutionary-based genetic algorithm optimization technique. In their work, four MOGAs were implemented to solve a process scheduling optimization problem; a two and a five objective MOGA with two different schedule building rules used for each of them. The first schedule builder uses a rule of choosing the fastest unit to complete the task, while the second schedule builder chooses the first suitable unit that is free for the job. The MOGA can be used as a method of handling the infeasibility constraint and it can also provide the insight to the user to optimize several conflicting objectives. So, one could allow some infeasibility for one objective, if better results could be obtained for the other objectives.

#### 2.6.2.4 Simulation-based Approaches

Simulation-based approaches to scheduling use a discrete simulation model of the application as a surrogate to the system being scheduled. These approaches often use scheduling rules or heuristics to drive the execution of a simulation model forward to meet scheduling goals. The design of a dynamic simulator for batch oriented processes, the Batch Operations Simulation System BOSS, was presented by Joglekar and Reklaitis (1984). The modular system described allows incorporation of dynamic models of individual processing steps and has the possibility of accommodating multiple product processing routes. Processing discontinuities in the time history of the system is taken into account and a key feature of the simulator is the use of logic when assigning dynamic routes and equipments that can be affected for example by equipment availability. The necessary input data for the simulator are the following: the process topology, the fixed equipment parameters, the product task sequence and recipes, the process routing information, the production schedule and the initial condition of the plant.

Bernstein *et al.* (1992) described an interactive simulation-based decision support system for a multipurpose batch plant. The system can be used both in an offline mode, for evaluation of master production schedules and long-term capacity planning and debottlenecking studies, and in an online mode, for short-term planning, scheduling, and decision-making. The difficult aspect of scheduling intermediates (when is there sufficient equipment to start processing an intermediate?) was tackled by keeping track and assessing the status of all batches in the process. The updated process information from the plant was collected from a link to the plant's distributed control system. Moreover, the menu-driven format of the interface with the user allows running simulations and provides interpretations of the results in an easy-to-understand format,

even for users with limited knowledge of the simulation model.

Goodall and Roy (1996) developed a hybrid system to develop good production schedules, called the batch process scheduler (BPS), using techniques from the areas of artificial intelligence and discrete event simulation (DES). The authors attempted to account for all the inherent constraints in the plant and overcome usual simplifying assumptions that have to do with the piping network and the arrangement of the valves which control the routing of a product. The dynamic connectivity constraint on the availability of plant items to actually make a connection with another item was addressed. They introduced an AND/OR plant item structure, and used the simulation module to provide an updated input to the control module which determines the activities to schedule.

The abbreviations that have been used in this chapter together with their corresponding explanations are gathered in table 2.1.

## 2.7 Concluding remarks

The batch process synthesis problem is usually assumed as solved when the planning and scheduling problems are considered (Rippin, 1983b). It is assumed that the sequence and the nature of the process tasks for each product have been fixed. In all the reviewed literature for scheduling and planning, whether the scheduling approach was exact or heuristic, the identity and sequence of operations (tasks) for a given product were given. The batch route was always known in advance and it was only the assignment of the tasks to the equipment units and the batch sizes that needed to be determined. Furthermore, the processing time of each equipment was assumed given for the scheduling problem. The processing time, which is the sum of at least the charging time, the operating and the discharging time, might vary because of the batch size or the equipment size. However, it is always assumed to be known for each equipment unit and product in most scheduling problems.

On the subject of batch control, various methods have been suggested for the rejection of disturbances and minimization of the deviation from the batch operations model. However, even when on-line optimization is performed, the initial batch operations model need to be available in advance, in a form of setpoint trajectories.

In regard to the individual equipment unit (task) optimization, a lot of work has been presented based on rigorous models and requiring significant computational effort and skills to solve the optimal batch operations problem. For batch reaction, in many cases the final processing time was fixed, and insights provided from the reaction kinetics was not exploited to the full extent. For batch distillation, several investigators worked with quasi-steady state, short-cut or dynamic models in order to find the optimal reflux policy. However, the solutions required an initial value for the reflux ratio vector and the models assumed constant relative volatility. But most importantly, the sequence of

Abbreviation	Explanation
AI	Artificial Intelligence
BH	Bayesian Heuristic
BOSS	Batch Operations Simulation System
BPS	Batch Process Scheduler
CST	Constraint Satisfaction Techniques
DAEs	Differential and Algebraic Equations
DES	Discrete Event Simulation
FCFS	First Come First Served
FIS	Finite Intermediate Storage
FMS	Flexible Manufacturing Systems
GA	Genetic Algorithm
HIM	Heuristic Improvement Method
IDP	Iterative Dynamic Programming
ILC	Iterative Learning Control
IMS	Idle Matrix Search
JSP	Job-shop Scheduling Problem
LCA	Life Cycle Analysis
LP	Linear Programs
LTI	Linear Time-Invariant
MEI	Minimum Environmental Impact
MINLP	Mixed Integer Non Linear Programs
MILP	Mixed Integer Linear Programs
MIS	Mixed Intermediate Storage
MOGA	MultiObjective Genetic Algorithm
MPC	Model Predictive Control
NCO	Necessary Conditions of Optimality
NIS	No Intermediate Storage
NLP	Non-Linear Programming
NP	Non-deterministic Polynomial time
OX	Order crossover operator
PMX	Partially Mapped crossover operator
RAES	Rapid Access Extensive Search
SA	Simulated Annealing
SI	Shortest Imminent processing time
STN	State-Task Network
SQP	Successive Quadratic Programming
NUCM	Non-Uniform Continuous time Modelling
MIBLP	Mixed Integer BiLinear Program
UDM	Uniform time Discretization Model
UIS	Unlimited Intermediate Storage
ZW	Zero Wait

Table 2.1: Abbreviations used in chapter 2 and their corresponding explanations

attainable products (main or cut-offs) was given *a priori* and the number of control intervals for each product was also determined in advance. For batch crystallization, work appeared for the operation on the invariant points, where the risk for cocrystallization of solids is high and therefore separation is infeasible. Recycle was considered, but the composition of the recycle stream was assumed to be known from the beginning and with recycle the maximum yield for a given feed is not realized. Additionally, no systematic procedure for specifying the operating temperatures was provided and the feasibility of the precipitation for a given salt was not checked.

As for the problem of synthesis of batch processes, several papers have used the term, but haven't addressed the actual problem. Their work is really that of the design of a batch processing plant. Recycle was considered in many cases, and the plant was in a periodic steady state for which the batch sizes and equipment unit sizes were determined, in order to maximize profit. However, interesting work appeared on the possibility of merging tasks in one unit, (Birewar and Grossmann, 1990), (Iribarren *et al.*, 1994). Allgor *et al.* (1996) opened the discussion for the optimal design of a batch processes plant where insights from the processing models can be used to investigate the effect of the operating policy of one task to the downstream tasks.

## 2.8 Thesis objective

The objective of this thesis is to address the batch process synthesis problem and provide a methodology for identifying the necessary sequence of batch reaction and separation tasks for the conversion of raw materials to purified final products. For the synthesis to be complete, the operation models for each task in the sequence need to be generated. Insights obtained from thermodynamic and process knowledge (kinetic models and phase diagrams) can provide information for efficient and feasible design of the operation, requiring neither the use of complex process models nor significant computational effort or skills.

The interaction between the tasks and the effect on subsequent tasks or the requirements on the previous tasks for a final task to achieve all product (end) objectives need to be addressed at the synthesis level. The feasibility of achieving the intermediate objectives for each task in the sequence needs to be addressed at the batch operations model generation level. It is also necessary to point out the connection between these two levels for the successful synthesis of batch processes for achieving all objectives in a feasible, near optimal way.

The remaining part of this thesis is structured in the following way: in the next chapter the entire methodology for the synthesis of batch processes as well as for the generation of the batch operations model for batch reaction and separation is provided in the form of four rule-based algorithms operating at two levels; the necessary computational tools for the application and verification of

these algorithms are described afterwards; subsequently, several case studies illustrate the various developed algorithms; and finally, conclusions and future work are considered in the last chapter of the thesis.

# METHODOLOGY

## 3.1 Introduction

The synthesis of batch processes entails the identification of the necessary tasks and their sequence, in order for a specified product to be obtained. This sequence is alternatively called a batch route or production path. Batch processes can be described in terms of the task, whether it is mixing, reaction, separation or any combination of the above. However, in order to be able to fully characterize the tasks, it is necessary to define them in terms of sub-tasks, such as heating, cooling, charging and so on. It is also essential to identify the impact of the individual sub-task on the total task. This is done in many cases, by identifying the relationship between properties and operational principles, which also help to define the different sub-tasks and their end. The feasibility of an operational sequence is defined through state variables or supplementary variables that do not violate the constraints that are imposed on them. However, the objective for the optimum synthesis of batch processes is to minimize the operating time and/or operating costs. As there is a trade off between these two objectives, ultimately an optimization problem would have to be formulated and solved, where appropriate weights can be given to time and operating costs.

In this chapter, the developed framework for the solution of the synthesis problem is presented. This Ph.D. work was focused in generating feasible solutions, but since thermodynamic insights were employed to produce these solutions, it can be argued how close these solutions are to optimality. The methodology for the solution of the synthesis problem is illustrated in figure 3.1, where the two levels of the methodology and the algorithms of each level are shown. At the higher level 1, the synthesis algorithm generates the batch route. Once the tasks are identified, the rule-based algorithms for batch reaction and separation provide the batch operations model for each task, at the lower level 2. The batch operations model is the sequence of sub-tasks necessary to achieve the end objectives of the respective reaction or separation task, which is equivalent in effect to an operating profile. The sub-tasks are defined, in this thesis, as operations where the manipulated variables remain constant for the sub-task duration, let that variable be temperature, heating/cooling rate, reflux ratio, etc.



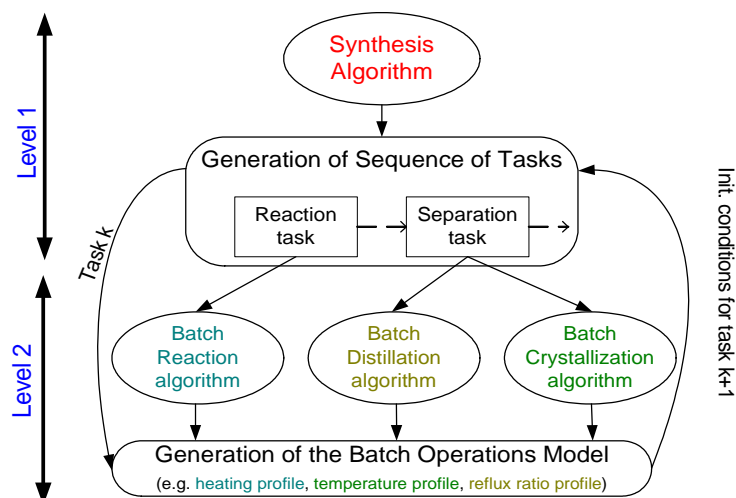


Figure 3.1: Block diagram of the methodology for the synthesis of batch processes as well as the generation of the batch operations model for each task

The two levels of the methodology are connected with each other, in the sense that the output of the one serves as the input of the other. The synthesis algorithm generates an initial estimate of the intermediate objectives for each task. The lower level algorithms are invoked and their outcome is returned to the higher level synthesis algorithm providing the current state of the mixture through the production path and allowing more detailed calculations to be made from the synthesis algorithm. Due to the interconnection between the two methodology levels, the lower level batch reaction and separation algorithms are presented first and the synthesis algorithm which integrates them is presented last.

In four sections, the equal in number developed algorithms are presented in the following order: batch reaction (one and two phases), batch distillation, batch crystallization and synthesis algorithm. Before each algorithm is presented, a subsection containing the necessary background theory for the development of the algorithm is included. The algorithms are then introduced, where any developed theory is presented first, the formulated set of rules comes next and finally the actual step-by-step description of the algorithm is supplied.

## 3.2 Task: Batch Reaction

### 3.2.1 Introduction

Batch reactors are easy to use and suitable for the production of low-volume and high-value-added specialty chemicals, fine chemicals, polymers, pharma-

ceuticals and biochemicals (Rippin, 1983a). The reactions usually take place in the liquid phase. Batch reactors consist of a closed vessel, a stirring system and some temperature control system such as an external jacket and/or internal coil for the heating/cooling of the reactant mixture. They are dynamic, which means that the concentrations of the reactants-products and/or the temperature of the reactor change with time.

The theoretical background necessary for the algorithms for the generation of the batch operations model for a batch reactor is provided, while required extensions and new definitions are presented next. The developed set of rules for the one-phase and the two-phase algorithms and their stepwise description follow.

### 3.2.2 Theoretical background

A complete operational cycle of a well mixed batch reactor consists of the following five stages:

1. Charging of the reactants: charging time  $t_i$
2. Occurrence of the chemical reaction(s): reaction time  $t_f$
3. Removal of the reactant mixture: discharging time  $t_o$
4. Cleaning and preparation of the reactor: preparation time  $t_p$
5. Non productive period: dead time  $t_d$

The total time for a complete operational cycle for a batch reactor is equal to:

$$t_t = t_i + t_f + t_o + t_p + t_d \quad (3.1)$$

It is noted that the only time that is connected to the chemical operation is the reaction time  $t_f$ . All the other times depend on the physical design characteristics of the reactor (e.g. reactor volume, pump flows) and are therefore predefined. In this thesis, the operation of the reactor during the time of reaction  $t_f$  is the main interest.

As a result of mixing, the concentrations of the reactants-products and the temperature are independent of the position inside the reactor. Finally, the reactor can be operated either isothermally or non isothermally.

The design equations for the operation of batch reactors isothermally and non isothermally for the case of multiple reactions are given in the following section.

#### General Batch Reactor Design Equations

The general dynamic mass balance (Aris, 1969) that gives the rate of change of the holdup of component  $c$  in a batch reactor, where  $R$  independent reactions take place is:

$$\frac{dN_c}{dt} = V \sum_{j=1}^R \nu_{jc}(r)_j ; i = 1, 2, \dots, N \quad (3.2)$$

where  $V$  is the volume of the reactant mixture,  $N_c$  is the number of moles of component  $c$ ,  $\nu_{jc}$  is the stoichiometric coefficient of component  $c$  that takes part in reaction  $j$  and  $(r)_j$  is the intensive rate of reaction  $j$  independent of component  $c$ . The expression for the intensive rate of reaction  $j$  that is independent of component  $c$  has to do with whether the reaction is reversible or not, and with the reaction order.

Additionally, for non isothermal operation of the batch reactor, the energy balance for the case when perfect mixing is valid is given by:

$$\left( \sum_{c=1}^N N_c C_{pc} \right) \frac{dT}{dt} = -V \sum_{j=1}^R (\Delta H_{rT})_j (r)_j + Q - W \quad (3.3)$$

where  $N_c$  and  $C_{pc}$  are the number of moles and the liquid heat capacity (in  $KJ/kmol.K$ ) of component  $c$ , respectively,  $V$  is the volume of the reactant mixture,  $(\Delta H_{rT})_j$  is the heat of reaction for reaction  $j$ ,  $Q$  is the rate of heat transfer from/to the system and  $W$  is the mechanical work ( $kJ/s$ ) due to mixing.

Note:  $(\Delta H_{rT})_j$  is negative for exothermic reactions and positive for endothermic reactions.

In this thesis, it is assumed that the mechanical work  $W$  due to mixing is negligible and hence equal to zero.

#### Isothermal operation

For the isothermal operation of the batch reactor,

$$\frac{dT}{dt} = 0 \quad (3.4)$$

and the differential equation 3.3 becomes algebraic.

#### Adiabatic operation

For the adiabatic operation of the batch reactor, the transfer rate of the heat to or from the system is  $Q = 0$ .

### **Yield and Selectivity**

In systems with multiple reactions, the reactants are converted to desired products and partially to unwanted byproducts. Consequently, the obtained amount of the desired product is generally smaller than what would be achieved if the reactants were exclusively converted to the desired product. Two variables that are often used for the analysis of multiple reactions are yield and selectivity.

If  $D$  represents one desired product and  $A$  is the main limiting reactant, then the total relative yield  $Y_{DA}$  of product  $D$  is defined as:

$$Y_{DA} = \frac{\text{moles of A converted to D}}{\text{total moles of A consumed}} \quad (3.5)$$

The total functional yield  $Y'_{DA}$  is defined according to the original amount of  $A$  charged in the batch reactor.

$$\text{Total Yield } Y'_{DA} = \frac{\text{moles of A converted to D}}{\text{total moles of A charged}} \quad (3.6)$$

Another variable often used in the analysis of multiple reactions is the selectivity of a desired reaction. Selectivity  $S_{DU}$  is defined as:

$$\text{Selectivity } S_{DU} = \frac{\text{moles of A converted to D}}{\text{moles of A converted to U}} \quad (3.7)$$

where  $D$  represents the desired product and  $U$  the byproduct.

For a batch reactor, the instantaneous yield and selectivity are described according to the rates of production and consumption of the reactants in the chemical system.

### 3.2.3 Batch Reaction Algorithm

The algorithms developed for the operational design of a batch reactor are rule based algorithms. The algorithms provide the model of the operation in the form of a sequence of sub-tasks. The formulated rules based on thermodynamic and process insights are used, in order to recognize the end of a sub-task due to a forthcoming violation of a constraint. The rules are also employed to identify the next sub-task in the sequence that will prevent the corresponding violation.

There are two problems to be investigated where in both cases the objective is to obtain the specified product(s) in a feasible manner at minimum time and/or cost. In the first problem the set of reactions take place in the liquid phase, which is the only phase in the system, while in the second problem a vapour phase is also present. In both problems there are certain specified operational limitations (constraints) on temperature and in the second case also on pressure. These lower and upper limits for the operating conditions can be due to process design, safety risk and chemical reaction hazard (e.g. temperature where run away reaction occurs or product quality is adversely affected, e.g. a gel is formed).

In both problems, the specified product(s) can be obtained once a number of end objectives are met, which are related to the product(s). There are two end (product) objectives for the reaction task investigated in this thesis, namely a specified molefraction of the limiting reactant in the reaction of interest (the aim is to be as low as possible, e.g. close to zero) and the yield of the desired product(s) (the aim is to be as high as possible). It is satisfactory if either of the end objectives is reached, while remaining feasible during the whole reaction task.

### 3.2.3.1 Further on Selectivity

As mentioned earlier, in multiple reactions systems, there are reactions that yield either one of the products or intermediate compounds, which react further to produce the final product(s). On the other hand, there are also reactions that either consume valuable reactants and/or produce unwanted byproducts. Therefore, the question of desired reactions or reactions of interest arises, as expressed in one of the end objectives.

The simple existence of desired and competing (undesired) reactions is what makes selectivity and an imposed constraint important. An extension to the earlier description of instantaneous selectivity is given below:

*Selectivity  $S_{ij}$  of reaction  $i$  over competing reaction  $j$  ( $i \neq j$ ) within a time interval is defined as the ratio between the reaction rate of reaction  $i$  to reaction rate of reaction  $j$ .*

$$\text{Selectivity } S_{ij} = \frac{\text{reaction rate of desired reaction}}{\text{reaction rate of competing/unwanted reaction}} \quad (3.8)$$

When the selectivity is described as the selectivity of one reaction over another, then it can also cover the cases when the competing reaction is one where its limiting reactant is different from the limiting reactant for the desired reaction. For example, the competing reaction could be a reaction where the desired product further reacts to form a byproduct. Such a reaction is unwanted and should be suppressed, since it jeopardizes the yield of the desired product.

A selectivity value equal to unity means that the reaction rate of the desired reaction is equal to that of the unwanted reaction. Obviously, the objective is to have the desired reaction promoted as much as possible and to limit the extent of the unwanted reaction. This means that the selectivity should be greater than unity and preferably at a high value. This is the reason why a constraint imposed on selectivity is important.

Thus, one of the goals for the reaction task is to keep the selectivity as high as possible or at least above a constraint at all times, until the product objectives are reached. In this way, the reactions are driven in a way that favour the reaction(s) of interest and suppress the competing and unwanted reactions. Keeping the selectivity high ensures that undesired formation of byproducts is limited. In that way the molefraction of the desired product in the outflow of the reactor is as high as possible. Furthermore, by making sure that the percentage of the reactant that is converted to desired product instead of undesired byproduct is the highest, the yield of the desired products is maximized.

Selectivity can also be used as a comparison criterion, in order to identify the first operation in a sequence of sub-tasks. This can be done by comparing different operations (such as adiabatic or isothermal operations) in terms of the total selectivity of the desired reaction over the competing/unwanted reaction,

at a specific point in time  $t$ . The comparison criterion of selectivity  $S_{function}$  is defined in the following equation:

$$S_{function} = \frac{\frac{\text{moles of desired product (at } t\text{)}}{\text{product's stoichiometric coefficient}}}{\frac{\text{moles of byproduct (at } t\text{)}}{\text{byproduct's stoichiometric coefficient}}} \quad (3.9)$$

Obviously, the operation that has the highest value of  $S_{function}$  should be chosen as the starting point.

Furthermore, the selectivity can also be used to identify the end of an operation. By estimating the effect of the current operation on the development of selectivity and its final value at the end of the reaction task, one can take action if the present operation does not drive selectivity to sufficiently high values. Calculating the instantaneous change of selectivity, one can also estimate the projection of selectivity at a specific point, namely when the end objective is reached.

The change of selectivity over time or versus the molefraction of the limiting reactant in the respective desired reaction can be documented. The variation over the corresponding molefraction is more useful than that over time, since one knows the desired molefraction at the end of the reaction task (given end objective). The selectivity tangent with respect to the molefraction  $x^{reac}$  of the limiting reactant of the reaction of main interest is given in the next equation.

$$\frac{\Delta S}{\Delta x^{reac}} = \frac{S_{current} - S_{previous}}{x_{current} - x_{previous}} = s_x \quad (3.10)$$

where the subscripts *current* and *previous* refer to the latest and the previous points of calculation. Since the desired end molefraction  $x_{end}$  is known, the end selectivity  $S'_{end}$  can be approximated at every interval.

$$S'_{end} = S_{current} + s_x(x_{end} - x_{current}) \quad (3.11)$$

where  $S_{current}$  and  $x_{current}$  refer to the corresponding variables at the end of each interval.

Using equations 3.10 and 3.11, one can estimate the direction that selectivity is going. If the selectivity tangent has the wrong sign and is too steep, then there is a risk that the end selectivity, as it is approximated, is below the selectivity constraint. This is also a sign that the current operation mode does not promote selectivity and therefore its end should be identified.

### 3.2.3.2 Promoting Selectivity of the Desired Reaction over the Unwanted Reaction

As stated earlier, identifying a future violation of the selectivity constraint can be used to end an operation that does not favour the corresponding selectivity. However, what is most important is to determine an operation that will promote the selectivity of the desired reaction over the competing/unwanted reaction.

It is important to make a distinction between irreversible and reversible reactions, when a decision for the promotion of those reactions needs to be taken. For the case of irreversible reactions, it is easy to prove that the ratio of the activation energy of the desired reaction to the activation energy of the competing/unwanted reaction can solely determine the operation that promotes selectivity.

As shown and proven in appendix A, if the activation energy ratio of the desired reaction over the competing reaction is larger than unity ( $\frac{E_a^1}{E_a^2} > 1$ ), then *heating* promotes selectivity  $S_{12}$ . This means that selectivity  $S_{12}$  at a higher temperature  $T_2$  is greater than the selectivity at the lower temperature  $T_1$ . On the other hand, if the activation energy ratio of the desired reaction over the competing reaction is smaller than unity ( $\frac{E_a^1}{E_a^2} < 1$ ), then *cooling* will promote the desired selectivity.

For the case of reversible reactions, comparing the heat of reaction for the set of reactions taking place, the terms endothermic, exothermic and the relative terms more/less endothermic and more/less exothermic can be used to describe the reactions. In order to make easier that comparison, a new variable (relative enthalpy measure for a reaction set)  $\epsilon^r$  is introduced to describe the extent of the enthalpy change in a reaction, in relation to the rest of the reactions. The value of this variable for each reaction is given according to how much exothermic or endothermic it is.

This indicator variable is positive for endothermic reactions and has a negative value for exothermic reactions. In that way, the least endothermic reaction will have a value of  $\epsilon^r$  equal to +1. In similar manner, the least exothermic reaction will have a value of  $\epsilon^r$  equal to -1. If there are three endothermic reactions, for the most endothermic  $\epsilon^r = +3$  while the intermediate one will have a value of  $\epsilon^r = +2$ . Likewise, for the exothermic reactions.

For a set of reactions, characterizing each reaction by  $\epsilon^r$  and ordering them in decreasing order arranges the reactions from the most endothermic to the most exothermic one. This indicator variable can be used to determine what is thermodynamically favourable for the promotion of a desired reversible reaction, in some occasions. As shown in appendix A, if the desired reaction is endothermic  $\epsilon_1^r > 0$  and the competing reaction is exothermic  $\epsilon_2^r < 0$ , then *heating* promotes selectivity  $S_{12}$ . On the other hand, if the desired reaction is exothermic  $\epsilon_1^r < 0$  and its competing reaction is endothermic  $\epsilon_2^r > 0$ , then *cooling* promotes selectivity  $S_{12}$ .

So, as long as the  $\epsilon^r$  values of two competing reactions [[have]] different sign, one can easily conclude whether heating or cooling will promote the desired reaction. However, when either both competing reactions are exothermic or both of them are endothermic ( $\epsilon^r$  values of the same sign), no definite decision can be made before the equilibrium constants of the reactions are calculated and the extent of reactions are determined (Appendix A).

For reversible reactions, the discussion on their selectivity is based on the assumption that equilibrium is reached. Certainly, the time needed to reach

equilibrium depends on the reaction kinetics and could differ significantly for the desired and the competing reaction. However, it is more interesting to determine what promotes selectivity when the time needed to reach equilibrium for the competing reactions is comparable.

### 3.2.3.3 Definitions

A set of definitions is given in this section that is used later in this thesis in the algorithm for the operational design of a batch reactor.

- The point in time in a specific sub-task  $i$  when the approximate predicted value of selectivity  $S'_{end}$  is below the selectivity constraint  $S_{min}$  is set as  $t_{stop,S}$ .
- The point in time in a specific sub-task  $i$  when the end objective of the yield of the desired product is satisfied is set as  $t_{yield}$  and can be the end of the reaction task.
- The point in time in a specific sub-task  $i$  when the end objective of the molefraction of the limiting reactant in the desired reaction is reached and no constraint is violated is set as  $t_{x^{reac}}$  and is the end of the reaction task.
- The point in time within a specific sub-task  $i$  where the temperature in the reactor is equal to  $(T_{up} - T_{slack})$  is set as  $t_{stop,T_{up}}$ .
- The point in time within a specific sub-task  $i$  where the temperature in the reactor is equal to  $(T_{low} + T_{slack})$  is set as  $t_{stop,T_{low}}$ .
- The point in time within a specific sub-task  $i$  where the pressure in the reactor is equal to  $(P_{up} - P_{slack})$  is set as  $t_{stop,P_{up}}$ .
- The point in time within a specific sub-task  $i$  where the pressure in the reactor is equal to  $(P_{low} + P_{slack})$  is set as  $t_{stop,P_{low}}$ .

### Slack Variables

Shifting from one batch operation (sub-task) to another, because of the violation of a constraint, might be infeasible unless slack variables are introduced. In most cases when a set of reactions take place, the overall enthalpy change is either exothermic or endothermic. The existence of an overall heat effect that is either released or absorbed makes it impossible to run a batch reactor to the specified upper or lower limits of the operating conditions and expect to stay on (and not violate) those limits, especially when the response of the system to changes might be slow.

Specifically, when the overall reaction heat effect is exothermic and the upper temperature limit is reached, then even if cooling is applied to keep the



temperature constant or decrease it, a temperature overshoot will take place. Similarly, when the upper limit of the pressure is reached, then even if cooling or vapour release is applied, the response to the change takes time and pressure exceeds the limit. In this way the switch from the previous operation, whether that is adiabatic operation or heating, will be infeasible.

On the other hand, when the overall reaction heat effect is endothermic and this time the lower temperature limit is hit, then a temperature undershoot will occur, even if heating is applied to keep the temperature constant or increase it. Similarly, when the lower limit of the pressure is hit, then even application of heating or avoiding the removal of vapour might not be sufficient and since the response to the operation mode change takes time, pressure will cross over the limit. In this way a feasible switch from the previous operation, whether that is adiabatic operation or cooling, will not be possible.

Thus, the introduction of slack variables to keep away from the upper and lower limits of the operating conditions is necessary. Particularly, when the overall reaction heat effect is exothermic and the shift happens from an operation of heating to adiabatic, cooling or isothermal operation specifically at  $T_{up}$  then a  $T_{slack}$  equal to 1-2 °C should be used. In the same shift, but with the overall reaction enthalpy change being endothermic, a smaller  $T_{slack}$  up to 1 °C should be used. Similarly for pressure where for exothermic reactions  $P_{slack}$  should be up to 0.1atm, while for endothermic reactions it should be up to 0.05atm. When the change occurs between a sub-task of cooling to an adiabatic, heating or isothermal operation sub-task specifically at  $T_{low}$  where the overall reaction enthalpy change is endothermic, then a bigger  $T_{slack}$  equal to 1-2 °C should be used. If the reactions are exothermic, a smaller  $T_{slack}$  up to 1 °C should be used. Similarly, for endothermic reactions  $P_{slack}$  should be up to 0.1atm, while for exothermic reactions it should be up to 0.05atm, respectively. The specific slack values will however depend upon the actual reaction enthalpy and reactor design.

The set of rules for the one-phase and the two-phase algorithms is formulated in the following subsection. The rules identify the necessary sub-tasks and their ends as well as the subsequent sub-tasks until the product objectives are met. The step-by-step descriptions of the two algorithms are presented last.

### 3.2.3.4 Batch Reaction Algorithm Set of Rules

The developed algorithm provides an operational model for a batch reactor. The operational model is given in the form of a sequence of sub-tasks. The sub-tasks considered are isothermal and adiabatic operation, heating and cooling with reaction taking place and also heating and cooling without any reaction occurring. The first sub-task in the sequence is decided according to rule A1.1.

#### Rule A1.1: selection of first sub-task

- i. The starting point for the batch reaction, namely the first sub-task ( $i = 1$ ) in the operational sequence, is selected from a set of isothermal and adiabatic operations. The first sub-task is chosen as the one where the selectivity  $S_{function}$  is the highest at a given point in time close to the start of the reaction and where no other operational constraint is violated. This point in time where the comparison is made could be, for example, the point in the time horizon where  $\xi_j \geq 0.00001$  kmol for all reactions  $j$  in the set and for all the operations compared. Alternatively, conversion  $X_j$  could be chosen as a dimensionless variable, where again  $X \geq 0.00001$ .*
- ii. In the case where the selectivity  $S_{function}$  is the same for more than one operation, then the first sub-task is chosen as the one where the reaction rate for the reaction of interest is the largest.*

Selectivity  $S_{function}$  is defined in equation 3.9. The operational constraints that should be obeyed include mainly temperature and pressure bounds and a lower limit for selectivity. The point in time where the comparison is made is such that obviously all competing reactions in the system have started taking place.

The reason why the selectivity  $S_{function}$  should be as high as possible is that in that way the starting point for the selectivity is the most feasible. Trying to have the highest selectivity all the time will accomplish the yield objective for the product, while ensuring a feasible operation.

The end of each operational sub-task is marked by the identification of an imminent violation of one of the process or supplementary constraints. The supplementary constraint used in the algorithm is selectivity or the prediction of selectivity at the time when the end objective for the molefraction of the limiting reactant in the desired reaction is satisfied. The end of each sub-task is determined according to the following rules. Furthermore, the identification of the next sub-task  $i + 1$  is also rule-based supported by thermodynamic or process insights.

**Rule A1.2: sub-task end (selectivity violation)**

*If the predicted selectivity value  $S'_{end}$  is below the lower permitted limit for the selectivity constraint, then the current operational sub-task  $i$  has reached its end and unless one of the end objectives are satisfied the next sub-task needs to be identified.*

In order to be feasible at all times, it is the selectivity at the end of the reaction task ( $S'_{end}$ ) that one should be concerned about and try to make sure to keep above the selectivity constraint. However, since the projected value of selectivity  $S'_{end}$  is a very strict criterion, the satisfaction of an alternative more loose end objective, namely the yield of the desired product, can be what will define the end of the reaction task. The identification or not of another sub-task in the sequence depends on the relation of the actual selectivity at

$t_{yield}$  to the selectivity constraint  $S_{min}$ . That is all explained in the following rule.

**Rule A1.3: identification of final sub-task**

*In the case when  $S'_{end}$  violates the selectivity constraint, but if at time  $t_{yield}$  the actual selectivity does not violate the lower selectivity bound, then the current sub-task is the last in the sequence and at time  $t_{yield}$  the generation of the operational model for the reaction task is completed.*

If on the other hand, both the predicted selectivity value  $S'_{end}$  and the actual selectivity at time  $t_{yield}$  violate the selectivity constraint, then the end of the current sub-task is identified as point  $t_{stop,S}$ , according to rule A1.2. When rule A1.2 is applicable, the succeeding sub-task  $i + 1$  is identified based on the next rules.

**Rule A1.4: subsequent sub-task identification (selectivity violation)**

*In case the selectivity constraint  $S_{min}$  is violated, the subsequent sub-task is identified according to what kinetically and thermodynamically favours the desired reaction.*

- i. For irreversible reactions, if the activation energy ratio of the desired reaction to the unwanted reaction is larger than unity, then adding heat to the system in relation to its current status will promote the desired reaction.*
- ii. For irreversible reactions, if the activation energy ratio of the desired reaction to the unwanted reaction is smaller than unity, then removing heat from the system in relation to its current status will promote the desired reaction.*
- iii. For reversible reactions, if the desired reaction has a positive  $\epsilon^r$  value and the unwanted reaction has a negative  $\epsilon^r$  value, then adding heat to the system in relation to its current status will promote the desired reaction.*
- iv. For reversible reactions, if the desired reaction has a negative  $\epsilon^r$  value and the unwanted reaction has a positive  $\epsilon^r$  value, then removing heat from the system in relation to its current status will promote the desired reaction.*
- v. For reversible reactions, if both the desired reaction and the unwanted reaction have positive (or negative)  $\epsilon^r$  values, then the equilibrium constants and the extent of reactions need to be calculated first before a decision can be taken.*
- vi. If there is more than one competing reaction to the desired reaction, then the comparison is primarily done with the most competing reaction of the two. The criteria to establish the most unwanted reaction are the following: the desired product is consumed, the limiting reactant is converted to byproduct and the reaction rate is high. The most unwanted reaction is the one that features the most of the above criteria. In case all the competing reactions share the same criteria and different operations promote the corresponding selectivities  $S_{1j}$ , then the competing reaction that has the smallest selectivity  $S_{1j}$  is the most*

unwanted, where subscript 1 refers to the desired reaction and  $j$  to its competing reactions.

**Rule A1.5: subsequent sub-task design (selectivity violation)**

*When rules A1.4i and A1.4iii are applicable, then the succeeding sub-task is identified as heating. The amount of heat added is chosen in accordance with the heat capacity for the batch reactor,  $Q_{min} < Q < Q_{max}$ .*

*When rules A1.4ii and A1.4iv are applicable, then the succeeding sub-task is identified as cooling. The amount of heat removed is chosen in accordance with the cooling capacity for the batch reactor,  $Q_{min} < Q < Q_{max}$ .*

When the selectivity constraint is violated and the succeeding sub-task is identified as heating or cooling and the amount of heat added or removed is chosen from a feasible range, then it is obvious that from sub-task  $i + 1$  a set of alternative sequences can be generated. Any amount of heat can be chosen, because the resulting operation is feasible according to the heating/cooling capacity of the reactor. However, there is a trade-off between the operating costs and the operation time for the chosen amount of heat. As a rule, the higher the amount, the higher the operating costs, since more steam or cooling water is used, and the shorter the operation time. Nevertheless, a set of alternative sequences can be generated and a limited search can pinpoint the fastest one, if that is the objective. Alternatively, one can select the sequence with the lowest operating costs, if that is more important. Obviously, the most important objective of the optimization, time or cost, will define the best sequence.

An adjustment to rule A1.5 is needed if the yield of the desired product at the end of sub-task  $i$  is close to the end objective.

**Rule A1.6: subsequent/final sub-task design (selectivity violation)**

*i. If rules A1.4i and A1.4iii apply, then the succeeding sub-task is identified as heating. If additionally the yield of the desired product at the end of sub-task  $i$  is close to the end objective ( $Y'_{DA} - Y_{DA,i} < 10\%$ ), then the heating rate can be chosen as a specific value that ensures the non-violation of the selectivity and the maximum temperature constraint when the end objective of the yield of the desired product is met.*

*ii. If rules A1.4ii and A1.4iv apply, then the succeeding sub-task is identified as cooling. If additionally the yield of the desired product at the end of sub-task  $i$  is close to the end objective ( $Y'_{DA} - Y_{DA,i} < 10\%$ ), then the cooling rate can be chosen as a specific value that ensures the non-violation of the selectivity and the minimum temperature constraint when the end objective of the yield of the desired product is met.*

If the heating/cooling rate suggested according to rule A1.6 is outside the feasible range, then the rule above cannot be applied. On the other hand, one can obviously choose to disregard rule A1.6 from the beginning and select the

heating or cooling rate within the feasible range. In that way, there is the risk that for some of the alternatives generated the operating costs are higher than what is necessary to reach the end objective, but at the same time the end objective is reached faster. It depends on what is more important for the generation of the operating model, time or costs.

Limitations on the operating conditions for the batch reactor can also be used to identify the end of a particular sub-task and the succeeding sub-task, according to the following rules.

**Rule A1.7: sub-task end ( $T_{up}$  violation)**

*When the temperature of the batch reactor  $T$  is about to violate the upper temperature limit  $T_{up}$ , then the end of the current sub-task is identified at point  $t_{stop, T_{up}}$ .*

**Rule A1.8: subsequent sub-task identification ( $T_{up}$  violation)**

*If the upper bound of the operating temperature is the constraint that is violated, then the next sub-task  $i + 1$  should be cooling. Alternatively, if the overall reaction enthalpy change is endothermic, then adiabatic operation can be another option.*

*The rate at which heat is removed is found as the amount of heat needed to keep the temperature below the constraint during the entire sub-task  $i + 1$ , until another constraint is violated or any of the end objectives is satisfied.*

**Rule A1.9: sub-task end ( $T_{low}$  violation)**

*When the temperature of the batch reactor  $T$  is about to violate the lower limit  $T_{low}$ , then the end of the current sub-task is identified at point  $t_{stop, T_{low}}$ .*

**Rule A1.10: subsequent sub-task identification ( $T_{low}$  violation)**

*If the lower bound of the operating temperature is violated, then the next sub-task  $i + 1$  could be heating. Alternatively, if the overall reaction is exothermic, then adiabatic operation can be another option.*

*The rate at which heat is to be added is the amount of heat needed to keep the temperature above the constraint during the entire sub-task  $i + 1$ , until another constraint is violated or any of the end objectives are satisfied.*

An initial estimate of the heating or cooling rate that is necessary for the succeeding task to be feasible, according to rules A1.8 and A1.10, can be found using the heats of reaction and the reaction rates at the end of sub-task  $i$ . Considering the rates for all of the reactions in the system at the end of sub-task  $i$ , multiplying with the respective heats of reaction and summing up will give the amount (rate) of energy that the system produces or absorbs.

If the system is in total exothermic and heat is produced, then the calculated heating rate (as described above) can be counterbalanced with cooling. However, especially in the case when one has to switch from a heating operation

to a cooling operation, the cooling rate that will prevent overshooting of the temperature above the maximum constraint should be up to 10-30 times higher than the calculated value, as a rule of thumb. The above mentioned number is referred to according to experience obtained from simulation of various case studies.

Similarly, if the system is in total endothermic and heat is absorbed, then the calculated cooling rate (as described earlier) can be counterbalanced with heating. Particularly, when at the end of a cooling operation, the suggested succeeding sub-task is a heating operation, then as a rule of thumb, in order to avoid the undershooting of the temperature below the minimum constraint at the switch over, the heating rate used should be up to 10-30 times higher than the calculated value.

However, the actual heating/cooling rate can be found with the means of dynamic simulation, as described in rules A1.8 and A1.10.

### **Two-phase batch reactor**

In the case when a second phase is present in the batch reactor, which for the purpose of this thesis is only vapour, then the effect of pressure becomes very important. In such a two-phase reactor, the set of reactions take place in the liquid phase, but due to the operating conditions a vapour phase is formed.

For a closed system, the formation of vapour leads to a pressure increase. One way to decrease the pressure of the system would obviously be to release the produced vapour from the reactor. However, there might be cases where it is undesirable to remove the vapour phase from the system and that should be avoided as much as possible.

The effect that temperature and pressure limitations have on the feasibility of the operation for the two-phase batch reactor can also be used to identify the end of a particular sub-task and the succeeding sub-task, according to the following rules.

Two cases are discussed, first when heating promotes the desired reaction and second when cooling promotes the desired reaction.

#### **- Case a: Heating promotes the desired reaction(s)**

When heating favours the desired reaction, then this is the operation mode to follow for most and preferably all the time. However, that could mean a possible violation of the upper temperature and/or pressure limit, depending on the starting conditions of the process.

The constraint that is violated first becomes active and provided that one wants to continue the heating operation, then one has to maintain operation at that specific constraint. For that purpose, the concept of a  $\Delta P$  and a  $\Delta T$  is introduced. If pressure is close to violating the upper limit, one has to keep the pressure between  $P_{up} - \Delta P$  and  $P_{up}$ . On the other hand, if the temperature constraint is close to violation, one has to keep the temperature between  $T_{up} - \Delta T$  and  $T_{up}$ .

**Rule A1.11: sub-task end ( $P_{up}$  violation)**

*If the pressure of the batch reactor is about to violate the upper pressure limit  $P_{up}$ , then the end of the current sub-task is identified as point  $t_{stop, P_{up}}$ .*

**Rule A1.12: subsequent sub-task identification ( $P_{up}$  violation)**

*If the upper limit of the operating pressure  $P_{up}$  is about to be violated, then the succeeding sub-task  $i + 1$  is an operation mode that removes heat from the system. When heating promotes the desired reaction, then the succeeding sub-task could be heating with simultaneous removal of the vapour from the system, if that is an option.*

The removal of heat from the system compared to its current status can also be interpreted in a different way than by application of direct cooling. Thus, heating at a lower rate, if that is sufficient to keep the pressure below the  $P_{up}$  constraint, could be a viable operation for the succeeding sub-task in the sequence.

Since, the presented problem is multi-constrained, one might be confronted with a case where the violation of two contradicting constraints is imminent. So, for example, in the case when either the lower limit for the operating temperature  $T_{low}$  or the upper limit for the operating temperature  $T_{up}$  is also close to violation together with  $P_{up}$ , then rule A1.12 is complemented by the next rule.

**Rule A1.13: subsequent sub-task identification ( $P_{up}$  and  $T$  violation)**

- i. If the upper limit of the operating pressure  $P_{up}$  as well as the lower limit of the operating temperature  $T_{low}$  are about to be violated, then the succeeding sub-task  $i + 1$  could be more heating and concurrent removal of vapour from the system.*
- ii. On the other hand, if the upper limit of the operating pressure  $P_{up}$  as well as the upper limit for the operating temperature  $T_{up}$  are about to be violated, then the succeeding sub-task  $i + 1$  should be continuous removal of vapour from the system and possibly heating, if the cooling from the vapour release dominates the provided heating.*

As it was mentioned earlier on page 47, once pressure is close to violating the upper limit, the operation range for the pressure should be kept between  $P_{up} - \Delta P$  and  $P_{up}$ . The imminent violation of the  $P_{up} - \Delta P$  limit is discussed in the following rule. It should be noted that the smaller the  $\Delta P$ , the more efficient the operation.

**Rule A1.14: subsequent sub-task identification ( $P_{up} - \Delta P$  violation)**

*If the pressure of the batch reactor is about to drop below  $P_{up} - \Delta P$ , then the succeeding sub-task  $i + 1$  should be ongoing vapour release and simultaneous*

heating at an appropriate higher rate. If the  $\Delta P$  is sufficiently large, then the succeeding sub-task could also be just heating without vapour release.

**Rule A1.15: subsequent sub-task identification ( $P_{low}$  violation)**

*If the operating pressure is about to violate the lower limit  $P_{low}$ , then the succeeding sub-task  $i + 1$  should be terminating the vapour release together with complementary heating.*

In the case when first the upper limit for the temperature constraint  $T_{up}$  is close to being violated, the actions to be taken are given in the following rules, which are complementary to rule A1.7.

**Rule A1.16: subsequent sub-task identification ( $T_{up}$  violation)**

*If the upper limit of the operating temperature  $T_{up}$  is about to be violated, then the succeeding sub-task  $i + 1$  is an operation that removes heat from the system. When heating promotes the desired reaction, then the succeeding sub-task could be heating with simultaneous removal of the vapour from the system, provided that the vapour release can remove the supplied energy from heating.*

**Rule A1.17: subsequent sub-task identification ( $T_{up}$  and  $P$  violation)**

- i. If both the upper limit of the operating temperature  $T_{up}$  and that of pressure  $P_{up}$  are close to violation, then the succeeding sub-task  $i + 1$  could be appropriate heating with simultaneous vapour release.*
- ii. On the other hand, if both the upper limit of the operating temperature  $T_{up}$  and the lower limit of the operating pressure  $P_{low}$  are about to be violated, then the succeeding sub-task  $i + 1$  could be terminating the vapour release and cooling. In the case that the overall reaction is endothermic, then adiabatic operation could also be an option.*

**Rule A1.18: subsequent sub-task identification ( $T_{up} - \Delta T$  violation)**

*Similarly to rule A1.14, if the temperature of the batch reactor is about to drop below the value of  $T_{up} - \Delta T$ , then the succeeding sub-task  $i + 1$  could be ongoing vapour release and simultaneous heating at an appropriate higher rate. If the  $\Delta T$  is sufficiently large, then the succeeding sub-task could also be just heating without vapour release.*

**Rule A1.19: subsequent sub-task identification ( $T_{low}$  violation)**

*In case the actual lower limit of the operating temperature  $T_{low}$  is close to being violated, then the succeeding sub-task  $i + 1$  should be terminating any vapour release together with heating at a higher rate.*

Rules A1.11 to A1.19 refer to the case where the desired reaction is promoted



by heating and these rules cover possible constraint violations that signal the end of a sub-task. Once the end of sub-task is identified, supplementary rules provide the respective actions needed to prevent the violation. The following rules cover the case where cooling favours the desired reaction.

- **Case b: Cooling promotes the desired reaction(s)**

Cooling is the preferable operation in this case. However, depending on the starting conditions of the process, that could mean a possible violation of the lower limit of the temperature and/or pressure constraint. Similarly to before, the constraint that is first violated becomes active and one wants to keep operation within a region of  $\Delta P$  or  $\Delta T$ . This means that either pressure has to be maintained between  $P_{low}$  and  $P_{low} + \Delta P$  or temperature has to be maintained between  $T_{low}$  and  $T_{low} + \Delta T$ .

**Rule A1.20: sub-task end ( $P_{low}$  violation)**

*When the batch reactor pressure is about to drop below the lower pressure limit  $P_{low}$  and violate that constraint first, then the end of the current sub-task is identified as point  $t_{stop, P_{low}}$ .*

**Rule A1.21: subsequent sub-task identification ( $P_{low}$  violation)**

*If the lower limit of the operating pressure  $P_{low}$  is about to be violated, then the succeeding sub-task  $i + 1$  could terminate any vapour release and heat mildly. If terminating the vapour release is sufficient to increase the pressure and can dominate some additional cooling, then this option is selected. Otherwise, in case the overall reaction is exothermic, then adiabatic operation could be the preferable feasible operation.*

**Rule A1.22: subsequent sub-task identification ( $P_{low}$  and  $T$  violation)**

- i. If both the lower limits for the operating pressure  $P_{low}$  and temperature  $T_{low}$  are threatened, then termination of the removal of vapour is necessary. If the overall reaction is exothermic, then either adiabatic operation or mild cooling can be applied. However, if the overall reaction is endothermic, then complementary heating is the necessary operation.*
- ii. If the lower limit of the operating pressure  $P_{low}$  as well as the upper limit of the operating temperature  $T_{up}$  are about to be violated, then the succeeding sub-task  $i + 1$  should be the termination of any vapour release and mild cooling, where the latter will depend on the overall reaction enthalpy.*

**Rule A1.23: subsequent sub-task identification ( $P_{low} + \Delta P$  violation)**

*If the lower pressure limit has been reached once and the current operation causes an imminent violation of the  $P_{low} + \Delta P$  value, then the succeeding sub-task should be cooling.*

**Rule A1.24: subsequent sub-task identification ( $P_{up}$  violation)**

*If the actual upper limit of the operating pressure  $P_{up}$  is about to be violated, then the succeeding sub-task  $i + 1$  should strong cooling.*

In the case when first the lower limit for the temperature constraint  $T_{low}$  is close to violation, the actions to be taken are given in the following rules, which are complementary to rule A1.9.

**Rule A1.25: subsequent sub-task identification ( $T_{low}$  violation)**

*If the lower limit of the operating temperature  $T_{low}$  is close to violation, then the succeeding sub-task  $i + 1$  should either be mild heating or adiabatic operation, in case the overall reaction is exothermic.*

**Rule A1.26: subsequent sub-task identification ( $T_{low}$  and  $P$  violation)**

- i. If both the lower limits for the operating temperature  $T_{low}$  and pressure  $P_{low}$  are about to be violated, then if the overall reaction is exothermic, adiabatic operation can be the next sub-task or mild heating if necessary to avoid constraint violation. No vapour should be removed from the system.*
- ii. If the lower limit of the operating temperature  $T_{low}$  as well as the upper limit of the operating pressure  $P_{up}$  are close to violation, then the succeeding sub-task  $i + 1$  will have to be removal of vapour from the system with simultaneous heating.*

**Rule A1.27: subsequent sub-task identification ( $T_{low} + \Delta T$  violation)**

*If the lower limit for the temperature has been reached once and the current operation causes an imminent violation of  $T_{low} + \Delta T$ , then the succeeding sub-task should be cooling.*

**Rule A1.28: subsequent sub-task identification ( $T_{up}$  violation)**

*If the actual upper limit of the operating temperature  $T_{up}$  is close to violation, then the succeeding sub-task should be strong cooling.*

Now the rules have been formulated. Therefore, the batch reaction algorithm can be presented next.

**3.2.3.5 Stepwise Description of the Batch Reaction Algorithm: One liquid-phase**

The developed algorithm is illustrated as a block diagram in figure 3.2. It covers the case, where a set of reactions take place in the liquid phase, which is the only phase present in the system. The operating temperature should be within a feasible range. The specification of the algorithm is as follows.

**Given:**

- The identity of the mixture compounds (both reactants and products), the initial feed charge (holdup) and the composition of the feed. The thermodynamic models, the set of reactions taking place and their respective kinetics.
- The end objectives for the reaction task, namely the end molefraction for the limiting reactant in the reaction of interest and the desired yield for the specified product(s).
- The feasible range of operating conditions for the batch reactor regarding temperature, in terms of upper and lower limits. Also, the lower limit for the selectivity constraint.
- The experimental or simulated data for isothermal and adiabatic operation within the feasible operating conditions limits.

**Calculate:**

- The necessary sequence of operational sub-tasks in order to reach the specified end objectives for the product(s) in minimum time and/or cost.
- The temperature or heating/cooling rate profile that will ensure the feasible operation of the batch reactor.

The algorithm is described in a stepwise fashion below.

1. From the given information, identify the desired reactions and the unwanted reactions. Determine the values of the (relative reaction enthalpy measure)  $\epsilon^r$  for each of the reactions.
2. Based on the information of the previous step, determine whether heating or cooling promotes the desired reaction over its competing reactions.
3. Retrieve the experimental data for isothermal and adiabatic operation within the feasible limits of the operating conditions. Alternatively, simulate the above mentioned operations until at least one of the end objectives is satisfied.
4. Calculate the selectivity function  $S_{function}$  for all the isothermal and adiabatic operations available.
5. Check whether the available operations are feasible, which means that the operating conditions remain within the feasible range. For an operation to be feasible, the selectivity constraint should not be violated at  $t_{yield}$  or  $t_{xreac}$ . Identify the feasible operation(s).
6. Set sub-task number  $i = 1$ . Identify the first sub-task in the operational sequence among the available operations, according to rule A1.1, based on a check on selectivity.

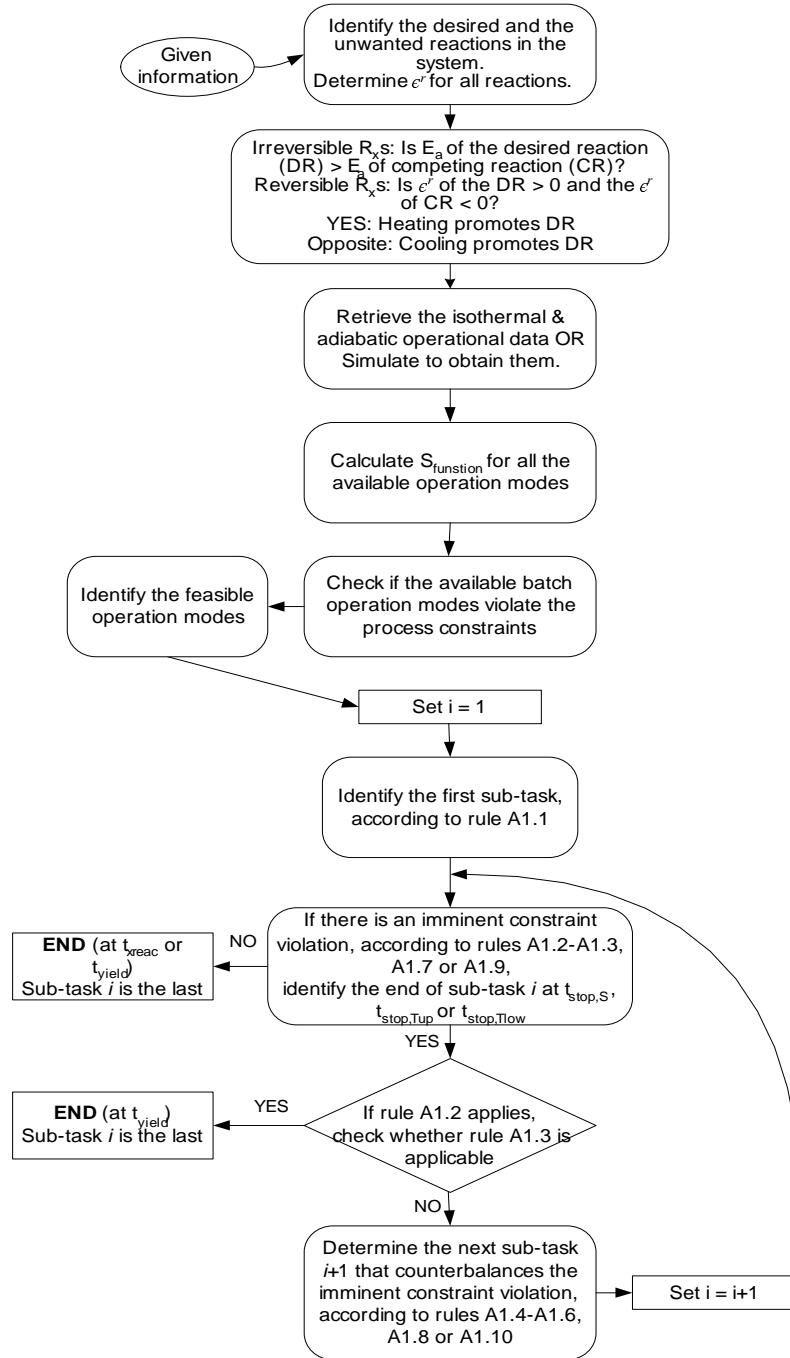


Figure 3.2: Block diagram of the algorithm A1a for operation model generation for a reaction task (one-phase reactor)

7. Identify the end of sub-task  $i$ , if any of rules A1.2 to A1.3, A1.7 or A1.9 are applicable.  
 If rules A1.2 and A1.3 apply, then sub-task  $i$  is the last one in the sequence and the *end* of the operation model generation for the batch reaction task is reached.  
 If rule A1.2 applies, then an imminent violation of the selectivity constraint is identified.  
 If rule A1.7 applies, then the violation of the upper limit of the operating temperature  $T_{up}$  is close.  
 If rule A1.9 applies, then sub-task  $i$  moves towards the violation of the lower limit of the operating temperature  $T_{low}$ .
8. Determine the next sub-task  $i + 1$  as an operation that counterbalances the imminent constraint violation that marked the end of sub-task  $i$ .  
 When the selectivity constraint is about to be violated, then the next sub-task is identified according to rules A1.4 to A1.6.  
 When the upper limit of the operating temperature  $T_{up}$  is about to be crossed, then the next sub-task is identified according to rule A1.8.  
 When the lower limit of the operating temperature  $T_{low}$  is close to violation, then the next sub-task is identified according to rule A1.10.
9. Repeat from step 7, until at least one of the end objectives is reached.  
 The *end* of the operational modelling for the batch reactor is either reached at one of the repetitions of step 7, or at the point when no constraint is violated and one of the end objectives is met.

The algorithm described above is referred to as Algorithm A1a.

### 3.2.3.6 Stepwise Description of the Batch Reaction Algorithm: Two-phase

The following algorithm is an extension of Algorithm A1a. It covers the case, where a set of reactions take place in the liquid phase, while a vapour phase is also present in the system. Both the operating temperature and pressure should be within a feasible range. The algorithm is illustrated in the block diagram in figure 3.3, where the differences from Algorithm A1a are highlighted in bold. The additional necessary information for the algorithm compared to the algorithm covering the case of a one-phase reactor is listed below.

**Given (additionally):**

- The feasible range of operating conditions for the batch reactor regarding pressure, in terms of upper and lower limits.
- The experimental or simulated data for operation with constant addition or removal of heat (constant rate) within the feasible limits of the heating/cooling capacity.

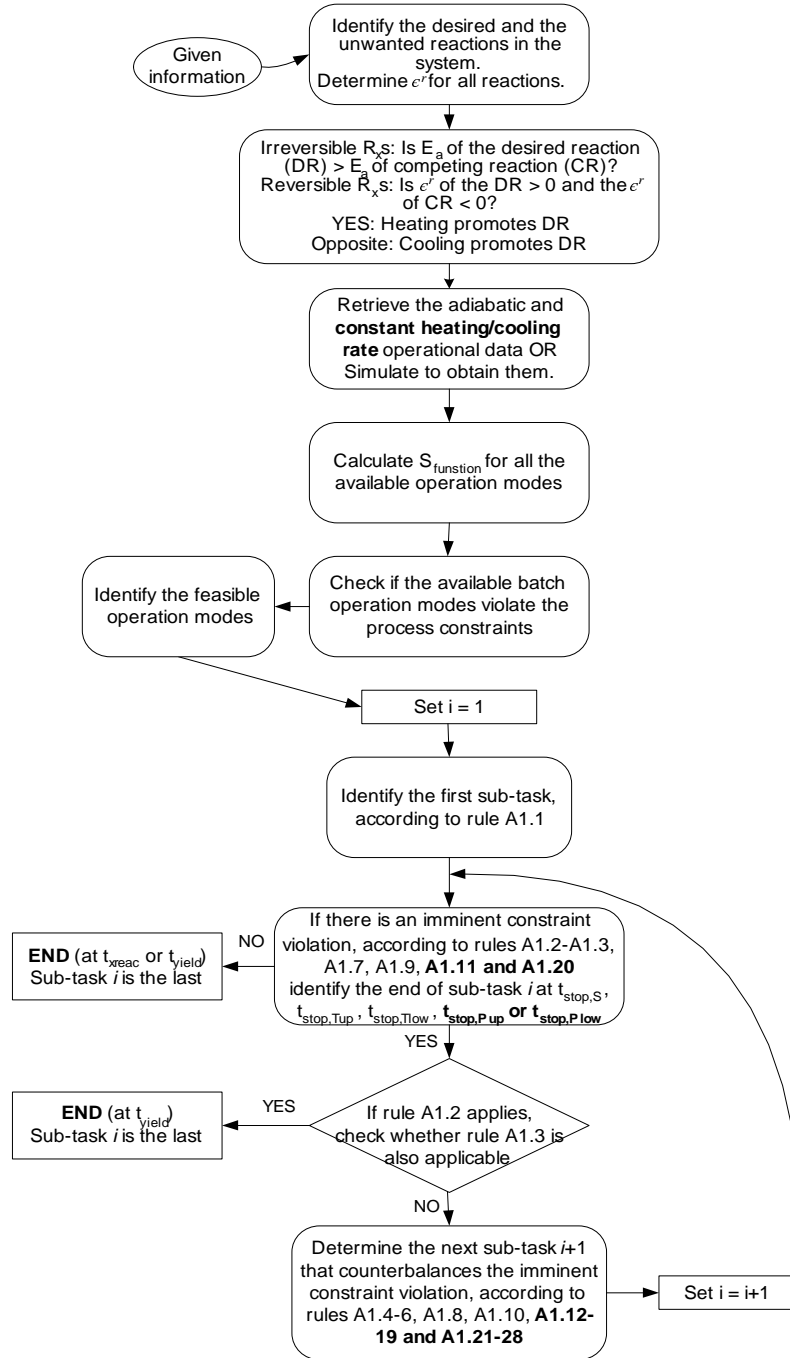


Figure 3.3: Block diagram of the algorithm A1b for operation model generation for a reaction task (two-phase reactor)

**Calculate:**

- The sequence of sub-tasks needed in order to reach in a feasible manner the specified end objectives for the product(s) in minimum time and/or cost.
- The corresponding temperature or heating/cooling profile as well as the regulation of the release valve for the removal or not of vapour from the reactor.

The additional steps for this algorithm compared to those of Algorithm A1a are given below.

- 1 - 2. The first two steps in the two algorithms are the same.
3. Additionally, retrieve the operational data for addition or removal or heat at a constant rate.
- 4 - 6. Steps 4 to 6 in the two algorithms are the same.
7. Identify the end of sub-task  $i$ , also if rules A1.11 and A1.20 are applicable.  
 If rule A1.7 applies, then the violation of the upper limit of the operating temperature  $T_{up}$  is close.  
 If rule A1.9 applies, then the violation of the lower limit of the operating temperature  $T_{low}$  is close.  
 If rule A1.11 applies, then the violation of the upper limit of the operating pressure  $P_{up}$  is close.  
 If rule A1.20 applies, then the violation of the lower limit of the operating pressure  $P_{low}$  is close.
8. Determine the next sub-task  $i + 1$  as an operation that counterbalances the imminent violation of the constraint that marked the end of sub-task  $i$ .  
 If the upper limit of the operating pressure  $P_{up}$  is about to be violated, then the next sub-task is identified according to rule A1.12 and the pressure is maintained within a belt of  $\Delta P$  ( $[P_{up} - \Delta P, P_{up}]$ ) with the help of rule A1.14.  
 If the lower limit of the operating pressure  $P_{low}$  is about to be violated, then the next sub-task is identified according to rule A1.21 and pressure is maintained between  $P_{low}$  and  $P_{low} + \Delta P$  with the help of rule A1.23.  
 If the upper limit of the operating temperature  $T_{up}$  is close to violation, then the next sub-task is identified according to rule A1.16 and the temperature is maintained between  $T_{up} - \Delta T$  and  $T_{up}$  with the help of rule A1.18.  
 If the lower limit of the operating temperature  $T_{low}$  is close to violation, then the next sub-task is identified according to rule A1.25 and temperature is maintained within a belt of  $\Delta T$  ( $[T_{low}, T_{low} + \Delta T]$ ) with the help

of rule A1.27.

In case more than one constraint is close to violation, then the different actions and corresponding sub-tasks are investigated with rules A1.13, A1.17, A1.22 and A1.26.

9. Repeat from step 7, until at least one of the end objectives is reached.

The algorithm described above is referred to as Algorithm A1b.

In summary, the algorithms generate the batch operations model by assigning in an iterative way a sequence of sub-tasks, in terms of isothermal or adiabatic operation, heating or cooling at a specific rate and opening or closing valves. These actions can easily be performed by a dynamic simulation engine. Dynamic simulations can also be performed (interactively) to support decision making in steps 7-8.

The strong feature of the algorithm is the identification of the desired and unwanted reactions in a set and the utilization of selectivity to identify sub-tasks and their end. An objective of the algorithm is to promote selectivity, in order to ensure the product recovery objective. Selectivity can only be employed, however, when there is more than one reaction taking place.

## 3.3 Task: Batch Distillation

### 3.3.1 Introduction

Batch distillation is probably the oldest separation process in the chemical processing industry for the separation of liquid mixtures and the most frequently used unit operation in batch processes. There can be many configurations for the distillation column, but the main components of it are: i) the vertical vessel with trays/plates, where the separation takes place, ii) the reboiler, where the feed is usually charged, iii) the condenser and iv) a reflux drum from where the liquid (reflux) can be recycled back to the column.

The nature of batch distillation and its operation at unsteady state require dynamic models for its complete description that cover a whole range of operations. However, the developed algorithm for the generation of the batch operations model for a batch distillation column is based on non rigorous models. A theoretical analysis of the batch distillation column equations and the different operation modes is provided in the following sections. The theoretical background includes a subsection on the driving force approach for continuous columns. This approach is then extended to batch distillation and a new operation mode is also introduced. The set of developed rules for the algorithm is presented next and the stepwise description of the algorithm follows. Finally, some further discussion to the order of products obtained when azeotropes are present is delivered.



### 3.3.2 Theoretical Background

Simple distillation, also known as differential distillation or *Rayleigh distillation*, is the most elementary example of batch distillation. Figure 3.4 shows a simple distillation still. The initial mixture is fed to the reboiler and vapour is removed from the top and condensed in the condenser. The vapour is rich with the most volatile component and as it is removed the liquid remaining in the still is enriched with the less volatile component. Lord Rayleigh (Rayleigh, 1902) proposed the following analysis for this process for a binary system.

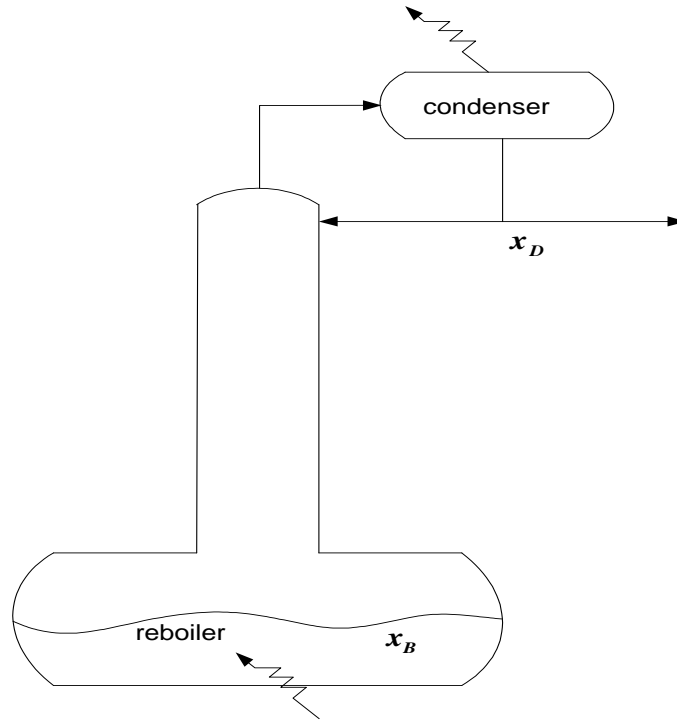


Figure 3.4: Schematic of a Simple Distillation Operation

#### 3.3.2.1 Simple Distillation Equations

Let  $F$  be the initial binary feed and  $x_F$  the composition of the more volatile component in the feed. Let  $B$  be the amount of the material remaining in the still,  $x_B$  the still composition of the more volatile component and  $x_D$  the composition of the distillate  $dB$  produced during an infinitesimal time interval  $dt$ . The differential material balance for the most volatile component can then be written as:

$$\begin{aligned}
x_D dB &= d(Bx_B) = Bdx_B + x_B dB \\
\int_F^B \frac{dB}{B} &= \int_{x_F}^{x_B} \frac{dx_B}{x_D - x_B} \\
\ln \left( \frac{B}{F} \right) &= \int_{x_F}^{x_B} \frac{dx_B}{x_D - x_B}
\end{aligned} \tag{3.12}$$

In this simple distillation process, it is assumed that the vapour formed within a short period is in thermodynamic equilibrium with the liquid. Therefore, the composition of the distillate  $x_D$  is related to the liquid composition in the still  $x_B$  by an equilibrium relation of the functional form  $x_D = f(x_B)$ . For a system following the ideal behavior given by Raoult's law, this functional form can be approximated using the concept of constant relative volatility ( $\alpha$ ). The equilibrium relationship between the vapour composition  $y$  ( $x_D$ ) and the liquid composition  $x$  ( $x_B$ ) of the more volatile component in a binary system is then given by:

$$y = \frac{\alpha x}{(\alpha - 1)x + 1} \tag{3.13}$$

The simple distillation still can be looked upon as a single equilibrium stage where a vapour and a liquid are in contact with one another and the transfer takes place between the two phases. However, even though simple distillation marks the first analysis of batch distillation processes, a complete separation using this process is unattainable, unless the relative volatility of the mixture is infinite. Therefore, simple distillation is only restrictively applied to laboratory scale distillation, for very easily separable mixtures or when no high purity products are required.

### 3.3.2.2 Batch Distillation Column Equations

When a number of equilibrium stages ( $N$ ) are stacked one above the other where successive vaporization and condensation are allowed, then the vapour in the condenser is enriched and the liquid in the reboiler is depleted, in terms of the more volatile component. This multistage layout is a typical representation of a distillation column. A classical schematic of a batch distillation column is illustrated in figure 3.5.

The initial feed is supplied to the reboiler at the bottom of the column. The column consists of perforated plates, such that the upward flow of vapour in the column is permitted. The vapour is condensed in the condenser and the liquid from the top is refluxed back across each plate. The assumption of negligible total liquid and vapour holdup on the perforated plates and the condenser can be made. Under this simplification, the multistage batch distillation column, as described in Diwekar (1995), also follows the Rayleigh equation 3.12 for

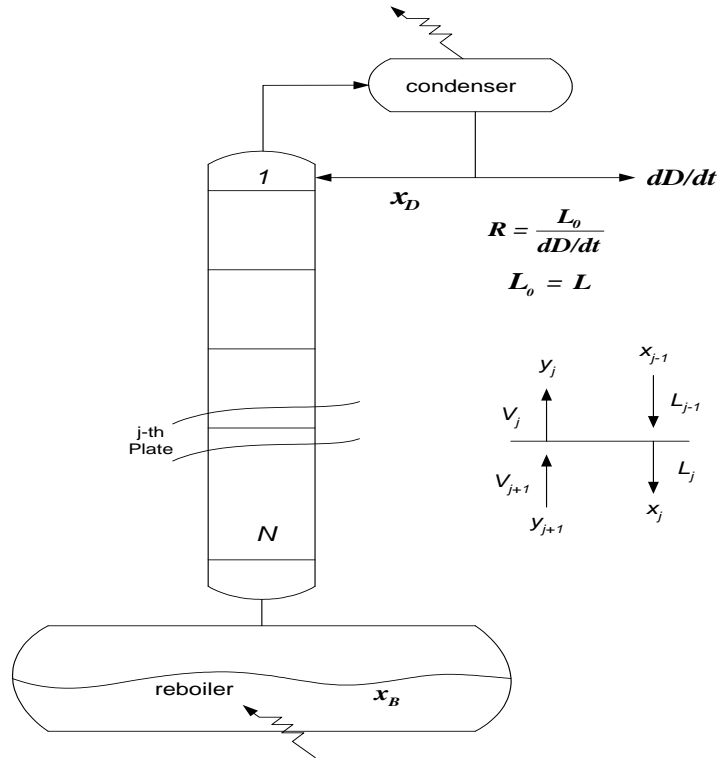


Figure 3.5: Schematic of a Batch Distillation Column

simple distillation. The difference between the two processes lies in the functional relationship between distillate composition  $x_D$  and bottom composition  $x_B$ , which for the multistage batch distillation column is governed by multiple equilibrium stages.

An evaluation of the functional form of the relationship between  $x_D$  and  $x_B$  requires the calculation of material (and energy) balances across each plate, due to the presence of reflux and column internals. As shown in figure 3.5 the plates are numbered starting from the top of the column. In the calculations around the  $j$ -th plate, there are four streams involved: liquid stream  $L_{j-1}$  and vapour stream  $V_{j+1}$  are entering and liquid stream  $L_j$  and vapour stream  $V_j$  are leaving the  $j$ -th plate. The internal streams in the column are given in kmol/hr. If the liquid and vapour enthalpies are denoted by  $H^L$  and  $H^V$  respectively, then the material and energy balances around the  $j$ -th plate can be written as follows:

Material balance:

$$L_{j-1} + V_{j+1} = L_j + V_j \quad (3.14)$$

Energy balance:

$$L_{j-1}H_{j-1}^L + V_{j+1}H_{j+1}^V = L_jH_j^L + V_jH_j^V + losses + H_{mix} \quad (3.15)$$

where  $H_{mix}$  is the heat of mixing.

If the following assumptions are made: constant latent heat of vaporization and ideal system, then the energy balance equation (3.15) is reduced to the equimolar overflow assumption  $L_{j-1} = L_j = L$  and  $V_{j+1} = V_j = V$ . The resulting assumption makes it possible to widen the range of application of the well known McCabe and Thiele graphical method (McCabe and Thiele, 1925) to cover batch distillation. Considering the overall and the most volatile component material balances around the condenser and the  $j$ -th plate respectively leads to the following equations:

$$V = L + dD/dt = dD/dt(R + 1) \quad (3.16)$$

$$Vy_j = Lx_{j-1} + (dD/dt)x_D \quad (3.17)$$

where  $dD/dt$  is the distillate rate,  $D$  in kmol,  $L$  represents the liquid flow rate refluxed back to the column from the condenser and  $R$  represents the reflux ratio defined as  $R = L/(dD/dt)$ .

Substituting for  $V$  from equation 3.16, equation 3.17 can be expressed in terms of the reflux ratio  $R$ :

$$y_j = \frac{R}{R+1}x_{j-1} + \frac{1}{R+1}x_D \quad (3.18)$$

The equation above is an equation for a straight line in the  $x$ - $y$  plane. This equation is the same as the line of operation for the rectifying section of a continuous distillation column. This is not a surprising conclusion, since the batch distillation column represented in figure 3.5 essentially performs the rectifying operation and is also called a batch rectifier. Once one knows the reflux ratio  $R$  and the number of trays in the column, the bottom composition  $x_B$  can be calculated with the McCabe-Thiele graphical method, as shown in figure 3.6.

### 3.3.2.3 Batch Distillation Operation Modes

The selection of the column operation has significant effect on the product quality. There are two fundamental modes of operating batch distillation columns:

- Constant reflux ratio
- Variable reflux ratio

Operating with a constant reflux ratio, as observed in continuous distillation, the composition of the distillate  $x_D$  and therefore the composition of the product varies over time. The reason for that is because after a point in time, the

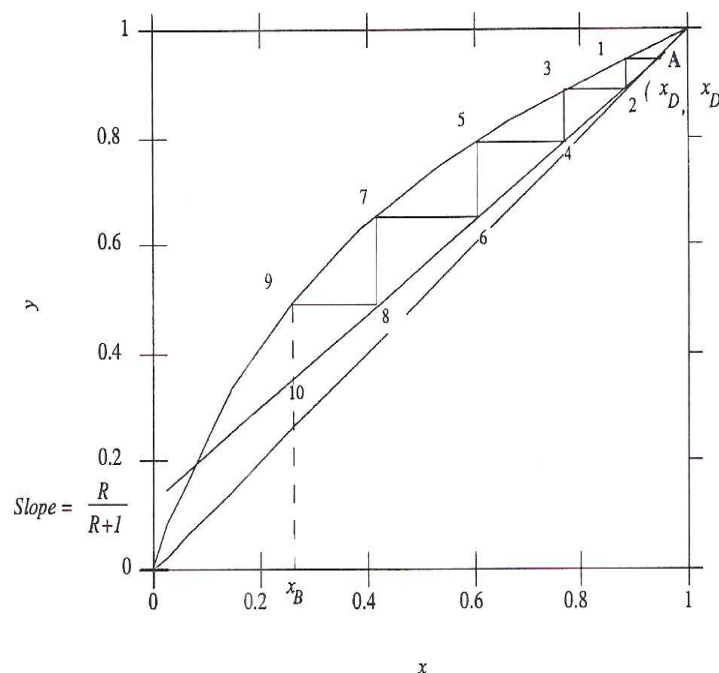


Figure 3.6: McCabe-Thiele method for the calculation of bottom composition  $x_B$

reflux ratio used is not high enough to maintain the desired distillate composition, which as a consequence contains less of the more volatile component as the distillation progresses. On the other hand, a constant distillate composition can be achieved by continuously varying the reflux ratio, so that it is sufficiently high, until the recovery objective for the specified product is satisfied.

Designing the operation of a distillation column with constant reflux ratio might seem easy, since one only has to choose the value of the reflux ratio once. However, the reflux ration can not be chosen arbitrarily. If it is too small the separation might be infeasible and the product specifications, such as product purity, might be unattainable. From another point of view if it is too high, the separation might be excessively energy consuming. Determining a reflux ratio profile is more demanding than the constant reflux ratio mode, but in that way the achievement of the product specifications is ensured. Nonetheless, choosing the exact value of the reflux ratio is a sensitive issue, since one has to keep the balance between operating at as low reflux ratio as possible, which is however sufficiently high for the product specifications to be achieved. The reasons behind the objective to operate at the lowest possible reflux ratio at all times are explained in the following section.

### 3.3.2.4 Driving Force Approach

The definition of the driving force, as it is used in this thesis, is adapted from Bek-Pedersen *et al.* (2000). The term “driving force” (denoted  $F_{Di}$ ) is based on a new definition, which is to some extent different than the classical definition by Chilton and Colburn (1935). The definition of the driving force is the difference in compositions of compound  $i$  in two co-existing phases that may or may not be in equilibrium. Thus, for the case of the typical batch distillation column considered here, using equation 3.18 gives:

$$F_{Di} = |y_i - x_i| = \frac{-1}{R+1}x_i + \frac{1}{R+1}x_D \quad (3.19)$$

The existence of a driving force is what makes the separation possible. As the size of the driving force for a given separation approaches zero, the separation of the species involved becomes difficult. That is why if an azeotrope is present, at the azeotropic composition the driving force is zero (since  $y_i=x_i$ ) and no further separation is possible. On the other hand, as the driving force increases in size, the separation of the species involved becomes easy, because the difference in composition between the phases is large. Operating at the largest driving force leads to highly energy efficient distillation column designs (Bek-Pedersen *et al.*, 2000). From equation 3.19 it is obvious that for a specific feed composition  $x_F$ , the largest driving force corresponds to the minimum reflux ratio. Therefore, it is desirable to operate at a low reflux ratio, which corresponds to a large driving force and near minimum energy requirements for the distillation column.

The concept of the driving force applied to batch distillation is described in the following section as part of the theory developed for the batch distillation algorithm.

## 3.3.3 Batch Distillation Algorithm

In order to determine a near optimal reflux ratio profile for the separation of a mixture of compounds with a batch distillation column, a new method has been developed in this thesis. This algorithm uses simple equations for the distillation column as described in the previous section (equations 3.18 - 3.19). It also uses a group of equations (3.20 - 3.23) that derive from the extension of the driving force approach to batch distillation and a suggested operation mode, developed for the algorithm and described in the following sections. In addition, the algorithm is based on a set of rules used for both the overall separation synthesis (based on distillation) and the generation of the operational model for each separation task. Furthermore, the algorithm uses the McCabe-Thiele graphical method to find quickly and without the use of rigorous models the bottom composition for each sub-task in the sequence.

### 3.3.3.1 Driving Force Approach extended to Batch Distillation

The approach of the driving force for continuous distillation (Bek-Pedersen *et al.*, 2000) can be applied in batch distillation to identify the minimum reflux ratio  $R_{min}$  needed to perform the separation. In this way, the first necessary step to ensure the feasibility of a separation is taken, by operating at reflux ratios larger than the limiting value. For a specific distillate composition  $x_D$ , the minimum reflux ratio  $R_{min}$  for a specific feed composition ( $x_i = x_F$ ), as indicated in equation 3.19 corresponds to the largest driving force  $F_{Di}$ . The largest driving force is actually the difference in composition between the liquid and the vapour phase for the most volatile component and can be calculated from the measured or estimated vapour-liquid equilibrium (VLE) data for a binary system. The minimum reflux ratio for a specific feed composition is then given by the following equation:

$$R_{min} = \frac{x_D - x_F}{F_{Di}(x_F)} - 1 \quad (3.20)$$

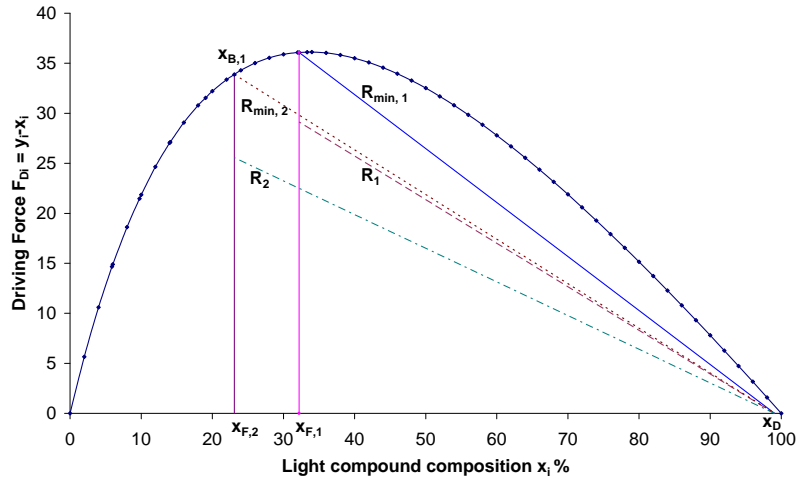


Figure 3.7: Driving force  $F_{Di}$  as a function of composition  $x_i$

However, the minimum reflux ratio can not be used, since it can only be supported by an infinite number of equilibrium stages. Thus, for a specific number of theoretical plates a reflux ratio  $R$  larger than the minimum value has to be used. That reflux ratio is found with the help of the computational tool PDS (Hostrup, 2002), developed in CAPEC, to match the given number of plates  $N$  for the column. It can be shown in figure 3.7 that as the distillation progresses and more of the most volatile component is removed, its composition in the still moves to the left (decreases). If the objective is to keep the distillate composition constant, then the reflux ratio has to be gradually increased. This

is so, because the actual reflux ratio used  $R_1$  moves towards the minimum reflux ratio for the corresponding composition in the still  $R_{min,2}$ . At that point, since the minimum reflux ratio  $R_{min,2}$  should not be used, a new reflux ratio  $R_2$  has to be chosen. Otherwise, the purity of the distillate will be endangered.

### 3.3.3.2 Near Optimal Reflux Ratio Operation Mode

In this thesis, a variation of the second mode of operation (variable reflux ratio mode) for a batch distillation is considered. However, the reflux ratio is varied in discrete steps. In that way, the reflux ratio is changing with time, but for a specific period it remains constant. The assumption is then made that for that period of time  $i$  both the reflux ratio is constant and the distillate composition  $x_D$  remains constant at an average value  $x_{Dav}$  that has an allowed minimum. Considering a constant distillate composition  $x_{Dav}$ , equation 3.12 becomes:

$$B_i = F_i \frac{x_{Dav} - x_{F,i}}{x_{Dav} - x_{B,i}} \quad (3.21)$$

The amount distilled over a period of time of constant reflux ratio is given from the material balance around the complete column:

$$D_i = F_i - B_i \quad (3.22)$$

In the above equations  $F_i$  is the initial charge, in kmol,  $x_{F,i}$  is the initial feed composition,  $x_{Dav}$  is the allowed minimum value for the distillate composition,  $D_i$  is the amount distilled in period  $i$  and  $B_i$  and  $x_{B,i}$  are the amount remaining in the still, in kmol, and its corresponding composition by the end of period  $i$  operated with a specific constant reflux ratio.

The duration for period  $i$  of constant reflux ratio can be found from integration of equation 3.16.

$$\begin{aligned} \int_0^T dt &= \int_0^D \frac{R+1}{V} dD \\ T_{period,i} &= \frac{R_i+1}{V_i} D_i \end{aligned} \quad (3.23)$$

From this point on in this thesis the subscript  $i$  to denote the period of time in the above equations will be implied.

Operating at a low reflux ratio (large driving force) leads to highly energy efficient distillation column designs, as it has already been mentioned. However, another advantage is that the separation is also faster. It can easily be proven using equation 3.23 that the time needed to reach a still composition  $x_{B,2}$  is less if it is done in two steps, operating first at constant reflux ratio  $R_1$  until a still composition  $x_{B,1}$  is reached ( $x_{B,1} > x_{B,2}$ ) and then operating at a constant reflux ratio  $R_2$  ( $R_2 > R_1$ ) until the desired still composition  $x_{B,2}$  is reached, than if the distillation column is operated constantly at the higher



reflux ratio  $R_2$ .

The set of rules for the batch distillation algorithm is formulated in the following subsection. The rules identify the necessary sub-tasks, their design and their ends as well as the subsequent sub-tasks until both the product(s) objectives are met. The sub-tasks for batch distillation are defined as periods of time, where the reflux ratio and vapour boilup rate remain constant. Thus, in the following subsections the term period  $i$  is also used instead of sub-task  $i$ .

### 3.3.3.3 Batch Distillation Algorithm Set of Rules

For a mixture of  $NC$  compounds, the number of adjacent pairs between which a split is made is  $NC - 1$ . For the case, where the goal is to obtain all  $NC$  compounds as products of a certain purity, then the minimum number of separation tasks is  $NC - 1$ . The developed algorithm, which will also be referred to as algorithm A2, is divided in two levels. The first level deals with the synthesis of the separation tasks based on batch distillation by identifying the sequence of obtaining possible products. The second level generates for each separation  $k$ , the necessary sequence of sub-tasks for obtaining each corresponding product with a specified purity and recovery.

#### Level 1 rules

##### Rule A2.1: separation task $k$ identification

*For a considered system, separation task  $k$  in a sequence is chosen as the split between the most volatile and the second most volatile compound, when no minimum boiling azeotrope is formed between the mentioned binary pair. The product in the sequence is the most volatile compound and the desired product purity is set as the distillate composition for the algorithm.*

However, since the recovery of a product is usually less than a 100 % there will always be a residue of the product that has just been distilled when the next separation task  $k+1$  is examined. In this case, the following two rules will always have to be considered.

##### Rule A2.2: separation task identification (intermediate cut removal)

*i. For the binary pair of the most volatile and second most volatile compound in the considered system (referred from now on as the "binary pair"), if the composition of the most volatile compound in this pair is above a maximum value  $x_F^{bin}$ , as described in appendix B (equations B.5 - B.8), an intermediate cut has to be distilled in order not to compromise the specified objectives (purity and recovery) of the next high purity product in the sequence.*

*ii. The intermediate cut should be removed at a constant reflux ratio with a*

value greater than or equal to the reflux ratio used in the last sub-task in the operational sequence of the previously obtained product, until  $x_F < x_F^{bin}$ .

iii. An intermediate cut will not be necessary, if the second and third most volatile compounds in the system form a minimum boiling azeotrope, which will then be the next product in the sequence.

The actual value of  $x_F^{bin}$  strongly depends on the distillate composition used in the algorithm for the separation task  $k + 1$  succeeding the intermediate cut removal (or in case no intermediate is needed succeeding the previous task), as indicated by equations B.5 - B.8.

**Rule A2.3: subsequent separation task identification**

*If the composition of the most volatile compound is below the maximum value  $x_F^{max}$ , then the binary pair between which the split will take place is the second and third most volatile compounds in the system. The next product in the sequence is then the second most volatile compound.*

The presence of azeotropes in the system has an effect upon the sequence of attained products. Minimum boiling azeotropes will always be in the sequence of products obtained in a batch rectifier. The composition of the feed compared to the corresponding azeotropic composition will determine the rest of the products in the sequence, according to the following rules.

**Rule A2.4: separation task identification (min. boil. azeotrope)**

i. *If the binary pair considered forms a minimum boiling azeotrope, then the next separation task  $k+1$  in the sequence is chosen in order to remove the azeotrope. The next product attained is the azeotrope and the distillate composition used in the algorithm, normally specified according to the desired product purity, is replaced by the azeotropic composition.*

ii. *In this case, the split occurs in principle between the azeotrope and one of the compounds of the binary pair, depending on the relation of the feed and azeotropic composition.*

**Rule A2.5: subsequent separation task identification (after azeotrope removal)**

*If the azeotropic composition is smaller than the feed composition for the corresponding binary pair in terms of the more volatile compound, then after the azeotrope is removed the next compound that can be obtained pure is the more volatile component in the binary pair (the split is between the azeotrope and the more volatile component in the binary pair). In case the desired product is the less volatile compound, the specific batch distillation configuration can not be used and the separation task of removing the azeotrope should be abandoned. Another batch distillation configuration, such as an inverted distillation column could then be used.*

**Rule A2.6: subsequent separation task identification (after azeotrope removal)**

*If the azeotropic composition is higher than the feed composition for the corresponding binary pair in terms of the more volatile compound, then after the azeotrope is removed the next compound that can be obtained pure is the less volatile component in the binary pair (the split is between the azeotrope and the less volatile component in the binary pair). In case the desired product is the more volatile compound, the specific batch distillation configuration can not be used and the separation task of removing the azeotrope should be abandoned.*

Rules A2.5 and A2.6 are further explained in figure 3.10 in section 3.3.3.5, where the two individual cases are identified. Additionally, the maximum amount of the remaining compound that can be distilled once the azeotrope is removed is given in equations 3.24 and 3.25, for the two cases, respectively.

At the second level of the algorithm, the operational model for each of the individual separation tasks in the identified sequence from level 1 is generated. The application of the algorithm gives the reflux ratio and vapour boilup rate profile for each of these separation tasks, when the objective is to obtain each product with specified purity and recovery. The algorithm has to be applied individually for each of the minimum  $NC - 1$  separation tasks.

The relationship between level 1 and 2 is significant. The information from level 1 regarding separation task  $k$  is passed on to level 2 and once the operational model is generated, the end point for separation task  $k$  is sent on back to level 1. This information serves as the given input for the next considered separation task  $k+1$ . The iteration continues until all specified products are obtained either as distillates or as the column bottom. An illustration of the relationship between the two levels is given in figure 3.8.

At level 2, the suggested reflux ratio profile is identified in advance as a sequence of sub-tasks. The sub-tasks for the batch distillation process are defined as operation at constant reflux ratio and vapour boilup rate. In the algorithm the values for these variables are specified for each sub-task together with the time that each sub-task needs. Thus, this is the operational model for the batch distillation. It is important to point out that the reflux ratio is varied in steps in order to keep the distillate composition constant. The same applies to the vapour boilup rate.

**Level 2 rules**

**Rule A2.7: first sub-task design (V)**

*For the considered system, the initial vapour boilup rate used in period  $i=1$  for separation task  $k$  in the sequence is set to be approximately double the amount of the total feed charge per time unit.*

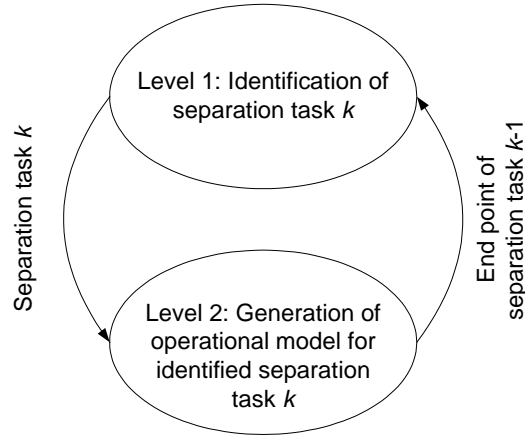


Figure 3.8: Data flow between levels 1 and 2 of the Batch Distillation Algorithm (for identification and generation of separation sequences and their operational model)

The need for the vapour boilup rate to be changed in the course of distillation may arise. The most common reason is flooding. The following rule will have to be considered.

**Rule A2.8: sub-task design ( $R$  vs  $V$ )**

*If the reflux ratio calculated to be used in the considered period  $i$  is above the flooding value ( $R_{max}(V)$ ) for the specific vapour boilup rate, then a new lower vapour boilup rate will have to be chosen. The new vapour boilup rate should be as high as possible, but still sufficiently low, in order for the reflux ratio chosen to be below its corresponding flooding value.*

The relationship between vapour boilup rate  $V$  and reflux ratio  $R$  and the identification of flooding in the column can be found through dynamic simulation for a given feed and column design. For a specific vapour boilup rate  $V$ , DYN-SIM in ICAS can be used to determine the reflux ratio value where flooding occurs, by gradually increasing  $R$ .

The bottom composition at the end of each period  $i$ , used to calculate the amount of distillate  $D$  obtained, the amount of bottom  $B$  remaining in the column and the duration of each period is determined according the following rule.

**Rule A2.9: sub-task end**

*The bottom composition at the end of period  $i$  is determined using the graphical method of McCabe-Thiele. The bottom composition  $x_B$  is identified as the*

liquid composition from plate  $j$ , when no significant change in the liquid composition between the adjacent plates  $j$  and  $j+1$  takes place ( $e = x_j - x_{j+1} \leq 0.01$ ).

The recovery of a product  $y_{km}^s$  is one of the two end objectives for the corresponding separation task and is used in order to identify the last sub-task of the operational sequence according to the next rules. The superscript  $s$  stands for separation and the subscripts  $k$  and  $m$  denote the separation task  $k$  and the product  $m$  in the overall batch route, respectively.

**Rule A2.10: final sub-task identification**

*If the difference between the desired specified recovery  $y_{km}^s$  (%) for the corresponding separation task  $k$  and the recovery at the end of the particular period  $i$ ,  $y_{km,i}^s$  (%) is less than 10%, then the next period is identified as the final period, i.e.  $N = i + 1$ .*

**Rule A2.11: operations model generation end for separation task  $k$**

*If the current period of time  $i$  is identified as the final period of the sequence  $N$ , then the suggested operational model satisfies the desired recovery  $y_{km}^s$  of product  $m$  and the generation of the operational model for separation task  $k$  is completed.*

**Rule A2.12: complete batch operations model generation end**

*i. If the bottom composition  $x_B$  at the end of period  $i=N$  meets the desired purity specification for the least volatile compound in the initial mixture, then the generation of the overall batch route with the operations model for each task is completed. The last product is collected from the bottom of the column.*  
*ii. Alternatively, the bottom composition  $x_B$  could also meet the desired purity specification for the second heaviest compound in the initial mixture, in case a minimum boiling azeotrope is obtained as the previous product in the sequence and the corresponding feed composition was larger than the azeotropic composition.*

### 3.3.3.4 Stepwise Description of the Batch Distillation Algorithm

The algorithm is illustrated in figure (3.9). The necessary prerequisite information for the algorithm is listed below.

**Given:**

- The identity of the mixture compounds, the initial feed charge, the composition of the feed (also the composition of the adjacent binary pairs, such as  $x_1 + x_2 = 1$ )
- The desirable recovery and purity for each specified product(s).

- The measured or estimated vapour-liquid equilibrium data for the adjacent pairs to separate.
- The column geometry (mainly number of plates  $N$ ) and the relationship between the vapour boilup rate and the reflux rate. From that the relationship between the vapour boilup rate and limiting values of the reflux ratio can be derived.

**Calculate:**

- The sequence of attainable products.
- The reflux ratio and vapour boilup rate profile that ensure that the specified end objectives for each of the products in the sequence are reached.

The algorithm is described in a stepwise fashion below.

**Level 1**

1. Set separation task  $k=1$ .  
Rank the mixture compounds by increasing normal boiling point. In this list any azeotropes present in the system must be included. Choose the separation task  $k$  as the split between the most volatile and the second most volatile compound. Set the distillate composition for the algorithm, according to rules A2.1 to A2.6.  
Set period of time  $i=1$ .

**Level 2**

2. Recover from the given information of the column geometry the relationship between the vapour boilup rate and the reflux ratio, in order to locate operating problems, such as flooding and weeping.
3. Choose the vapour boilup rate according to rule A2.7.
4. Retrieve the vapour-liquid equilibrium data at the system pressure for the binary pair between which the split is chosen or between which the azeotrope takes place and calculate the driving force for the binary pair.
5. For the specific feed composition  $x_{Fi}$ , ( $i=1,N$ ) and the distillate composition  $x_D$  as this has been determined by the rules associated to step 1, calculate the minimum reflux ratio required for this separation using equation 3.20.
6. Calculate the reflux ratio to be used that matches the specified number of plates of the distillation column, according to the Hostrup (2002) method.
7. Check the reflux ratio calculated in step 5 in relation to the vapour boilup rate used. Adjust, if necessary, the vapour boilup rate according to rule A2.8.

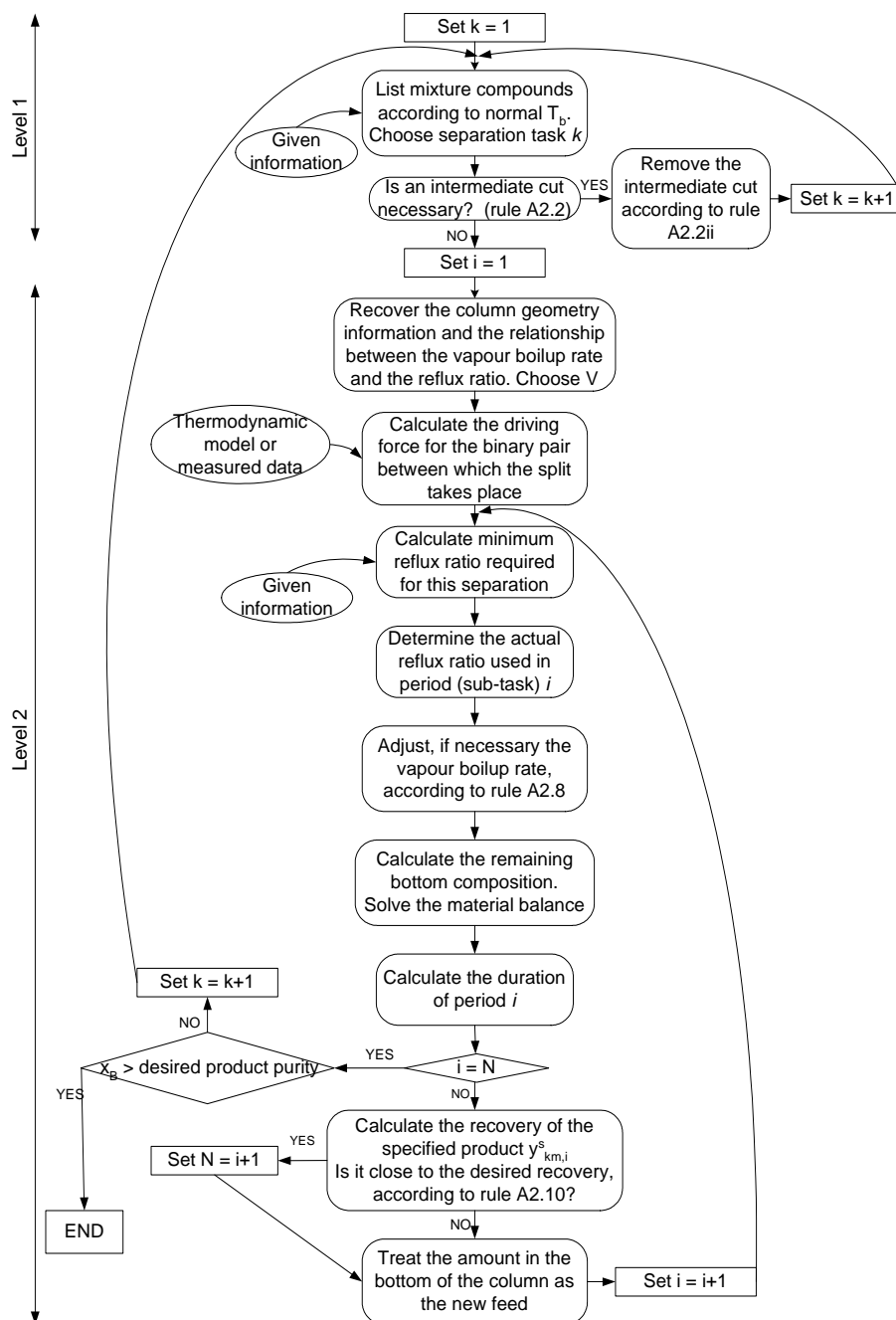


Figure 3.9: Block diagram of the algorithm A2 for the generation of a sequence of separation tasks based on batch distillation as well as the generation of the operational model for each separation task

8. Determine the bottom composition  $x_B$  at the end of period  $i$ , using the graphical method of McCabe-Thiele. Identify  $x_B$  according to rule A2.9. Calculate the amount  $D$  distilled in this period and the amount  $B$  remaining in the column, using equations 3.21 - 3.22.
9. Calculate the duration of period  $i$  for which the column is operated at constant reflux ratio  $R$  determined in step 5, using equation 3.23.
10. Check whether the current period  $i$  is the final in the sequence of sub-tasks ( $i = N$ ). If  $i \neq N$ , go to step 11.  
Otherwise, rule A2.11 applies. Check whether the conditions of rule A2.12 are also met.  
If the conditions are not satisfied, set  $k = k+1$  and repeat the algorithm from step 1.  
If rule A2.12 is true, the last product of the sequence can be collected from the bottom of the column and the synthesis and operations model design of batch distillation is completed.
11. Calculate the recovery of the product at the end of this period and identify if possible, according to rule A2.10, the value of  $N$ .
12. Assign the bottom composition  $x_B$  and the amount in the bottom  $B$  at the end of this period  $i$  as the feed composition  $x_F$  and the feed  $F$  for the next period  $i + 1$  ( $x_{B,i} = x_{F,i+1}$  and  $B_i = F_{i+1}$ ). Set  $i = i + 1$  and go to step 5.

The algorithm described above will be from now on referred to as Algorithm A2.

### 3.3.3.5 Framework for the synthesis and design of batch separation processes based on distillation

The algorithm described in the previous section, as already mentioned, is divided in two levels. The first level takes care of the generation of a batch route (sequence of separation tasks) for the separation of a mixture to its components. The second level performs the individual operational design for each of the separation tasks identified in the sequence. The two levels are described in more detail below.

**Level 1** At the first level the synthesis of separation processes based on batch distillation is performed. The synthesis involves the identification of the separation tasks and the order in which they are performed. Each separation task in this case is carried out with batch distillation and it is performed in the same operation unit. Identifying the order of the separation tasks implies finding the sequence of products, final and intermediate, that need to be distilled.



For a non-azeotropic mixture, the sequence of products is easily found by ranking the compounds according to increasing boiling point (decreasing volatility). The necessity to identify an in-between separation task where an intermediate product of less purity is obtained is explored in the algorithm. For the case of more complicated mixtures when minimum boiling azeotropes are present, the removal of each azeotrope is considered as a separation task in the sequence and the product obtained is the azeotrope. The presence of azeotropes, however, complicates the acquirement of a simple sequence of decreasing volatility compounds.

As soon as a minimum boiling azeotrope is present, the azeotrope will inevitably be one of the products distilled in the batch rectifier. Since the temperature where the azeotrope is obtained is lower than the boiling points of the pure compounds, the azeotrope will be distilled first in the sequence of products. However, the identity of the compounds distilled afterwards depends on the composition of the feed.

For a binary pair (compounds A and B) forming an azeotrope (A-B), there are three possible products in the sequence that can be obtained, namely A, B and A-B. Two individual cases can be identified as shown in figure 3.10:

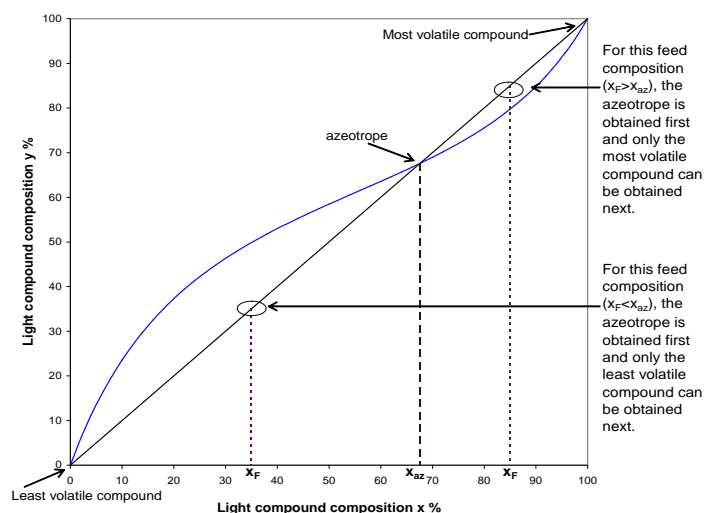


Figure 3.10: xy-diagram for a binary pair forming a minimum boiling azeotrope

- Case 1:  $x_F > x_{az}$ . The composition of the feed in terms of the more volatile compound A is larger than the azeotropic composition ( $x_F$  lies on the right hand side of the azeotrope). The azeotrope is the first product in the sequence. As the azeotrope is distilled the composition in the column moves along the diagonal towards the more volatile compound, until pure A remains in the column. Obviously, the next product that can

be obtained is compound A, since in this case the less volatile compound has already been removed with the azeotrope. From the lever rule, the maximum amount of pure compound A that can be distilled is given:

$$A = \frac{x_F - x_{az}}{1 - x_{az}} F \quad (3.24)$$

where  $F$  is the total amount of the feed in terms of the binary pair. The larger the difference between the feed composition  $x_F$  and the azeotropic composition  $x_{az}$ , the smaller the amount of the azeotrope distilled and the larger the amount of compound A, which is the next product in the sequence, that can be obtained nearly pure.

- Case 2:  $x_F < x_{az}$ . The composition of the feed is smaller than the azeotropic composition ( $x_F$  lies on the left hand side of the azeotrope). Yet again, the minimum boiling azeotrope is the first product in the sequence. However, this time as the azeotrope is distilled the composition in the column moves along the diagonal towards the less volatile compound B, until in the end pure B remains in the column. Clearly, the only product that can be distilled next in the sequence is compound B, since the more volatile compound has already been removed with the azeotrope. From the lever rule, the maximum amount of pure compound B that can be distilled is given:

$$B = \frac{x_{az} - x_F}{x_{az}} F \quad (3.25)$$

The larger the difference between the feed composition  $x_F$  and the azeotropic composition  $x_{az}$ , the larger also the amount of compound B, that can be obtained nearly pure.

For the case of a multicomponent batch distillation, Bernot *et al.* (1990) and (1991), has proposed a methodology to obtain a feasible sequence for the separation of the mixture. The sequence of products obtained is based on the location of the feed with respect to the batch distillation regions. For a simple ternary system (compounds A, B and C), where two of the mixture compounds form a minimum boiling azeotrope A-B, the separation sequencing is shown in figure 3.11.

For feed I, the composition  $x_F$  in terms of the binary pair forming the azeotrope (A and B) is smaller than the azeotropic composition, which corresponds to case 2 described above. The minimum boiling azeotrope is the first product in the sequence and the less volatile compound B is obtained next. The heavier compound C is obtained last. Similarly, for feed II, which corresponds to case 1, the minimum boiling azeotrope is still the first product in the sequence. The more volatile compound A is next and the last compound obtained is the heavier compound C. The arrows starting from the feed and ending at heavy compound C show how the composition in the column changes

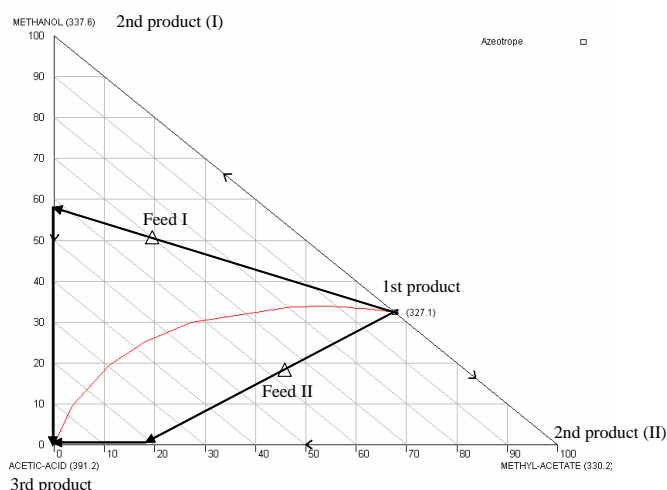


Figure 3.11: Sequence of products for a ternary system with a minimum boiling azeotrope present

as the various products in the sequence are distilled.

**Level 2** At the second level, which is a lower level, the design of the operation for each separation task is performed. The batch route for the separation of a mixture to its components is generated in level 1. As mentioned earlier, the batch route for this case is a sequence of separation tasks (splits) performed in the batch distillation column. The operational design for the individual separation task performed in order to achieve a specific product is carried out at level 2.

In a similar sense for the overall synthesis, the design of the task is realized by the identification of a sequence of sub-tasks (periods) with the final objective of achieving a product of specified purity and recovery. The sub-tasks for the batch distillation process have been defined as operation at constant reflux ratio and vapour boilup rate. Level 2 in the algorithm consists of an iterative procedure that yields the values for these variables for each period along with the duration of each sub-task. The reflux ratio profile generated can then be verified either experimentally or through dynamic simulation. The verification through dynamic simulation can be considered as part of the procedure for the generation of a reflux ratio profile. Verification and appropriate adaptation of the duration of each period might be necessary before the suggested reflux ratio can be used as an initial point for further optimization.

In summary, an algorithm was developed for generating a piecewise constant reflux ratio profile, capable of achieving the specified product(s) objectives of

purity and recovery, while providing at a higher level the order of obtainable products when multicomponent mixtures are considered. Determining whether an intermediate cut is necessary before a high purity product can be obtained is also available in the developed algorithm. In the case where minimum boiling azeotropes are present, the identified order of possible products is different, since certain products can not be obtained depending on the feed composition compared to the azeotropic composition.

The strong feature of the algorithm is the use of the driving force approach to identify the minimum reflux ratio for a considered composition. Using only the VLE data of the adjacent binary pairs, the reflux ratio values for each interval are found *a priori*. The generated reflux ratio profile does not need rigorous models, it is less demanding in computational effort and it can also be used as a very good starting point for a dynamic optimization problem.

## 3.4 Task: Batch Crystallization

### 3.4.1 Introduction

Separating a mixture of components by fractional crystallization might seem simple, but we do not know yet how to sequence simple operations, such as heating, cooling, evaporating, etc. to accomplish several industrial applications. According to Cisternas and Rudd (1993) the legal system recognizes that the design of even moderately complicated fractional crystallization processes is beyond the ordinary skill of “one versed in the art” and novel process designs can usually be patented.

An algorithm has been developed for the synthesis and design of batch crystallization processes based on information obtained from solid-liquid equilibrium phase diagrams. The developed algorithm identifies *a priori* a series of sub-tasks and their nature, in order to meet specified end objectives for the separation, namely a desired recovery for one or more solutes (products).

Since the algorithm is based on phase diagrams, some theoretical background on composition plots, the representation of material balance lines on them and the lever rule are provided in the following subsection. The next subsection introduces the developed set of rules for the identification of the solid whose precipitation is feasible, and for the identification and design of the necessary sub-task. The case where the desired solid recovery can only be achieved with an alternate solids precipitation is presented next and the number of necessary precipitations is determined. Last, the algorithm is described step-by-step.

### 3.4.2 Theoretical Background

In crystallization, graphical methods can be used for the sequencing of batch operations and the identification of crystallization paths. Composition phase diagrams can serve to map the system to be separated, the equilibria present

and the results of various process manipulations, such as evaporation, dilution, mixing and solids separation.

A short introduction to the theoretical background for batch crystallization synthesis is given. This includes composition plots and the representation of material balances in them, the lever rule, equilibrium lines and phase diagrams and the classification of phase systems separated by fractional crystallization.

### 3.4.2.1 Composition plots

The composition of a three component system,  $S$ ,  $A$  and  $B$ , can be represented on a two-dimensional graph, such as figure 3.12.  $S$  denotes the solvent from which solutes  $A$  and  $B$  are selectively crystallized. If the composition of  $S$  is  $x\%$  and of  $A$  is  $y\%$ , then the composition of  $B$  is  $z\% = 100 - x - y$ . The composition of the system can be represented either with triangular coordinates  $(x, y, z)$  or with Cartesian coordinates  $(X, Y)$ .

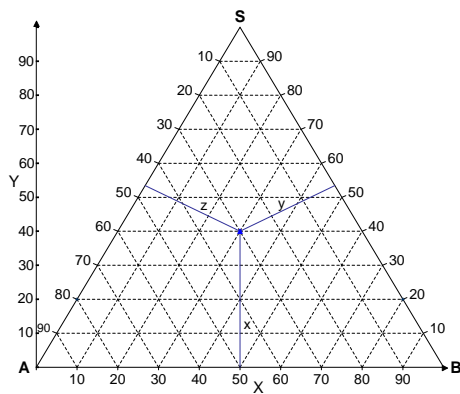


Figure 3.12: Cartesian and triangular coordinates in an equilateral plot

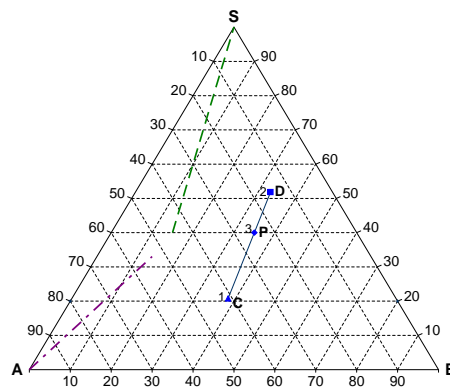


Figure 3.13: Construction lines and material balances represented in an equilateral plot

The interchange from triangular to Cartesian coordinates is:

$$\begin{aligned} X &= x/2 + z \\ Y &= x \end{aligned} \quad (3.26)$$

The composition of a quaternary system,  $S$ ,  $A$ ,  $B$  and  $C$ , can also be represented on a two-dimensional graph  $S$  denotes the solvent from which solutes  $A$ ,  $B$  and  $C$  are selectively crystallized. If the composition of  $A$  is  $x\%$ , of  $B$  is  $y\%$  and of  $C$  is  $z\%$ , then the composition of  $S$  is  $w\% = 100 - x - y - z$ . The composition of the system can be plotted in a 3D space using the tetrahedral space model (coordinates  $x, y, z, w$ ), such as in figure 3.14. The sides

of the tetrahedral, like  $ABS$  (Solids  $A$ ,  $B$  and Solvent  $S$ ) and  $BCS$ , are actually two-component plus solvent triangular diagrams, which have been covered above.

The composition of the quaternary system can also be projected from a 3D onto a 2D space. The graph of the projection, also known as *Jänecke projection*, is shown in figure 3.15. Jänecke (1906) set out the rules for drawing phase boundaries and working with the graphs to visualize process operations. All the solutions illustrated in a Jänecke projection are saturated. The Jänecke projection is based on the assumption of the sum of salts being equal to a 100%. The key point is that changing the amount of water in the system does not move the position of the composition point on the projection surface.

So, for any system with an actual composition  $(x, y, z, w)$  what is plotted in the projection diagram is the solvent-free composition of the system  $(x^{sf}, y^{sf}, z^{sf})$ . The solvent-free composition is given with triangular coordinates that can easily be changed to Cartesian coordinates, according to equation 3.26. Additionally, the composition of the solvent in Cartesian coordinates in the 3D space is  $Z = w$ .

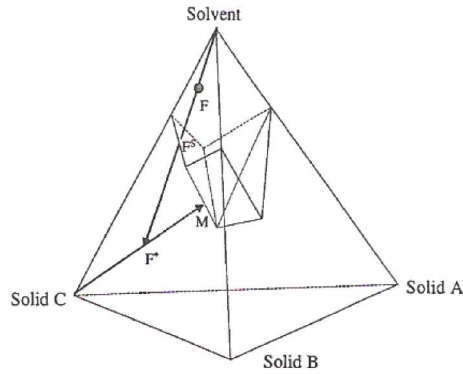


Figure 3.14: 3D representation of a phase diagram in the tetrahedral space model [(Takano, 2000)]

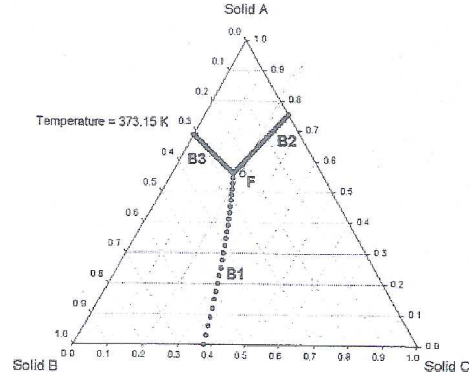


Figure 3.15: 2D representation of a phase diagram in a Jänecke projection [(Takano, 2000)]

### 3.4.2.2 Material Balance lines

Various process manipulations can be represented on the triangular phase diagram based on the principle of mass conservation. As shown in figure 3.13, if any two systems with compositions represented by points 1 and 2 are mixed together, then the locus of compositions of the resulting system 3 will be on the straight line connecting points 1 and 2. This straight line is called a tie line. A tie line is a line connecting the compositions of the two phases/systems in a phase diagram.

The majority of the process operations for crystallization can be represented on the phase diagram. So for an evaporation or dilution operation, where solvent is respectively removed or added to a given system, the composition of the residue must plot somewhere along a line starting from the solvent apex, such as the bold dashed line in figure 3.13. The composition of the residue obviously moves along the line towards the solvent apex when dilution takes place and away from it when solvent is removed (evaporation). Similarly, the precipitation of a solid  $A$  will move the composition of the residue along the dash-dot line away from the solid apex.

### Lever Rule

Applying the Lever Rule on a tie line of the phase diagram allows one to obtain information such as the amount of solvent that needs to be removed (evaporation) or added (dilution) to achieve a specific slurry or the specific amount of solid that will precipitate from a given slurry.

The Lever rule is:

*The relative amounts of two coexisting phases are **inversely** proportional to their distance from a point.*

Thus, for a system with composition of point 3 in figure 3.13,  $C_o$ , that splits into amount  $s$  of system 1 with composition  $C_s$  and into amount  $l$  of system 2 with composition  $C_l$ , the following equations apply:

$$\begin{aligned}(s + l)C_o &= sC_s + lC_l \\ C_o &= \frac{s}{s + l}C_s + \frac{l}{s + l}C_l \\ C_o &= f_s C_s + (1 - f_s)C_l\end{aligned}\tag{3.27}$$

where  $f_s$  is the fraction of amount  $s$  in system 3.

By rearranging

$$C_o - C_l = f_s(C_s - C_l)\tag{3.28}$$

Finally, fractions  $f_s$  and  $f_l$  are given:

$$\begin{aligned}f_s &= \frac{C_o - C_l}{C_s - C_l} \\ f_l &= \frac{C_o - C_s}{C_l - C_s}\end{aligned}\tag{3.29}$$

In terms of lengths of the tie line where points 1, 2 and 3 are located, fractions  $f_s$  and  $f_l$  can be represented as such:

$$\begin{aligned}
 f_s &= \frac{\overline{PD}}{\overline{CD}} \\
 f_l &= \frac{\overline{CP}}{\overline{CD}}
 \end{aligned}
 \tag{3.30}$$

The use of the Lever Rule and tie lines give meaning to phase diagrams and allow pencil and paper analysis of even complex phase diagrams.

### 3.4.2.3 The phase diagram

At equilibrium, all systems of any given composition will consist of one or more phases. In fractional crystallization, the phase diagrams considered are those of solid-liquid equilibrium diagrams, which mean that a solution phase always needs to be present. There can be many solid phases, one for each of the different salts crystallizing. A phase can exist over a range of temperatures and compositions.

The phase diagram represents a set of equilibrium curves on a composition map, which indicate the phases present at a given temperature and composition. The location of these equilibrium lines change with temperature including that solid phases may appear or disappear.

### 3.4.2.4 Types of phase systems

Fractional crystallization systems are typically composed of the solutes that need to be separated and the solvent from which they selectively crystallize. Three basic types of phase systems are recognized (Fitch, 1970):

#### Type I:

Solutes crystallize without forming either solid solutions or compounds among themselves (double salts). They may, however, form compounds with the solvent (hydrates).

#### Type II:

Solutes crystallize as compounds (double salts).

#### Type III:

Solutes crystallize in solid solutions.

This thesis deals with the first two types of systems. A typical phase diagram for a Type I system at a temperature  $T$  is shown in figure 3.16, while a typical phase diagram for a type II system is illustrated in figure 3.17.  $ABS$  is a hydrate of the double salt formed between  $A$  and  $B$  and this is the reason it is located inside the phase diagram and not in the  $AB$  axis.

In figure 3.16, solutions with a composition along the bold curve between regions  $a$  and  $b$  are saturated with respect to component  $A$ ; those along the bold curve between regions  $a$  and  $c$  with component  $B$ . Region  $a$  consists of



unsaturated solution and no solid phase. Regions  $b$  and  $c$  consist of saturated solution and one solid phase, salt  $A$  and  $B$  respectively. In figure 3.17, solutions along the bold curve between regions  $a$  and  $e$  are saturated with respect to component  $ABS$  and region  $e$  consists of saturated solution and one solid phase, salt  $ABS$ . In the phase diagram of Type I system, region  $d$  consists of a saturated solution (with the composition of point  $Inv$ ) and two solid phases. In the phase diagram of Type II system, the remaining area (regions  $d_1$  and  $d_2$ ) consists of a saturated solution (with the composition of either point  $Inv1$  or point  $Inv2$ ) and two solid phases, namely solid  $A$  and  $ABS$  or solid  $ABS$  and  $B$ .

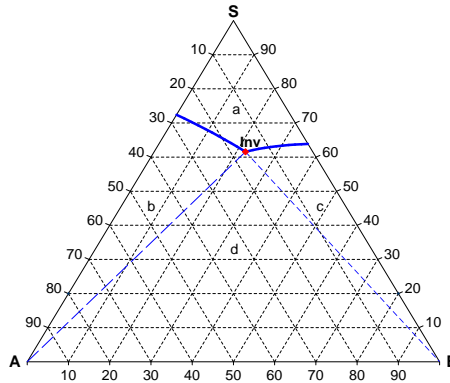


Figure 3.16: A typical phase diagram for a Type I system

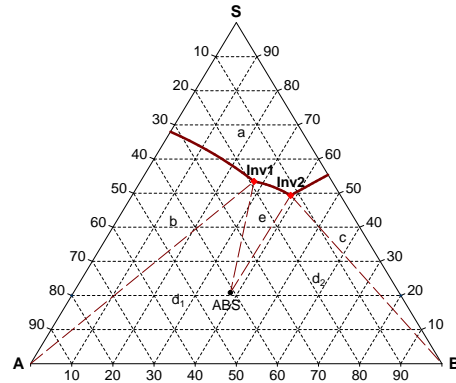


Figure 3.17: A typical phase diagram for a Type II system

In figures 3.16-3.17 above, the bold lines denote the solubility curves or single saturation curves for the solids that precipitate at one temperature. If the feed lies in a saturated region with respect to one component, then once the solid precipitates the remaining liquid in equilibrium has a composition that lies on the saturated curve. Two solubility curves meet at an invariant point  $Inv$ , shown as a red rhombus in the figures above, which is a multiple saturation point. For a ternary system, the invariant point is saturated with two solids while for a quaternary system the invariant points are saturated with three solids. The dashed lines in the figures are the borders of the saturated two-phase regions, one solid and one liquid. These dashed lines denote the change from a region saturated with one solid to a region saturated with two solids, the latter being a “three phase region”. These lines always start from a point that denotes a solid in the diagram and end up to an invariant point that is saturated at least with the respective solid.

#### 3.4.2.5 Solubility Index

For a solution saturated in a component  $s$  the solubility index  $SI$ , which is an expression for the degree of saturation, equals to unity. The solubility  $SI$

for salt  $s$  is defined as the activity product of salt  $s$  divided by its solubility product:

$$SI_s = \frac{\prod_i a_i^{\nu_{s,i}}}{K_s} \quad (3.31)$$

where  $a_i$  is the activity of component  $i$  calculated as the product of activity coefficient and composition,  $\nu_{s,i}$  is the stoichiometric coefficient of component  $i$  for the reaction (formation) of solid type  $s$  and  $K_s$  is the solubility product calculated from Gibbs free energy at the standard state.

The solubility index can be used to determine whether a mixture is located in the saturated region ( $SI_s \geq 1$ ) or the unsaturated region ( $SI_s < 1$ ) for a specific solid  $s$ . The solubility index calculation is particularly useful for the case of a solution with more than two salts dissolved.

Additionally, the solubility index calculation can be used to determine the amount of solvent that needs to be removed or added in order to obtain a specific amount of solid. As shown in figure 3.14 moving from point  $F$  to point  $F^*$ , it is only the amount of solvent that changes and both points are represented with the same point in the Jänecke projection diagram. Separating the solid that precipitates from point  $F^*$  yields a mother liquor, in equilibrium with the solid, represented by point  $M$  in figure 3.14. Moving from point  $F^*$  to point  $M$  it is only the amount of solid that has been removed that changes in the actual composition. That amount can be found using the lever rule. As a result, the solvent-free composition of point  $M$  is known.

Furthermore, point  $M$  lies on the saturation surface for the precipitating solid, which means that the solubility index is equal to 1. Solving equation 3.31, the composition of the solvent ( $w$ ) is found and thus the actual amount of the solvent. The difference in the amounts of solvent in the original feed  $F$  and the mother liquor  $M$  gives the amount of solvent that needs to be removed or added. Once the composition of the solvent ( $w$ ) is found, the actual composition of components  $A, B$  and  $C$  at point  $M$  is described as  $(1 - w) * x^{sf}, (1 - w) * y^{sf}, (1 - w) * z^{sf}$ , respectively.

### 3.4.3 Batch Crystallization Algorithm

An algorithm has been developed for the synthesis of batch crystallization, where the sequence of operational sub-tasks is identified, such as evaporation, leaching, dilution, heating or cooling. Furthermore, the design of each sub-task is also described in the algorithm in terms of the operating conditions, such as temperature or amounts of solvent that need to be removed or added.

This algorithm uses simple principles and methods, such as the conservation of mass and the lever rule, and it is solely based on the solid-liquid equilibrium phase diagram. It also uses a set of rules for the identification of the sequence of products whose precipitation is feasible (separation synthesis) and for the

operational design of each sub-task. These rules are based on insights from the understanding of the phase diagrams.

### 3.4.3.1 Batch Crystallization Algorithm Set of Rules

The identity of the solid precipitating depends on the feed composition or in terms of the phase diagram, it depends on the location of the feed in the diagram in relation to the position of the invariant point(s). In order for the solid to crystallize, the amount of solvent might have to be modified by means of evaporation or dilution.

However, before this operation and its conditions are chosen, the solid whose precipitation is feasible needs to be identified. The following rules can be used to identify whether the specified desired product can be precipitated from the given feed and also to determine under which conditions that precipitation is feasible.

#### Feasibility of precipitation

The case of a ternary system of a solvent  $S$  (50,100) and two solids A and B ( $(X_{solid}, Y_{solid}) = (0,0)$  and  $(100,0)$  respectively) is shown in figure 3.18.  $(X,Y)$  denotes the position in the triangular diagram in Cartesian coordinates. The feed  $F$  has  $(X_F, Y_F)$  coordinates and the coordinates of the invariant point(s) are denoted by  $(X_{inv,i}, Y_{inv,i})$ . In this case, two solids precipitate at the invariant point. The precipitation of a single solid is feasible in the following situations.

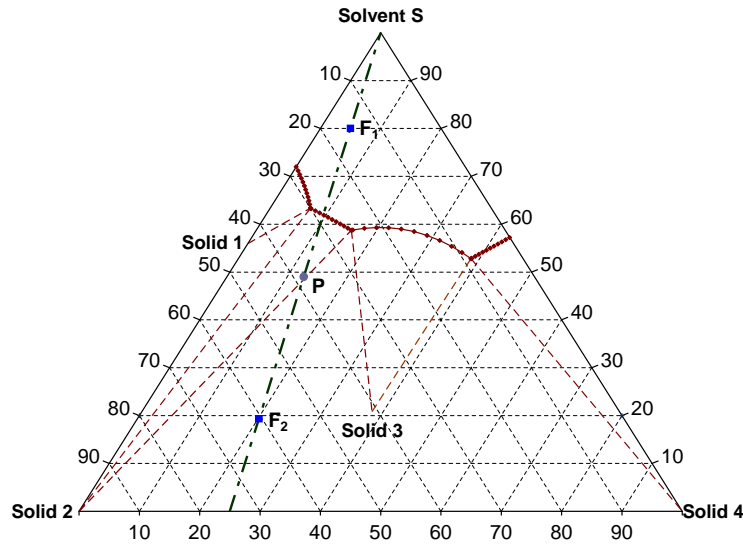


Figure 3.18: Solid-liquid phase diagram for a ternary system with evaporation axis

**Rule A3.1: single solid precipitation feasibility check**

*The precipitation of a single solid is feasible, if the evaporation/dilution line that connects the solvent and the feed does not pass through any of the invariant points*

Once the previous rule is applicable, then the identity of the solid to precipitate can be determined, as stated by the next rules. The following cases can be distinguished, according to the position of the feed in relation to the invariant point(s):

**Rule A3.2: task identification (identity of solid to precipitate)**

*Equation 3.32 is satisfied if the evaporation/dilution line lies to the left of the considered invariant point*

$$X = \frac{50 * (Y_{inv,i} - Y_F) - X_F * (Y_{inv,i} - 100)}{100 - Y_F} < X_{inv,i} \quad (3.32)$$

*and the solid that will precipitate is the one with the smaller  $X$  coordinate of the two solids precipitating at the specific invariant point (solid 2 in figure 3.18, ( $X_{solid2} < X_{solid3}$ )).*

**Rule A3.3: task identification (hydrate involved)**

*However, when the two solids precipitating at the considered invariant point are a pure salt and its hydrate, then the exactly opposite precipitation is feasible (than the one identified by rule A3.2), namely the solid with the larger  $X$  coordinate of the two.*

Equation 3.32 might be satisfied for more than one invariant point. In that case, the identity of the solid crystallizing is determined according to the invariant point that has the smallest  $X_{inv}$ .

**Rule A3.4: task identification (identity of solid to precipitate)**

*Equation 3.33 is satisfied if the evaporation/dilution line lies to the right of the considered invariant point*

$$X = \frac{50 * (Y_{inv,i} - Y_F) - X_F * (Y_{inv,i} - 100)}{100 - Y_F} > X_{inv,i} \quad (3.33)$$

*and the solid that will precipitate is the one with the larger coordinate  $X$  of the two solids precipitating at the specific invariant point.*

**Rule A3.5: task identification (hydrate involved)**

*The exception to rule A3.4 is that if equation 3.33 is satisfied and the two solids precipitating at the invariant point are a pure salt and its hydrate, then the precipitation is feasible for the solid with the smaller coordinate  $X$  of the two.*

Once again, equation 3.33 might be satisfied for more than one invariant point. In that case, the identity of the solid crystallizing is determined according to the invariant point that has the largest  $X_{inv}$ .

For a four-component system or a multicomponent system, the identity of the solid whose precipitation is feasible from a given solution (feed) is found with the help of the solubility index.

**Rule A3.6: task identification (multicomponent system)**

*For the mass composition of the feed, the solid that has the highest solubility index  $SI_s$  is identified as the solid whose precipitation is feasible. Alternatively, adjusting the solvent amount such that only one solid has a solubility index  $SI_s = 1$  provides the saturation conditions for the first precipitating solid.*

**Identification of operational sub-task**

The operation needed to obtain the feasible solid is identified according to the following rules.

**Rule A3.7: sub-task identification (evaporation)**

***Evaporation** will be necessary in order to obtain the identified pure solid, in the case when either equation 3.32 or 3.33 is satisfied and the  $Y$  coordinate of the feed is larger than that of the considered invariant point ( $Y_F > Y_{inv,i}$ ).*

When rule A3.7 applies, the feed actually lies either in an unsaturated region or it is situated in the saturated region for the specific solid whose feasible precipitation has been determined and further evaporation will yield more solid.

**Rule A3.8: sub-task design (evaporation)**

*The maximum evaporation ratio is given according to the lever rule:*

$$\text{Maximum evaporation ratio} = \frac{\overline{F_1P}}{\overline{PS}} \quad (3.34)$$

*and the amount of the solvent to be evaporated is found by multiplying 99 % of the maximum evaporation ratio with the considered feed.*

The amount of solvent to evaporate is chosen to be about 1 % less than the

maximum, in order to avoid ending up in a “three phase region” where cocrystallization occurs. In the above equation, point  $P$  is the point of intersection of evaporation axis and the line that connects the solid precipitating and the specific invariant point, from which the feasibility of the precipitation of the solid was identified according to one of the equations 3.32 - 3.33.

Evaporating less than the maximum ensures that the resulting slurry is positioned in a region of the phase diagram where only one pure salt precipitates.

**Rule A3.9: sub-task identification (further evaporation)**

*For the case when  $Y_F < Y_{inv,i}$  and the following equation is satisfied for the identified precipitating solid*

$$Y_F > \frac{Y_{inv,i} - Y_{solid}}{X_{inv,i} - X_{solid}} X_F + \frac{X_{inv,i} Y_{solid} - Y_{inv,i} X_{solid}}{X_{inv,i} - X_{solid}} \quad (3.35)$$

*then further **evaporation** is the operation needed to achieve a higher yield for the solid and the amount of solvent to remove is still found according to rule A3.8*

If the above equation 3.35 is satisfied, the feed actually lies in the saturated region for the solid identified.

**Rule A3.10: sub-task identification (dilution)**

*For the case when  $Y_F < Y_{inv,i}$  and the following equation is satisfied for the identified precipitating solid*

$$Y_F < \frac{Y_{inv,i} - Y_{solid}}{X_{inv,i} - X_{solid}} X_F + \frac{X_{inv,i} Y_{solid} - Y_{inv,i} X_{solid}}{X_{inv,i} - X_{solid}} \quad (3.36)$$

*then **dilution** is the operation needed in order to guarantee the precipitation of the pure identified solid.*

If equation 3.36 is satisfied, the feed lies in the “three phase region” where two solids precipitate. This is an unwanted situation because it compromises the purity requirement of the precipitated solids. If the feed ends in the “three phase region” because of shifting to another temperature, then the dilution operation has to proceed the heating/cooling operation that will achieve the higher or lower temperature.

**Rule A3.11: sub-task design (dilution)**

*The minimum dilution ratio is given according to the lever rule:*

$$\text{Minimum dilution ratio} = \frac{\overline{F_2P}}{\overline{PS}} \quad (3.37)$$

*and the amount of the solvent to be added is found by multiplying 101 % of the minimum dilution ratio with the considered feed.*

Similarly to rule A3.8, the amount of solvent to add is chosen to be about 1 % more than the minimum, in order to make certain that the resulting slurry is located in a region of the phase diagram where only one pure salt precipitates.

However, if the identified solid is a hydrate of a pure salt and the desired product is the pure salt, then a different operational sub-task should be identified for the case that rule A3.10 applies. The operation is identified according to the two supplementary rules that follow:

**Rule A3.12: sub-task identification (evaporation, hydrate involved)**

*If equation 3.36 is satisfied and the identified solid (according to rules A3.3 or A3.5) is a hydrate of a pure salt, then an additional feasibility check will have to be performed. If equation 3.35 is satisfied for the pure salt (solid = pure salt), then **evaporation** is the operation that is needed to obtain the pure salt. The amount of solvent to be removed is found according to rule A3.8 for the pure salt.*

When rule A3.12 is applicable, the feed lies in a “three phase region” where two solids precipitate. This region is located between the saturated region for the hydrate and the saturated region for its pure salt. In this case, point  $P$  in equation 3.34 is the point of intersection of the evaporation axis and the line that connects the pure salt precipitating and the second invariant point that is saturated with the pure salt. For that invariant point and the pure salt, either equation 3.32 or equation 3.35 is valid, depending on the relationship of  $Y_F$  with  $Y_{inv}$  ( $Y_F > Y_{inv}$  or  $Y_F < Y_{inv}$  respectively).

**Rule A3.13: sub-task identification (dilution, hydrate involved)**

*If equation 3.36 is satisfied and the identified solid (according to rules A3.3 or A3.5) is a hydrate of a pure salt, then if it is equation 3.36 that is also satisfied for the pure salt (solid = pure salt), then **dilution** is the operation that is needed to obtain the pure salt. The amount of solvent to be added is found according to rule A3.11 for the pure salt.*

For a four-component system or a multicomponent system, the identity of the operational sub-task needed to obtain the feasible solid is found according to the following rules.

**Rule A3.14: sub-task identification (evaporation, multicomponent system)**

*If the solubility index  $SI$  of all the solids in the system is less than unity, then the feed lies in an unsaturated region and **evaporation** is the necessary operational sub-task.*

**Rule A3.15: sub-task identification (dilution, multicomponent system)**

*If there are more than one solid whose solubility index  $SI$  is greater than unity, then the feed lies in a multi-phase region where more than one solids precipitate and **dilution** is the necessary operational sub-task.*

**Rule A3.16: sub-task design (multicomponent system)**

*The amount of solvent to evaporate or add is found as the difference between the amount of solvent in the original feed and the amount of solvent in the resulting mother liquor at the point where the solubility index of the precipitating solid is equal to unity.*

The position of the mother liquor in the phase diagram is easily found as the interception of the precipitating solid - slurry connecting line and the corresponding equilibrium line. Since for the solvent-free composition diagram, moving from the slurry (same position as the original feed) to the mother liquor the only difference is the amount of the precipitated solid, then the amount of the remaining solid in the mother liquor can easily be found. It is for that mother liquor composition that the amount of solvent needs to be found, where  $SI_s = 1$ .

**Determination of operating conditions**

The operating conditions of the crystallization in terms of temperature are chosen from the candidate set of potential operation point temperatures based on the following rules for the maximization of solid recovery.

**Rule A3.17: sub-task design (temperature)**

*The operating temperature for the crystallization is chosen, such that first the precipitation of the desired product is feasible and secondly in order for the resulting slurry after the removal or addition of solvent to have the highest possible slurry density. The slurry density is given by the following ratio:*

$$\text{Slurry Density} = \frac{\overline{SLML}}{\overline{SolidML}} \quad (3.38)$$

$SL$  refers to the point indicating the composition of the resulting slurry, while  $ML$  points out the composition of the mother liquid in equilibrium with the precipitating solid.  $Solid$  denotes the position of the precipitating solid in the phase diagram. For the case of quaternary systems, the position of the resulting slurry in the Jänecke projection diagram is the same as that of the feed and it is according to that point that the highest slurry density is chosen.

It is obvious from figure 3.19 that the position of the invariant point can move significantly with temperature. The choice of the operating temperature for the crystallization is therefore important, since it might mean feasible precipitation of the desired product or not. It can also be noticed that crystallization of solid  $A$  at  $0^\circ\text{C}$  would yield very small amounts of solid in comparison to crystallization at  $100^\circ\text{C}$  where the slurry density is highest.



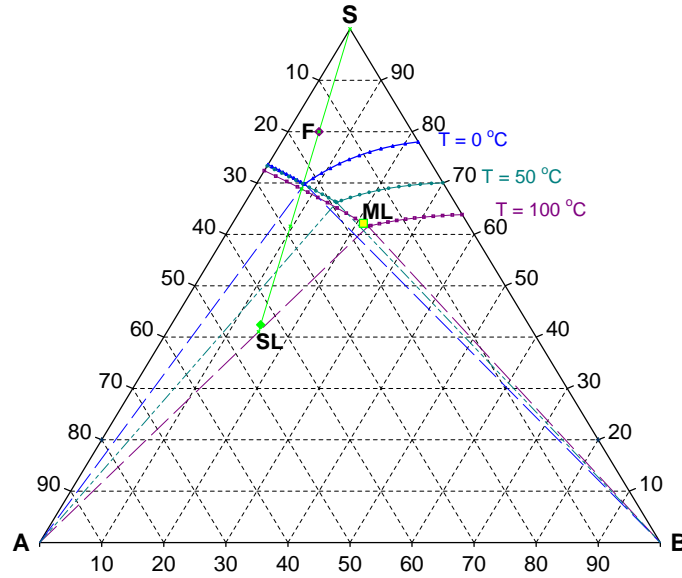


Figure 3.19: Selection of operating temperature for the crystallization based on slurry density

#### 3.4.3.2 Identification of alternate solids precipitation

The separation of a desired salt from a solution with a specified recovery might not be possible with a single precipitation of the salt at a specific temperature. However, the desired recovery might be achieved with an alternate solids precipitation (between the desired salt and a second salt in the system) at two temperatures  $T_1$  and  $T_2$  ( $T_{low}$  and  $T_{high}$ ). In order to identify when this case appears, some of the feasibility criteria mentioned above (i.e. rules A3.2-A3.5 and A3.17) are applied.

For a starting feed point  $F_1$  in the diagram and for a chosen temperature  $T_1$ , picked out according to rule A3.17, there is usually one solid precipitating by means of evaporation or dilution, unless the evaporation/dilution axis passes through the invariant point. The maximum evaporation ratio or the minimum dilution ratio, in order to achieve the largest amount of solid crystallizing, are given respectively by equations 3.34 and 3.37. The location of the slurry  $SL_1$  can be located exactly on the diagram, according to rules A3.8 and A3.11.

The composition of the mother liquor  $ML_1$  ( $X_{ML_1}, Y_{ML_1}$ ) in equilibrium with the solid precipitating is located in the ternary diagram on the equilibrium (saturation) line for the precipitating solid. If one considers the mother liquor as a new feed point, then the identity of the solid that will precipitate at a different temperature  $T_2$  (selected according to rule A3.17) is determined according to equations 3.32 or 3.33. The location of the slurry  $SL_2$  can be located exactly on the diagram, according to rules A3.8 and A3.11.

In this case, the evaporation or dilution needed can be calculated to be such that the resulting slurry  $SL_3$  has a composition given by the intersection of the evaporation/dilution axis and the line connecting the precipitating solid (vertex of triangle) and point  $SL_1$ . That guarantees that the resulting mother liquor after this precipitation will be the same as  $ML_1$ . The cyclic operation is then established, since one only has to move between points  $ML_1$ ,  $SL_2$ ,  $ML_2$  and  $SL_3$  until the desired product recovery is achieved. In figure 3.20  $ML_1 = SL_2$ .

For a mixture where the specified product recovery can be achieved with an alternate solids precipitation at two temperatures  $T_{low}$  and  $T_{high}$ , the number of precipitations  $p$  needed can be calculated in advance.

*In practice, only three slurry densities are necessary for that reason, namely the ones corresponding to points  $SL_1$  ( $p = 1$ ) and  $SL_3$  ( $p = 2i - 1, i = 2, \dots, n$ ) where the first identified solid precipitates and to point  $SL_2$  ( $p = 2i, i = 1, \dots, n$ ) where the second solid precipitates.*

The letter  $p$  denotes the  $p_{th}$  precipitation taking place in total, while  $i$  refers to the individual solid precipitation number.

The exact compositions of points  $F_1, SL_1, ML_1, SL_2, ML_2$  and  $SL_3$  are known, since they are found according to the rules and procedure described earlier. Additionally,  $ML_1 = ML_p$ ,  $p = 2i - 1$  for  $i = 1, \dots, n$ ;  $SL_3 = SL_p$ ,  $p = 2i - 1$  for  $i = 2, \dots, n$  and  $SL_2 = SL_p$ ,  $ML_2 = ML_p$  where  $p = 2i$  for  $i = 1, \dots, n$ .

The necessary slurry densities to calculate the total recovery of a precipitating solid are found, as described below. Firstly, in order to move from the original feed to a slurry composition that will give the highest solid yield, solvent might have to be removed or added. The evaporation/dilution ratio  $(ev - d)_1$  is given:

$$\text{Evaporation/Dilution ratio } (ev - d)_1 = \frac{\overline{F_1 SL_1}}{\overline{SL_1 S}} \quad (3.39)$$

where point S denotes the solvent S.

The resulting slurry is found by subtracting or adding the amount of solvent that is evaporated from or added to the original feed  $F_1$ :

$$\text{Amount of slurry } SL_1 = (1 \pm (ev - d)_1)F_1 \quad (3.40)$$

From the lever rule, the slurry density of the resulting slurry is found and the exact amount of the solid that will precipitate is calculated by multiplying the slurry density with the amount of the slurry, as shown in equation 3.41:

$$\text{Slurry Density } \varrho_{SL,p} = \frac{\overline{SL_p ML_p}}{\overline{Solid_s ML_p}} \quad (3.41)$$

$$\text{Amount of solid pptd} = \varrho_{SL,p} SL_p$$

In the above equations,  $p$  denotes the precipitation number which takes place in series,  $s$  denotes the solid that crystallizes each time and  $SL$  is the amount of the slurry (e.g. in kg). As shown in figure 3.20, for the first precipitation  $p = 1$  and  $s = 1$  ( $s \in [1, 2]$ ).

The amount of the mother liquor in equilibrium with the precipitated crystals of solid  $s$  after precipitation number  $p$  is given by the following equation:

$$ML_p = ML_{p-1}(1 \pm (ev - d)_p)(1 - \varrho_{SL,p}) \quad (3.42)$$

For the case when  $p = 1$ ,  $ML_0$  corresponds to the original feed  $F_1$ .

The resulting mother liquor is treated as a new feed and the precipitation of the second solid at a different temperature is feasible. In order for the precipitation of a single solid to be feasible, solvent might have to be removed or added. The evaporation/dilution ratio is in general:

$$\text{Evaporation/Dilution ratio } (ev - d)_p = \frac{\overline{ML_{p-1} SL_p}}{\overline{SL_p S}} \quad (3.43)$$

For the case when  $p = 1$ , the above equation 3.43 is reduced to equation 3.39.

The recovery  $y_{ps}^s$  of the precipitating solid  $s$  after each precipitation that yields the respective solid is given from the following fraction:

$$\begin{aligned} \text{recovery } y_{ps}^s &= \frac{\text{Amount of solid } s \text{ precipitated (pptd)}}{\text{Amount of solid } s \text{ in slurry } SL_p} \\ \text{recovery } y_{ps}^s &= \frac{\varrho_{SL,p} SL_p}{x_{solid,s} SL_p} = \frac{\varrho_{SL,p}}{x_{solid,s}} \end{aligned} \quad (3.44)$$

where the superscript  $s$  denotes separation in this thesis (alternatively,  $r$  denotes reaction). The evaporation or dilution operation has no effect to the amount of the solids present, so the amount of solids in the considered feed (or previous mother liquor) is the same as in the resulting slurry. The slurry density  $\varrho_{SL,p}$  is given by equation 3.41 and  $x_{solid,s}$  is the weight fraction composition in triangular coordinates of the respective solid  $s$  for point  $SL_p$ , which is easily found by transforming the Cartesian coordinates for point  $SL_p$  to triangular coordinates.

As indicated earlier, for the precipitation of the first identified solid  $s$ , there are only two relevant slurry densities corresponding to points  $SL_1$  and  $SL_3$ . This means, in principle, that there are also only two values for the recoveries of the specified solid  $y_{11}^s$  and  $y_{31}^s$  ( $=y_{p1}^s, p = 2i - 1, i = 2, \dots, n$ ). Regarding the precipitation of the second solid, there is only one relevant slurry density corresponding to point  $SL_2$ , which means there is only one value for the recovery of the specified solid  $y_{22}^s$  ( $=y_{p2}^s, p = 2i, i = 1, \dots, n$ ), which is the same for each precipitation of the second solid.

Depending on whether the desired product is the first or the second solid precipitating, two cases can be distinguished:

1. The desired product is the first solid precipitating.

If the original amount in the feed of the first precipitating solid is  $SOLID_1$ , then according to equation 3.44, the amounts separated at the various specific solid precipitations ( $i = 1, n$ ) are:

$$\begin{aligned} \text{Solid pptd in precipitation } (i=)1 &= y_{11}^s SOLID_1 \\ \text{Remaining solid after precipitation } 1 &= (1 - y_{11}^s) SOLID_1 \\ \text{Solid pptd in precipitation } (i=)2 &= y_{31}^s (1 - y_{11}^s) SOLID_1 \\ \text{Remaining solid after precipitation } 2 &= (1 - y_{31}^s)(1 - y_{11}^s) SOLID_1 \end{aligned} \quad (3.45)$$

The amount of the solid in question remaining in the resulting mother liquor ( $ML_1$ ) does not change with evaporation or dilution or precipitation of the second solid. Similarly to equations 3.45, the  $i_{th}$  precipitation of the first precipitated solid is given from the equation below:

$$\text{Solid pptd in precipitation } i = y_{31}^s (1 - y_{31}^s)^{i-2} (1 - y_{11}^s) SOLID_1 \quad (3.46)$$

Dividing the sum of the amounts of solids crystallized in the individual precipitations for solid 1 with the original amount of the solid in the feed ( $SOLID_1$ ) yields the total recovery achieved for the first precipitating solid:

$$\text{Total recovery of 1st solid precipitating} = y_{11}^s + \sum_{i=2}^n y_{31}^s (1 - y_{31}^s)^{i-2} (1 - y_{11}^s) \quad (3.47)$$

2. The desired product is the second solid precipitating.

If the original amount in the feed of the second precipitating solid is  $SOLID_2$ , then according to equation 3.44, the amounts separated at the various specific solid precipitations ( $i = 1, n$ ) are:

$$\begin{aligned} \text{Solid pptd in precipitation } (i=)1 &= y_{22}^s SOLID_2 \\ \text{Remaining solid after precipitation 1} &= (1 - y_{22}^s) SOLID_2 \\ \text{Solid pptd in precipitation } (i=)2 &= y_{22}^s (1 - y_{22}^s) SOLID_2 \\ \text{Remaining solid after precipitation 2} &= (1 - y_{22}^s)^2 SOLID_2 \end{aligned} \quad (3.48)$$

Similarly to equations 3.48, the  $i_{th}$  precipitation of the second precipitated solid is given from the equation below:

$$\text{Solid pptd in precipitation } i = y_{22}^s (1 - y_{22}^s)^{i-1} SOLID_2 \quad (3.49)$$

The total recovery achieved for the second precipitating solid is found by dividing the sum of the amounts of solids crystallized in the individual precipitations for solid 2 with the original amount of the solid in the feed ( $SOLID_2$ ):

$$\text{Total recovery of 2nd solid precipitating} = \sum_{i=1}^n y_{22}^s (1 - y_{22}^s)^{i-1} \quad (3.50)$$

Substituting the specified value for the total recovery on the left hand side of either equation 3.47 or 3.50, one can solve to find the number of precipitations  $i$  for the individual solid. The total number of alternate precipitations in series is then found to be  $p = 2i - 1$  for the case when the desired product is the first identified precipitating solid (at temperature  $T_1$ ). For the case when the desired product is the second identified precipitating solid (at temperature  $T_2$ ), then the total number of precipitations needed is  $p = 2i$ .

#### 3.4.3.3 Stepwise Description of the Batch Crystallization Algorithm

The algorithm illustrated as a block diagram is shown in figure (3.21). For the application of the algorithm, the prerequisite information is:

**Given:**

- The identity of the solvent and the solutes and the initial feed charge and composition.
- The temperature range of operating the crystallizers and the desired product(s) recovery, i.e. the goals of the crystallization.
- The solid-liquid equilibrium phase diagram for the set of potential temperatures of operation.
- When the phase diagram needs to be estimated, the identity of the various forms that the dissolved salts might precipitate at different temperatures and over different composition ranges, such as hydrates and double salts, need to be included in the component list.

**Calculate:**

- The sequence of solids precipitating and the necessary operational sub-tasks to obtain each identified solid.
- The operating conditions of the individual sub-tasks, in terms of operating temperature and amount of solvent removed or added.

The algorithm is described in a stepwise fashion below.

1. Generate the solid-liquid equilibrium phase diagram for the operational temperature range.
2. Set sub-task (precipitation) number  $p = 1$   
For the specific feed, identify the solid that precipitates over the permitted temperature range according to rules A3.1 to A3.5.
3. Identify the operating temperature for the sub-task according to rule A3.17
4. Identify the sub-task according to rules A3.7, A3.9-A3.10 and A3.14-A3.15, in terms of evaporation or dilution. Additionally, when the identified solid is a hydrate of a pure salt, check against rules A3.12 to A3.13 before identifying the specific sub-task.
5. Calculate the exact amount of solvent to remove or add according to rules A3.8, A3.11 or A3.16, i.e. design the sub-task action.
6. Knowing the exact location of the slurry on the phase diagram, compute the recovery of the solid for the individual sub-task.
7. Calculate the overall recovery of the precipitated solid at sub-task  $p$ .
8. Check whether the desired or maximum product(s) recovery has been achieved for all the specified products, i.e. are the goals satisfied.  
If yes, the *end* of the batch crystallization synthesis has been reached and the suggested operational model satisfies all end objectives.  
Otherwise, proceed to step 9.

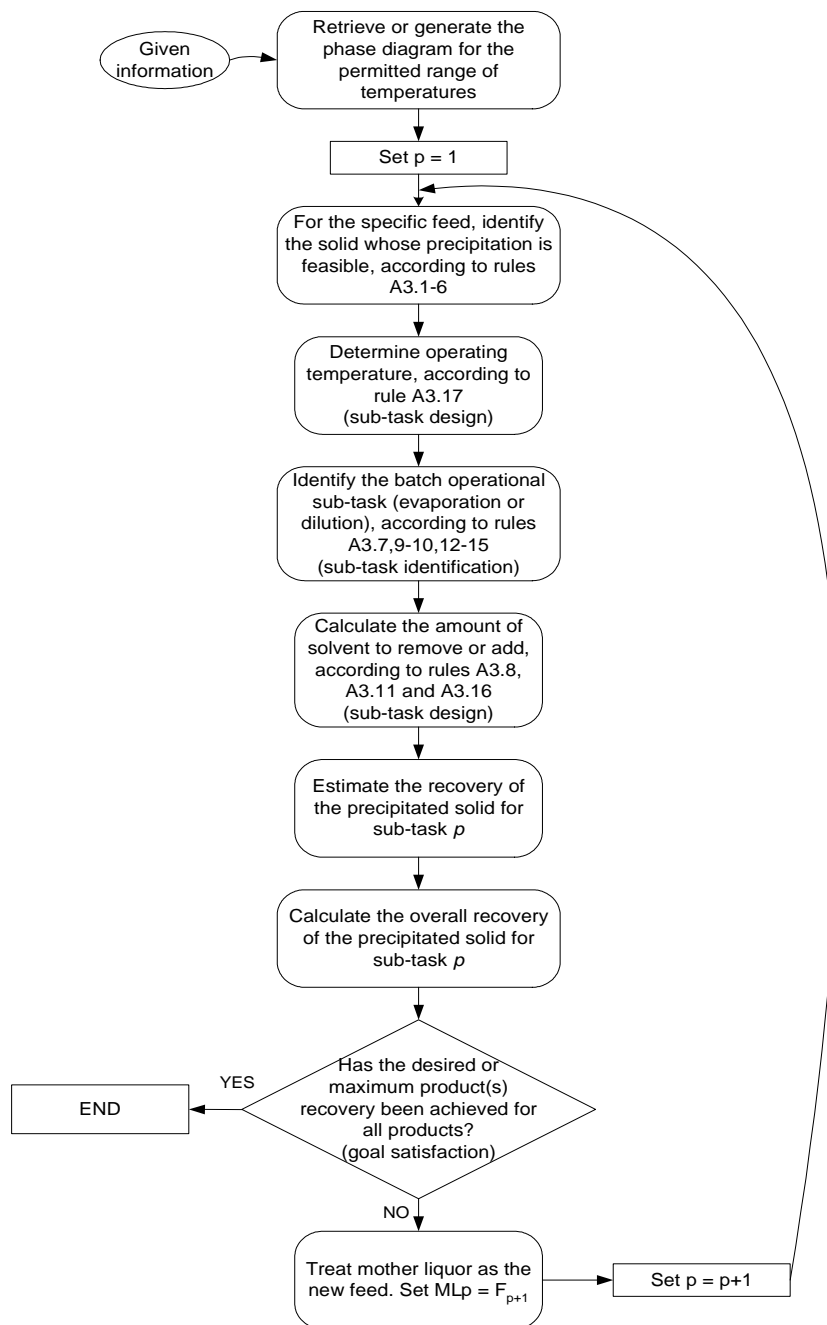


Figure 3.21: Block diagram of the algorithm A3 for the generation of a sequence of separation tasks based on batch crystallization as well as the generation of the operational design for each separation task

9. Treat the resulting mother liquor after the separation of the precipitated solid as the new feed for the next sub-task  $p + 1$ . Go to step 2.

The algorithm described above will be from now on referred to as Algorithm A3.

In summary, the developed algorithm for the synthesis and design of batch crystallization provides a sequence of sub-tasks, such as isothermal evaporation or dilution and heating or cooling that are accompanied by solid-liquid separation. The end objective for the crystallization is the achievement of a desired or maximum recovery for one or more solids. The algorithm consists mainly of a repetitive procedure that identifies the type of operation for each sub-task (synthesis) and its conditions (design), based on solid-liquid phase diagrams. Access to these diagrams is easy, through the utility toolbox of ICAS, which is described in chapter 4 of this thesis.

The feasibility of the precipitation of a solid from a given feed is examined for a range of temperatures and both the operating temperature and the amount of solvent necessary to be removed or added are determined. The operating temperature is chosen so that the amount of solid precipitating from the resulting slurry is the highest. The removed or added solvent amount is calculated in such way as to avoid regions in the diagram, where two or more solids precipitate, since this is not effective separation. All the decisions taken based on the phase diagrams are accurate, since the exact coordinates of the solubility curves are given and the equations for the evaporation/dilution lines, the “precipitated solid-slurry-mother liquor” lines and their intersections can be exactly calculated.

Furthermore, theory has been developed to identify in advance the number of precipitations needed to achieve a desired recovery for a solid, when its specified recovery can only be achieved with an alternate solids precipitation at two different temperatures  $T_{low}$  and  $T_{high}$ .

## 3.5 Synthesis of Batch Processes

### 3.5.1 Introduction

The problem of the synthesis of batch processes is usually regarded already solved when scheduling or plant design problems are considered. The generation of the actual sequence of tasks necessary to recover a set of desired products by converting a given set of raw materials is handled in the developed algorithm. The algorithm generates a sequence of reaction and separation tasks and the intermediate objectives for each task in the sequence. The synthesis algorithm also integrates the previously developed algorithms, which provide the batch operations model for each identified task in the sequence. Thus, the solution to the synthesis problem is the complete batch route with the corresponding operational models for each task.



The theoretical background for the synthesis algorithm comes from a separation synthesis methodology for continuous processes (Jaksland, 1996) and is presented in the next subsection. The extension to batch processes and the inclusion of reaction tasks in the sequence is considered next. A set of developed rules for the systematic identification and positioning of separation tasks in the sequence follows and the stepwise description of the algorithm concludes the synthesis section.

### 3.5.2 Theoretical Background

The algorithm presented in Jaksland (1996) is used as the basis for the identification of the separation technique for each of the separation tasks needed, in order to obtain the final products from a set of raw materials. This algorithm is based on thermodynamic insights, where the relationship between compound properties and separation techniques is identified.

The Jaksland algorithm consists of two levels, each of which is divided in 6 sub-algorithms. At the first level, all possible binary pairs from the considered mixture are identified together with existing azeotropes. For each pair the binary property ratios (for the properties in table 6 of appendix C) are computed and the largest property ratio identifies the most feasible separation technique for the specified pair. After a step where a screening process is performed, the largest (remaining) ratio indicates the first separation task (first split between the selected binary pair) and the corresponding separation technique.

At the second level, pure component and mixture properties are employed to simultaneously sequence and select the separation tasks and corresponding separation techniques. Including mixture properties, at this level, allows one to verify the choice of separation tasks from level 1, consider also separation techniques that require MSAs (Mass Separating Agents; techniques also given in table 6 of appendix C) and determine improved estimates of the operating conditions. At the end of this level, a physically feasible flowsheet is produced together with feasible alternatives for each separation task.

In summary, the Jaksland algorithm with the objective of determining physically feasible flowsheets is based on exploiting the largest driving force for every separation and therefore suggests a flowsheet with a sequence of the easiest separations. However, the existing algorithm determines flowsheets for continuous processes and does not consider the dynamic nature of batch processes.

In this Ph.D.-project, it is specifically the first level sub-algorithms that are used (entirely or partly) and extended, in order to identify a feasible sequence of reaction and separation tasks for batch processes. The extension considered in this thesis is the inclusion of reaction tasks in the generated batch route and the identification and positioning of a particular separation task, based on mixture and reaction analysis and the extent of feasibility for the corresponding identified separation technique. The flexibility of batch processes and the ability of obtaining more than one pure product from a batch separation unit are also considered.

### 3.5.3 Batch Processes Synthesis Algorithm

The suggested methodology for the synthesis of batch processes is based on a set of rules. The developed set of rules deals with the synthesis of batch processes in a similar manner to the level 1 synthesis of the Jaksland algorithm. Considering the possible composition of the outflow of a batch reactor (in terms of compound identities), the most feasible separation technique is identified. Mixture analysis provides knowledge of existing azeotropes and separation boundaries for the various batch reactor effluent mixtures. The knowledge gained from the mixture analysis for the raw materials as well as the reactor product mixtures provides the insights for the positioning of separation tasks necessary to ensure the purity and recovery objectives for the products.

For the case when more than one set of reactions needs to take place, each set corresponds to a reaction task. These reaction tasks together with a separation task in the end provide the initial sequence of tasks. However, the concluding sequence of reaction and separation tasks is found once the necessity of arranging separation tasks prior, between and after the reaction tasks is determined, based on the developed set of rules.

Once the reaction/separation sequence and the individual separation techniques are identified, the actual estimates for the operating conditions for each task are determined in a piecewise fashion (for each sub-task in the main task considered). Similarly to level 2 of the Jaksland algorithm for continuous processes, the developed algorithms for batch reaction, distillation and crystallization are used to determine the operation model for each task. The operation models provided by the above mentioned algorithms complete the synthesis of batch processes.

#### 3.5.3.1 Developed Theory

For a mixture of  $NC$  compounds the possible binary pair combinations are found to be  $\frac{(NC-1)NC}{2}$ . However, the binary pairs between which a split can be made can only be the adjacent pairs of the mixture, which are  $NC - 1$ . The identity of the adjacent pairs depends on the considered property.

The compounds of the mixture need to be listed in decreasing order for all the properties in table 6 of appendix C. The binary property ratios  $r_{ij}$  for the respective adjacent pairs can then be calculated and listed.

$$r_{ij} = \frac{p_{jA}}{p_{jB}} \quad (3.51)$$

where  $p_{jA} \geq p_{jB}$ . Subscripts  $i$  and  $j$  refer to the adjacent binary pair and to the property considered, respectively. Subscripts  $A$  and  $B$  indicate the two components of the binary pair  $i$ .

Specifically, for the case of (batch) distillation, which is related to normal boiling point and vapour pressure, any existing minimum boiling azeotrope should be added to the list of compounds of the considered mixture when

the property ratios of the adjacent binary pairs are calculated for the two specific properties. If the feed composition of the azeotropic pair is known compared to the azeotropic composition, then one of the two compounds in the azeotropic pair can be eliminated from the list of compounds of the considered mixture. The identity of the compound that needs to be eliminated has been discussed earlier in section 3.3.3.5. The reason why the specific compound can be eliminated is that once the minimum boiling azeotrope is obtained, one of the two components is no longer present in the mixture.

If the values of  $r_{ij}$  are not close to unity, a separation technique is, in principle, likely to be able to exploit the differences in property  $j$  for the binary pair  $i$ . The significance of the deviation from unity varies for different property-separation technique relationships. However, in all cases a property ratio close to unity indicates a difficult separation task (the “closeness” also varies for different properties).

For a binary pair  $i$ , the feasibility of a separation technique  $k$ , which is related to property  $j$  is found according to (Jaksland, 1996):

If,  
 $r_{ij} \leq m_{kj}$ , then separation technique  $k$  is **infeasible** for binary pair  $i$ .  
 $m_{kj} \leq r_{ij} \leq M_{kj}$ , then separation technique  $k$  is **feasible** for binary pair  $i$ .  
 $M_{kj} \leq r_{ij} \leq N_{kj}$ , then separation technique  $k$  is **most feasible** for binary pair  $i$ .  
 $N_{kj} \leq r_{ij} \leq n_{kj}$ , then separation technique  $k$  is **feasible** for binary pair  $i$ .  
 $r_{ij} \geq n_{kj}$ , then separation technique  $k$  is **infeasible** for binary pair  $i$ .

The values for  $m_{kj}$ ,  $M_{kj}$ ,  $N_{kj}$  and  $n_{kj}$  for the individual separation techniques and properties are given in table 6 of appendix C. Screening out the infeasible separation techniques for each binary pair is easy and it is the next step. The property ratios that suggest an infeasible separation technique should be removed from each property list.

In the Jaksland algorithm, the “possibility distribution”  $\mu(r_{ij})$  (Qian and Lien, 1995) is used to determine the extent to which a separation is feasible for a binary separation task, for the case of just feasible separations. The “possibility distribution”  $\mu(r_{ij})$  is given:

$$\mu(r_{ij}) = \frac{r_{ij} - m_{kj}}{M_{kj} - m_{kj}} \quad (3.52)$$

Obviously, from equation 3.52,  $\mu(r_{ij})$  is between 0 and unity for just feasible separations. If  $\mu(r_{ij})$  was used to compare the extent of feasibility for the most feasible separations, then in those cases it would be greater than unity. For the most feasible separations  $\mu(r_{ij})$  is set to unity, since the scale difference for the values of  $m_{kj}$  and  $M_{kj}$  does not allow the use of  $\mu(r_{ij})$  as a reliable measure of comparison.

However, for the property ratios identifying a separation technique as very

feasible, their scaled values can be used for comparison of the extent of the feasibility of these separations. The separation feasibility index  $M_{kj}$  is used for this purpose.

$$sr_{ij} = \frac{r_{ij}}{M_{kj}} \quad (3.53)$$

After the screening, comparing the “possibility distribution”  $\mu(r_{ij})$  and the scaled binary property ratios  $sr_{ij}$  for the remaining adjacent binary pair property ratios, the separation technique that should be used is identified by the largest  $\mu(r_{ij})$  or  $sr_{ij}$  of all.

Once the separation technique is identified, the exact sequence of attainable products is determined from the application of the developed batch operations model design algorithms of this thesis for batch separation, which would be equivalent to level 2 of the Jaksland algorithm for continuous processes.

Furthermore, in the case where more than one set of reactions is needed to obtain the final product then the property ratios for the adjacent binary pairs for the specified reaction product can also be used to identify whether a separation task is necessary or desirable between two consecutive reaction tasks.

Specifically in the case where more than one set of reactions is necessary to obtain the final product, the presence of separation boundaries needs to be identified in advance, especially when the final product is involved and its recovery is endangered.

The issues of separation boundaries as well as the insights derived from reaction kinetics analysis are discussed during the development of the following set of rules for the synthesis of batch processes.

### 3.5.3.2 Batch Processes Synthesis Algorithm Set of Rules

The set of rules have been developed for the identification and sequencing of the necessary batch operations, in terms of reaction and separation tasks. The rules are based in some cases on basic chemical engineering knowledge and common logic, while others derive from thermodynamic and process insights.

The primary sequence of major batch tasks, such as reaction and separation, is determined from the following rule.

#### Rule S.1: initial sequence of tasks identification

*Given a set of raw materials and the objective to obtain one or more final products of specific purity, then at least one reaction task and at least one separation task is needed.*

#### Rule S.2: number of separation tasks identification

*If more than one final product is desired, then the minimum number of separation tasks is that of the number of specified products minus one.*

The exact identity of the separation technique for the separation task is found according to the next rule as the one that is the easiest and most feasible separation.

**Rule S.3: separation technique identification**

*The separation technique for a separation task is identified from the largest scaled binary property ratio  $sr_{ij}$  or "possibility distribution"  $\mu(r_{ij})$  for the adjacent binary pairs of compounds present in the system.*

*Subsequently, the second largest  $sr_{ij}$  or  $\mu(r_{ij})$  can identify the second easiest separation, and so on.*

**Rule S.4: separation batch operations model identification**

*Once the separation technique is identified, the application of the corresponding batch separation algorithm will provide the exact sequence of obtained products and thus the exact sequence of separation tasks.*

For the above rule, a separation task is defined as a task performed to obtain one product or otherwise is a split between the attained product and its adjacent compound. The adjacent compound is found in terms of the property on which the separation technique is indicated.

The question whether a separation task is necessary before a reaction task is discussed in the following rules.

**Rule S.5: sep. task prior to 1<sup>st</sup> reaction task identification (raw materials)**

*If the raw materials for the reaction task are not of the required purity, then a separation task may be advantageous before the next reaction task.*

**Rule S.6: no separation task prior to 1<sup>st</sup> reaction task (impurities and reaction)**

*If the impurities are inert and do not take part in the given set of reactions, then a separation task is not necessary prior to the reaction task.*

**Rule S.7: no separation task prior to 1<sup>st</sup> reaction task (impurities and separation)**

*If the impurities do not form any separation boundary, such as an azeotrope, with the final product(s), then a separation task is not necessary prior to the reaction task.*

*If there is more than one reaction task and a separation task is identified in the sequence after the first reaction task, then the impurities should not form a separation boundary with the specified (intermediate) product of the first reaction task.*

**Rule S.8: sep. task prior to 1<sup>st</sup> reaction task identification (impurities and reaction)**

*If the impurities take part in the given set of reactions and form byproducts by consuming the limiting reactant, then a separation task may be necessary prior to the reaction task.*

*The separation task might be avoided if the selectivity of the desired reaction over the competing reaction, where the impurities are consumed, is very high and therefore in practice the competing reaction is suppressed.*

**Rule S.9: sep. task prior to 1<sup>st</sup> reaction task identification (impurities and separation)**

*If either the impurities or their byproducts form any separation boundaries, such as an azeotrope, with the final product, then a separation task is necessary before the first reaction task.*

If rules S.8 and S.9 apply and the impurities are not removed, then the recovery of the product will be undermined. However, if the concentration of the impurities is very small and the objective for the product recovery is sufficiently flexible to allow limiting reactant to be converted to byproduct or part of the desired product to be removed as waste (e.g. azeotrope), then the preceding separation task to the reaction task can be omitted. The conversion of the limiting reactant to a byproduct instead of a desired product is affecting the product's recovery, as discussed in rule S.6, but small conversion might be allowed. The presence of an azeotrope between an impurity and a product will affect the product's purity objective, as discussed in rule S.7, but a small amount might have a sufficiently small effect.

The next rules are used to identify the placement of a separation task between two consecutive reaction tasks in the sequence of reaction and separation tasks. Obviously, the necessity of such an intermediate separation task exists only when the final product is obtained after at least two set of reaction tasks.

**Rule S.10: sep. task identification between two consecutive reaction tasks**

*When there is more than one reaction task needed for the final product to be produced, the identification of a separation task between two reaction tasks is decided by comparing the reactant mixtures at the end of the respective reaction tasks.*

After the separation technique is chosen for each of the respective reactant mixtures (the outflows of two succeeding reaction tasks), then the scaled binary property ratio  $sr_{ij}$  (eq. 3.53) or the "possibility distribution"  $\mu(r_{ij})$  (eq. 3.52) for the adjacent binary pairs where the respective products are involved are compared.

**Rule S.11: sep. task identification between two consecutive reaction tasks (feasibility/easiness of separation)**

*The largest scaled binary property ratio  $sr_{ij}$  or “possibility distribution”  $\mu(r_{ij})$  among the adjacent binary pairs for the respective (intermediate or final) products, indicates that a corresponding separation task is easiest.*

*If that is the separation task after the first reaction task of the two, then a separation task might be introduced between the two reaction tasks in the sequence.*

The presence of separation boundaries and their relation to the respective products (at the end of each reaction task) can also be used to determine whether a separation task has to be introduced between the two reaction tasks.

**Rule S.12: sep. task identification between two consecutive reaction tasks (byproduct-final product separation boundary)**

*If any of the byproducts of the first reaction set (of the two compared) form any separation boundary with the final product that endangers the achievement of the final product objectives, then a separation task needs to be introduced in the sequence before the second reaction task is performed. The separation task will be responsible for removing the byproducts or in other words for purifying the respective intermediate product.*

**Rule S.13: sep. task identification between two consecutive reaction tasks (reaction kinetics)**

*If the desired reaction in the second reaction task (of the two compared) is of at least second order and its rate increases the smaller the volume of the reactant mixture is, then a separation task is desirable before the second reaction task, so that only the intermediate reactant (product of the first reaction task) is provided to the second reaction task.*

For a second order irreversible reaction  $A + B \Rightarrow C$ , the rate of the reaction is given by:

$$\begin{aligned} r &= kC_A C_B V \\ r &= k \frac{N_A}{V} \frac{N_B}{V} V \\ r &= k \frac{N_A}{V} N_B \end{aligned} \tag{3.54}$$

where  $r$  is the reaction rate (kmol/hr),  $k$  is the Arrhenius rate constant,  $C_A$  and  $C_B$  are the concentrations of reactants  $A$  and  $B$ ,  $N_A$  and  $N_B$  are the number of moles of the reactants and  $V$  is the volume of the reactant mixture.

It is obvious from equation 3.54, that for the same reaction and operating conditions, constant  $k$  and holdup  $N_A$  and  $N_B$  are the same. It is actually the

volume of the reactant mixture that has an effect on the reaction rate and for a second or higher order reaction it will increase as volume  $V$  decreases.

The end objectives for the individual tasks of the reaction-separation sequence are found according to the following rules. The only known objectives in the beginning are the product objectives at the end of the final task in the sequence, namely the recovery and purity of the final product. If the number of tasks in the sequence is greater than two, then some assumptions have to be introduced (rules S.15 and S.16), in order to be able to find all the end objectives of the respective tasks in the sequence.

**Rule S.14: total recovery expression**

*For every task in the sequence ( $k = 1, \dots, N$ ), a recovery  $r_k$  is assigned. The total recovery  $r_T$  of the final product is found to be the product of the recoveries of the respective reaction and separation tasks in the sequence.*

$$r_T = \prod_{k=1}^N r_k \quad (3.55)$$

where recovery  $r_k$  for a specific reaction task is given by equation 3.6. For a separation task,

$$r_k = \frac{\text{moles of specified product obtained}}{\text{total moles of specified product charged}} \quad (3.56)$$

**Rule S.15: purity specification of intermediate separation tasks**

*For the intermediate separation tasks, the desired purity for the respective product is set to  $p_k^s \geq 0.99$  for very feasible separations and to  $p_k^s \geq 0.98$  for just feasible operations.*

where superscript  $s$  denotes a separation task.

The second end objective for the final product (purity) will provide a second equation, in addition to equation 3.55, that can be used to find the respective task recoveries  $r_k$ . However, when  $k > 2$ , then the following assumption has to be made.

**Rule S.16: (initial) intermediate task recovery specification**

*If the number of tasks in the proposed sequence is greater than two, then initially it will be assumed that all the recoveries for the reaction and separation tasks are the same,  $r_k = r$ .*

For the last two tasks in the sequence, the exact recoveries can be found solving the system of equation 3.55 and the resulting equation for the final product purity, a system of two equations and two unknown variables.

The necessity of a final separation task in the sequence is discussed in the following rule.



**Rule S.17: final separation task identification**

*If the provided reactants for the final **reaction** task in the sequence are of high purity and the yield of that task is sufficiently high, then it should be investigated whether the objectives for the final product can be achieved without a final separation task in the sequence.*

Once again, solving the system of the two equations for the product recovery and purity for the two last tasks in the sequence (the sequence without the final separation task), it can be calculated whether a feasible recovery for the last reaction task ( $r_N < 1$ ) is sufficient to achieve the final product objectives.

It is important to point out that once the sequence of the various tasks is identified, the individual operational design is handled by the developed algorithms for batch reaction and separation.

If the objectives for the final product can not be satisfied with the intermediate recoveries suggested from rules S.15 to S.17, one can set more strict intermediate objectives for the respective tasks. In that way, higher recoveries may be set as objectives and for the separation tasks purer products may be required.

**3.5.3.3 Stepwise Description of the Batch Processes Synthesis Algorithm**

The algorithm illustrated as a block diagram is shown in figure (3.22). For the application of the algorithm, the following prerequisite information must be provided.

**Given:**

- The identity of the mixture compounds (both reactants and products) and the composition of the feed (raw materials). The thermodynamic models, the set of reactions taking place and their respective kinetics.
- The identity of the final product(s) and their end objectives, namely the desired purity and recovery.
- The identity of any separation boundaries present in the respective mixture considered for separation.

**Calculate:**

- The sequence of reaction and separation tasks necessary to achieve the specified end objectives for the product(s), in minimum time and/or cost.
- The intermediate objectives at the end of each task in the sequence, in terms of recovery (and purity for the separation tasks) of the intermediate products that lead to the final product as well as of the final product.

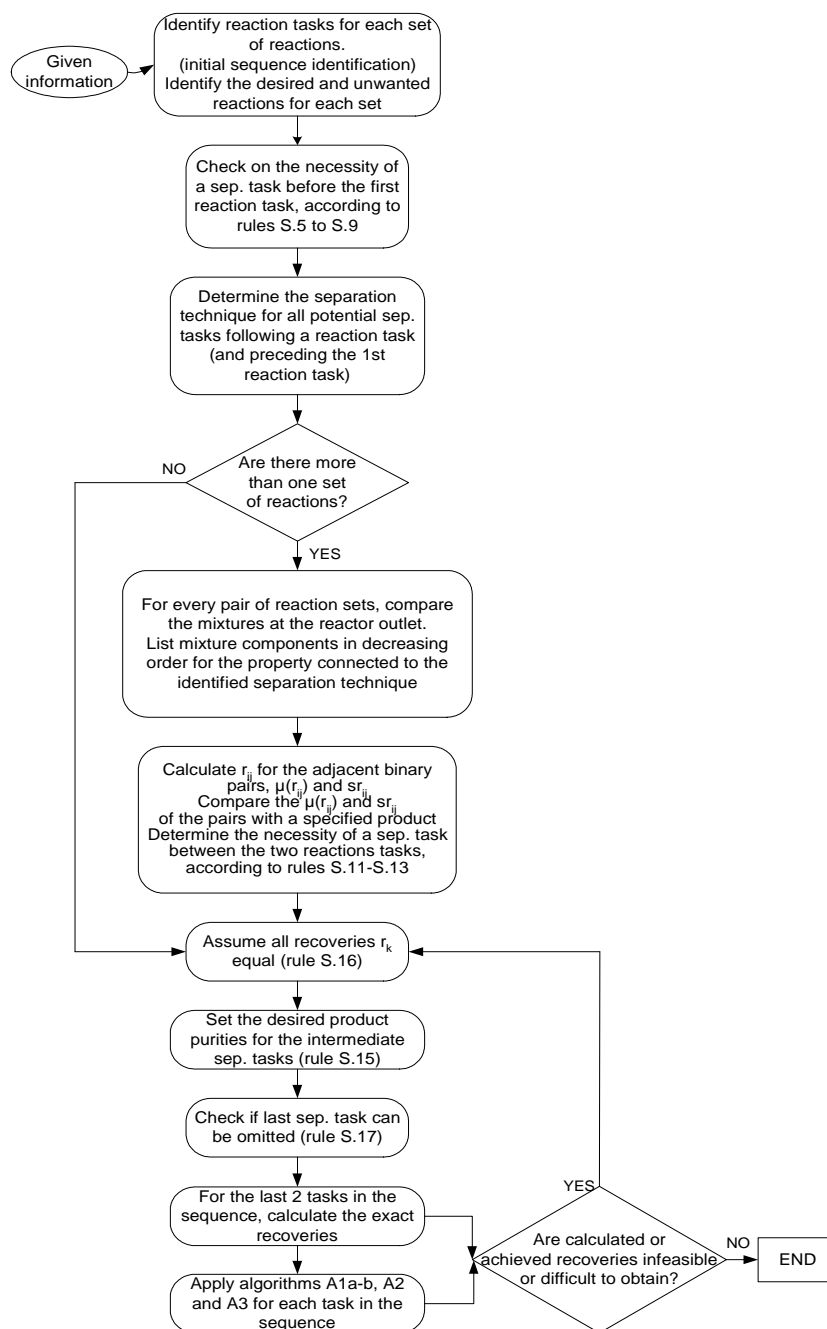


Figure 3.22: Block diagram of the algorithm S for the generation of a batch route (sequence of reaction and separation tasks) together with the batch operations model for each task

The algorithm is described in a stepwise fashion below.

1. For each set of reactions, identify a reaction task. Identify the desired reactions and the unwanted reactions in each set. Identify an initial sequence of tasks, where only the reaction tasks are present and a potential final separation task.
2. Determine whether a separation task is necessary before the first reaction task, according to rules S.5 to S.9.
3. Identify the separation technique for the respective separation tasks in the sequence, according to rule S.3. Identify separation techniques for all potential separation tasks following a reaction task.
4. When there are more than one reaction sets in the sequence, compare the reactant mixtures at the end of two succeeding reaction tasks. If there is only one set of reactions, go to step 9.
5. List the mixture components in decreasing order for the property that identified the respective separation technique.
6. Calculate the binary property ratios for the adjacent binary pairs, as well as the “possibility distribution”  $\mu(r_{ij})$  or the scaled binary property ratios  $sr_{ij}$ .
7. From the  $\mu(r_{ij})$  or the  $sr_{ij}$  of the binary pairs containing a specified product, determine the feasibility and its extent for the separation task where the specified product (final or intermediate) will be obtained.
8. Apply rules S.11 to S.13 and identify any necessary separation task between two succeeding reaction tasks.
9. Assume initially that all recoveries  $r_k$  are equal for the tasks in the sequence (rule S.16).
10. Set the desired product purities for any intermediate separation tasks, according to rule S.15.
11. Determine whether the last separation task can be omitted, according to rule S.17.
12. For the last two tasks in the sequence, find the exact recoveries by solving the system of equations 3.55 and that of the final product purity.
13. Apply the developed batch reaction and separation algorithms to obtain the operational model for each task, given the intermediate end objectives for each task.

14. If any recovery is found infeasible ( $r_k$  close to or greater than unity) at step 12 or difficult to obtain at step 13, adjust the initial assumption of step 9 and repeat from there. The adjustment (choosing a higher  $r_k$ ) should be made for recoveries of very feasible separation tasks and generally for the first recoveries in the sequence.

The algorithm described above will be from now on referred to as Algorithm S.

In summary, an algorithm was developed for the synthesis of batch processes, which systematically builds on the simplest sequence of reaction and separation tasks by adding separation tasks either before the first reaction task, between two reaction tasks or after the last reaction task. The resulting batch route, which achieves the specified products objectives, is provided together with the intermediate objectives for each task in the sequence. Once the task is identified along with its goal, the sub-tasks synthesis and design are performed by the corresponding reaction and separation algorithms. The final state from these algorithms is compared against the goal and returned to the synthesis algorithm, in order to improve the intermediate objectives of the remaining tasks in the sequence.

The integration of the developed reaction and separation algorithms in the synthesis algorithm provide the overall production sequencing and the accompanying batch operations models for all the tasks. The actual position of the separation tasks in the sequence is based on the feasibility and easiness of the identified separation technique and whether the separation smoothes the progress of the reaction task that follows. The strong feature of the algorithm is the use of the relationship between compound properties and separation process principles to identify the easiest separation technique and the insights gained from the analysis of the reaction kinetics used to identify ways to ease and make faster the reaction tasks.



# COMPUTATIONAL TOOLS

## 4.1 Introduction

A number of tools are necessary for the application of the methodology and algorithms developed in this thesis. Furthermore, these tools are also necessary for the verification of the batch routes and operational models generated from the various algorithms. Originally, definition tools for feed streams or units are required and tools used to add compounds, thermodynamic models and reactions to the system are also needed. An analysis and utility toolbox to analyze any given mixture and a synthesis tool for separation technique identification are necessary for the generation of the batch route. Moreover, for the individual tasks in the generated sequence, tools that may be used to produce vapour-liquid and solid-liquid equilibrium diagrams are also needed, since the solution of distillation or crystallization synthesis and design problems are based on these diagrams. Finally, a simulation engine for verification is also essential. All these kinds of tools are made available in the ICAS package, where they can be used in an integrated manner.

A general description of the main computational tools needed in this thesis follows. Additionally, the tools used for each individual algorithm described in the previous chapter are outlined separately. In those sections, the particular features of each tool are highlighted and it is pointed out where in the algorithms they are used.

### 4.1.1 ICAS - Integrated Computer Aided System

At the Computer Aided Process Engineering Center (CAPEC) at the Technical University of Denmark, an Integrated Computer Aided System (ICAS) has been developed for process modelling, synthesis/design, analysis, control and simulation and is used both for teaching purposes and by the industrial member companies of CAPEC. The description of the ICAS package is given by Gani *et al.* (1997). The respective computational tools are present as toolboxes and then during the solution of a problem the user can move from one toolbox to another to solve problems requiring more than one tool. From any toolbox,

it is possible to invoke the simulation engine to perform steady state and/or dynamic simulation. So the solution of a process synthesis problem in a step-wise form in ICAS would be to first define the feed stream, then analyze the mixture (invoking the analysis and utility toolbox), then generate a flowsheet (with synthesis toolbox), then optimize the flowsheet (design toolbox) and finally verify the design (simulation toolbox).

Some of the features available in ICAS as toolboxes are:

- Property prediction: Tools include CAPEC database, pure component property prediction (ProPred), mixture property prediction (TML), model parameter estimation (TML) and thermodynamic model selection (TMS).
- Modelling: Computer aided model generation (ModDev), model analysis, translation and solution (MoT) plus addition of user-defined models (MoT).
- Process synthesis and design: Tools include computer aided flowsheet generation (CAPSS), design of reactive/azeotropic distillation (PDS), configuration of distillation columns (PDS), solvent search/design (ProCamd).
- Reactions: Tools include reaction database, kinetic model parameter estimation, reaction path synthesis based on data (RAS).
- Simulation: The ICASsim simulation engine allows steady state simulation, while DYNISIM is a dynamic simulation system. BRIC in particular is connected to DYNISIM and it is used for batch operations records and simulation.
- Control: Design and analysis of control systems, including a MPC toolbox for model predictive control.
- PDS: Process design studio for azeotropic and reactive distillation design and analysis.
- BRIC: Batch operation records and simulation.

#### 4.1.2 The CAPEC Database and reaction database

A knowledge base consisting of information related to the properties of the compounds of a given system and the reactions that might take place between them is a basic tool needed for this methodology. The CAPEC database (Nielsen *et al.*, 2001) includes collected and screened experimental data of pure component data for approximately 13200 pure compounds, mixture data, solvent data and solubility data from open sources (literature). A really important feature of the database is that it allows the user to add new data and new compounds.

The reaction database is a database of reactions, where a number of reactions are already present and most significantly new reactions can also be added.

### 4.1.3 ProPred: Property prediction

In connection to adding new compounds in the CAPEC database, a computational tool for the prediction of pure compound properties is required. A lot of the products developed in a batch mode are novel compounds that do not appear in any known databases (such as the DIPPR databank). In this case, it is necessary that a trustworthy prediction of the properties of these compounds is performed before they can be added to the database and used in the solution of a problem.

ProPred is a tool integrated into ICAS directly for that purpose. ProPred is an interactive program, where via a graphical interface the user can build a molecule by connecting fragments (CH<sub>2</sub>, CH<sub>3</sub>, OH etc.). While building, the predicted properties for the molecule are shown continuously. Presently the program can predict properties using the Joback and Reid (1987), Constantinou and Gani (1994) and Marrero and Gani (2001) group contribution methods as well as some correlation based methods. As an extra feature to improve usability with respect to complex compounds it is possible to define new groups and their contributions for all or some of the prediction methods.

### 4.1.4 Utility toolbox

A number of calculations are available in the *property window* of ICAS. An essential calculation for the developed methodology is the calculation of phase diagrams. That possibility is given in the utility toolbox of ICAS. The computations of driving force curves (VLE calculation) as well as solid-liquid equilibrium diagrams are available. Acquiring these diagrams is basically the first step to the synthesis/design problem of batch separation considered in this thesis. The easy access to these diagrams is a useful feature, since they form the base of an easy and visual way of attacking the synthesis/design problem, also for many complex separations.

Additionally, PT-flash calculations are necessary for the analysis of the mixture considered and the solubility index *SI* calculation is essential in determining the design of batch crystallization of quaternary systems.

### 4.1.5 PDS: Process Design Studio

The computational tool Process Design Studio (PDS), integrated into the ICAS package is used in this thesis to determine the reflux ratio for each period in the sequence of sub-tasks generated by the distillation algorithm. The special feature of the tool used in the algorithm is the analysis of the feasibility of achieving a specified distillate composition and product recovery from a specific feed, by manipulating the reflux ratio to match the number of plates in the column. In the distillation design part of PDS, given the identity of the mixture compounds, the thermodynamic model, desired products and number of plates, the program returns the minimum reflux ratio and the feed stage location. For



the case of batch distillation, the relationship between feed, products, reflux ratio and number of plates can be analyzed and determined.

However, PDS can also be used to compute binary and ternary azeotropes, phase diagrams, distillation boundaries and residue curves. In that way, it can be used for preliminary mixture analysis of a system to be separated by distillation. A number of thermodynamic models can be used within PDS and ICAS. PDS is connected to a thermodynamic model library, which have activity coefficient models (various forms of UNIFAC) and mixed GE-EOS models.

#### 4.1.6 CAPSS

The binary property ratio matrix generated in CAPSS for a multicomponent mixture is used for the sequencing and identification of the separation technique needed for continuous processes (Jaksland, 1996). In this thesis, the same binary ratio matrix is used for the generation of the complete batch route, involving the production and separation of specified products. The largest property ratios are used to identify the easiest separation technique for a specific split. Moreover, the property ratios are used to identify the position of a separation task in a series of reaction and separation tasks.

#### 4.1.7 BRIC and Dynamic simulator

The generated operational model for the individual tasks (separation and reaction) from the algorithms of this thesis has been verified through dynamic simulation. The possibility provided by BRIC is to simulate a sequence of batch operation steps/runs (corresponding to a sequence of sub-tasks), where a number of variables can be changed from one run to the other. In that way, the step-wise changed reflux ratio profile for a distillation column can be simulated, where the reflux ratio and vapour boilup rate values can be changed gradually. Other options provided are changing the heat input to e.g. a reactor or modifying the feed stream from one run to the other, in order to enable charging. A number of conditions that will indicate the end of each step can be chosen, such as time (operation step  $n$  must be completed within  $t$  hours) and composition (molefraction of component A in stream  $s$  must be less than  $x$ ), ICAS User's Manual (Gani, 2002).

BRIC also offers the option of data reconciliation. Temperature, pressure and composition profiles can be obtained for each stream and unit defined in the problem. The data collected are gathered in an MS excel file and can therefore very easily be manipulated. In that way, one can without much effort verify whether operational constraints are respected and end objectives are met. Additionally, secondary properties can be determined and used in the algorithms, such as the approximation of end selectivity (knowing the current selectivity and its tangent).

BRIC calls DYNISIM to perform the dynamic simulation. The flowsheet needs to be drawn first using a set of different unit options available, such as reactors,

flashes, distillation columns, crystallizers, tank mixers, etc.. There are different simulation strategies that can be used (ODE or DAE) and different methods of solution that can be applied, such as explicit Euler or Runge-Kutta (RK) or backward differential formula (BDF). In this thesis, the ODE option was used and the method of solution was BDF with no scaling.

## 4.2 Batch Reaction Algorithm Tools

A reaction database is necessary for the batch reaction algorithm, since reaction is what differentiates this algorithm from the rest of the operational design algorithms for separation. The reaction database in ICAS can be used to retrieve available reactions from a list of defined reactions as well as to add new reactions. The feature of adding new reactions makes it possible to apply the algorithm for every batch reactor whose set of reactions is known and is given with either an Arrhenius kinetic model or in an equilibrium correlation form. However, since in a batch reactor we are interested in the change of holdup with time, the reaction rate is preferably given as an Arrhenius type rate law. When adding a new reaction, one can specify whether the reaction is reversible or not, the order of the reaction and provide the pre-exponential factor and the activation energy for all the reactions.

The heat of reaction is an essential variable for the algorithm and it can easily be calculated from the standard enthalpies of formation  $H_f^o$  for all products and reactants. However, if there are any compounds that are not present in the database, then ProPred can be used to predict the pure compound properties, add the compound to the database and continue with the simulation of the batch reactor.

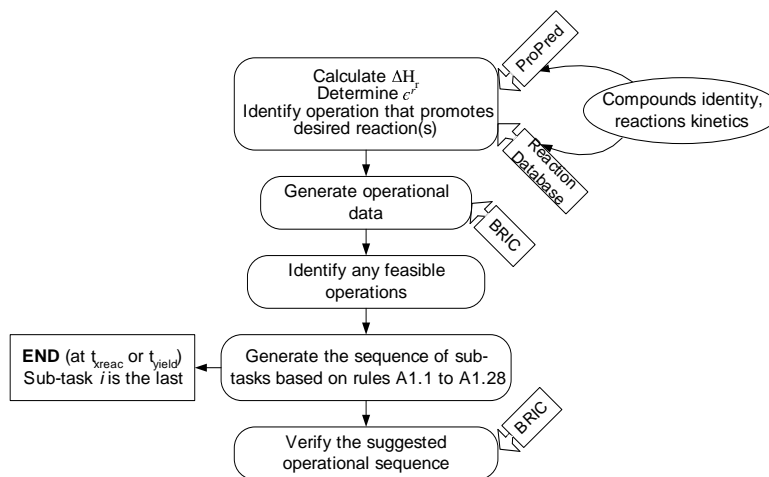


Figure 4.1: Use of computational tools in the batch reaction algorithms A1a-b

If the operational data for isothermal and adiabatic operation are not available, then the dynamic simulator invoked by BRIC can be used to generate the data. The operation, namely isothermal, adiabatic or constant heating rate, can be defined and the data can be collected until a terminal objective is satisfied (e.g. molefraction of a compound in the reactor). Furthermore, BRIC can be used to simulate a series of sub-tasks where the heating input changes from one step to another. The end of each step can be identified by an imminent violation of a constraint (temperature or pressure). An illustration of the use of the computational tools needed in the various steps of the batch reaction algorithm is given in figure 4.1.

### 4.3 Batch Distillation Algorithm Tools

The computational tool Process Design Studio (PDS) in the ICAS package is used to determine the reflux ratio for each period in the sequence of sub-tasks, which is the actual operational model of each separation task. Process Design Studio is a primarily synthesis tool developed by Hostrup (2002) and implemented in ICAS. The special feature of the tool used in the algorithm is the analysis of the feasibility of achieving a specified distillate composition and recovery from a specific feed, by manipulating the reflux ratio to match the number of plates in the column. The calculations in PDS are done in principle for a continuous distillation column. However, they can still be used for the case of a batch distillation column and it is yet again the total number of plates that one should try to match to the reflux ratio. Even though the batch distillation column considered only has a rectifying section, it is still the composition of the bottom plate that satisfies the mass balance.

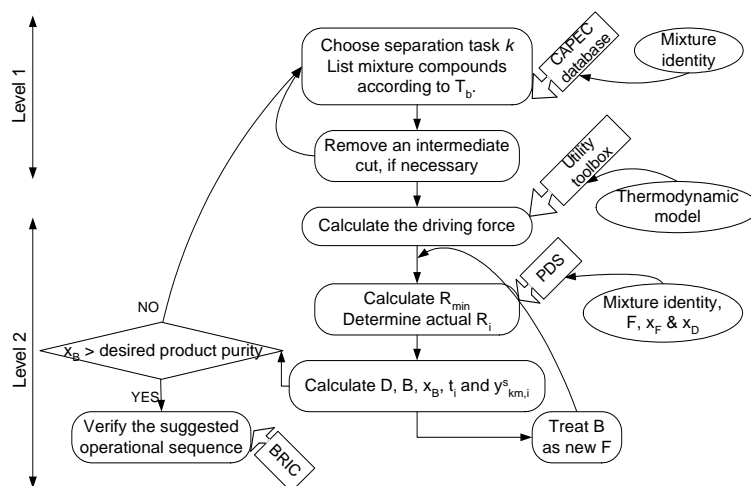


Figure 4.2: Use of computational tools in the batch distillation algorithm A2

Another element in the ICAS package that has also been available to use in the algorithm is the mixture property calculation feature. When no vapour-liquid equilibrium data are available, it is essential that they are estimated in order to calculate the driving force curves. In order to do so, accurate properties of the pure compounds and reliable thermodynamic models should be available. For the case when a compound is not present in the database and no accessible properties are present, it is necessary that the properties for this compound are predicted with ProPred. Once the pure compound properties are predicted, the compound can be added to the database and further on calculations, such as VLE calculations can be performed.

Moreover, BRIC is used to simulate the generated sequence of sub-tasks, where the reflux ratio changes from one step to the next. The end of each sub-task can be identified after a specified time or at the imminent violation of the distillate composition that is not allowed to drop below a specified  $x_D$ . An illustration of the use of the computational tools needed in the various steps of the batch distillation algorithm is given in figure 4.2.

## 4.4 Batch Crystallization Algorithm Tools

The utility toolbox in ICAS, which is actually the property calculation feature invoked from the mixture specification of a stream, is used for the generation of the solid-liquid equilibrium diagram. The solubility of the selected solvent and solutes is plotted in a triangular diagram. The generated data are given in Cartesian coordinates  $(X, Y)$ . Additionally, the mass compositions of the ions plus the solvent are also given. The latter information can be particularly useful in the case of quaternary systems for calculating the amount of solvent, since for quaternary systems the Cartesian coordinates only give information for the solvent-free composition of the solutes. Once the phase diagram is acquired, then the algorithm can be applied. The phase diagram can also be plotted as multiple curves with the temperature varying.

Another feature of the utility toolbox that is used especially in the case of quaternary systems is the solubility index  $SI_s$  calculation. This calculation can be used to determine the feasibility of the precipitation of a given solid for a specific feed. Moreover, the solubility index calculation can also be used to determine the amount of solvent needed to remove or add in order for a specific amount of solid to precipitate. The difference in the amount of solvent in the considered feed and the amount of solvent in the corresponding mother liquor when  $SI_s = 1$  for the precipitating solid  $s$  equals the amount of solvent to be removed or added (if the difference is negative).

The dynamic simulator Dynsim is finally used to verify the sequence of sub-tasks generated. Each sub-task is simulated as two steps, the one being evaporation of the solvent, where its end is marked by the removal of the exact amount of solvent. The second step is the separation of mother liquor from the precipitated solid. An illustration of the use of the computational tools needed

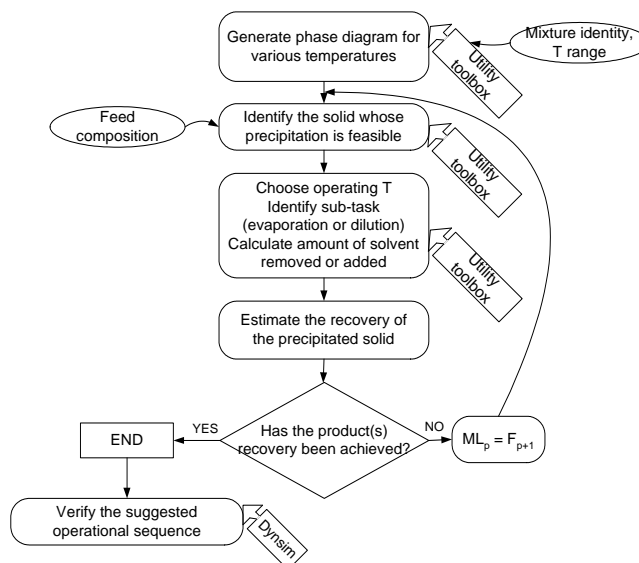


Figure 4.3: Use of computational tools in the batch crystallization algorithm A3

in the various steps of the batch crystallization algorithm is given in figure 4.3.

## 4.5 Batch Synthesis Algorithm Tools

The main computational tool used in this algorithm is the binary ratio matrix generated in CAPSS for a multicomponent mixture. A key feature of the algorithm is the identification of the separation technique that is the most feasible for a given separation. For a given mixture, which in the synthesis algorithm is regularly the outlet of a batch reactor, the binary property ratios are calculated for all the component pairs in the mixture. For each property the ratios of the adjacent pairs are compared to the respective feasibility indexes ( $m_{kj}$  and  $M_{kj}$ ) and the feasibility of the separation technique connected to the respective property is decided for the binary pair in question. CAPSS has a further step, in which the most feasible separation technique is identified for the mixture. Furthermore, the most feasible separation technique following a reaction task can also be identified. This is done, in principle, by comparing the various  $sr_{ij}$  and  $\mu(r_{ij})$  for the binary pairs, where a desired product (intermediate or final) is involved.

Additionally, in the first step of CAPSS, the mixture analysis is performed and the separation boundaries of the mixture are identified. Alternatively, PDS can be used for the identification of azeotropes present in the mixture and particularly the azeotropes between impurities, by-products and the final

or intermediate products are important to be identified in the first steps of the algorithm. Obviously for the reaction tasks, the reaction database of ICAS is necessary to obtain all the reactions or it needs to be used to add the missing reactions. Moreover, if a component is not present in the CAPEC database, then its properties need to be predicted with ProPred and then added to the component database. Finally, the entire environment of ICAS is used for the simulation of the batch route. The use of the computational tools needed in the various steps of the batch synthesis algorithm is illustrated in figure 4.4.

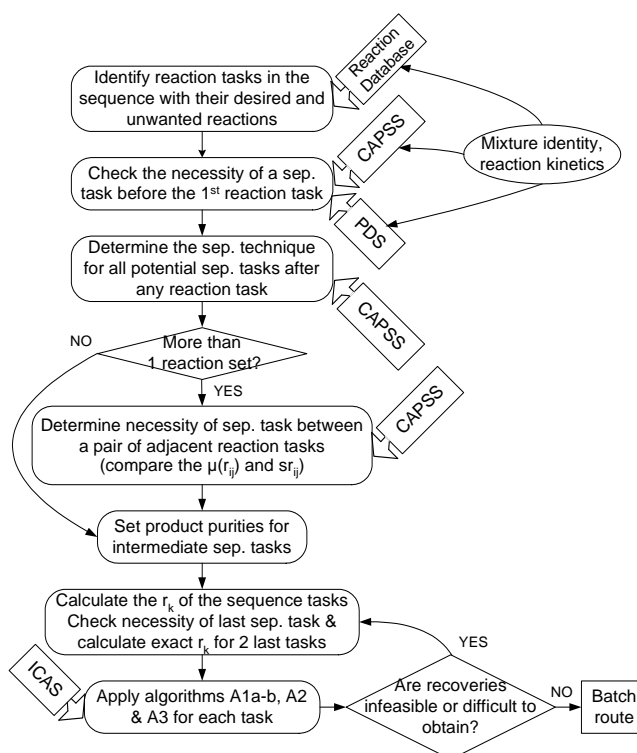


Figure 4.4: Use of computational tools in the batch synthesis algorithm S



# APPLICATION EXAMPLES

## 5.1 Introduction

The various algorithms developed for the batch processes synthesis and the generation of operation models for batch processes are applied and verified through a number of case studies. First algorithm A1a is applied to a reaction system where only one phase is present, while in the second example algorithm A1b is applied to a batch reactor, where the presence of vapour has implications on the operation because of pressure constraints. The third and fourth case studies handle the operational modelling of batch distillation columns with algorithm A2. The former case concerns the separation of a ternary non-azeotropic mixture, while the latter case separates a binary azeotropic system. Two cases of ternary electrolyte systems and that of a quaternary system are considered next, where the application of algorithm A3 is necessary. Finally, the synthesis of batch processes is examined in the last example.

## 5.2 Conceptual example: Operational modelling of a liquid phase reaction

This problem was adapted from the series of papers by Allgor *et al.* (1996), (1999) and Allgor and Barton (1999). The problem serves as a conceptual example for the application and verification of the algorithm for the operational modelling of batch reaction, where there is only one phase present. For this example, only the first set of reactions from the original paper is considered. The reactions take place in a closed batch reactor, where reactants  $R_1$  and  $R_2$  (8 and 4 kmoles, respectively) and solvent  $S$  (5.8 kmoles) are added. For the sake of the algorithm, it is considered that only one liquid phase is present in the system and operational constraints relate only to temperature. The assumption of one phase can be quite realistic, since the considered system is closed, no constraints on pressure are present and the main desired reaction takes place in the liquid phase.

The identity of only one of the reactants was given, namely of  $R_1$  as allyl



alcohol, and of the solvent  $S$  as toluene. Reactant  $R_2$  is chosen as methane, and the set of reactions is adjusted as follows:



The reaction rate constants for the above set of reactions are adapted from the paper and are given in table 5.1. The operating range for the reactor temperature is set for the application of algorithm A1a between  $T_{low}$  and  $T_{up}$  ( $T_{low} = 300K$  and  $T_{up} = 360K$ ). Additionally, the constraint for the selectivity is set to  $S_{min} = 15$ .

Reaction no	$E_a$ ( $Jmol^{-1}$ )	$k_o$
1	78240	$7.5 \cdot 10^4$
2	45605	1.01
3	103345	$1.22 \cdot 10^{11}$
4f	32217	$3.58 \cdot 10^{-2}$
4b	91211	$7.33 \cdot 10^9$

Table 5.1: Reaction rate constants for the set of reactions in the one-phase batch reactor

The objective for the reaction task is to obtain at least 97% of compound  $I_2$ , which is considered as the product of the reaction task. The limiting reactant whose molefraction would signify the end of the reaction task is  $R_2$  ( $x_{R_2} = 0.0001$ ). Alternatively, the more loose criterion would be the yield of the intermediate product  $I_1$  ( $Y'_{I_1} = 0.995$ ).

**Problem statement:** Given the identity and composition (initial holdup) of the reactants, the set of reactions and their kinetics as well as the product specifications, determine the batch operations model for the reaction task to achieve the specified end objectives for the product, preferably in minimum time and/or cost.

**Problem solution:** Algorithm A1a for the synthesis of feasible operational sequences for a batch reactor is applied. Dynamic process simulation is applied to analyze and verify the generated operational sequences.

Steps 1-2: From the set of reactions taking place, some are desired, since they yield the product, while others are competing reactions that need to be suppressed. The specified product for this reaction task is compound  $I_2$ , which is produced in reaction 3 from the intermediate product  $I_1$ , which is produced in reaction 1. On the other hand, one of the reactants, namely compound  $R_1$ , is also consumed in reaction 2, instead of desired reaction 1. Furthermore,

reaction 2 is unwanted because the intermediate product  $I_1$  is consumed there to produce byproduct  $A$ , instead of product  $I_2$ . The forward part of reaction 4 is also unwanted, since the  $I_1$  is consumed there, endangering the recovery of the specified product  $I_2$ .

Therefore, the selectivity of reaction 1 over reaction 2  $S_{12}$  should be as high as possible and kept above the constraint  $S_{min}$ . In that way the rate of reaction 1 will always be higher than the rate of reaction 2. Similarly, selectivities  $S_{34}$  and  $S_{32}$  should be kept above the selectivity constraint. For this example, selectivity  $S_{34}$  has been very high and always above the constraint, because for the reversible reaction 4 the reverse reaction yielding product  $I_2$  is favoured over the forward reaction. Selectivities  $S_{12}$  and  $S_{32}$  follow a similar course versus the molefraction of the limiting reactant, so the results shown are based on selectivity  $S_{12}$ .

In the case of irreversible reactions, the activation energies  $E_a$  of the reactions in question determine whether heating or cooling promotes selectivity. All of the desired reactions have an activation energy that is larger than the activation energy of their competing reactions ( $E_a^1 > E_a^2, E_a^3 > E_a^4, E_a^3 > E_a^2$ ), as can be seen in table 5.1. In this case, *heating* promotes the desired reaction over the competing reaction that it is compared to.

Steps 3-4: Data for isothermal and adiabatic operation for this example are generated by dynamic simulation at temperatures in the given range. The end point for all the simulations is the molefraction of the limiting reactant  $R_2$ , which is set close to zero ( $x_{R_2} = 0.0001$ ). The feasibility of the operation is checked against the temperature and selectivity constraints.

Steps 5-6: Obviously, the isothermal operations do not violate the temperature constraints, but in all cases the selectivity is below the constraint at the time when the looser criterion of  $Y'_{I_1} = 0.995$  is satisfied. Regarding the adiabatic operations, either the selectivity constraint is violated if the initial temperature is too low or the temperature rises above the upper limit if the initial temperature is too high, as shown in table 5.2. Therefore, none of these operation modes can be identified as feasible, since either the temperature or the selectivity constraint is eventually violated.

Since none of the above operations are feasible, the generation of an operational sequence can be performed in the next steps. The first sub-task in the sequence is found, among the available data of isothermal and adiabatic operations. The operation with the highest selectivity  $S_{function}$  without violation of any constraint is chosen. Isothermal operation at a temperature of 300K is the best starting point, because the selectivity of the desired reaction over the competing reaction is the highest among the available operations, and is selected as the first sub-task in the sequence.

Steps 7-8: The actual selectivity of the chosen operation for the first sub-task may not violate the constraint, however the projected value  $S'_{end}$  indicates that operating isothermally will cause the selectivity constraint eventually to be violated. Thus, the end of the first sub-task is identified at  $t_{stop,S}$ . The next sub-task was identified, according to rule A1.5i, as heating. At this point, ac-

Isothermal operation		Operating time (hr)	
Temperature (K)	$S_{12}$ when $Y'_{I_1} = 0.995$		
300	$1.89 < S_{min}$	8.4	
309	$2.76 < S_{min}$	5.8	
320	$4.35 < S_{min}$	3.8	
330	$6.17 < S_{min}$	2.7	
340	$9.48 < S_{min}$	1.9	
350	$13.37 < S_{min}$	1.4	
Adiabatic operation		Temperature (K)	Operating time (hr)
Initial temperature (K)	$S_{12}$ when $Y'_{I_1} = 0.995$		
300	$6.93 < S_{min}$	332.93	3.2
309	$12.12 < S_{min}$	349.18	2.0
320	23.73	$367.99 > T_{up}$	1.2
330	41.50	$384.34 > T_{up}$	0.8
340	53.76	$400.32 > T_{up}$	0.6
350	51.51	$415.87 > T_{up}$	0.5

Table 5.2: Feasibility check of the isothermal and adiabatic operations

cording to rule A1.6, heating was supplied at various indicative amounts from a range of available heat input and a number of alternative feasible operational sequences were generated. The end of the second sub-task was suggested because of an imminent violation of the upper limit of temperature. Since the heating amounts for this sub-task were different, the operating times for the different alternatives varied.

Steps 7 and 8 of the algorithm are repeated and the end of sub-task 2 is found as  $t_{stop, T_{up}}$ . The slack variable for the temperature for this example is set to 1.5-2K. According to rule A1.9, a cooling operation should be the third sub-task in the sequence and the cooling rates were found based upon rule A1.9. For all the generated alternative sequences, the projected value of the selectivity constraint is violated at some point  $t_{stop, S}$ . The end objective of  $Y'_{I_1} = 0.995$  is neither reached before the  $T_{low}$  constraint is violated and for the sequences that it is reached, the actual selectivity is below  $S_{min}$ .

There is only one sequence where  $S > S_{min}$  for  $Y'_{I_1} = 0.995$ , which is sequence 1 as seen in table 5.3, where the final objective is reached with no constraint violation. It is only for that sequence that the third sub-task is the final and where  $t_{yield}$  signifies the end of the reaction task. For the remaining sequences, the end of the third sub-task is at  $t_{stop, S}$ . The next sub-task in sequences 3-7 is identified as heating and the specific heating rate is chosen according to rule A1.7i, since  $Y'_{I_1} - Y_{I_1,3} < 10\%$ . The heating operation is the final sub-task, since selectivity is above the constraint  $S_{min}$  at the time  $t_{yield}$  when the recovery objective is satisfied.

The generated sequences are presented in table 5.3, where also the corresponding information related to the number, type and sequence of sub-tasks

and the respective times of operation are given, providing the operational model for the reaction task. Additionally, for every sub-task the imminent violation that signals the end of the corresponding sub-task is given. The application of the algorithm A1a for the generation of the operational model for a batch reactor has generated seven alternative operational sequences. The number of alternative sequences was decided at the second sub-task when the heating rate was selected arbitrarily between the lower and upper limit of the heating capacity,  $Q_{min} < Q < Q_{max}$ .

The information provided together with the sequence of sub-tasks, in terms of operational times and variables, was used to verify the feasibility of the alternatives and to compute the performance criteria through dynamic simulation. BRIC in connection to the dynamic simulation engine of ICAS has been employed for the verification and data collection of the alternatives. Results for selectivity  $S_{12}$  and the temperature profile of the reactor are given in figures 5.1 and 5.2 versus the molefraction of the limiting reactant  $R_2$  (note: the starting point of the sequences is at  $x_{R_2} = 0.225$ , which means that as time progresses we move from the right to the left of the diagram  $X$  axis).

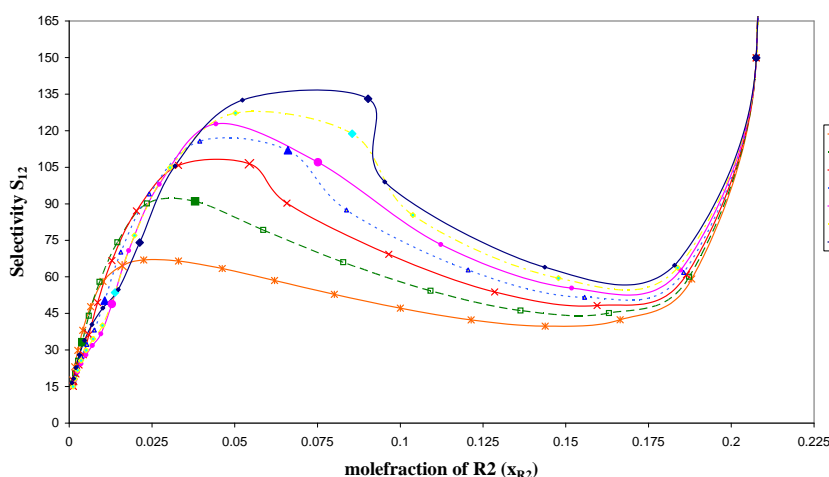


Figure 5.1: Selectivity  $S_{12}$  versus  $x_{R_2}$  for the generated operational sequences

In the beginning of the operational sequence (see upper right hand corner of figure 5.1), the selectivity is very high (infinity) because the second reaction has not started yet. However, isothermal operation at a low temperature causes a steep drop of selectivity, as it can be seen in figure 5.1. The end of the first sub-task is indicated in the figure with enlarged points for all the alternatives sequences, which for the first sub-task is the same point. The other enlarged points in figure 5.1 indicate the end of the second and third sub-task for the alternatives sequences. The 2<sup>nd</sup> sub-task of heating raises the selectivity as expected and the 3<sup>rd</sup> sub-task of cooling has the opposite effect. The switch

Operational sequence no	Sub-task 1	Sub-task 2	Sub-task 3	Sub-task 4	Total operat. time (hr)
1	Isothermal op. (0.1 hr) $T = 300K$ $S'_{end}$	Heating (1.08 hr) $Q_{12} = 1100MJ/hr$ $T_{up} - T_{slack}$	Cooling (0.6 hr) $Q_{13} = -200MJ/hr$ $Y'_{I_1} = 0.995 (S = 17.7)$		1.78
2	Isothermal op. (0.1 hr) $T = 300K$ $S'_{end}$	Heating (0.7 hr) $Q_{22} = 2200MJ/hr$ $T_{up} - T_{slack}$	Cooling (0.5 hr) $Q_{23} = -1300MJ/hr$ $S'_{end} (= 12.1)$	Adiabatic op. (0.3 hr) $Q_{24} = 0$ $Y'_{I_1} = 0.995 (S = 16.3)$	1.6
3	Isothermal op. (0.1 hr) $T = 300K$ $S'_{end}$	Heating (0.54 hr) $Q_{32} = 3300MJ/hr$ $T_{up} - T_{slack}$	Cooling (0.5 hr) $Q_{33} = -2200MJ/hr$ $S'_{end} (= 6.1)$	Heating (0.42 hr) $Q_{34} = 600MJ/hr$ $Y'_{I_1} = 0.995 (S = 15.1)$	1.56
4	Isothermal op. (0.1 hr) $T = 300K$ $S'_{end}$	Heating (0.45 hr) $Q_{42} = 4400MJ/hr$ $T_{up} - T_{slack}$	Cooling (0.4 hr) $Q_{43} = -3100MJ/hr$ $S'_{end} (= 6.6)$	Heating (0.6 hr) $Q_{44} = 250MJ/hr$ $Y'_{I_1} = 0.995 (S = 15.5)$	1.55
5	Isothermal op. (0.1 hr) $T = 300K$ $S'_{end}$	Heating (0.39 hr) $Q_{52} = 5500MJ/hr$ $T_{up} - T_{slack}$	Cooling (0.4 hr) $Q_{53} = -4000MJ/hr$ $S'_{end} (= -6.4)$	Heating (0.69 hr) $Q_{54} = 420MJ/hr$ $Y'_{I_1} = 0.995 (S = 15)$	1.58
6	Isothermal op. (0.1 hr) $T = 300K$ $S'_{end}$	Heating (0.34 hr) $Q_{62} = 6600MJ/hr$ $T_{up} - T_{slack}$	Cooling (0.4 hr) $Q_{63} = -4000MJ/hr$ $S'_{end} (= -1.5)$	Heating (0.7 hr) $Q_{64} = 300MJ/hr$ $Y'_{I_1} = 0.995 (S = 15)$	1.54
7	Isothermal op. (0.1 hr) $T = 300K$ $S'_{end}$	Heating (0.31 hr) $Q_{72} = 7700MJ/hr$ $T_{up} - T_{slack}$	Cooling (0.3 hr) $Q_{73} = -5000MJ/hr$ $S'_{end} (= 11.5)$	Heating (0.8 hr) $Q_{74} = 150MJ/hr$ $Y'_{I_1} = 0.995 (S = 16.6)$	1.51

Table 5.3: Generated family of alternative operational sequences for application example 5.2

point between the second and third sub-task is reached at different molefractions for each alternative sequence depending on the amount of heating used in the second sub-task. For the second sub-task the higher the amount of heating used, the shorter the operating time (larger  $x_{R_2}$  at the end of the sub-task), but also the higher the selectivity achieved. For the final sub-task of heating, the selectivity continues to drop (at reactions end), but while it is not so obvious from figure 5.1 the drop is actually less steep than for the cooling sub-task.

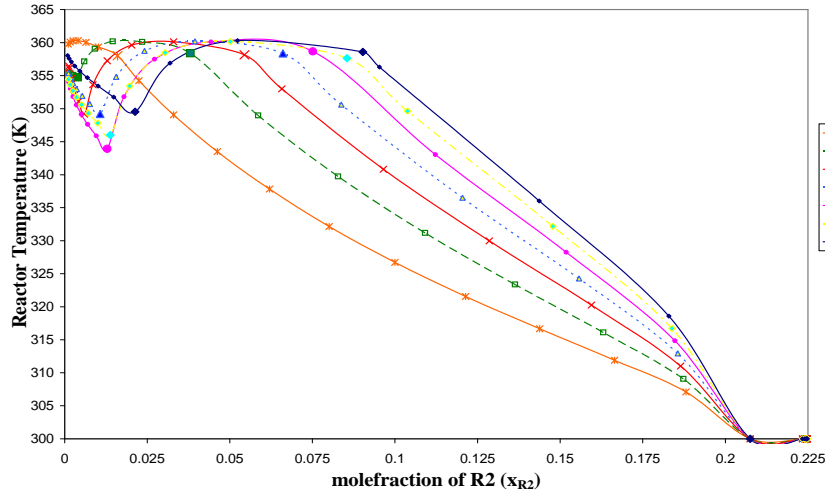


Figure 5.2: Reactor temperature versus  $x_{R_2}$  for the generated operational sequences

From the temperature profiles shown in figure 5.2, it can be noted that the slope of the temperature curve for the second sub-task depends upon the various heating rates and obviously the higher the heating rate, the steeper the slope. All the generated alternatives are verified to be feasible, since no selectivity and temperature constraints are violated. It can also be seen in figures 5.1 - 5.2, that the objective of  $x_{R_2}$  being close to zero is clearly satisfied.

The fastest operational sequence from the generated alternatives is no 7, as it can be seen in table 5.3. However, it also seems to be the one with the maximum operating costs, since the amounts of heat added or removed are the largest. The operating costs for the heating and cooling sub-tasks in the sequences were calculated in terms of amounts of cooling water and steam needed (appendix D) and are shown in figure 5.3. Sequence no 1 has the minimum operating costs, but also the longest total operating time.

The decision of which operational sequence to choose can be taken after a number of variables are considered. The chosen sequence should maximize the amount of product that can be sold trying to satisfy the market demand and minimize at the same time the production cost per product unit. For that reason a profit function would have to be determined and optimized.

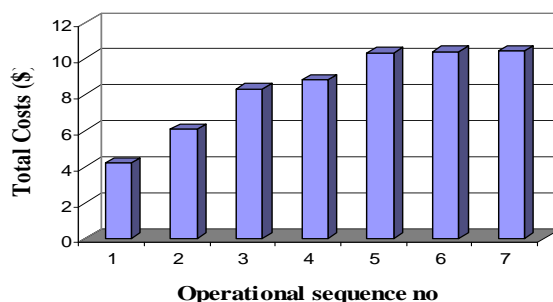


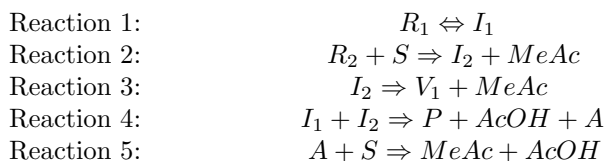
Figure 5.3: Total operating costs for the generated operational sequences

### 5.3 Operational modelling of two-phase reaction system

An industrial example was adapted, in order to demonstrate the application of the algorithm for the operational design of a batch reactor where both liquid and vapour are present and constraints exist on both temperature and pressure. The product of the particular process is an active pesticide ingredient for crop protection.

A set of reactions take place in a closed batch reactor, where reactant  $R_1$  and solvent  $S$  (26.75 and 80.39 kmoles, respectively) are originally added at ambient temperature. The identity of the solvent  $S$  is acetic acid. The second reactant  $R_2$  is fed at a rate of 11.32 kmoles/hr over a period of six hours. The first reactant and solvent are heated to 80 °C before the addition of the second reactant is commenced.

At first, there is only one liquid phase present in the system, but as the temperature increases and once all the reactions start taking place volatile compounds are produced and at some point a vapour phase appears. However, the desired product  $P$  remains in the liquid phase because it is a very heavy compound. The specific problem is treated only after that point, where two phases are present in the system. For reasons of confidentiality, the identity of the compounds in the set of reactions taking place is not given. The set of reactions is the following:



The kinetic parameters for the above set of reactions have been obtained from reaction calorimetry and are given in table 5.4, where subscripts f and b denote the reaction forwards and backwards, respectively.

Reaction no	$E_a/R$ (K)	$k_o$ ( $hr^{-1}$ or $m^3 kmol^{-1} hr^{-1}$ )
1 <sub>f</sub>	9959.1	$8.82 \cdot 10^{10}$
1 <sub>b</sub>	9959.1	$8.82 \cdot 10^{12}$
2	10861.2	$7.86 \cdot 10^{10}$
3	0	0.492
4	9959.1	$5.292 \cdot 10^{16}$
5	0	$3.6 \cdot 10^3$

Table 5.4: Reaction rate constants for the set of reactions in the two-phase batch reactor

The operating range for the reactor temperature is set for the application of algorithm A1b between  $T_{low}$  and  $T_{up}$ . The permitted pressure range is limited between  $P_{low}$  and  $P_{up}$  ( $P_{low} = 1$  atm and  $P_{up} = 2$  atm). Additionally, the constraint for the selectivity is set to  $S_{min} = 15$ . The available heating unit has a maximum capacity of  $Q_{max} = 600$  MJ/hr.

The objective for this reaction task is to obtain at least 85% of the maximum yield for the final product  $P$ . The limiting reactant whose molefraction would signify the end of the reaction task is  $R_1$  ( $x_{R_1} = 0.01$ ). Even though the limiting reactant of the main reaction of interest (reaction 4) is compound  $I_1$ , it is easier to monitor the progress of selectivity  $S_{43}$  versus the molefraction of  $R_1$ , because it has a monotonic decrease. On the other hand, selectivity  $S_{43}$  versus the molefraction of  $I_1$  (intermediate product from reaction 1 and reactant in reaction 4) does not give a clear picture, since compound  $I_1$  is consumed as fast as it is produced. Alternatively, the more loose criterion would be the desired yield of the final product  $P$  ( $Y'_P = 0.85$ ).

**Problem statement:** Given the identity and composition (initial holdup) of the reactants, the set of reactions and their kinetics as well as the product specifications, determine the operational model for the reaction task to achieve the specified end objectives for the product, preferably in minimum time and/or cost.

**Problem solution:** Algorithm A1b for the synthesis of feasible operational sequences for a batch reactor is applied. Dynamic process simulation is applied to analyze and verify the generated operational sequences.

The identity of the reactants and the products is known, but four out of the ten compounds are not present in the database, namely  $R_1$ ,  $R_2$ ,  $I_1$  and  $P$ . This means that the respective heats of formation are missing and the heat of reaction can not be calculated for all of the reactions.

ProPred in ICAS was used to calculate the properties for the missing compounds and also to add them in the database, so that they can be used in the dynamic simulation of the batch reactor.



Steps 1-2: Reaction 1 is the isomerization of reactant  $R_1$  to the intermediate  $I_1$ , while reaction 2 of the solvent  $S$  and the second reactant  $R_2$  yields the intermediate  $I_2$ . Reaction 4 between the two intermediates yields the final product  $P$ . The three earlier mentioned reactions are highly desirable, since they produce either intermediate or final products. On the other hand, reaction 3, being the decomposition of the intermediate  $I_2$ , is competing with reaction 4 and is unwanted in relation to reaction 2. Furthermore, reaction 5 is competing with reaction 2, in the sense that they have a common reactant. Based on the above, it is advantageous if the selectivity of reaction 4 over reaction 3 is as high as possible ( $S_{43} > S_{min}$ ). The same applies to the selectivity of reaction 2 over reactions 3 and 5 ( $S_{23} > S_{min}, S_{25} > S_{min}$ ).

The desired reactions (2 and 4) and the unwanted reactions which they are compared to (3 and 5) are all irreversible reactions. In this case, their activation energies will determine the appropriate operation that will promote selectivity. Both the desired reactions (2 and 4) have an activation energy that is larger than the activation energy of competing reaction 3 ( $E_a^2 > E_a^3$  and  $E_a^4 > E_a^3$ ) and the activation energy of desired reaction 2 is also larger than that of competing reaction 5 ( $E_a^2 > E_a^5$ ). In this case, *heating* promotes the desired reactions over their competing reactions.

Steps 3-5: Data for different heating rates and adiabatic operation are generated by dynamic simulation with the same terminal point ( $x_{R_1} = 0.01$ ). No cooling operations were generated, since cooling does not promote the desired reactions. The selectivity function  $S_{function}$  is calculated for all the above operations and their feasibility is checked against the process constraints.

All the operations are found infeasible, because of at least one constraint violation (when  $Y_P' = 0.85$ ). For adiabatic operation and low heating rates, the lower temperature limit is violated. For intermediate heating rates the upper pressure constraint is violated, while for higher heating rates both the temperature and pressure upper limits are violated. Each violation can be seen in table 5.7.

Step 6: Since none of the above operations remain feasible until the product objective is satisfied, the first sub-task of the operational sequence is selected as the one that has the highest  $S_{function}$ . As can be expected, heating at the highest permitted rate is the best starting point. As stated, *heating* promotes the desired reactions over their competing reactions and therefore, the higher the heating the higher the selectivity ( $S_{function}$ ).

Steps 7-9: The constraint that is close to violation because of the heating operation is actually the upper pressure limit, so the end of sub-task 1 is found at  $t_{stop, P_{up}}$ . The next sub-task was identified according to A1.14ii as heating with simultaneous removal of vapour from the system. The amount of heat added is as high as possible but also such that the actual pressure constraint is not violated. The second sub-task is ended, according to rule A1.17, because of the imminent violation of the  $P_{up} - \Delta P$  pressure limit. Since heating promotes the desired reactions, then according to rule A1.19 the next sub-task is further

heating at a higher rate with continuous removal of vapour from the system.

The information related to the generated operational sequence is given in table 5.5 and it can be used for the verification of the sequence and further comparison if necessary. The temperature and pressure profiles of the reactor are given in figures 5.4 and 5.5. The total operating time for the sequence is 2.96 hr.

Sub-task no	Operation	Heating rate	End of sub-task	Operating time (hr)
1	Heating	600 MJ/hr	$P_{up}$	0.65
2	Heating + vapour release	265 MJ/hr	$P_{low}$	0.71
3	Heating + vapour release	465 MJ/hr	$Y'_P$	1.60

Table 5.5: Generated sequence of sub-tasks for the two-phase reactor

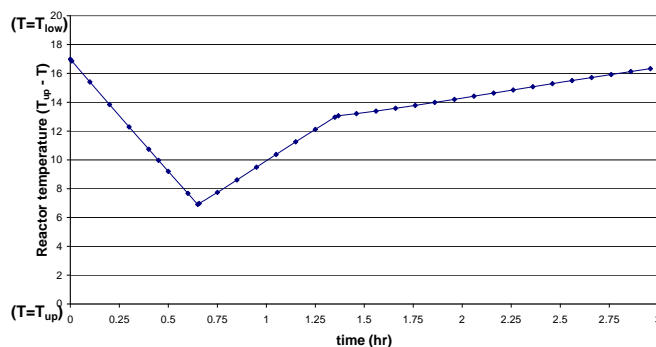


Figure 5.4: Reactor temperature profile for the generated operational sequence in the two-phase batch reactor

The presentation of the temperature profile is given as a difference between the upper temperature limit and the actual reactor temperature ( $T_{up} - T$ ). In that way the values fluctuate between 0 K, when  $T = T_{up}$ , and 20 K, which is  $T_{up} - T_{low}$ . The temperature, at the point where both phases start to be present, is close to  $T_{low}$ .

From the temperature and pressure profiles, it can be noted that heating at the highest rate (sub-task 1) increases both the temperature and the pressure of the reactor. However, it is the upper pressure limit that is reached first. In the next two sub-tasks, the temperature is decreased, even though heating is applied, because of the cooling from evaporation and removal of the volatile compounds. The vapour release dominates the heating provided and therefore the temperature decreases. In the last sub-task, when the heating provided is at a higher rate than during the second sub-task, the decrease is not as steep as in the second sub-task.

From the pressure profile of the reactor, given in figure 5.5, one can see that

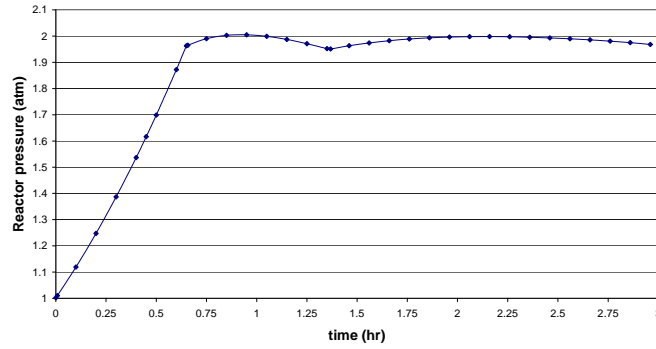


Figure 5.5: Reactor pressure profile for the generated operational sequence in the two-phase batch reactor

once the pressure approaches the upper pressure limit, it is actually maintained close to the limit during the last two sub-tasks of the sequence. According to rule A1.15, pressure was not allowed to drop below  $P_{up} - \Delta P = 1.95$  atm. The pressure was allowed to vary within  $\Delta P$  during the last two sub-tasks.

The smaller  $\Delta P$  is, which means that operation is maintained closer to the actual upper limit  $P_{up}$ , the faster the operating time for the sequence. As an indication of the above, the suggested sequence (sequence I) is selectively compared with two alternative sequences, one where  $P_{up} - \Delta P = 1.9$  atm (sequence II) and another where  $P_{up} - \Delta P = 1$  atm (sequence III). The results from this comparison are given in table 5.6. The time in parenthesis is the respective total operating time.

Operational sequence no	Sub-task Operation	End of sub-task	Operating time (hr)
I	Heating (600 MJ/hr)	$P_{up}$	0.65
$\Delta P =$	Heating + vap. release (265 MJ/hr)	$P_{up} - \Delta P$	0.71
0.05 atm	Heating + vap. release (465 MJ/hr)	$Y_P'$	1.60 (2.96)
II	Heating (600 MJ/hr)	$P_{up}$	0.65
$\Delta P =$	Heating + vap. release (265 MJ/hr)	$P_{up} - \Delta P$	0.94
0.1 atm	Heating + vap. release (505 MJ/hr)	$Y_P'$	1.39 (2.98)
III	Heating (600 MJ/hr)	$P_{up}$	0.65
	Heating + vap. release (265 MJ/hr)	$T_{low}$	1.61
$\Delta P =$	Heating (600 MJ/hr)	$P_{up}$	0.21
1 atm	Heating + vap. release (525 MJ/hr)	$Y_P'$	0.66 (3.13)

Table 5.6: Comparison of generated operational sequence for the two-phase reactor

The first sub-task is the same for the three compared options, being the best starting point for the process with the given constraints (heating capability for

the reactor). Since the violation of the same constraint signifies the end of the first sub-task, the second sub-task is the same for all operational sequences. However, the operating time for the second sub-task varies, because the value for the  $\Delta P$  range is different (violated constraint  $P_{up} - \Delta P$ ). The succeeding sub-tasks (no 3 and 4) are then found accordingly.

The first sub-task for the suggested sequence was chosen among a number of constant heating operations. The infeasibility of these operations and the superiority of the suggested operational sequence from the algorithm is shown in table 5.7. For the cases where  $T_{up} - T > 20$  K, then it is the lower limit for the temperature that is violated, while when  $T_{up} - T < 0$  K, the upper limit for the temperature is violated. In fact, as it can be seen in the table, at least one of the temperature or pressure constraints is violated in all the constant heating operations.

Operation MJ/hr	Time (hr)	$T_{up} - T$ (K) at $Y'_P = 0.85$	P (atm) at $Y'_P = 0.85$
Adiabatic	7.41	36.2	1.40
Heating (100 MJ/hr)	4.24	24.7	1.92
Heating (200 MJ/hr)	3.05	13.8	$2.58 > P_{up}$
Heating (300 MJ/hr)	2.48	6.4	$3.12 > P_{up}$
Heating (400 MJ/hr)	2.14	0.7	$3.58 > P_{up}$
Heating (500 MJ/hr)	1.89	-3.8	$3.98 > P_{up}$
Heating (600 MJ/hr)	1.71	-7.6	$4.36 > P_{up}$

Table 5.7: Duration and feasibility check for the constant heating operations for the two-phase reactor

The two case studies presented above showed that operating on a profile instead of constant operation can primarily achieve the product objectives in a feasible way. Operation on a profile is also a faster alternative and less costly in operation than a constant operation mode. However, it has been shown that there is an obvious trade-off between fast operating time and operating costs. Taking advantage of selectivity ensures the recovery objective for the specified product and suppresses the production of unwanted byproducts.

The application of the algorithms provides with feasible operational sequences that meet both path and terminal constraints. The active constraints change from one interval to the next, but preventive actions are taken so none of the constraints are violated. The use of slack variables help keep away from the actual constraints and the approximation of the end selectivity helps identify the course of selectivity and take the right action, so as to keep it as high as possible.

For the case where one liquid phase is present, the suggested sequence of sub-tasks consists of various intervals that i) keep selectivity the highest, ii) make sure that  $T < T_{up}$  and iii) guarantee that selectivity in the end is above a minimum  $S_{min}$ . The suggested sequence shows similarities to the Srinivasan

and Bonvin (2004) optimal solutions, even though their manipulated variable is the feed rate of one of the reactants. In the present algorithm, the manipulated variable is the heat input to the batch reactor, which is provided in a constant rate and changes accordingly from one interval to the other. The switch times are linked to the path constraints.

Similarly, for a two-phase system, the suggested sequence has i) an interval where the heat input is the maximum, ii) an interval where the active constraint is kept away from violation and iii) an interval where again the active constraint is kept away from violation and the recovery objective for the product is met. The suggested sequence of sub-tasks from the algorithms is feasible and can be used as initial sequence for a dynamic optimization problem.

## 5.4 Separation of ternary non-azeotropic system by batch distillation

A problem given in Perry's Handbook, 7th ed. (chapter 13, example 10) was considered, (Perry *et al.*, 1997). A ternary system of benzene, monochlorobenzene (MCB) and o-dichlorobenzene (o-DCB) needs to be separated by distillation. The mixture charge is 45.4 kmol with a composition of 25% benzene, 50% MCB and 25% DCB, which is to be distilled in a conventional batch still consisting of a reboiler, a column containing 10 theoretical stages, a total condenser, a reflux drum, and distillate accumulators.

The objectives for the separation task are to recover at least 95% of all three components with a 99% purity.

**Problem statement:** Given the identity and composition (initial holdup) of the mixture to be separated as well as the product specifications, determine the operational model for the separation task in order to achieve the specified end objectives for the products, preferably in minimum time and/or cost.

**Problem solution:** Algorithm A2 for the synthesis of feasible operational sequences for a batch distillation column is applied. Dynamic process simulation is applied to analyze and verify the generated operational sequence.

Step 1: The first separation task is identified in the first step of the algorithm. The compounds of the ternary mixture are ranked by increasing boiling point, namely benzene (353.2K), MCB (404.9K) and o-DCB (453.6K). No azeotropes are present in the mixture. Based on the above information, the first separation task is identified as the split between benzene and MCB and the acquired product will be benzene. The distillate composition for the algorithm is set as  $x_D = 0.999$ .

Steps 2-3: The column geometric specifications are given in appendix E. The reflux ratio for which flooding occurs is given versus the vapour boilup rate used in figure E.1 (appendix E). The vapour boilup rate is chosen, according

to rule A2.7 as  $V = 100 \text{ kmol/hr}$ .

Steps 4-6: The vapour-liquid equilibrium data for the binary pair of benzene and MCB are predicted using the UNIFAC v1 par model for the liquid phase and the ideal gas model for the vapour phase, at  $P = 1 \text{ atm}$ , where the models are selected from the thermodynamic specification in ICAS. The driving force is calculated as the difference between the liquid and the vapour composition, shown in figure 5.6.

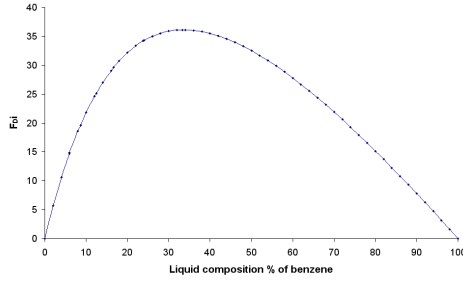


Figure 5.6: Driving force diagram for benzene - MCB separation

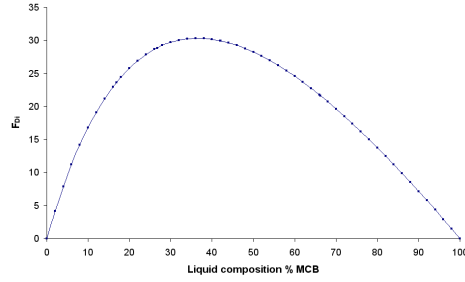


Figure 5.7: Driving force diagram for MCB - o-DCB separation

The feed composition at the beginning of the first time period is  $x_{F1} = 0.333$ . The distillate composition has been set to  $x_D = 0.999$ . Based on these values and the driving force  $F_{Di}$  for  $x_{F1} = 0.333$ , the minimum reflux ratio is calculated to be  $R_{min,1} = 0.844$ .

The actual reflux ratio used in the first time period, which corresponds to the number of plates of the column is found with Process Design Studio (PDS) in ICAS. The binary feed mixture is saturated liquid, the distillate composition is set to  $x_D = 0.999$  and the bottom composition is found for 95% recovery of benzene. The reflux ratio values that correspond to 12 plates (10 plates, a reboiler and a total condenser) are between 1.294 and 1.526. The reflux ratio for the first period is set to  $R_1 = 1.294$ .

Steps 7-9: The chosen reflux ratio is below the flooding value  $R_{max}(V)$  for the vapour boilup rate used, according to figure E.1. At the end of the first period, the bottom composition  $x_B$  is found with the graphical McCabe-Thiele method. The bottom composition is identified, for the first time period, from the 10<sup>th</sup> plate (rule A2.9). Solving equations 3.21 - 3.22, the amount of distillate collected in the holding tank at the end of the first period as well as the remaining total holdup of the column are calculated.

The duration of the first sub-task is predicted from equation 3.23 as  $t_1 = 0.0979 \text{ hr}$ .

Steps 10-12: The recovery of benzene at the end of the first period is approximately  $y_1^s = 37.6\%$ . Since  $y_{ben}^s - y_1^s > 10\%$ , the next period is not the final one,  $i + 1 \neq N$ .

The remaining amount in the bottom  $B_1$  is assigned as the feed  $F_2$  for the

second time period. The bottom composition  $x_{B1}$  is also considered to be the feed composition  $x_{F2}$ . Steps 5-12 are repeated until the final sub-task in the sequence for obtaining product benzene is identified.

The application of algorithm A2 provided the batch operational model for the first separation task, where benzene was obtained, as the sequence of six sub-tasks with a total time  $t_{ben} = 0.4384hr$ . BRIC in connection to the dynamic simulation engine of ICAS was employed for the verification of the operational model.

The only additional constraint for the rigorous simulation was imposed on the distillate composition, which was not allowed to drop below the purity objective. However, for the final sub-task the active constraint was the purity of benzene in the distillate accumulator. The stepwise reflux ratio profile for obtaining pure benzene is given in table 5.8.

Period no	Minimum reflux ratio $R_{min}$	Reflux ratio R	Vapour boilup rate V	Simulated time (hr)
1	0.844	1.294	100	0.0854
2	1.225	1.969	100	0.0421
3	1.809	2.65	100	0.0610
4	2.476	3.865	100	0.0413
5	3.644	6.654	80	0.1166
6	5.41	11.962	80	0.1147

Table 5.8: Batch recipe for obtaining first pure product benzene in example 5.4

The batch recipe suggested follows initial operation at total reflux until steady state is reached after  $t_{ss} = 0.0541hr$ . The total simulation time for the sequence of six sub-tasks is  $t_{ben}^{sim} = 0.4611hr$  ( $t_{ss}$  not included). At the end of the sequence both product objectives were reached (product purity = 99% and product recovery = 96.58% > 95%).

Once the first product is obtained, the second separation task needs to be identified. The composition of remaining benzene in the binary pair is above the maximum allowed  $x_F^{max}$ , so according to rule A2.2 an intermediate cut has to be distilled before the next pure product can be obtained.

Knowing the amount already distilled and the remaining holdup in the column, the composition of benzene in the binary pair is calculated  $x_F^{bin} = 0.0169$ . The maximum allowed binary composition  $x_F^{max}$  that does not jeopardize the fulfillment of the second product's objectives is found from equation B.5 (appendix B) as  $x_F^{max} = 0.0095$ . However, the removal of the intermediate product needs to lower  $x_F^{bin}$  below  $x_F^{max}$ , since that value corresponds to distillate composition  $x_{D2} = 1$ . If the distillate composition is  $x_{D2} = 0.999$ , then according to equation B.4  $x_F^{bin}$  (appendix B), needs to be lowered to 0.00857.

The reflux ratio used for the removal of the intermediate cut is the same as in the last sub-task of the sequence for obtaining benzene ( $R_7 = 11.962$ ). For the third separation task, the binary pair considered is MCB and o-DCB. The feed composition is  $x_F = 0.668$  and the required distillate composition is  $x_D = 0.999$ . Once the driving force curve is calculated for the pair, figure 5.7, steps 3-12 of algorithm A2 are repeated to generate the batch operational model for obtaining pure MCB. The suggested sequence consists of 4 sub-tasks with a predicted total time  $t_{MCB} = 0.6643hr$ . The sequence is described in table 5.9.

Period no	Minimum reflux ratio $R_{min}$	Reflux ratio R	Vapour boilup rate V	Simulated time (hr)
8	0.557	1.05	80	0.374
9	0.931	1.615	80	0.2301
10	1.536	2.58	80	0.0553
11	2.517	5	80	0.1215

Table 5.9: Batch recipe for obtaining second pure product MCB in example 5.4

The total simulation time for the sequence of four sub-tasks is  $t_{MCB}^{sim} = 0.7809hr$ . At the end of the sequence both product objectives were reached (product purity = 99% and product recovery = 95%). At the end of this sequence, the composition of the heaviest component in the reboiler is  $x_B = 0.949$ , which does not satisfy the purity of objective for this product. A final sub-task is necessary, where an intermediate cut is distilled, in order to bring the o-DCB purity in the reboiler in the desired value ( $R_{12} = 17$ ).

Accumulated results are given in table 5.10 and in figures 5.8 - 5.12. In a total time of  $t = 1.4867hr$  after the first operation with total reflux, the initial charge is separated in its components. Benzene is collected in distillate accumulate no 1, while MCB is collected in distillate accumulate no 3 and the heavy o-DCB is collected from the reboiler. Both the purity and the recovery objectives for all the products are achieved.

The distillate composition for the entire operation (full sequence) is given as a function of time in figure 5.8. Initially the reflux ratio profile used keeps the distillate composition rich in benzene, which is the blue line in figure 5.8. When the distillate is collected as an intermediate product in holding tank 2, its composition becomes more and more rich in MCB. The reflux profile used next causes the distillate composition to be rich in MCB, illustrated with the pink line in the figures. The last intermediate product is collected for the enrichment of the reboiler composition and achievement of the purity objective for the final product o-DCB, which is collected from the reboiler, as shown in figure 5.9.

The reflux ratio profile for the entire operation is given as a function of time in figure 5.10. The vertical dashed lines indicate the switch times between



	Distillate accumul. 1	Distillate accumul. 2	Distillate accumul. 3	Distillate accumul. 2
Number of sub-tasks	6	1	4	1
Total time of operation, hr	0.4611	0.074	0.7809	0.1487
Accumulated distillate				
Total (kmol)	11.0714	0.4786	21.7823	1.0547
Mole fractions				
Benzene	<b>0.9901</b>	0.4099	0.0088	0.1860
MCB	0.0009	0.5901	<b>0.99</b>	0.8011
o-DCB	0	0	0.0011	0.0129
Reboiler composition				
Mole fractions				
Benzene	0.0106	0.0054	0	0
MCB	0.6519	0.6522	0.0515	0.01
o-DCB	0.3375	0.3424	0.9485	<b>0.99</b>

Table 5.10: Accumulated results for the separation of benzene - MCB - o-DCB mixture

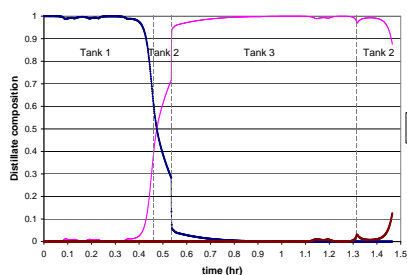


Figure 5.8: Distillate composition over time for benzene - MCB - o-DCB separation

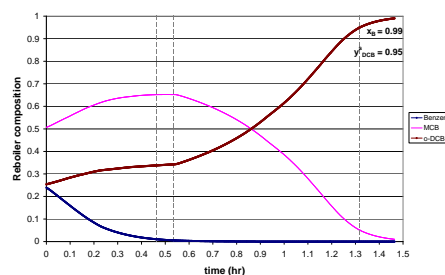


Figure 5.9: Reboiler composition over time for benzene - MCB - o-DCB separation

the different separation tasks, where different products and intermediates are collected in various tanks. Each separation task consists of one or more sub-tasks, where the reflux ratio is kept constant. The temperature profiles for the condenser and the reboiler are presented in figure 5.11. As expected, for the first and the third separation tasks, where almost pure benzene and MCB, respectively, are distilled, the condenser temperature is close to the boiling points of the pure compounds. Similarly, the reboiler temperature, given as an orange line, approaches in the end the boiling point of pure o-DCB.

It should be noted that both intermediate products are collected in the same holding tank (no 2), which means that the amount and composition shown in

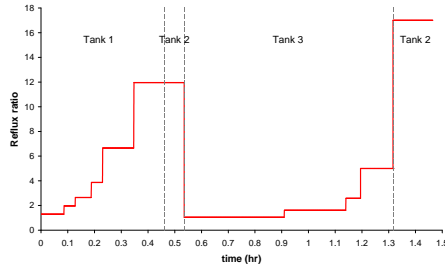


Figure 5.10: Reflux ratio profile for benzene - MCB - o-DCB separation

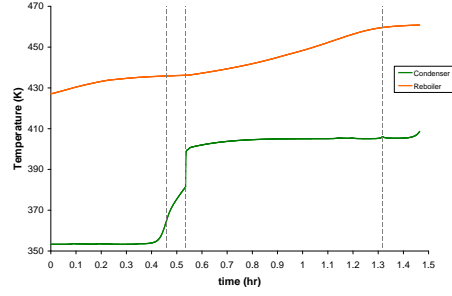


Figure 5.11: Condenser and reboiler temperature profile for benzene - MCB - o-DCB separation

the last column of table 5.10 are of the mixed cut-offs. This amount can be recycled to the next batch for further separation. The distillate accumulate as a function of time in the various holding tanks is given in figure 5.12. One can notice that the accumulate in tank no 2 for the last period starts exactly at the point it ended in sub-task 7 at time  $t = 0.5351$  hr ( $= 0.4611 + 0.074$ ). Accumulates in tanks no 1 and 3 start from zero.

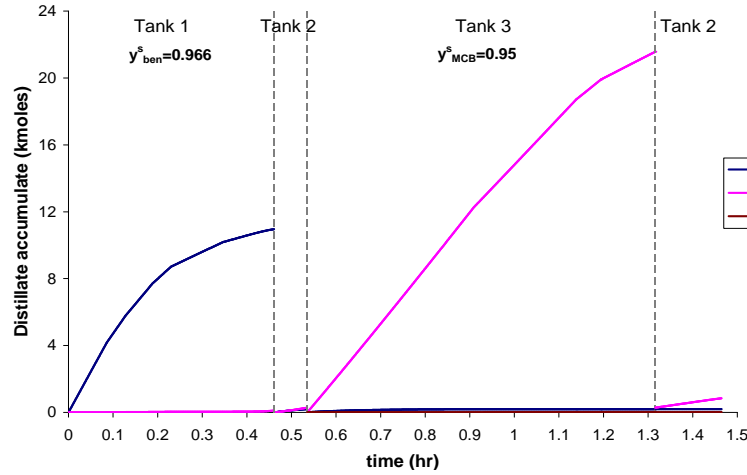


Figure 5.12: Distillate accumulate in various tanks as function of time for benzene - MCB - o-DCB separation

Comparing the two sub-sequences for obtaining pure benzene and pure MCB, namely reflux ratio profiles  $R_1$ - $R_6$  and  $R_8$ - $R_{11}$ , with constant reflux ratio operation shows the superiority of the stepwise reflux ratio operation. After the steady state condition was reached, constant reflux ratio operation was used (at various  $R$  values, given in table 5.11), until the point  $t$  where the desired

purity objective was not compromised. For the case of the benzene product, a constant reflux ratio below the value of  $R = 6.38$  leads to infeasible operation, because the recovery objective can not be achieved together with the purity objective. Operating at reflux ratio values above  $R = 6.38$ , both end objectives are satisfied, but require longer total operation time. The generated sequence from the algorithm is 44% faster compared to operation with the smallest constant reflux ratio, where both product objectives are achieved ( $R = 6.38$ ). Furthermore, about 46% less reflux is returned to the distillation column in the former operation compared to the latter.

Reflux ratio	Product purity %	Product recovery %	time (min)	Total reflux $L$ (kmoles)
1.294	99	44.6	6.3	6.6
1.969	99	70.6	12.6	15.98
2.65	99	81.3	17.5	24.76
3.865	99	89.5	25.1	39.79
6.38	99	95	49.4	69.48
6.654	99	95.3	51.3	72.92
11.962	99	98.4	88.1	135.2
$R_1 - R_6$	99	96.6	26.3	37.64

Table 5.11: Comparison of suggested reflux ratio profile with constant reflux ratio operation (for product benzene) in example 5.4

Similar results are obtained from the comparison of the suggested batch operations model with operation at constant reflux ratio when attaining pure MCB. It was observed that operation with constant reflux ratio values below  $R = 3.83$ , after the intermediate cut is removed, means that the product objectives can not both be satisfied. The stepwise reflux ratio operation suggested by the algorithm is actually 41.1% faster and with 58.2% less reflux returned to the column compared to the operation with the smallest constant reflux ratio, where both product objectives are achieved ( $R = 3.83$ ).

## 5.5 Separation of binary azeotropic system by batch distillation

A binary mixture of methanol (MeOH) and methyl-acetate (MeAc) needs to be separated by batch distillation. The mixture charge is 50 kmoles with a composition of 15% MeOH and 85% MeAc. This mixture is to be distilled in a batch still consisting of a reboiler, a column containing 18 theoretical stages, a total condenser, a reflux drum, and a distillate accumulator.

The objective is to collect a 99 % purity MeAc product from the reboiler, with a recovery of at least 95% of the maximum.

**Problem statement:** Given the identity and composition of the components in the mixture to be separated, and the product specifications, identify the separation task and determine an operational model, to achieve the specified product objectives, preferably in minimum time and/or cost.

**Problem solution:** Algorithm A2 for the synthesis of feasible operational sequences for a batch distillation column is applied. Dynamic process simulation is applied to analyze and verify the generated operational sequence.

The binary pair forms a minimum boiling azeotrope at  $T_{az} = 327.1K$  with a composition of 67.63% MeAc. In this case, the minimum boiling azeotrope is the first product to be obtained in the batch rectifier. Since the feed composition is above the azeotropic composition, after the azeotrope is distilled the next product that can be obtained is MeAc, according to rule A2.5. The maximum recovery of 99% pure MeAc is found to be 27.409 kmoles.

The distillate composition in the algorithm is set close to the azeotropic composition,  $x_D = 0.3227$ . The vapour boilup rate is chosen to be  $V = 100 \text{ kmoles/hr}$ . The vle data for the binary pair of MeOH and MeAc are predicted using the UNIFAC vle 1 par model for the liquid phase and the ideal gas model for the vapour phase, at  $P = 1 \text{ atm}$ . The driving force as a function of the liquid composition of MeOH is shown in figure 5.13.

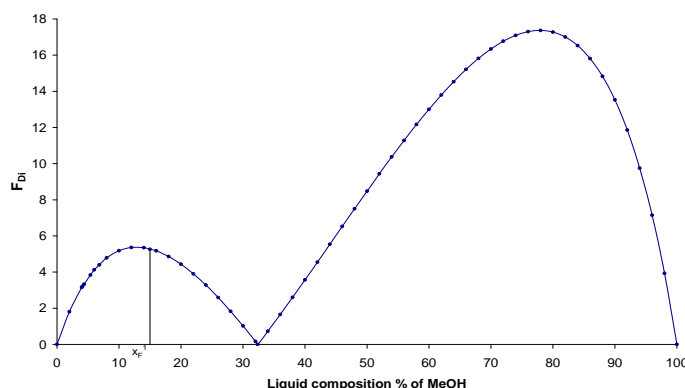


Figure 5.13: Driving force diagram for MeOH - MeAc separation

For the calculation of the minimum reflux ratio from equation 3.20, the feed and distillate compositions used are that of MeOH, so that  $x_D > x_F$ . The application of the algorithm provides a sequence of three sub-tasks with a predicted total time of  $t_{az} = 1.523 \text{ hr}$ . The sequence is described in table 5.12.

Dynamic simulation is employed to verify the suggested recipe through BRIC. The end of each sub-task was found when the distillate composition dropped below  $x_D = 0.3227$ . The active constraint for the last sub-task was the purity of MeAc in the reboiler  $x_B = 0.99$ . The total simulation time for the suggested

sequence is  $t_{az}^{sim} = 1.619hr$ . At the end of the sequence the remaining MeAc in the reboiler is 99% pure and 95.8% of its maximum recovery is obtained. Thus both product specifications have been achieved. The composition of the reboiler as function of time is given in figure 5.14, while the temperature of the distilled azeotrope throughout the sequence is shown in figure 5.15. The vertical dashed lines in the two figures indicate the switch times between the three sub-tasks of the suggested batch operations model.

Period no	Minimum reflux ratio $R_{min}$	Reflux ratio $R$	Vapour boilup rate $V$	Simulated time (hr)
1	2.283	4.775	100	1.134
2	4.39	8.23	100	0.224
3	7.859	14	100	0.261

Table 5.12: Batch recipe for removing the minimum boiling azeotrope in example 5.5

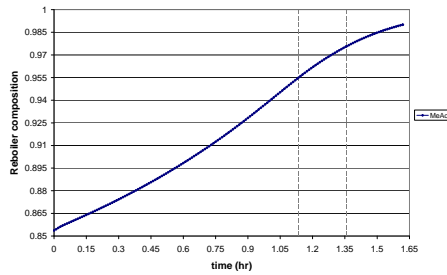


Figure 5.14: Reboiler composition over time for MeOH - MeAc separation

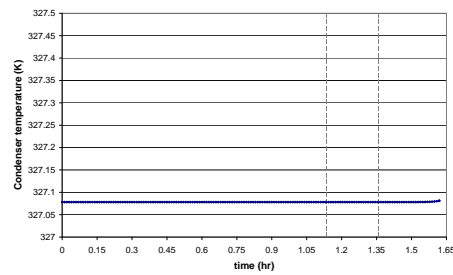


Figure 5.15: Condenser temperature profile for MeOH - MeAc separation

The suggested sequence was compared with constant reflux ratio operation. In that case, it was found that for low values of the reflux ratio ( $R < 9.96$ ), the recovery objective for the methyl-acetate product could not be achieved. For higher values of the reflux ratio, the operating time was significantly longer than the one achieved by the suggested operational sequence. Compared to the operation with the lowest constant reflux ratio, where both product objectives are achieved ( $R = 9.96$ ), the stepwise reflux ratio operation suggested by the algorithm is actually about 38% faster.

The previous two case studies for batch distillation demonstrated that, in general, a stepwise reflux ratio profile is much faster than a constant reflux ratio operation, which has a sufficiently high value for achieving both product objectives, recovery and purity. The suggested reflux ratio profile from the A2

algorithm guarantees the accomplishment of the products purity and recovery. The constant values for the reflux ratio for each interval are found *a priori* based on the VLE data of the binary pairs considered and an available computational tool for the synthesis of continuous distillation columns. No rigorous models for batch distillation columns are necessary to find the suggested profile.

The reflux ratio profile can serve as a very good starting point for an optimization problem. Dynamic simulation has shown that the switch times between the intervals need to be redefined. However, the difference between the calculated switch times and the simulated times is not so big. The sensitivity to this difference can be expected to decrease once the feed charge to the distillation column increases. For the small feeds considered in examples 5.4-5.5, the actual differences are small, but compared to the period duration, the deviation is significant enough to prevent the purity objective to be fulfilled if the calculated times are kept.

An important feature of the algorithm is the identification of the need of intermediate cuts when multicomponent mixtures are considered. It has also been shown that a mixture can be separated in high purity compounds, without compromising the product recovery. For multicomponent mixtures, the order of the products obtained is determined and it is easy to generate the reflux ratio profiles to obtain these products, considering each time the adjacent binary pairs.

For the azeotropic mixture that has been considered, the suggested reflux ratio profile guaranteed that the desired product MeAc distilled with the azeotrope was the minimum. If the reflux ratio was not sufficiently large, then the distillate composition would become greater than the azeotropic composition, which means that unnecessary MeAc would have been removed. This could compromise the recovery objective for the MeAc product collected from the reboiler. On the other hand, if the reflux ratio was too large, then longer operating time and larger operating costs would be necessary for the product objectives to be met. Consequently, an appropriate reflux ratio profile is also necessary to quickly remove an azeotrope and to obtain after that the desired product.

## 5.6 Separation of ternary electrolyte systems by batch crystallization

### 5.6.1 Separation of Type I ternary system

Sodium chloride needs to be recovered from a ternary aqueous mixture of sodium chloride (NaCl), potassium chloride (KCl) and of course water. The feed charge is 100 kg and the mass composition of the ternary system is water 80%, NaCl 15% and KCl 5%. The crystallizer can be operated within a temperature range of 0 to 100 °C.

The objective of the separation is to recover 95% of the dissolved NaCl.

**Problem statement:** Given the identity of the solvent and the solutes, the feed charge and composition, the operating temperature of the crystallizer, and the product specifications, determine the sequence of solids precipitating, the necessary sequence of operational sub-tasks and their operating conditions, in order to reach the specified product objectives.

**Problem solution:** Application of algorithm A3 for the synthesis of batch crystallization based on solid-liquid phase diagram.

Steps 1-2: In the first step of the algorithm, the ternary phase diagram is generated for the operational temperature range. The thermodynamical model used for the liquid phase is an extended UNIQUAC model for aqueous salt and ideal gas for the vapour phase. No hydrates or double salts need to be added in the component list for the estimation of the phase diagram.

The feed Cartesian coordinates are  $X_F = 45$ ,  $Y_F = 80$  as transformed from the triangular coordinates, according to equation 3.26. Once the phase diagrams are generated, the positions of the invariant points are also known for the temperature range. From the given feed, the precipitation of NaCl is actually feasible at any temperature within the given range, since equation 3.32 is satisfied. The solid-liquid equilibrium phase diagram is shown in figure 5.16, where only the minimum and the maximum temperature data are drawn for simplicity.

Steps 3-4: The operating temperature for the precipitation of NaCl is chosen so that the resulting slurry density is the maximum. As seen from figure 5.16, the slurry density (and thus the yield) increases as temperature increases. Therefore, the temperature for the crystallizer is set to the maximum value of  $T_1 = 100^\circ\text{C}$ .

As already mentioned, equation 3.32 is satisfied for the feed and additionally  $Y_F > Y_{inv}$ , which means that the feed is located in the unsaturated region and the necessary sub-task for precipitation of NaCl is evaporation at  $100^\circ\text{C}$ .

Steps 5-7: The amount of solvent evaporated is about 99% of the maximum evaporation and the resulting slurry is point  $SL_1$  (35.6, 42.4). The mother liquor in equilibrium with  $SL_1$  is found to be point  $ML_1$  (52.17, 62.135) and the slurry density is  $\rho_{SL_1} = 0.3176$ . The recovery for the precipitated NaCl for the first sub-task is easily calculated to be  $y_{1,NaCl}^s = 0.735$ , which is below the desired objective.

Steps 8-9: The mother liquor  $ML_1$  resulting after the precipitated salt is recovered, is treated as a new feed, in order to identify the second sub-task in the sequence. Steps 2-8 are repeated for that reason.

The precipitation of NaCl is not feasible at any temperature for the new considered feed (except of course for  $T_1 = 100^\circ\text{C}$ ). The salt that will precipitate in the second sub-task is KCl. Since  $Y_{F_2} < Y_{inv}$  and equation 3.35 is satisfied, hence the mother liquor  $ML_1$  lies in the saturated region for KCl. Operating at the lowest temperature gives the largest slurry density and therefore, the

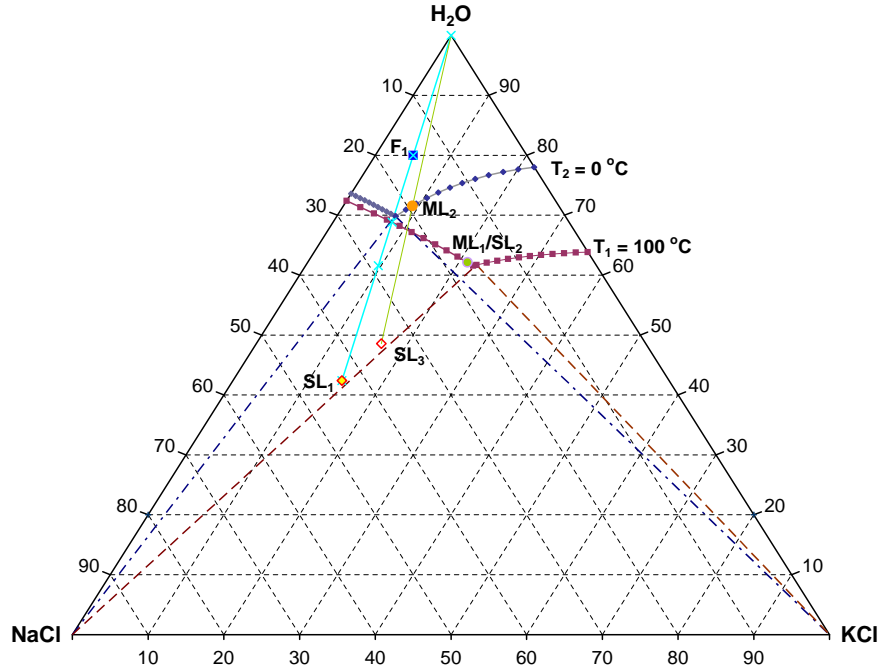


Figure 5.16: Generated operational path for the type I system illustrated on the ternary phase diagram

temperature for the second sub-task is chosen to be  $T_2 = 0^\circ\text{C}$ . Since the desired salt is not KCl, there is no reason for further evaporation that maximizes the recovery. Therefore, the second sub-task is plain cooling crystallization at  $T_2 = 0^\circ\text{C}$ . The mother liquor in equilibrium with the current slurry is  $ML_2$  (44.91, 71.566). The slurry density is  $\rho_{SL_2} = 0.1318$  and the recovery for the precipitated KCl is  $y_{2,KCl}^s = 0.625$ .

Once again, mother liquor  $ML_2$  is treated as a new feed ( $F_3$ ). It is checked whether the precipitation of NaCl is feasible at  $T_1 = 100^\circ\text{C}$ , so that alternate precipitation of NaCl and KCl is used for the satisfaction of the recovery objective for NaCl. The precipitation of NaCl is feasible for  $T > 20^\circ\text{C}$  and the highest recovery is at  $T_1 = 100^\circ\text{C}$ . Evaporation is necessary since  $ML_2$  lies in the unsaturated region and the amount of evaporated solvent is chosen such that the resulting slurry  $SL_3$  (40.796, 48.589) is in equilibrium with a mother liquor of a composition of  $ML_1$ . The slurry density is  $\rho_{SL_3} = 0.218$  and the recovery for the precipitated NaCl is  $y_{3,NaCl}^s = 0.6245$ .

Solving equation 3.47, it is found that the desired recovery  $y_{NaCl}^s = 0.95$  is achieved after the third precipitation of NaCl ( $i = 3$ ). The total number of alternate precipitations in series is then found to be  $p = 2i - 1 = 5$ . Actually the total recovery achieved should be  $y_{total}^s = 0.9626 > 0.95$ . The operational



sequence of sub-tasks for the desired recovery of the dissolved NaCl is given in table 5.13.

Sub-task no	Operation	Temperature °C	Salt pptd	Simulated yield
1	Evaporation 65.278 kg water	100	NaCl	73.5%
2	Cooling crystallization	0	KCl	62.5%
3	Evaporation 9.194 kg water	100	NaCl	90.1%
4	Cooling crystallization	0	KCl	85.9%
5	Evaporation 3.452 kg water	100	NaCl	96.25% > 95%

Table 5.13: Operational sequence for the batch crystallizer for the separation of the type I ternary system

The suggested sequence was verified by dynamic simulation in ICAS. For each sub-task the temperature and the vaporization were given. For simulation purposes, the sub-tasks of evaporative crystallization at  $T_1 = 100^\circ\text{C}$  are done in two steps, first the removal of solvent and then the solid-liquid separation. The desired vaporization, as provided in table 5.13, was given as an evaporation rate in kmol/hr and the operation time was set to an hour.

The objective of this example was to provide the operational path for the recovery of the specified salt in terms of sub-tasks (e.g. evaporation, dilution, temperature swift, solid-liquid separation) and operating temperatures and it was not attempted to establish operating times. Moreover, the time needed for the evaporation depend on the heat removal capabilities of the unit and it was considered out of the scope of this example to proceed in that direction.

### 5.6.2 Separation of Type II ternary system

The ternary system of water, sodium sulphate ( $\text{Na}_2\text{SO}_4$ ) and ammonium sulphate ( $(\text{NH}_4)_2\text{SO}_4$ ) is investigated for the recovery of the dissolved sodium sulphate. The mass composition of the mixture is 80% water, 15%  $\text{Na}_2\text{SO}_4$  and 5%  $(\text{NH}_4)_2\text{SO}_4$  and the feed charge is 100 kg. The permitted temperature range of the crystallizer is 0 to 100 °C. For the estimation of the phase diagram, the information that the pure salts precipitate also in other forms, such as sodium sulphate decahydrate and sodium ammonium sulphate tetrahydrate, is given.

The objective for the separation is the maximization of the recovery of  $\text{Na}_2\text{SO}_4$ , at the lowest operating temperatures, when only pure solutes are allowed to precipitate.

**Problem statement:** Given the identity of the solvent and the solutes, the

feed charge and composition, the operating temperature of the crystallizer, and the product specifications, determine the sequence of solids precipitating, the necessary sequence of operational sub-tasks and their operating conditions, in order to reach the specified product objectives.

**Problem solution:** Algorithm A3 for the synthesis of batch crystallization based on solid-liquid phase diagram is applied.

The phase diagram generated, shown in figure 5.17, is by far more complicated than that of the Type I system discussed in the previous example. Unwanted hydrates and double salts precipitate at different temperatures. For the given feed ( $X_F = 45, Y_F = 80$ ), the precipitation of  $\text{Na}_2\text{SO}_4$  is not feasible for all temperatures, but only for temperatures  $T \geq 30^\circ\text{C}$ . For temperatures below  $30^\circ\text{C}$ , the decahydrate form precipitates. The lowest temperature where  $\text{Na}_2\text{SO}_4$  precipitates is chosen as  $T_1 = 30^\circ\text{C}$ . Since the feed is in the unsaturated region (equation 3.32 is satisfied and  $Y_F > Y_{inv}$ ), evaporation is the first sub-task.

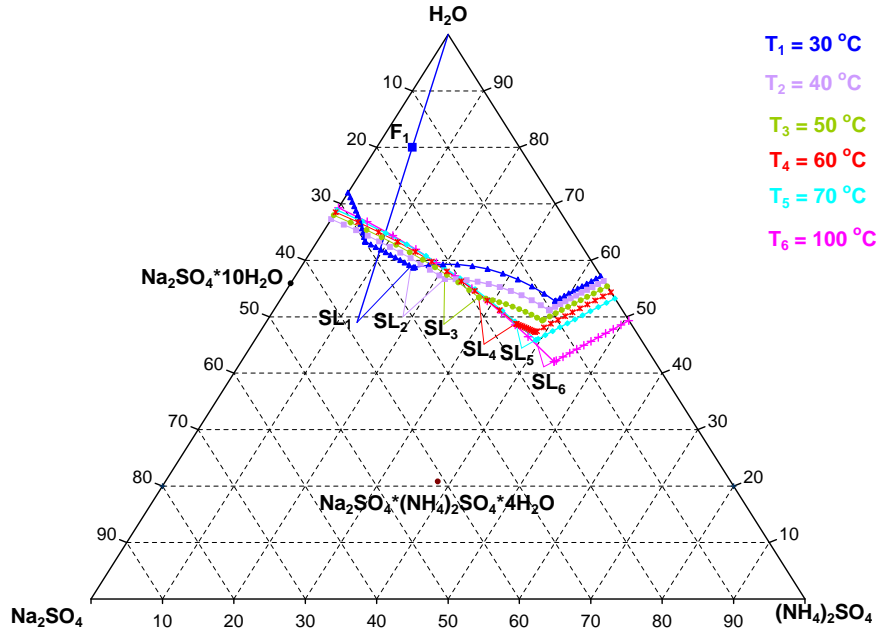


Figure 5.17: Generated operational path for the type II system illustrated on the ternary phase diagram

The amount of water evaporated and the resulting slurry are found according to rule A3.8. The mother liquor in equilibrium with the precipitated solid can either be used for the precipitation of the decahydrate at low temperatures or

for the precipitation of  $\text{Na}_2\text{SO}_4$  for  $T \geq 30^\circ\text{C}$ . Therefore, since the objective is the recovery of  $\text{Na}_2\text{SO}_4$  and no alternative salts precipitation can be applied in 2 different temperatures, the next sub-task is chosen to be evaporation at the next lowest temperature  $T_2 = 40^\circ\text{C}$ . Similarly, the amount of water evaporated and the resulting slurry are found according to rule A3.8 and the mother liquor is found from the tie line.

The sequence of sub-tasks leading to the maximum recovery of  $\text{Na}_2\text{SO}_4$  from the given feed is based on the following information and constraints. The constraint of operating at the lowest temperature needs to be taken into consideration. Furthermore, from the phase diagram the information gained is that the obtained mother liquor from the precipitation of  $\text{Na}_2\text{SO}_4$  at temperature  $T$  can only be used for further precipitation of the salt at higher temperatures. Moreover, it can be calculated that at lower temperatures than  $T$  either the decahydrate form or the double salt precipitates.

The precipitation of  $(\text{NH}_4)_2\text{SO}_4$  is not feasible from the mother liquors obtained at low temperatures. The precipitation of  $\text{Na}_2\text{SO}_4$  at the maximum temperature  $T = 100^\circ\text{C}$  results in a mother liquor where alternate precipitation between  $(\text{NH}_4)_2\text{SO}_4$  and  $\text{Na}_2\text{SO}_4$  is possible at two temperatures  $T = 60^\circ\text{C}$  and  $T = 100^\circ\text{C}$  respectively. However, the recovery of  $\text{Na}_2\text{SO}_4$  does not increase so much at every repetitive cycle and such an alternate salt precipitation was not applied.

The last sub-task of the sequence is evaporative crystallization at the highest temperature  $T = 100^\circ\text{C}$ . The maximum recovery achieved is  $y_{total}^s = 0.8925$ . The sequence of sub-tasks suggested, in order to achieve the maximum recovery of  $\text{Na}_2\text{SO}_4$  from the given feed at the lowest operating temperatures is given in table 5.14.

Sub-task no	Operation	Temperature $^\circ\text{C}$	Salt pttd	Simulated yield %
1	Evaporative crystallization 60.776 kg	30	$\text{Na}_2\text{SO}_4$	44.2%
2	Evaporative crystallization 5.815 kg	40	$\text{Na}_2\text{SO}_4$	65.1%
3	Evaporative crystallization 3.701 kg	50	$\text{Na}_2\text{SO}_4$	77.1%
4	Evaporative crystallization 2.756 kg	60	$\text{Na}_2\text{SO}_4$	84.7%
5	Evaporative crystallization 1.120 kg	70	$\text{Na}_2\text{SO}_4$	87.5%
6	Evaporative crystallization 1.033 kg	100	$\text{Na}_2\text{SO}_4$	89.2%

Table 5.14: Operational sequence for the batch crystallizer for the type II ternary system

The suggested sequence was verified by dynamic simulation in ICAS. The temperature and the evaporation rate used in each sub-task are given in table 5.14. The crystallizer was not operated at temperatures between 70 and 100 °C, since the slurry density resulting from the evaporation of  $ML_5$  at those temperatures was too small. It can also be seen in table 5.14 that the recovery from sub-task 5 to sub-task 6 improves only very little, but it would improve even less if sub-task no 6 was evaporative crystallization at  $T_6 = 80^\circ\text{C}$ , and so on.

Alternatively, if there was no limitation on operating at the lowest temperature, the suggested sequence would be completely different. Evaporation at  $T_1 = 100^\circ\text{C}$  would be chosen as the first sub-task, since the recovery is highest at the highest temperature. The resulting mother liquor could then be treated as a new feed and further evaporation at the highest temperature  $T = 100^\circ\text{C}$  would result to a similar recovery of  $\text{Na}_2\text{SO}_4$  of  $y_{total}^s = 0.89257$ .

This example was used in order to highlight the possibility of generating a sequence of sub-tasks for the recovery of a solid, when specific requirements for the operating conditions are present, such as operating at the lowest temperature.

## 5.7 Separation of quaternary electrolyte system by batch crystallization

Sodium sulphate needs to be recovered from a quaternary aqueous mixture of sodium chloride ( $\text{NaCl}$ ), sodium carbonate ( $\text{Na}_2\text{CO}_3$ ), sodium sulphate  $\text{Na}_2\text{SO}_4$  and of course water. The feed charge is 100 kg and the mass composition of the quaternary system is water 70%,  $\text{NaCl}$  9%,  $\text{Na}_2\text{CO}_3$  3% and  $\text{Na}_2\text{SO}_4$  18%. The temperature of the crystallizer should be in the range of 0 to 100 °C.

The objective of the separation is to obtain pure  $\text{Na}_2\text{SO}_4$  at the maximum possible recovery, or with a yield of at least 80% ( $y_{\text{Na}_2\text{SO}_4}^s \geq 0.8$ ), when only pure solutes are allowed to precipitate.

**Problem statement:** Given the identity and composition of the components in the mixture to be separated, and the product specifications, identify the order of the precipitated salts and determine the necessary operational model, in order to achieve the specified product objectives.

**Problem solution:** Algorithm A3 for the synthesis of feasible operational sequences for a batch crystallizer is applied. Dynamic process simulation is applied to verify the generated operational sequence.

Step 1: First the phase diagram is generated for the given temperature range. The same thermodynamic model is used as in the previous crystallization examples. A number of additional solid forms are added to the component list, other than the dissolved pure salts, since they precipitate at various temper-

atures. The additional solids are the mono-, hepta- and decahydrate form of sodium carbonate, the decahydrate form of sodium sulphate and the double salt berkeyite (sodium carbonate disulphate). The complete component list used in this example is:  $\text{H}_2\text{O}$ ,  $\text{NaCl}$ ,  $\text{Na}_2\text{CO}_3$ ,  $\text{Na}_2\text{SO}_4$ ,  $\text{NaCl}\cdot\text{H}_2\text{O}$ ,  $\text{NaCl}\cdot 2\text{H}_2\text{O}$ ,  $\text{Na}_2\text{CO}_3\cdot 2\text{Na}_2\text{SO}_4$  (berkeyite),  $\text{Na}_2\text{CO}_3\cdot\text{H}_2\text{O}$ ,  $\text{Na}_2\text{CO}_3\cdot 7\text{H}_2\text{O}$ ,  $\text{Na}_2\text{CO}_3\cdot 10\text{H}_2\text{O}$ ,  $\text{Na}_2\text{SO}_4\cdot\text{NaCl}$ ,  $\text{Na}_2\text{SO}_4\cdot 7\text{H}_2\text{O}$ ,  $\text{Na}_2\text{SO}_4\cdot 10\text{H}_2\text{O}$ .

The phase diagram for the quaternary system is calculated in ICAS and it is provided in terms of the 3D Cartesian coordinates ( $X, Y, Z$ ). The  $Z$  coordinate is actually found from the given mass composition of the solvent and ions, and the solvent amount can then be calculated. The phase diagrams calculated and an indication of the change of solids precipitating in various parts of the phase diagrams at various temperatures are given in figures 5.18 to 5.23. The feed is illustrated with a blue rhombus in the above mentioned figures and depending on the operating temperature it lies in various regions where different solids precipitate. As an indication, for the given feed the decahydrate of sodium sulphate precipitates at 0 °C, as shown in figure 5.18,  $\text{Na}_2\text{SO}_4$  precipitates at 50 °C (figure 5.21) and berkeyite precipitates at 100 °C (figure 5.23).

Therefore, from the mentioned figures it is obvious that the desired solid  $\text{Na}_2\text{SO}_4$  does not precipitate over the whole temperature range. The equilibrium lines move with temperature, changing the size of the regions within which the different solids precipitate. The size of the regions with temperature, and particularly the size of the region that the feed lies in, also has an effect on the amount of solid that can precipitate without co-crystallization taking place. The solubility curves in figures 5.18 to 5.23 are multiple saturation curves, where two solids precipitate. The two solids that precipitate on every curve are found to be the ones that the two regions on each side of the curve are saturated with. The invariant points for these solvent-free phase diagrams are the points where three saturation curves meet and three regions in the diagram have borders with them. These three regions for every invariant point and the solids they are saturated with define the solids that will precipitate on each invariant point. Needless to say that the solubility curves and the invariant points should be avoided if co-crystallization is undesirable.

Steps 2-3: The desired solid  $\text{Na}_2\text{SO}_4$  precipitates in its pure salt form at temperatures above  $T \geq 20^\circ\text{C}$ . However, for the given feed, it is only the temperature range between 30 °C to 85 °C that can be used for the precipitation of  $\text{Na}_2\text{SO}_4$ .

The operating temperature for the first sub-task is chosen to be  $T_1 = 30^\circ\text{C}$ , since at that temperature the precipitation of  $\text{Na}_2\text{SO}_4$  is feasible and the highest slurry density is achieved. Consequently, the maximum recovery of the precipitated salt will be for  $T_1 = 30^\circ\text{C}$ .

Steps 4-5: According to rule A3.14, since the solubility index for all the solids in the feed is below unity, then the feed lies in an unsaturated region. Thus, the chosen operation is evaporation at  $T_1 = 30^\circ\text{C}$ .

The amount of water needed to be evaporated is found according to rule A3.16. The solvent free composition of the mother liquor is necessary to apply rule A3.16. First, the position of the resulting mother liquor is found at the intercep-

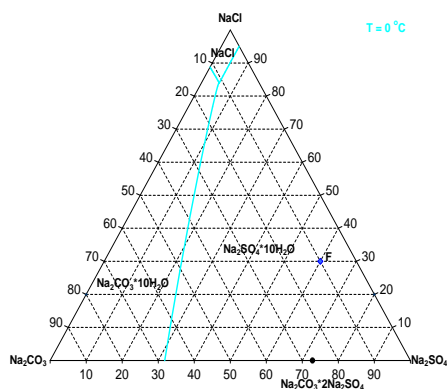


Figure 5.18: Solvent-free ternary phase diagram at T=0 °C

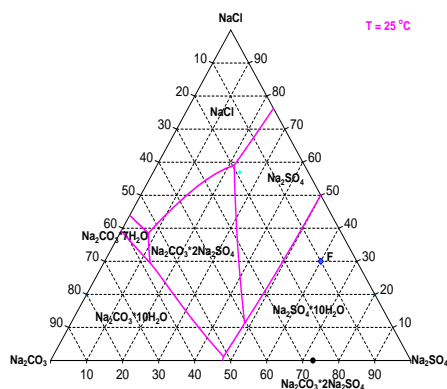


Figure 5.19: Solvent-free ternary phase diagram at T=25 °C

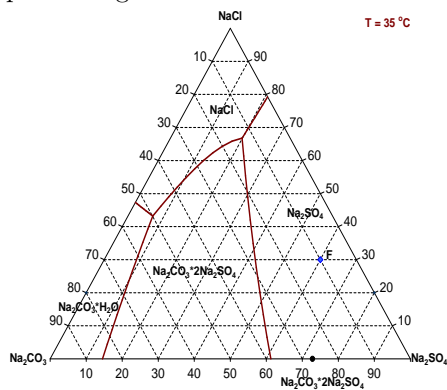


Figure 5.20: Solvent-free ternary phase diagram at T=35 °C

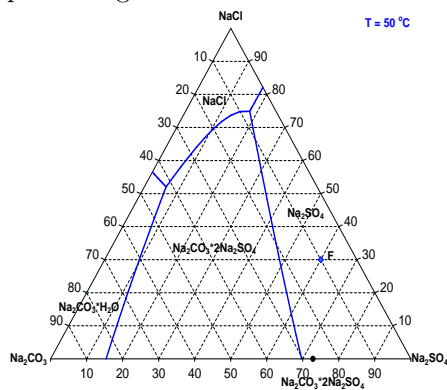


Figure 5.21: Solvent-free ternary phase diagram at T=50 °C

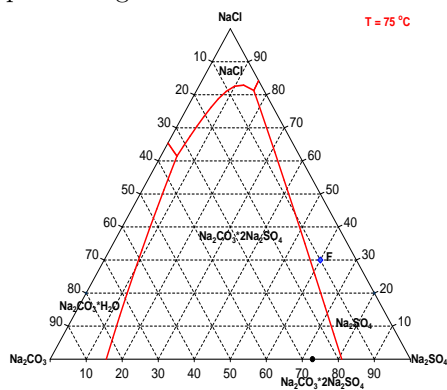


Figure 5.22: Solvent-free ternary phase diagram at T=75 °C

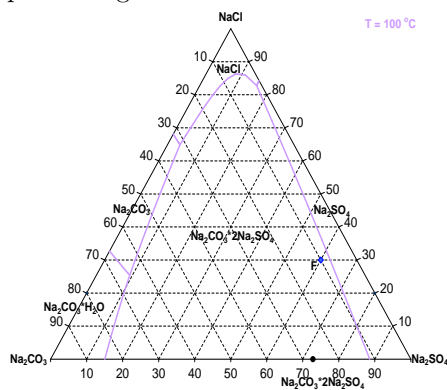


Figure 5.23: Solvent-free ternary phase diagram at T=100 °C

tion of the  $\text{Na}_2\text{SO}_4$  -  $SL_1$  line and the equilibrium line separating the region where  $\text{Na}_2\text{SO}_4$  precipitates and the region where  $\text{Na}_2\text{CO}_3 \cdot 2\text{Na}_2\text{SO}_4$  precipitates. From the Cartesian coordinates of  $ML_1$ , the triangular solvent free coordinates are found and also the amount of  $\text{Na}_2\text{SO}_4$  in the mother liquor, given that only sodium sulphate has precipitated.

For the calculated amount of solids in the mother liquor, the amount of water is found where the solubility index of  $\text{Na}_2\text{SO}_4$  equals to unity. The difference between the amount of water in the feed and the mother liquor  $ML_1$  is multiplied by 99% and the solvent evaporated is found.

Steps 6-9: The position of the slurry on the ternary phase diagram is exactly where the feed is located, since for the solvent free composition representation, the amount of solvent is irrelevant. The reason that the feed and the slurry are represented by the same point in the Jänecke projection diagram is because the amounts of dissolved salts are the same.

The position of the mother liquor is found as described above in step 5. The slurry density is found as the ratio  $\frac{SL_1 ML_1}{Solid ML_1}$ . The recovery of the dissolved  $\text{Na}_2\text{SO}_4$  in the first sub-task should be 78.846%. Since this is below the desired recovery, another sub-task is necessary. Mother liquor  $ML_1$  is treated as a new feed and steps 2-9 are repeated.

The precipitation of  $\text{Na}_2\text{SO}_4$  for the new feed is not feasible for temperatures above 30 °C, where the double salt berkeyite precipitates, or for temperatures below 15 °C, where the decahydrate of  $\text{Na}_2\text{SO}_4$  precipitates. It is actually for temperatures 20-25 °C that its precipitation is feasible. However, the slurry density is higher for  $T_2 = 25^\circ\text{C}$  and so further evaporation at that temperature is chosen.

The position of the new mother liquor  $ML_2$  is found in a similar manner as for sub-task 2. The amount of solvent evaporating is found according to rule A3.16. Knowing the position of  $SL_2$  and  $ML_2$ , the slurry density and the recovery of  $\text{Na}_2\text{SO}_4$  for the second sub-task are calculated. The total recovery of  $\text{Na}_2\text{SO}_4$  after two sub-tasks should be 81.732%.

The desired recovery of  $y_{Na_2SO_4}^s \geq 0.8$  has been achieved after two sub-tasks, but further improvement is investigated. The mother liquor  $ML_2$  is treated as a new feed, for which the precipitation of  $\text{Na}_2\text{SO}_4$  is not feasible for temperatures above 25 °C, where the double salt berkeyite precipitates, or for temperatures below 15 °C, where the decahydrate of  $\text{Na}_2\text{SO}_4$  precipitates.

At  $T = 20^\circ\text{C}$ , it is NaCl that precipitates. Since, this is one of the dissolved solutes allowed to recover, a third sub-task could be evaporation at  $T = 20^\circ\text{C}$ , but the recovery is quite small and the resulting mother liquor does not promote any significant improvement in the recovery of  $\text{Na}_2\text{SO}_4$  (sub-task 4) at  $T = 25^\circ\text{C}$ . Therefore, it was decided that the suggested operational sequence should consist only of two sub-tasks where  $\text{Na}_2\text{SO}_4$  is recovered. The sequence and the operating conditions for the crystallizer are given below in table 5.15.

Dynsim in ICAS was used to verify the feasibility of the suggested sequence.

Sub-task no	Operation	Temperature °C	Salt pttd	Simulated yield %
1	Evaporation 35.694 kg	30	Na <sub>2</sub> SO <sub>4</sub>	79.85
2	Evaporation 2.359 kg	25	Na <sub>2</sub> SO <sub>4</sub>	81.85 > 80%

Table 5.15: Operational sequence for the batch crystallizer for the separation of the quaternary electrolyte system

The necessary information given for each sub-task was temperature and the amount of solvent to be removed. The objective of this example was to provide the operational path for the maximum recovery of the specified salt of a quaternary system based on the solid-liquid phase diagram. The operational path is found in terms of sub-tasks and operating temperatures, with the further constraint that only the dissolved pure salts were allowed to be recovered.

The operational path is given graphically in figure 5.24. The solubility curves for a temperature of 20 °C are given with the green lines, the dashed pink lines define the different saturation regions for the quaternary system at a temperature of 25 °C, while the bold blue lines are for a temperature of 30 °C. For the two lower temperatures, the feed lies in the region saturated with the decahydrate of Na<sub>2</sub>SO<sub>4</sub> and it can easily be seen that the precipitation of Na<sub>2</sub>SO<sub>4</sub> for the given feed is feasible only at 30 °C. From the resulting mother liquor  $ML_1$ , which is the red point on the phase diagram, precipitation is feasible both at 20 °C and 25 °C, but the slurry density, as it can be seen from the graph, is higher at 25 °C. The slurry density is higher at 25 °C, because the distance from  $ML_1$  to the dashed line is further than to the green line. The resulting  $ML_2$  cannot be treated for the precipitation of Na<sub>2</sub>SO<sub>4</sub>, since it is situated in regions where either NaCl or the double salt that precipitates at 20 °C and 30 °C, respectively.

It should be noted that the feed  $F_1$  and the resulting mother liquors  $ML_1$  and  $ML_2$  lie on a straight line that passes through the Na<sub>2</sub>SO<sub>4</sub> vertex of the triangle. The more Na<sub>2</sub>SO<sub>4</sub> precipitates in succeeding sub-tasks at different temperatures the further the mother liquor lies from the vertex. For the furthest points, the pure salt that precipitates is NaCl. This is the reason that the maximum recovery of Na<sub>2</sub>SO<sub>4</sub> is realized as  $ML_2$ .

The crystallization examples that were presented proved how the solid-liquid equilibrium diagrams can be used for the synthesis of operational sequences, where the objective is to recover certain amounts of pure salts. It was shown that operating away from the invariant points eliminates the risk of cocrystallization. Switching from one operating temperature to another can be used to either alternately precipitate two solids or to achieve further precipitation of one solid. The latter case is in principle similar to pressure swing distillation,



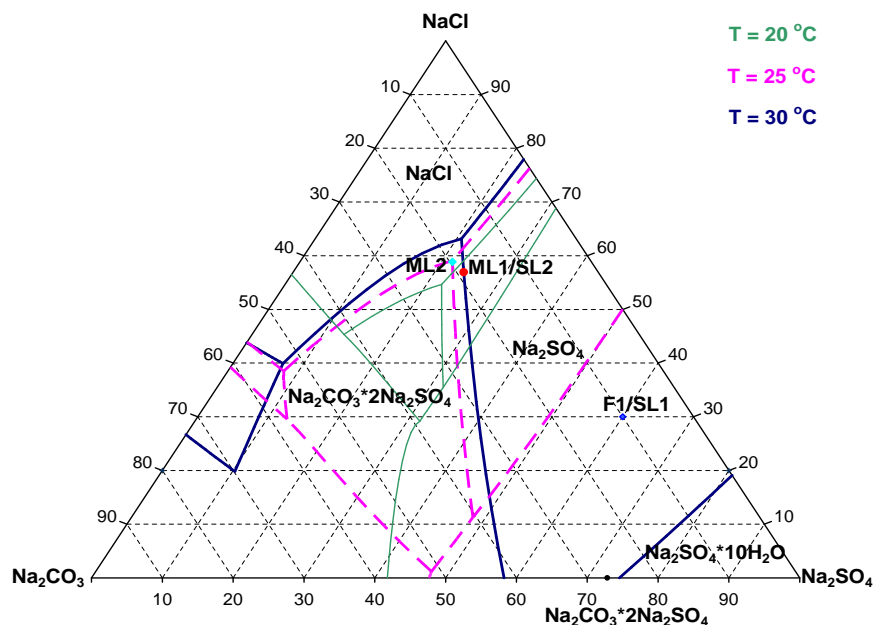


Figure 5.24: Generated operational path for the quaternary system illustrated on the ternary solvent-free phase diagram

where one takes advantage of the switch of the azeotrope position, in order to obtain more high purity product from the azeotropic composition.

The change in the solubility boundaries and regions has been most emphatically shown in the example with the quaternary system. In general, the mother liquor resulting from one precipitation, similar to an azeotrope, cannot be used for further precipitation in the same temperature. However, changing temperature, the size and the identity of the saturated regions also change and from that same mother liquor more desired solid can be precipitated.

The use of the ternary phase diagrams is a very easy way to illustrate the various operations, such as evaporation, dilution, temperature switch and the actually study of the phase diagram can lead to the decisions connected to the order and the identity of these operations. The developed algorithm additionally checks for the feasibility of the precipitation of a specified solid from a feed. This check can also be done by the phase diagram study, but correct identification can be difficult for borderline cases.

The systematic procedure for selecting the crystallization temperature was based on the feasibility of the precipitation of the solid and the maximum slurry density criterion. The crystallization examples showed that once the phase diagram is studied and understood, the generation of a sequence of operations for a specified recovery of pure solids is easy, even when different constraints on the operating temperature are present.

## 5.8 Generation of batch route (integrated example)

The problem adapted from Allgor *et al.* (1996) in section 5.2 is considered again, but for this case study the final product is reached after two set of reactions and the objective is to obtain high purity (99%) of compound  $P$  with a recovery of 90% ( $r_T = 0.9$ ). The proposed batch route to obtain product  $P$  in Allgor *et al.* (1996) is given in figure 5.25.

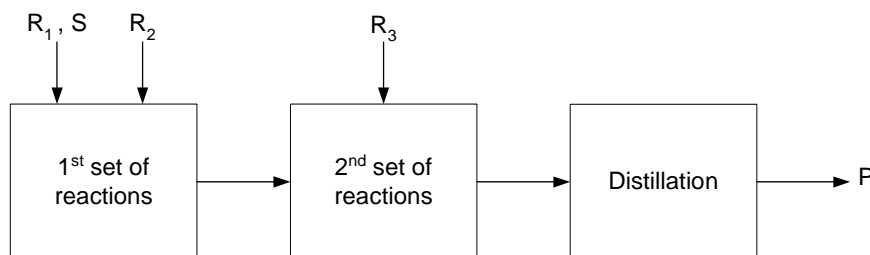


Figure 5.25: Suggested batch route for the adapted example (Allgor *et al.*, 1996)

The first set of reactions is given in example 5.2 in page 122 while the second set of reactions is:



which is the known methyl-tert-butyl ether synthesis from the reaction database. The lower and upper temperature limits for this reaction are  $T_{low} = 300K$  and  $T_{up} = 330K$ . Reactant  $R_3$  is methanol.

**Problem statement:** Given the identity and composition of the reactants, the set of reactions and their kinetics as well as the product specifications, determine the sequence of reaction and separation tasks necessary to achieve the specified end objectives for the product, preferably in minimum time and/or cost. Furthermore, determine the operational model for each task in the sequence.

**Problem solution:** Algorithm S for the synthesis of batch processes is applied to provide the batch route (sequence of batch tasks) for attaining product  $P$ . The algorithms for batch reaction (A1a) and separation (A2) are applied to provide the operational models for the respective tasks.

Step 1: Two reactions tasks are identified for the sequence from the two set of reactions. The desired and the unwanted reactions for the first set of reactions have been determined in section 5.2. Regarding the second set of reactions, the

single reaction is desired since it yields the final product. A final separation task for obtaining the product must come after the last reaction task. Thus, the sequence consists, initially, of these two reaction tasks and a subsequent separation task.

Step 2: The necessity of a separation task before the first reaction task is investigated next. The reactants for the first set of reactions ( $R_1$  and  $R_2$ ) are pure materials and according to rule S.5 no separation task needs to take place before the first reaction task. This is supported also by the fact that the solvent, even though it is present in high concentration, does not take part in any of the competing reactions (rule S.6) and therefore does not endanger the yield of the product. Furthermore, the solvent, which is considered an impurity for rules S.5 to S.10, does not form any azeotrope with the final product  $P$  (rule S.7) that would undermine the recovery of the product. The conclusion of the second step of the algorithm is that no separation task is necessary prior to the first reaction task.

Step 3: The scaled binary property ratios  $sr_{ij}$  or the “possibility distributions”  $\mu(r_{ij})$  for the adjacent binary pairs of compounds present in the system are given in appendix F for a number of properties. The largest  $sr_{ij}$  for both the reactant mixtures after the first and the second reaction task is the one for vapour pressure. The corresponding separation technique related to vapour pressure is distillation. Another property related to distillation is the normal boiling temperature. It should be pointed out that the  $sr_{ij}$  for the triple point pressure was the largest one, but the corresponding separation technique was screened out as infeasible because of the operating conditions ( $P < 0.001\text{atm}$ ). Alternatively, the computational tool of CAPSS in ICAS can be used to identify distillation as the separation technique for the two potential separation tasks. Steps 4-8: Since there are more than one reaction tasks in the sequence, the application of steps 4-8 of the algorithm is necessary to determine whether a separation task is necessary between the two reaction tasks. The reactant mixtures at the end of the respective reaction tasks are compared. The products that one should obtain from the two potential separation tasks are compound  $I_2$ , which is the (intermediate) product after the first reaction task and compound  $P$ , which is the final product after the second reaction task, respectively.

The property lists of the respective mixture components for normal boiling point and vapour pressure are given in tables F.2 - F.3 and F.6 in appendix F. The binary property ratios for the adjacent binary pairs with a specified product, as well as the “possibility distribution”  $\mu(r_{ij})$  or the scaled binary property ratios  $sr_{ij}$  are compared in tables 5.16 and 5.17.

It can easily be perceived that distillation is a **most feasible** separation technique for obtaining the respective products, with the various  $sr_{ij}$ s being by far greater than unity, and that for the  $R_3/\mathbf{P}$  pair in table 5.17, the extent of feasibility is the smallest. From the comparison made in tables 5.16 and 5.17, and according to rule S.12 it is obvious that the separation of the intermediate product  $I_2$  in a distillation column ( $sr_{ij} = 59.85$ ) after the first reaction task is much easier than the separation of the final product  $P$  ( $sr_{ij} = 6.56$  and

Separation task	Adjacent binary pair	$r_{ij}$	$sr_{ij}$
After first reaction task	$I_2/R_1$	89.77	59.85
After second reaction task	$R_1/\mathbf{P}$	9.84	6.56
	$\mathbf{P}/I_1$	13.62	9.08

Table 5.16: Comparison of the reactant mixtures after succeeding reaction tasks based on the property of vapour pressure

Separation task	Adjacent binary pair	$r_{ij}$	$sr_{ij}$
After first reaction task	$R_1/I_2$	1.39	1.36
After second reaction task	$\mathbf{P}/I_2$	1.23	1.21
	$R_3/\mathbf{P}$	1.03	1.01

Table 5.17: Comparison of the reactant mixtures after succeeding reaction tasks based on the property of boiling point

9.08). The intermediate product  $I_2$  is also the most volatile compound of that mixture, making it the first obtained product of the batch distillation. On the other hand, product  $P$  might need to be the second product obtained in the batch distillation column, if the recovery of the second reaction task is not sufficiently high and the unreacted  $I_2$  jeopardizes the purity of the final product.

The byproducts that come along from the first reaction task to the second, if an intermediate separation task does not take place, do not form any minimum boiling azeotropes with the final product  $P$  that endanger its recovery or purity (rule S.13). The presence of minimum boiling azeotropes in the two reactant mixtures compared is identified in table 5.18. Based on the previous statement alone, an intermediate separation task is not necessary. However, according to rule S.14 the reaction yielding the final product  $P$  in the second set is a second order reaction and its rate increases as the volume of the reactant mixture decreases (rule S.14). This implies that it is best for unnecessary byproducts to be removed before the second reaction task, so that the volume of the reactant mixture is minimized. The application of rules S.12 to S.14 indicates that a separation task should take place between the two reaction tasks.

Step 9: Each task in the sequence is assigned a recovery  $r_k$  ( $k=1,\dots,4$ ). So far, the sequence consists of a reaction task, a separation task by distillation, another reaction task and a final separation task also by distillation. According to rule S.17 and since there are more than two tasks in the sequence, the recoveries for each task are assumed initially equal ( $r_k=r$ ).

$$\begin{aligned}
 r_T &= r_1 r_2 r_3 r_4 = r^4 \\
 0.9 &= r^4 \\
 r &= 0.974
 \end{aligned} \tag{5.1}$$

List of compounds of reactant mixtures in decreasing boiling point $T_b$	
Sep. task after 1 <sup>st</sup> reaction task	Sep. task after 2 <sup>nd</sup> reaction task
B ( $T_b = 467.15K$ )	B ( $T_b = 467.15K$ )
A ( $T_b = 417.15K$ )	A ( $T_b = 417.15K$ )
C ( $T_b = 391.4K$ )	C ( $T_b = 391.4K$ )
C-A az. (90.87% C $T_{az} = 389K$ )	C-A az. (90.87% C $T_{az} = 389K$ )
C-B az. (94.87% C $T_{az} = 388.9K$ )	C-B az. (94.87% C $T_{az} = 388.9K$ )
S ( $T_b = 383.78K$ )	S ( $T_b = 383.78K$ )
S-B az. (99.85% S $T_{az} = 383.7K$ )	S-B az. (99.85% S $T_{az} = 383.7K$ )
S-C az. (87.16% S $T_{az} = 383.5K$ )	S-C az. (87.16% S $T_{az} = 383.5K$ )
$I_1$ ( $T_b = 372.7K$ )	$I_1$ ( $T_b = 372.7K$ )
$R_1$ ( $T_b = 370.23K$ )	$R_1$ ( $T_b = 370.23K$ )
$I_1 - C$ az. (67.33% $I_1$ $T_{az} = 369.2K$ )	$I_1 - C$ az. (67.33% $I_1$ $T_{az} = 369.2K$ )
$I_1 - S$ az. (59.81% $I_1$ $T_{az} = 368.5K$ )	$I_1 - S$ az. (59.81% $I_1$ $T_{az} = 368.5K$ )
$R_1 - S$ az. (63.53% $R_1$ $T_{az} = 367.4K$ )	$R_1 - S$ az. (63.53% $R_1$ $T_{az} = 367.4K$ )
$R_1 - C$ az. (67.92% $R_1$ $T_{az} = 366.6K$ )	$R_1 - C$ az. (67.92% $R_1$ $T_{az} = 366.6K$ )
$I_2$ ( $T_b = 266.25K$ )	$R_3$ ( $T_b = 337.85K$ )
	$R_3 - S$ az. (89.01% $R_3$ $T_{az} = 337K$ )
	$R_3 - C$ az. (88.92% $R_3$ $T_{az} = 336.5K$ )
	<b>P</b> ( $T_b = 328.35K$ )
	$P - R_3$ az. (69.09% P $T_{az} = 324.9K$ )
	$I_2$ ( $T_b = 266.25K$ )

Table 5.18: Comparison of the reactant mixtures resulting after succeeding reaction tasks in terms of separation boundaries

Since no initial separation task is necessary in the sequence, then the operational modelling for the first reaction task is the same as the one already performed in section 5.2. The fastest sequence of sub-tasks from the generated family of alternatives is chosen and considered as feed for the separation task that follows. The achieved recovery for that operational model is  $r_1 = 0.9776 > 0.974$ , hence the operational model is feasible and can be used in the sequence. The reaction time for the first task in the sequence is  $t_1 = 1.51hr$ . The outflow of the first batch reactor is given in table 5.19.

Compounds	Holdup (kmoles)	Compounds	Holdup (kmoles)
$R_1$	3.964649	C	0.000067
$I_1$	0.026496	S	5.8
A	0.049107	B	1.955287
$I_2$	1.955221		
Temperature		358.04 K	

Table 5.19: Holdup and temperature of the reactor effluent, for the first reaction task

Step 10: The split for the separation task occurs between compounds  $I_2$  and  $R_1$  and algorithm A2 is applied to that binary pair providing the operational model for the batch distillation column. The required recovery for the second task in the sequence is  $r_2 = 0.974$  and according to rule S.16 the required purity of the intermediate product  $I_2$  from the separation task is  $p_2 \geq 0.99$ , because the feasibility of the separation is very high. The operating time for the second task in the sequence  $t_2 = 0.159hr$ , out of which  $0.094 hr$  is time operated in total reflux and the time required to reach steady state, before the actual suggested reflux ratio profile can be applied.

After the operation of the first distillation column is modelled, the intermediate product is fed to the second reaction task. The feed coming from the batch distillation is given in table 5.20. Comparing the amounts of the intermediate product  $I_2$  in tables 5.19 and 5.20, it can be calculated that the recovery of the separation task is  $r_2 = 0.974$ , as required.

Compounds	Holdup (kmoles)
$R_1$	0.003054
$I_1$	0.000012
$I_2$	1.904411
S	0.002968

Table 5.20: Intermediate product from the first batch distillation column

Step 11: The necessity or redundancy of the last separation task is checked. If the last separation task is avoided, then this means that the effluent of the second reaction task has to satisfy both the product objectives, namely the product recovery and purity. Let  $N_P^{max}$  be the maximum amount of product  $P$  that can be produced. At the end of the first reaction task, the intermediate product  $I_2$  is equal to  $r_1 N_P^{max}$ . The product obtained from the intermediate separation task is  $I_2 = r_1 r_2 N_P^{max}$  and it has a purity of  $p_2$ . Along with  $I_2$ , other volatile compounds from the reactor effluent are present, which amount to  $r_1 r_2 \frac{1-p_2}{p_2} N_P^{max}$ . If the added reactant  $R_3$  to the second reaction task is equal to  $I_2$  coming from the separation task, then the produced final product  $P$  is  $r_1 r_2 r_3 N_P^{max}$ . The final product purity is  $p_3$  and the following equation should be valid.

$$\begin{aligned}
 \frac{P}{(I_2 + R_3) + P + otherVOC} &= p_3 \\
 \frac{r_1 r_2 r_3 N_P^{max}}{(2r_1 r_2 (1 - r_3) + r_1 r_2 r_3 + r_1 r_2 \frac{1-p_2}{p_2}) N_P^{max}} &= p_3 \\
 \frac{r_3}{2 - r_3 + \frac{1-p_2}{p_2}} &= p_3
 \end{aligned} \tag{5.2}$$

The final product purity is  $p_3 = 0.99$ , while the intermediate purity of the separation task is also  $p_2 = 0.99$ . Substituting these two values in equation 5.2

gives  $r_3 = 1$ . This means that the product objectives can be met only if all the intermediate product  $I_2$  is converted to the final product  $P$  in the last reaction task. Even if the purity  $p_2$  is higher, the second reaction task recovery needs to be very high. Therefore, it is decided that a final separation tasks needs to be in the sequence. Thus, the suggested sequence is as shown in figure 5.26.

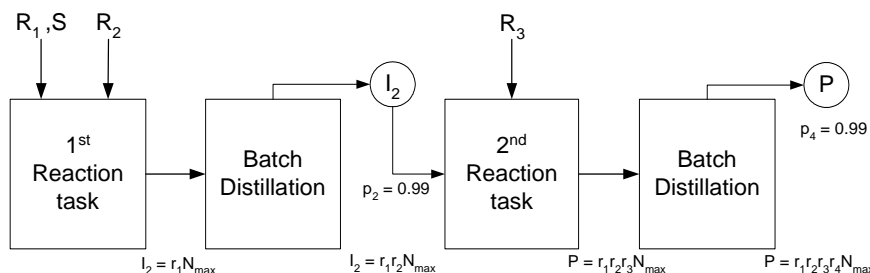


Figure 5.26: Suggested batch route for the case study from the Synthesis algorithm

Step 12: The recoveries  $r_3$  and  $r_4$  of the last two tasks in the sequence can be determined exactly, such that the product objectives are satisfied. The final product  $P$  can be obtained as the first product in the batch distillation column, but the more volatile component  $I_2$  will also be obtained. Furthermore, because of the minimum boiling azeotrope between product  $P$  and reactant  $R_3$ , compound  $R_3$  will also be part of the first distillation product. In order for the product purity to be satisfied, the following equation needs to be valid.

$$\frac{P}{(I_2 + R_3) + P} = \frac{r_1 r_2 r_3 r_4 N_P^{\max}}{(2r_1 r_2 (1 - r_3) + r_1 r_2 r_3 r_4) N_P^{\max}} = p_4 \quad (5.3)$$

$$\frac{r_3 r_4}{2(1 - r_3) + r_3 r_4} = p_4 = 0.99$$

Solving the system of the above equation and

$$r_1 r_2 r_3 r_4 = 0.9 \quad (5.4)$$

where  $r_1$  and  $r_2$  are already known, one can calculate the required recoveries  $r_3 = 0.9952$  and  $r_4 = 0.95$ .

Step 13: Regarding the operational model of the second reaction task, the fact that only one reaction takes place does not allow one to take advantage of selectivity for the design of the operation and how heating or cooling promotes the desired reaction over the unwanted one. From the analysis of the reaction kinetics, it is obvious that the reaction rate will be the highest for the maximum temperature  $T_{up}$ . Therefore, the operation for that reaction task is chosen as isothermal operation at  $T_{up}$  until the intermediate recovery  $r_3$  is reached. The feed to the final separation task is given in table 5.21 and the achieved recovery is  $r_3 = 0.9952$ , as required. The reaction time for the second reaction task in

the sequence is  $t_3 = 3.98hr$ . No account has been made for the time required to heat the intermediate product  $I_2$  from the distillate temperature to the required temperature for the reaction  $T_{up}$ , since this is strongly dependant on the involved heating capacity.

Compounds	Holdup (kmoles)	Compounds	Holdup (kmoles)
$R_1$	0.003054	S	0.002968
$I_1$	0.000012	$R_3$	0.008693
$I_2$	0.009104	P	1.895307

Table 5.21: Intermediate product mixture from the second batch reaction task

The operational model for the batch distillation column where the last separation task takes place as the split between compounds  $P$  and  $R_3$  is provided by algorithm A2, which is applied for the specific binary pair. The required recovery for the final task in the sequence, as it has already been determined, is  $r_4 = 0.95$  and the required purity of the final product  $P$  from the separation task is  $p_4 = 0.99$ . The operating time for the final task in the sequence  $t_4 = 3.412hr$ , out of which  $1.494 hr$  is time operated in total reflux in order to reach steady state, before the actual suggested reflux ratio profile can be applied.

The final product obtained as distillate from the second batch distillation task in the sequence is given in table 5.22. Comparing the amounts of the final product  $P$  in tables 5.21 and 5.22, it can be calculated that the recovery of the final separation task is  $r_4 = 0.95$ , as required. Furthermore, the total recovery for product  $P$  is  $r_T = 0.9$  and the purity is  $p_4 = 0.99$ . So, the batch route suggested is feasible in terms of reaching the end objectives for the product.

Compounds	Holdup (kmoles)	Compounds	Holdup (kmoles)
$R_1$	0.000311	S	0.000008
$I_1$	0.000002	$R_3$	0.008685
$I_2$	0.009104	P	1.8

Table 5.22: Final product obtained as distillate from the second batch distillation column

The total operating time for the suggested batch route is  $t_{total} = 9.061hr$ . It is noted again, that the only operation that has not be accounted for in the total time for the batch route is the heating needed to raise the temperature of the distillate product of the first distillation from its boiling point to the temperature at which the batch reactor is operated for the second reaction task. This time depends strongly on the available heating capabilities of existing heat exchangers. However, based on simulation the time that the distillation columns were operated in total reflux ratio, in order to reach steady state, prior to the application of the suggested reflux ratio profile has been included in the total time.



For the sake of comparison results are also given, in terms of operating time, for the alternative route (Allgor *et al.*, 1996) illustrated in figure 5.25. The first reaction task is the same as in the suggested route and the operating time is  $t_1 = 1.51hr$  and the recovery is still  $r_1 = 0.9776$ . The individual recoveries for the other tasks in the sequence are found by solving:

$$\begin{aligned} \frac{P}{(I_2 + R_3) + P} &= \frac{r_1 r_2 r_3 N_P^{max}}{(2r_1(1 - r_2) + r_1 r_2 r_3) N_P^{max}} = p_3 \\ \frac{r_2 r_3}{2(1 - r_2) + r_2 r_3} &= p_3 \end{aligned} \quad (5.5)$$

and substituting  $r_1 r_2 r_3 = r_T$  in equation 5.5. The solution of the equations yields a recovery for the second reaction task  $r_2 = 0.9954$  and a recovery for the separation task  $r_3 = 0.925$ .

The second reaction task is similarly found to be isothermal operation at  $T_{up}$ , which ensures the maximum reaction rate for the desired reaction and therefore the shortest operating time. The time needed to obtain the required recovery is  $t_2 = 22.13hr$ . Already at the completion of the second reaction task, the total time is  $t = 23.64hr$ . The operating time for the two consecutive reaction tasks is 161% slower than the total time of the suggested tasks sequence and also, as expected, the purity objective is not satisfied. The advantages of the suggested sequence are obvious when it comes to determining how much faster it is than the alternative route. No attempt was made to continue with the last separation task for the alternative route, since there is no doubt that the suggested sequence is much faster.

The application of the synthesis algorithm S for the last case study examined generated a batch route with an extra separation task than the batch route in the original paper. One would think that the addition of an extra task would increase the total operating time. On the contrary, adding this intermediate separation task decreased significantly the total batch time. The insights provided from the study of the reaction kinetics for the second reaction task pointed out the need for the intermediate separation task. The reasons that imposed the extra task were the fact that it was a very easy separation and consequently a fast one, but mainly because providing a smaller feed to the second reaction, without any unnecessary byproducts from the first reaction task, decreased the reaction volume and therefore the operating time for the second reaction task.

It was established that the simple batch route, which is usually the direct adaptation of the route used in the laboratory, allows room for a lot of optimization. The developed algorithm investigates in a systematic way the different scenarios for the sequences of reaction and separation tasks, starting from the simplest batch route and looking into the need of adding extra starting, intermediate and final separation tasks to ensure the achievement of all the

product's objectives.

A simple procedure for determining intermediate objectives for each task in the sequence was introduced. However, achieving these intermediate objectives depend on the potential of the batch operations model generation algorithms to provide a sequence of feasible sub-tasks that meets the end objectives for each task. The intermediate objectives for each task in the sequence and the final product objectives are interconnected with each other. Thus, for the application of the synthesis algorithm S, the developed batch reaction and separation algorithms A1-A3 need to be invoked and applied before a complete batch route with accompanying batch operations models for all the tasks can be generated.



# CONCLUSIONS

## 6.1 Achievements

The objective of this work has been to provide solutions to the batch process synthesis problem. This solution should be in the form of a feasible batch route for each product, namely the sequence of processing tasks necessary for obtaining the specified product, as well as the batch operations model for each task in the sequence. The batch operations model can be given as a sequence of sub-tasks necessary to achieve specified objectives for each task.

The main achievement of this work has been the development of a methodology that takes advantage of existing thermodynamic and process insights to provide feasible solutions to the synthesis and operational design problem of batch processes. The developed algorithms are easy to use, do not require extended knowledge of the process models for the different batch processes and because they are based on thermodynamic and process insights, they provide near optimum solutions. The developed methodology works at two levels, where at the upper level the batch route is generated and at the lower level a near optimum batch operations model is provided for each task in the batch route.

The developed algorithm for the generation of the batch route has been given in a systematic way together with its rules and a step-by-step procedure. The algorithm identifies the easiest and most feasible separation technique for each possible separation task and then methodically positions these separation tasks in the sequence, before, between or after a reaction task. Two criteria are mainly used for the determination of the actual positioning of the separation tasks in the sequence, namely the extent of feasibility and how easy the identified separation technique is, as well as whether the separation contributes to the acceleration of the progress of the succeeding reaction task. The solution to the synthesis problem is realized without the use of rigorous optimization techniques, where a superstructure of all the alternatives is considered, but rather based on thermodynamic and process insights; the latter being derived from reaction and mixture analysis.

An illustrative example was used to demonstrate the algorithm and its important aspects. When the generated solution was compared with the available route from the literature, it was found to be much faster when an extra inter-

mediate separation task was considered. The case study confirmed that there is space for optimization even when the synthesis problem is considered exclusively, without even the individual task optimizations to be considered. The simple batch routes usually adopted from the laboratory can be significantly improved at the synthesis level.

The strong feature of the algorithm is, firstly, the identification of the easiest and most feasible separation technique based on the relationship between pure compound properties and separation process principles and, secondly, the full utilization of the insights gained from the reaction kinetics analysis, in order to identify ways to make the reaction tasks easier and faster.

The minimization of the total operating time provided at the synthesis level of the methodology can further be complemented at the operational design level, where the individual tasks in the sequence are considered one by one. The objective is then to achieve the intermediate objectives of each task set at the synthesis level and to do so in minimum time. The concluding mixture state from the operational design algorithms is compared against the set goal and is then returned back to the synthesis algorithm, in order to improve the intermediate objectives of the remaining tasks in the sequence. If the set objectives could not be reached, the decision to relax them, but tighten others can be taken at the synthesis level. Thus, the developed reaction and separation algorithms are integrated with the synthesis algorithm, since the generation of the complete batch route depends on the application of all of these algorithms.

The single product line is considered in this thesis when a batch route is generated with the developed methodology, but the route can then be used as given data for solving scheduling and planning problems that arise in multiproduct or multipurpose batch plants.

The developed algorithms A1a and A1b for the operational design of batch reactors determine a sequence of operations, such as heating or cooling with vapour release or not, and isothermal or adiabatic operation, until a specific recovery is achieved for the desired product. Limitations in the amount of heating and cooling provided are taken into consideration. Since different amounts from the feasible range can be used, a set of feasible alternatives can be generated that achieve the end objective but differ in operating time and costs. An application example showed that there is an obvious trade-off between short operating time and operating costs. So, in the case where minimum time is the requirement, the maximum value for heating or cooling should be used.

A strong feature of the algorithm is the attempt to promote selectivity of the desired reactions, when there are competing reactions. In that way, the recovery objective for the specified product is guaranteed and the production of unwanted byproducts is suppressed. The first step is the categorization of the reactions of the given set into desired and unwanted reactions and the classification into exothermic and endothermic reactions. The desired reactions are then compared to their competing ones, in terms of their activation energies, their exothermicity or endothermicity and their extent of reaction, and the

operation that promotes mostly the desired reaction is identified as cooling or heating. The selectivity is then used as a path and terminal constraint in addition to temperature and pressure constraints, in order to identify sub-tasks and their end. The algorithms produce, in effect, the heating/cooling input profile necessary to remain feasible during reaction and also meet the terminal objectives. The output temperature and pressure profiles can be used as initial setpoint trajectories given in advance when the batch control problem is considered and on-line optimization is performed.

The application of the algorithms in two case studies produced a profile for the manipulated variable (heat input) that consisted of certain arcs. These arcs correspond to different sub-tasks. From one interval to the next, the constraints that become active change and the different sub-tasks in the sequence are the preventive actions that are taken such that none of the constraints are violated. The generated sequence shows a lot of similarities to the optimal solutions of Srinivasan and Bonvin (2004), in a qualitative way, as explained in section 5.3. Therefore, the generated sequence of sub-tasks seems to be able to be used as a good initial sequence for a dynamic optimization problem. This is very important, since for an optimization problem a substantial amount of time is usually spent in retrieving a good initial estimate. The initial estimate is crucial to whether the global optimum solution is reached instead of a local optimum.

The developed algorithm A2 provides the batch operations model for multicomponent batch distillation in the form of a piecewise constant reflux ratio profile. Two terminal objectives are considered for each specified product, namely purity and recovery. The algorithm without using any rigorous models generates *a priori* a reflux ratio profile that satisfies the product objectives.

An achievement of the algorithm is that it provides the sequence of attainable products and also determines the necessity of intermediate waste cut products, if the recovery or purity for the next in line high purity product is endangered. The sequence of attainable products is also determined for azeotropic mixtures, which according to the position to the feed means that one of the mixture components can not be obtained as high purity product. This happens because together with the minimum boiling azeotrope that is removed, the mixture is depleted of one of the two compounds forming the azeotrope.

The majority of researchers considered constant relative volatility for their models. However, the strong feature of the developed algorithm is the use of the driving force approach to identify the minimum reflux ratio for a considered composition. The vapour liquid equilibrium data used for that reason are not predicted based on constant relative volatility. Furthermore, considering any separation as the split between two components or the removal of an azeotrope, the multicomponent mixture can be separated into its constituents by considering a sequence of binary splits.

The only necessary data then are the VLE data of the adjacent binary pairs and the reflux ratio values for each interval are found *a priori*. It is important to

note that the number of intervals is not determined *a priori*, but is found during the course of the algorithm application. The algorithm finds the minimum reflux ratio for a given feed, determines a reflux ratio according to the number of plates using an available computational tool for the synthesis of continuous distillation columns and determines when the chosen reflux ratio will become infeasible. At that point the current bottom content is considered as a new feed and the procedure is continued until the product recovery objective is met. The reflux ratio profile is found such that the distillate composition is at least that of the product purity objective.

Two cases studies illustrated that a stepwise reflux ratio profile is much faster than a constant reflux ratio operation. In order for constant reflux ratio operation to even be feasible, in terms of achieving both product objectives, then an adequately high reflux value is necessary. However, that value is unnecessarily high for most of the operating time and is actually responsible for the longer operating time. It has also been shown that it is possible to separate a mixture in high purity compounds, without compromising the product recovery. In the case of the azeotropic mixture, it was demonstrated that an appropriate reflux ratio profile is needed both for the fast removal of the azeotrope but also such that the desired recovery objective for the product collected from the still is not compromised. A small reflux ratio could mean the unnecessary removal of desired product, while a too large reflux ratio would mean longer operating time and larger operating costs.

The suggested reflux ratio profile for each product was sufficient in terms of reflux ratio values, but dynamic simulation showed that the switch times between the intervals need to be redefined for the purity objective to be met. However, the generation of the reflux ratio profile does not need any rigorous batch process models, it is less demanding in computational effort and skills and it can obviously be used as a very good starting point for the dynamic optimization of the column.

The developed algorithm A3 for the synthesis and design of batch crystallization uses insights from the solid-liquid equilibrium phase diagrams to provide a sequence of sub-tasks that satisfies the product objectives. The terminal objective considered for the task is the maximum or a specified recovery for one or more solids. The sub-tasks considered are isothermal evaporation or dilution, shifting from one temperature to another by cooling or heating and solid-liquid separation.

A new feature of this algorithm is the feasibility check for the precipitation of a specified solid from a given feed over a temperature range and the identification of the actual precipitating solid for a given feed. This is done by comparing the feed coordinates with coordinates of the different invariant points. Usually this check is very easy to perform graphically with the phase diagram, but in the case where the evaporation/dilution line passes very close to an invariant point it might not be possible to make the correct evaluation. A set of equations have been determined particularly for these cases. Together

with the solid whose precipitation is feasible, the necessary sub-task in terms of evaporation or dilution is also identified.

The operating temperature for the sub-task is chosen through a systematic procedure. The slurry density is calculated for the temperatures in the feasible range and the temperature at which the largest amount of solid precipitates is selected. However, it should be noted, that operation close to the invariant points is avoided in this thesis, in order to avoid cocrystallization. Thus, the slurry position is found for evaporation that is less than the allowed maximum and for dilution that is more than the allowed minimum. It is among those slurry positions, that the best slurry density is found. Moreover, theory has been developed for the identification of the case where the desired or maximum recovery of a solid can not be achieved in a single precipitation and can only be achieved by repetitive alternate solids precipitation at two different temperatures. Equations have been established, in order to determine the necessary number of precipitations in advance.

As highlighted in three case studies, it is very simple to identify the necessary operations to recover certain amounts of pure salts, once one has the knowledge and understanding of the phase diagram. Particularly, it is very advantageous to understand how to exploit the change in the solubility boundaries and regions with temperature. Since two different solids might precipitate for the same point in the phase diagram, at two different temperatures, shifting from one operating temperature to another can be used to overcome an invariant point where no further precipitation is feasible.

In conclusion, the series of carried out application examples have shown that the thermodynamic and process insights embedded in the simple models can be exploited to provide solutions for the synthesis and operational design problem of batch processes, as the goal of this thesis was originally set to be. The synthesis algorithm can also be used for retrofit calculations in an existing production line, where the batch route used could be improved by the addition of intermediate separation tasks. This is more easily utilized in a batch plant, which is more flexible than a continuous one, since separation units are already available to be used for the extra separation tasks. It becomes then a scheduling problem to assign a separation unit to the new separation task.

The developed methodology relies a great deal on accurate information and good prediction of the pure component properties and the reaction kinetics. Inaccurate property values might result in the identification of a not so feasible separation technique for a separation task or the failure of not identifying a necessary intermediate separation task in the sequence. Inaccurate information on the standard enthalpy of formation could ultimately lead to identifying a wrong operation for the promotion of a desired reaction. Errors in the VLE diagram could result to infeasible reflux ratio profiles. Similarly, mistakes in the solid-liquid diagram could lead to identification of the wrong solid to precipitate or to infeasible separation, if the amount of solvent removed is actually more than necessary. Therefore, a key limitation of this methodology is to obtain



the information needed with a sufficient accuracy for the specific purpose.

## 6.2 Future Work

In this thesis, separation by reaction has not been considered. The algorithm for batch reaction could be extended to cover reactive separation. The reactive distillation could be considered as reaction taking place in the liquid phase in a vessel, where the formed vapour is fed continuously to a distillation column from which the volatile compounds are removed as distillate and the heavy compounds are returned to the reactor. A reflux ratio profile could be determined to ensure that the loss of heavy compounds to the distillate was minimized. The further complication is that the still composition does not only change because of the distillation but also because of the reactions taking place. Moreover, the vapour boilup rate cannot be considered constant as it also continuously changes. A simulation approach could be probably be used to identify operating constraints violation and determine appropriate actions to counter the upcoming violations.

The work on batch distillation was limited to regular rectifying distillation columns in this thesis. However, an algorithm for the operational design of inverted stripping distillation columns could similarly be developed. In the inverted distillation column, the feed is loaded in the condenser and the product is drawn from the reboiler. The minimum ratio of product refluxed back in the column can be found in a similar manner with the driving force approach, for each mixture composition in the condenser. As the heavy product is removed, the composition in the condenser becomes richer in volatile compounds. This type of distillation columns could be advantageous to use when the desired products is one of the heavy compounds of the mixture and would otherwise be collected last in a regular distillation column. Additionally, minimum boiling azeotropes could potentially be avoided with that kind of configuration.

It has not been the objective to include optimization in the work described in this thesis. However, it has been obvious that trade-offs between operating time and costs are present. The actual choice of operating conditions also has an effect on operating costs. For the case of batch crystallization, for example, switching between two temperatures far from each other for alternate solid precipitation could result to a lower number of precipitations needed to reach a specified recovery. However, the operating costs for heating and cooling could be very high. Cost considerations of this kind in the optimization of batch crystallization could prove to be beneficial. It might be better to operate at two temperatures that are closer to each other, even if that meant a higher number of precipitations for the same recovery.

The developed algorithms would also benefit from further validation from other case studies and literature examples.

# Appendices



# A

## Batch Reaction: Promoting reaction system selectivity through temperature change

The case of a batch reactor where multiple reactions take place, some being desired and others being unwanted, and where the objective is to promote the selectivity of the desired over the unwanted reactions is considered in this appendix.

The decisions taken for the promotion of a desired reaction over a competing/unwanted reaction depend on whether the reactions are reversible or irreversible.

For the case of irreversible reactions, the activation energies  $E_a$  determine the action that promotes selectivity. Let us consider two reactions, 1 and 2, that share a reactant  $A$  and yield the desired product  $P$  and a byproduct  $D$ , respectively.



where the reaction rates are given by  $r_1 = k_1 C_A C_B$  and  $r_2 = k_2 C_A C_C$ , respectively. The rate constant  $k$ , as expressed by its Arrhenius form, is  $k = k_o \exp(\frac{-E_a}{RT})$ .

If the activation energy ratio of the desired reaction over the competing reaction is larger than unity ( $\frac{E_a^1}{E_a^2} > 1$ ), then *heating* promotes selectivity  $S_{12}$ . This translates that selectivity  $S_{12}$  at a higher temperature  $T_2$  is greater than the selectivity at the lower temperature  $T_1$ .

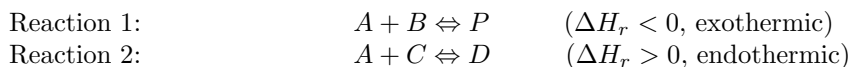
$$\begin{aligned} S_{12}(T_2) > S_{12}(T_1) &\Leftrightarrow \frac{k_1(T_2)C_A C_B}{k_2(T_2)C_A C_C} > \frac{k_1(T_1)C_A C_B}{k_2(T_1)C_A C_C} \\ \frac{k_1(T_2)}{k_2(T_2)} > \frac{k_1(T_1)}{k_2(T_1)} &\Leftrightarrow \frac{k_o^1 \exp(-E_a^1/RT_2)}{k_o^2 \exp(-E_a^2/RT_2)} > \frac{k_o^1 \exp(-E_a^1/RT_1)}{k_o^2 \exp(-E_a^2/RT_1)} \end{aligned} \quad (\text{A.1})$$

$$\begin{aligned} \exp \frac{(E_a^2 - E_a^1)}{RT_2} &> \exp \frac{(E_a^2 - E_a^1)}{RT_1} \\ \frac{(E_a^2 - E_a^1)}{RT_2} &> \frac{(E_a^2 - E_a^1)}{RT_1} \\ (E_a^2 - E_a^1) \left( \frac{1}{T_2} - \frac{1}{T_1} \right) &> 0 \end{aligned} \tag{A.2}$$

We have as given that  $[\frac{E_a^1}{E_a^2} > 1 \Leftrightarrow E_a^1 > E_a^2]$  and we know that by heating  $T_2 > T_1$ , which means that both amounts  $(E_a^2 - E_a^1)$  and  $(\frac{1}{T_2} - \frac{1}{T_1})$  in the last line of equation A.2 are negative. Thus, their product is positive and [[hence the statement]] that heating will promote the selectivity is correct.

It can similarly be proven that if the activation energy ratio of the desired reaction over the competing reaction is smaller than unity ( $\frac{E_a^1}{E_a^2} < 1$ ), then *cooling* will promote selectivity. It should be noted that the order of the reaction is irrelevant, since the concentrations are crossed out when comparing selectivity at two temperatures.

For the case of reversible reactions, a definite decision on the action that promotes selectivity can only be taken if the two reactions have a different sign of the heat of reaction, referring to the case when one is exothermic and the other one is endothermic. Let us consider two reversible reactions, 1 and 2, that share a reactant *A* and yield the desired product *P* and a byproduct *D*, respectively.



In the above case, where the desired reaction is exothermic and the competing reaction is endothermic, *cooling* promotes selectivity. This means that at a lower temperature  $T_2$ , selectivity  $S_{12}$  will be higher than the selectivity at a higher temperature  $T_1$ .

According to equation 3.7, the selectivity at equilibrium, for the above reaction set, is given by  $S_{12}(T_1) = \frac{N_P}{N_D}$ , where  $N_P$  is the number of moles of the desired product and  $N_D$  is the number of moles of the unwanted byproduct, at equilibrium. If cooling is applied, then the resulting temperature  $T_2$  will be lower than the original temperature  $T_1$ . According to Le Chatelier, the position of equilibrium will move in such a way as to counteract the change and in this case increase the temperature. This means that for the exothermic reaction 1 the position of the equilibrium will be moved to the right, while for the endothermic reaction 2, the position of the equilibrium will be moved to the left. At the new equilibrium, the number of moles of the desired product  $N'_P$  is greater than  $N_P$  and the number of moles of the unwanted byproduct  $N'_D$  is smaller than  $N_D$ .

Let us assume that the selectivity at the lower temperature  $S_{12}(T_2)$  is greater than the selectivity at the higher temperature  $T_1$ .

$$S_{12}(T_2) > S_{12}(T_1) \Leftrightarrow \frac{N'_P}{N'_D} > \frac{N_P}{N_D}$$

$$\frac{N'_P}{N_P} > \frac{N'_D}{N_D} \quad (\text{A.3})$$

We know that  $N'_P > N_P$ , which means that  $\frac{N'_P}{N_P} > 1$  and also that  $N'_D < N_D$ , which means that  $\frac{N'_D}{N_D} < 1$ . So the inequality in the last line of equation A.3 is correct and our initial assumption is valid.

It can similarly be proven that if the desired reaction is endothermic and the competing reaction is exothermic, then *heating* will promote selectivity.

However, for the cases when both the desired and competing reaction are exothermic or both of them are endothermic, no definite decision can be taken for the promotion of selectivity based on the degree of their exothermicity/endothermicity.

In the case when the two reversible reactions in question are both exothermic, then cooling will move the position of the equilibrium for both reactions to the left. So at the new equilibrium, the number of moles of the desired product  $N'_P$  will be greater than  $N_P$  and the number of moles of the unwanted byproduct  $N'_D$  will also be greater than  $N_D$ . The extent of their exothermicity can not help us decide how the selectivity will be affected.

The equilibrium constants for the reversible reactions (in page 174) at a temperature  $T_1$  are given by the following equation, (Aris, 1969).

$$K_1(T_1) = \frac{C_P}{C_A C_B} = \exp\left(\frac{-\Delta G_1}{RT_1}\right)$$

$$K_2(T_1) = \frac{C_D}{C_A C_C} = \exp\left(\frac{-\Delta G_2}{RT_1}\right) \quad (\text{A.4})$$

where  $\Delta G$  is the difference between the Gibbs free energy of the products and that of the reactants under standard conditions.

One should keep in mind the connection of the Gibbs free energy to the enthalpy of reaction  $\Delta H_r$  through the Gibbs-Helmholtz equation:

$$\left(\frac{\partial(\frac{\Delta G}{T})}{\partial T}\right)_P = -\frac{\Delta H}{T^2} \quad (\text{A.5})$$

If  $\xi_1$  is the extent of reaction 1 and  $\xi_2$  is the extent of reaction 2, then equation A.4 can be written:

$$K_1(T_1) = \exp\left(\frac{-\Delta G_1}{RT_1}\right) = \frac{C_P^o + \xi_1}{(C_A^o - \xi_1)(C_B^o - \xi_1)}$$

$$K_2(T_1) = \exp\left(\frac{-\Delta G_2}{RT_1}\right) = \frac{C_D^o + \xi_2}{(C_A^o - \xi_2)(C_C^o - \xi_2)} \quad (\text{A.6})$$

From the above equation A.6, one can solve to find the exact values of  $\xi_1$ , and  $\xi_2$ .

$$\xi = \frac{1}{2}(C_A^o + C_{B/C}^o + K^{-1}) + \frac{1}{2}[(C_A^o + C_{B/C}^o + K^{-1})^2 - 4C_A^o C_{B/C}^o + 4C_{P/D}^o K^{-1}]^{1/2} \quad (\text{A.7})$$

For a lower temperature  $T_2$  resulting from cooling and at a new equilibrium, the new extent of reactions  $\xi'_1$  and  $\xi'_2$  can be calculated from equation A.7 by substituting the equilibrium constant  $K_2$  at temperature  $T_2$  instead of  $T_1$ .

Without solving equation A.6, we only know that  $\xi'_1$  is greater than  $\xi_1$  and that  $\xi'_2$  is greater than  $\xi_2$ , since the position of the equilibrium is moved to the right by cooling. Selectivity at temperature  $T_1$  is given by

$$S_{12}(T_1) = \frac{C_P}{C_D} \Leftrightarrow S_{12}(T_1) = \frac{C_P^o + \xi_1}{C_D^o + \xi_2} \quad (\text{A.8})$$

and at temperature  $T_2$

$$S_{12}(T_2) = \frac{C'_P}{C'_D} \Leftrightarrow S_{12}(T_2) = \frac{C_P^o + \xi'_1}{C_D^o + \xi'_2} \quad (\text{A.9})$$

It is only after we have solved for  $\xi_1$ ,  $\xi_2$ ,  $\xi'_1$  and  $\xi'_2$  that we can determine whether the selectivity is favoured or not with cooling ( $S_{12}(T_2) > S_{12}(T_1)$ ) or  $S_{12}(T_2) < S_{12}(T_1)$  .

Of course the discussion on reversible reactions and their selectivity is based on the assumption that equilibrium is reached. For each reaction, the time needed to reach equilibrium depends on the reaction constants  $k$  of the forwards and backwards reaction and can be found, for example, for a first order reaction from, (Aris, 1969):

$$C = C^o \exp[-(k^f + k^b)t] \quad (\text{A.10})$$

It is obvious that the time needed to reach equilibrium could be very different for the desired and the competing reaction. Reaction kinetics should be taken into consideration when the effect of cooling or heating on selectivity of reversible reactions is studied, but maybe it is more important to determine what promotes selectivity when the time needed to reach equilibrium for both reactions is comparable.

# B

## Batch Distillation: Deciding on an intermediate cut

In this appendix, the case of separation of multicomponent mixtures by batch distillation and the need of the removal of an intermediate cut-off product, before a main product, is addressed. The composition of the mixture is considered and equations are generated that provide the relationship between the binary composition of the most volatile and second most volatile component in the mixture  $x_F^{bin}$  and the distillate composition  $x_D$  used in the developed algorithm for the separation task  $k+1$  succeeding the intermediate cut removal.

If the composition of the more volatile compound in the binary pair considered (in terms of normalized terms for the two components in the binary pair), is above a maximum value  $x_F^{bin}$ , then an intermediate cut has to be distilled in order not to compromise the specified objectives (purity and recovery) of the next product in the sequence.

The maximum value  $x_F^{bin}$  of the more volatile compound in the binary pair considered can be found if one knows the specified recovery values for each product as well as the desired product purities.

Let us consider a ternary non-azeotropic system of components A, B and C (as given in decreasing volatility order) with  $N_A$ ,  $N_B$  and  $N_C$  being the amounts (in kmols) of the components in the original feed. According to the distillation algorithm, the first separation task is that between components A and B and the first product is compound A.

Let the specified recovery for product A be  $y_A^s$  and the required product purity equal to  $x_{p1}$ . The distillation algorithm uses the required product purity as the distillate composition  $x_D$ . After the end of the first separation task, the remaining amounts of A, B and C are  $(1 - y_A^s)N_A$ ,  $N_B - \frac{1-x_{D1}}{x_{D1}}y_A^sN_A$  and  $N_C$ , respectively. The subscript 1 refers to the first separation task in the sequence.

Let the specified recovery for product B be  $y_B^s$  and the required product purity equal to  $x_{p2}$ . Regarding the next separation task in the sequence and the need or not for an intermediate cut, the following should be considered. If the composition of the more volatile compound (residue of A) in the binary



pair  $A - B$  is  $x_F^{bin}$ , then:

$$\frac{(1 - y_A^s)N_A}{N_B - \frac{1-x_{p1}}{x_{p1}}y_A^s N_A} = \frac{x_F^{bin}}{1 - x_F^{bin}} \quad (\text{B.1})$$

What should be the distillate composition  $x_{D2}$  used in the distillation algorithm for the second separation task, if that should provide high purity compound  $B$ ? The separation should then happen between compounds  $B$  and  $C$ . However, all of compound  $A$  remaining in the column will also be distilled, since it is more volatile than both  $B$  and  $C$ . Can the required recovery and purity objectives for  $B$  be obtained?

Meeting the recovery objective for product  $B$ , the amounts distilled at the end of the second separation task for each component are:

$$\begin{aligned} A &= \frac{x_F^{bin}}{1 - x_F^{bin}}(N_B - \frac{1 - x_{p1}}{x_{p1}}y_A^s N_A) \\ B &= y_B^s(N_B - \frac{1 - x_{p1}}{x_{p1}}y_A^s N_A) \\ C &= \frac{1 - x_{D2}}{x_{D2}}y_B^s(N_B - \frac{1 - x_{p1}}{x_{p1}}y_A^s N_A) \end{aligned} \quad (\text{B.2})$$

where one should note that  $x_{D2}$  is the distillate composition used in the algorithm for the binary pair  $B - C$ .

In order for the purity objective  $x_{p2}$  to be satisfied, the following equation should be in force.

$$\frac{y_B^s}{\frac{x_F^{bin}}{1-x_F^{bin}} + y_B^s + \frac{1-x_{D2}}{x_{D2}}y_B^s} = x_{p2} \quad (\text{B.3})$$

From the above equation, the relationship between the composition  $x_F^{bin}$  of the more volatile compound in the binary pair  $A - B$  and the distillate composition  $x_{D2}$  used in the distillation algorithm for the second separation task (split between binary pair  $B - C$ ) is given:

$$x_F^{bin} = \left(1 + \frac{x_{D2}x_{p2}}{(x_{D2} - x_{p2})y_B^s}\right)^{-1} \quad (\text{B.4})$$

The absolute maximum value that  $x_F^{bin}$  can take is found if one substitutes  $x_{D2}$  in equation B.4 with 1.

$$x_F^{max} = \left(1 + \frac{x_{p2}}{(1 - x_{p2})y_B^s}\right)^{-1} \quad (\text{B.5})$$

If there is no residue of the previously obtained product (component  $A$  in this case), then  $x_F^{bin}$  is equal to 0. From equation B.4, it turns out that the

minimum value for the distillate composition that can be used in the algorithm is:

$$x_D^{min} = x_{p2} \quad (\text{B.6})$$

as it is mentioned in rule A2.1.

It turns out that the distillate composition used in the algorithm for the second separation task in the sequence, which will guarantee the satisfaction of the purity objective for the specified product  $B$ , can be chosen from a range.

$$x_{p2} \leq x_{D2} < 1 \quad (\text{B.7})$$

for respective values of  $x_F^{bin}$ :

$$0 \leq x_F^{bin} < x_F^{max} \quad (\text{B.8})$$

For any value of  $x_F^{bin}$  greater than  $x_F^{max}$  an intermediate cut will have to be distilled before product  $B$  can be obtained with high purity  $x_{p2}$ . For a given value of  $x_F^{bin}$  smaller than  $x_F^{max}$ , the distillate composition used in the algorithm can be found from equation B.4, since  $x_{p2}$  and  $y_B^s$  are specified already.

If the distillate composition  $x_{D2}$  found from equation B.4 is considered to be too high, which might mean that the resulting reflux ratio profile suggested from the algorithm is too high, then one can still decide on an intermediate cut to be distilled off.

Alternatively, one can decide on the maximum value  $x_F^{max}$  by substituting  $x_{D2}$  in equation B.4 with a value which is less than 1 and equal to what one would consider an attainable maximum value for  $x_{D2}$ .



C

## Property - separation technique relationship

In the following pages tables 1 and 6 from Jaksland (1996) are reprinted with permission from C. Jaksland.

**Table 1:** List of important pure component properties and their classification

Property no.	Property	Classification	Primary/ Secondary	Method of prediction
p <sub>1</sub>	Kinetic diameter	structural	p <sub>n</sub>	literature
p <sub>2</sub>	van der Waals volume	structural	p <sub>n</sub>	databank
p <sub>3</sub>	Molecular diameter	structural	p <sub>n</sub>	literature
p <sub>4</sub>	Molecular weight	structural	p <sub>n</sub>	databank
p <sub>5</sub>	Radius of gyration	structural	p <sub>n</sub>	databank
p <sub>6</sub>	Molar volume	chemical	p <sub>c</sub>	databank, new method <sup>3</sup>
p <sub>7</sub>	Polarisability <sup>1</sup>	chemical	p <sub>n</sub>	literature
p <sub>8</sub>	Dipolemoment <sup>1</sup>	chemical	p <sub>n</sub>	databank, new method <sup>3</sup>
p <sub>9</sub>	Critical temperature	physical	p <sub>n</sub>	databank
p <sub>10</sub>	Critical pressure	physical	p <sub>n</sub>	databank
p <sub>11</sub>	Melting point	physical	p <sub>c</sub>	databank
p <sub>12</sub>	Heat of fusion at T <sub>m</sub>	chemical	p <sub>c</sub>	databank
p <sub>13</sub>	Triple point pressure	physical	p <sub>n</sub>	databank
p <sub>14</sub>	Triple point temperature	physical	p <sub>n</sub>	databank
p <sub>15</sub>	Boiling point	physical	p <sub>c</sub>	databank
p <sub>16</sub>	Vapour pressure	physical	p <sub>c</sub>	correlation
p <sub>17</sub>	Heat of vaporization	physical	p <sub>c</sub>	correlation
p <sub>18</sub>	Heat of reaction <sup>2</sup>	chemical	p <sub>c</sub>	predicted from p <sub>20</sub>
p <sub>19</sub>	Gibbs free energy <sup>2</sup>	chemical	p <sub>c</sub>	databank
p <sub>20</sub>	Heat of formation <sup>2</sup>	chemical	p <sub>c</sub>	databank
p <sub>21</sub>	Ion charge	physical	p <sub>n</sub>	literature
p <sub>22</sub>	Solubility parameter <sup>1</sup>	physical	p <sub>c</sub>	databank, new method <sup>3</sup>
p <sub>23</sub>	Refractive index <sup>1</sup>	physical	p <sub>c</sub>	databank, new method <sup>3</sup>
p <sub>24</sub>	Surface tension <sup>1</sup>	transport	p <sub>c</sub>	correlation, new method <sup>3</sup>
p <sub>25</sub>	Connectivity index <sup>1</sup>	structural	p <sub>n</sub>	literature
p <sub>26</sub>	Dielectric constant <sup>1</sup>	structural	p <sub>c</sub>	new method <sup>3</sup>
p <sub>27</sub>	Kirkwood function <sup>1</sup>	structural	p <sub>c</sub>	new method <sup>3</sup>
p <sub>28</sub>	Electrostatic factor <sup>1</sup>	structural	p <sub>c</sub>	new method <sup>3</sup> , literature
p <sub>29</sub>	Molecular refraction <sup>1</sup>	structural	p <sub>c</sub>	new method <sup>3</sup>
p <sub>30</sub>	Solvatochromic param. <sup>1</sup>	structural	p <sub>c</sub>	new method <sup>3</sup>
p <sub>31</sub>	Density <sup>1</sup>	chemical	p <sub>c</sub>	correlation
p <sub>32</sub>	Viscosity <sup>1</sup>	transport	p <sub>c</sub>	correlation
p <sub>33</sub>	Lennard Jones parameter <sup>1</sup>	transport	p <sub>p</sub>	correlation

<sup>1</sup>Pure component properties used in selection of a mass separating agent in addition to mixture properties (see chapter 3.4.2 and Appendix A).

<sup>2</sup>Pure component properties used in mixture analysis to estimate reactivity.

<sup>3</sup>See appendix A.

Figure C.1: List of important pure component properties

Table 6: Recommended values for separation feasibility indices

Separation process		$p_1$	$p_2$	$p_3$	$p_4$	$p_5$	$p_6$	$p_7$	$p_8$	$p_9$	$p_{10}$	$p_{11}$	$p_{12}$	$p_{13}$	$p_{14}$	$p_{15}$	$p_{16}$	$p_{17}$	$p_{18}$	$p_{19}$
Absorption <sup>1</sup>	m M	-	-	-	-	-	-	X	X	-	-	-	-	-	-	-	-	-	-	-
Azeotropic distillation <sup>1</sup>		-	-	-	-	-	-	X	X	-	-	-	-	-	-	-	-	-	-	-
Cryogenic distillation <sup>2</sup>	m M	-	-	-	-	-	-	-	-	-	-	-	-	-	-	-	-	-	-	-
Crystallisation <sup>1</sup>	m M	-	-	-	-	-	-	-	-	-	-	-	-	-	-	-	-	-	-	-
Desublimation	m M	-	-	-	-	-	-	-	-	-	-	-	-	-	-	-	-	-	-	-
Distillation <sup>2</sup>	m M	-	-	-	-	-	-	-	-	-	-	-	-	-	-	-	-	-	-	-
Extractive distillation <sup>1,2,4</sup>	m M N	-	-	-	-	-	-	X	X	-	-	-	-	-	-	-	-	-	-	-
Flash operation <sup>2</sup>	m M	-	-	-	-	-	-	-	-	-	-	-	-	-	-	-	-	-	-	-
Gas separation membranes	m M	-	1.07 1.10	-	-	-	-	-	-	-	-	-	-	-	-	-	-	-	-	-
Ion exchange	m M	-	-	-	-	-	-	-	-	-	-	-	-	-	-	-	-	-	-	-
Leaching <sup>1</sup>		-	-	-	-	-	-	X	X	-	-	-	-	-	-	-	-	-	-	-
Liquid-liquid extraction <sup>1</sup>		-	-	-	-	-	-	X	X	-	-	-	-	-	-	-	-	-	-	-
Liquid membranes	m M	-	-	-	-	-	-	-	-	-	-	-	-	-	-	-	-	-	-	-

Figure C.2: Property - separation techniques relationship

These methods require a mass separating agent which is identified from pure component properties  $P_7$ ,  $P_8$  and  $P_{22}$ - $P_{32}$  and mixture properties such as selectivity, solubility. <sup>2</sup>These separation techniques are, in addition to boiling point ratios and vapour pressure ratios, identified from pure component property values of heat of vaporisation. <sup>3</sup>Crystallisation is identified from melting point ratios as well as pure component property values of heat of fusion at melting point. <sup>4</sup>Extractive distillation is considered very feasible at a relative volatility between 1.0 and 1.5, feasible at a relative volatility between 1.5 and 2.0. At a relative volatility larger than 2.0, extractive distillation is considered infeasible since distillation is a competitive alternative. <sup>5</sup>Partial condensation is also related to vapour pressure computed within T and/or P limits of correlations. <sup>6</sup>In supercritical extraction the selection of the MSA is related to pure component properties  $p_9$ ,  $p_{10}$  in addition to  $p_7$ ,  $p_8$  and  $p_{22}$ .  $P_{32}$ .

Figure C.3: Property - separation techniques relationship, continued

# D

## Calculation of operational costs for case study 5.2

The costs of operation for the generated sequences are compared in terms of costs of cooling water and steam. It is assumed that cooling water is obtained at a temperature of 6-8 °C and the temperature rise is  $\Delta T = 10K$  before the water is disposed of. The amount of water necessary for the cooling sub-task in the sequences is found according to:

$$m_{H_2O} = \frac{Q_c t_{cooling}}{C_p \Delta T} MW_{H_2O} \quad (D.1)$$

where  $Q_c$  and  $t_{cooling}$  is  $Q_{13}$  and  $t_{i3}$  for the seven alternative sequences ( $i = 1, \dots, 7$ ), respectively. The  $C_p$  of water is found from the CAPEC database (Nielsen *et al.*, 2001) to be  $75.85 \frac{kJ}{kmol \cdot K}$ .

Regarding the heating sub-tasks in the sequences, it is assumed that steam at 100 psig is used and after the latent heat of steam is provided for the heating, saturated water is sent away from the process. The amount of steam needed for the heating sub-tasks in the sequences is found according to:

$$m_{steam} = \frac{Q_h t_{heating}}{\lambda} \quad (D.2)$$

where  $Q_h t_{heating} = Q_{12} t_{i2} + Q_{14} t_{i4}$  for the seven alternative sequences ( $i = 1, \dots, 7$ ). The latent heat of steam  $\lambda$  was found to be  $2067 \frac{kJ}{kg}$ , (Smith and VanNess, 1987).

The costs of cooling water and steam were found from Peters and Timmerhaus (1991) to be  $C_{H_2O} = 0.2\$/3.785m^3$  and  $C_{steam} = 3.2\$/1000lb$ , respectively. The actual amounts of cooling water and steam for the seven generated alternative sequences of sub-tasks as well as the operating costs because of heating and cooling are given in table D.1.



Operational sequence no $i$	$Q_{cooling}$ $Q_{13t_{i3}}$	$Q_{heating}$ $Q_{12t_{i2}} + Q_{14t_{i4}}$	$m_{H_2O}$ (kg)	$m_{steam}$ (kg)	$C_{cooling}$ (\$)	$C_{heating}$ (\$)	Total Costs (\$)
1	120 MJ	1188 MJ	2850.1	574.7	0.15	4.05	4.20
2	650 MJ	1540 MJ	15438.0	745.0	0.82	5.25	6.07
3	1100 MJ	2034 MJ	26125.9	984.0	1.38	6.93	8.31
4	1240 MJ	2130 MJ	29451.0	1030.5	1.56	7.25	8.81
5	1600 MJ	2434.8 MJ	38001.3	1177.9	2.01	8.29	10.30
6	1600 MJ	2454 MJ	38001.3	1187.2	2.01	8.36	10.37
7	1500 MJ	2507 MJ	35626.2	1212.9	1.88	8.54	10.42

Table D.1: Operational costs for the generated alternative sequences of sub-tasks based on heating and cooling

# E

## Column geometric specifications for case study 5.4

This appendix provides the column geometry specifications for the batch distillation column used in case study 5.4. This information is used for the dynamic simulation of the column. Additionally, the relationship between the vapour boilup rate  $V$  and the reflux ratio  $R_{max}$  where flooding takes place is also given. This relationship was obtained through dynamic simulation for the original feed and specific column design. For a specific vapour boilup rate  $V$ , DYN-SIM in ICAS was used to determine the reflux ratio value where flooding occurs, by gradually increasing  $R$ .

Stage	Active area ( $m^2$ )	Plate spacing (m)	Weir height (m)	Weir length (m)
Condenser	0.013	0.8	0.0038	0.003
1	0.013	0.8	0.0038	0.003
2	0.013	0.8	0.0038	0.003
3	0.013	0.8	0.0038	0.003
4	0.013	0.8	0.0038	0.003
5	0.013	0.8	0.0038	0.003
6	0.013	0.8	0.0038	0.003
7	0.013	0.8	0.0038	0.003
8	0.013	0.8	0.0038	0.003
9	0.013	0.8	0.0038	0.003
10	0.013	0.8	0.0038	0.003
11	0.013	0.8	0.0038	0.003
Reboiler	3.7	1.3	0.53	0.4

Table E.1: Column geometry

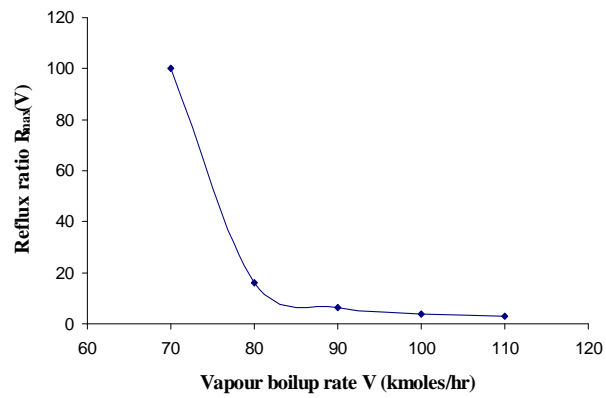


Figure E.1: Flooding reflux ratio value for example's column geometric specifications

# F

## Property lists for case study 5.8

The components of two mixtures are considered, namely the mixture after the first reaction task and the one resulting if both reaction tasks take place first. The compounds of the mixtures are listed in decreasing order for each property and the adjacent binary property ratios are calculated. The property lists are given below. Tables F.1 through F.3 consider the mixture after the first reaction task, while tables F.4 to F.6 consider the mixture after the second reaction task.

It can easily be realized, from a fast comparison of the property lists, that property  $p_{16}$ : vapour pressure has the largest scaled binary property ratio  $sr_{ij}$  of the remaining after the screening adjacent binary pair property ratios. This is true for both of the considered mixtures. The separation technique that is indicated from property  $p_{16}$  is distillation.

Property $p_2$ (van der Waals volume) list			
Compound	Adjacent binary pair	$r_{i2}$	Comment
C	C/A	1.06	
A	A/B	<b>1.52</b> > 1.1	$sr_{i2} = 1.382$
B	B/I1	1.09	
I1	I1/I2	1.18	
I2	I2/R1	1.15	
R1			
Property $p_4$ (molecular weight) list			
Compound	Adjacent binary pair	$r_{i4}$	Comment
A	A/C	1.02	
C	C/B	<b>1.44</b> < 1.7 and 1.9	Infeasible
B	B/I1	1.22	
I1	I1/R1	1.28	
R1	R1/I2	1.04	
I2			
Property $p_5$ (radius of gyration) list			
Compound	Adjacent binary pair	$r_{i5}$	Comment
A	A/C	1.07	
C	C/B	<b>1.20</b> > 1.03	$sr_{i5} = 1.165$
B	B/I1	1.09	
I1	I1/I2	1.11	
I2	I2/R1	1.12	
R1			
Property $p_6$ (molar volume) list			
Compound	Adjacent binary pair	$r_{i6}$	Comment
C	C/A	1.14	
A	A/I2	<b>1.60</b> > 1.08	$sr_{i6} = 1.481$
I2	I2/I1	1.04	
I1	I1/B	1.02	
B	B/R1	1.32	
R1			
Property $p_8$ (dipolemoment) list			
Compound	Adjacent binary pair	$r_{i8}$	Comment
A	A/I1	1.32	
I1	I1/R1	1.04	
R1	R1/C	<b>1.97</b> > 1.1	$sr_{i8} = 1.791$
C	C/I2	1.62	
I2			

Table F.1: Property lists for the mixture after the 1<sup>st</sup> reaction task

Property $p_9$ (critical temperature) list			
Compound	Adjacent binary pair	$r_{i9}$	Comment
B	B/A	1.10	
A	A/C	1.02	
C	C/R1	1.02	
R1	R1/I1	1.02	
I1	I1/I2	<b>1.28</b> > 1.2	$sr_{i9} = 1.067$
I2			
Property $p_{11}$ (melting point) list			
Compound	Adjacent binary pair	$r_{i11}$	Comment
C	C/I1	<b>1.27</b> $\geq$ 1.27	$sr_{i11} = 1$
I1	I1/R1	1.10	
R1	R1/I2	1.09	
I2			
Property $p_{13}$ (triple point pressure) list			
Compound	Adjacent binary pair	$r_{i13}$	Comment
I2	I2/R1	<b>99999</b> > 40	$sr_{i13} = 2500$
R1	R1/I1	2.41	Infeasible
I1			oper. conditions
Property $p_{14}$ (triple point temperature) list			
Compound	Adjacent binary pair	$r_{i14}$	Comment
C	C/I1	<b>1.27</b> > 1.20	$sr_{i14} = 1.058$
I1	I1/R1	1.10	
R1	R1/I2	1.09	
I2			
Property $p_{15}$ (boiling point) list			
Compound	Adjacent binary pair	$r_{i15}$	Comment
B	B/A	1.12	
A	A/C	1.07	
C	C/I1	1.05	
I1	I1/R1	1.01	
R1	R1/I2	<b>1.39</b> > 1.02	$sr_{i15} = 1.363$
I2		<b>1.39</b> > 1.17	$sr_{i15} = 1.188$
		<b>1.39</b> < 1.40	$\mu(r_{i15}) = 0.941$

Table F.2: Property lists for the mixture after the 1<sup>st</sup> reaction task, continued

Property $p_{16}$ (vapour pressure) list			
Compound	Adjacent binary pair	$r_{i16}$	Comment
I2	I2/R1	89.77	
R1	R1/I1	1.38	
I1	I1/A	9.38	
A	A/C	11.65	
C	C/B	<b>455.99</b> > 1.5	$sr_{i16} = \mathbf{303.99}$
B		<b>455.99</b> > 2.4	$sr_{i16} = 189.99$
		<b>455.99</b> > 15	$sr_{i16} = 30.4$
Property $p_{22}$ (solubility parameter) list			
Compound	Adjacent binary pair	$r_{i22}$	Comment
B	B/R1	1.11	
R1	R1/I1	1.09	
I1	I1/A	<b>1.20</b> > 1.01	$sr_{i22} = 1.188$
A	A/C	1.15	
C	C/I2	1.19	
I2			

Table F.3: Property lists for the mixture after the 1<sup>st</sup> reaction task, continued

Property $p_2$ (van der Waals volume) list			
Compound	Adjacent binary pair	$r_{i2}$	Comment
C	C/A	1.06	
A	A/P	1.41	
P	P/B	1.08	
B	B/I1	1.09	
I1	I1/I2	1.18	
I2	I2/R1	1.15	
R1	R1/R3	<b>1.78</b> > 1.1	$sr_{i2} = 1.619$
R3			
Property $p_4$ (molecular weight) list			
Compound	Adjacent binary pair	$r_{i4}$	Comment
A	A/C	1.02	
C	C/B	1.44	
B	B/P	1.02	
P	P/I1	1.19	
I1	I1/R1	1.28	
R1	R1/I2	1.04	
I2	I2/R3	<b>1.75</b> < 1.9	Infeasible
R3		<b>1.75</b> < 2.3	$\mu(r_{i4}) = 0.083$
Property $p_5$ (radius of gyration) list			
Compound	Adjacent binary pair	$r_{i5}$	Comment
A	A/C	1.07	
C	C/B	1.20	
B	B/I1	1.09	
I1	I1/P	1.01	
P	P/I2	1.11	
I2	I2/R1	1.12	
R1	R1/R3	<b>1.66</b> > 1.03	$sr_{i5} = 1.612$
R3			
Property $p_6$ (molar volume) list			
Compound	Adjacent binary pair	$r_{i6}$	Comment
C	C/A	1.14	
A	A/P	1.27	
P	P/I2	1.26	
I2	I2/I1	1.04	
I1	I1/B	1.02	
B	B/R1	1.32	
R1	R1/R3	<b>1.69</b> > 1.08	$sr_{i6} = 1.565$
R3			

Table F.4: Property lists for the mixture after the 2<sup>nd</sup> reaction task



Property $p_8$ (dipolemoment) list			
Compound	Adjacent binary pair	$r_{i8}$	Comment
A	A/R3	1.29	
R3	R3/I1	1.02	
I1	I1/R1	1.04	
R1	R1/P	1.18	
P	P/C	<b>1.68</b> > 1.1	$sr_{i8} = 1.527$
C	C/I2	1.62	
I2			
Property $p_9$ (critical temperature) list			
Compound	Adjacent binary pair	$r_{i9}$	Comment
B	B/A	1.10	
A	A/C	1.02	
C	C/R1	1.02	
R1	R1/I1	1.02	
I1	I1/R3	1.05	
R3	R3/P	1.03	
P	P/I2	<b>1.19</b> < 1.2	$\mu(r_{i9}) = 0.9$
I2			
Property $p_{11}$ (melting point) list			
Compound	Adjacent binary pair	$r_{i11}$	Comment
C	C/R3	<b>1.14</b> < 1.2	Infeasible
R3	R3/P	1.07	
P	P/I1	1.04	
I1	I1/R1	1.10	
R1	R1/I2	1.09	
I2			
Property $p_{13}$ (triple point pressure) list			
Compound	Adjacent binary pair	$r_{i13}$	Comment
I2	I2/P	1.16	
P	P/R3	4.81	
R3	R3/I1	<b>98447.37</b> > 40	$sr_{i13} = 2461.2$
R1	R1/I1	2.41	Infeasible
I1			oper. conditions
Property $p_{14}$ (triple point temperature) list			
Compound	Adjacent binary pair	$r_{i14}$	Comment
C	C/R3	<b>1.14</b> < 1.2	$\mu(r_{i14}) = 0.4$
R3	R3/P	1.07	
P	P/I1	1.04	
I1	I1/R1	1.10	
R1	R1/I2	1.09	
I2			

Table F.5: Property lists for the mixture after the 2<sup>nd</sup> reaction task, continued

Property $p_{15}$ (boiling point) list			
Compound	Adjacent binary pair	$r_{i15}$	Comment
B	B/A	1.12	
A	A/C	1.07	
C	C/I1	1.05	
I1	I1/R1	1.01	
R1	R1/R3	1.10	
R3	R3/P	1.03	
P	P/I2	<b>1.23</b> > 1.02	$sr_{i15} = 1.206$
I2		<b>1.23</b> > 1.17	$sr_{i15} = 1.051$
		<b>1.23</b> ≤ 1.23	Infeasible
Property $p_{16}$ (vapour pressure) list			
Compound	Adjacent binary pair	$r_{i16}$	Comment
R3	R3/I2	18.07	
I2	I2/R1	89.77	
R1	R1/P	9.84	
P	P/I1	13.62	
I1	I1/A	9.38	
A	A/C	11.65	
C	C/B	<b>455.99</b> > 1.5	$sr_{i16} = \mathbf{303.99}$
B		<b>455.99</b> > 2.4	$sr_{i16} = 189.99$
		<b>455.99</b> > 15	$sr_{i16} = 30.4$
Property $p_{22}$ (solubility parameter) list			
Compound	Adjacent binary pair	$r_{i22}$	Comment
R3	R3/B	1.09	
B	B/R1	1.11	
R1	R1/I1	1.09	
I1	I1/A	<b>1.20</b> > 1.01	$sr_{i22} = 1.188$
A	A/C	1.15	
C	C/P	1.08	
P	P/I2	1.10	
I2			

Table F.6: Property lists for the mixture after the 2<sup>nd</sup> reaction task, continued



# List of definitions

Batch Operations Model	The sequence of sub-tasks necessary to achieve the end objectives of the respective reaction or separation task, which is equivalent in effect to an operating profile.
Batch Process	A designed sequence of operations, which produces some outcome and occurs in a batch mode. A batch process is identified by the changes it creates to the properties of a compound or a mixture
Batch Route	The sequence of necessary tasks for a specified product to be obtained, otherwise called the production path
BRIC	Batch Records in ICAS, a tool for the simulation and data reconciliation of batch operations
CAPEC	Computer Aided Process Engineering Center, at the Department of Chemical Engineering, Technical University of Denmark
ICAS	Integrated Computer Aided System, an integration of computational tools developed at CAPEC
PDS	Process Design Studio, a tool for the design and configuration of distillation columns
Sub-task	A period or an operation where the manipulated variables remain constant for its duration, let that variable be temperature, heating/cooling rate, reflux ratio, etc.
Synthesis	The procedure by which the identity and sequence of the tasks needed to obtain a specified product are determined



# Nomenclature

## Symbols

$(\Delta H_{rT})_j$	heat of reaction for reaction $j$
$(ev - d)_p$	evaporation or dilution ratio for the $p^{th}$ precipitation
$(r)_j$	intensive rate of reaction $j$ , kmol/hr
$\alpha$	relative volatility
$\Delta G_j$	difference in the Gibbs free energy of the products and of the reactants for reaction $j$ , $kJ/mol$
$\Delta P$	variable used to keep pressure close to its upper or lower limits, within a pressure zone
$\Delta T$	variable used to keep temperature close to its upper or lower limits, within a temperature zone
$\epsilon^r$	Indication variable that describes the extent of the enthalpy change in a reaction, in relation to the rest of the reactions in a set
$\mu(r_{ij})$	possibility distribution
$\nu_{jc}$	stoichiometric coefficient of component $c$ taking part in reaction $j$
$\varrho_{SL,p}$	slurry density for the $p^{th}$ precipitation
$\xi_j$	extent of reaction $j$
$B$	bottom amount remaining in the distillation column, kmol
$D$	distillate amount, kmol
$E_a^i$	activation energy for reaction $j$
$F$	feed charge in a batch distillation column, kmol
$f_s, f_l$	solid and liquid fractions that a saturated feed splits into during crystallization
$F_{Di}$	driving force
$H_f^o$	standard enthalpy of formation, $kJ/kmol$

---

$k$	Arrhenius rate constant
$k_o^j$	pre-exponential factor for the Arrhenius rate constant for reaction $j$
$L$	liquid flow rate refluxed back to the column, kmol/hr
$N$	number of equilibrium stages in a distillation column
$N_c$	number of moles of component $c$
$NC$	total number of components
$P$	pressure, atm
$p_k^s$	desired purity of specified product for intermediate separation tasks $k$ in the batch route
$p_j$	pure component property
$P_{slack}$	slack variable for keeping pressure away from its upper and lower limits
$Q$	rate of heat transfer from/to the system
$R$	reflux ratio
$r_k$	product recovery for the individual task $k$ in the batch route
$r_T$	total recovery of a final product for the whole batch route
$r_{ij}$	adjacent binary ratio value (components ranked after increasing $p_j$ )
$R_{max}(V)$	maximum reflux ratio value for a specific vapour boilup rate, where flooding occurs
$R_{min}$	minimum reflux ratio
$S'_{end}$	approximation of end selectivity at the desired end mole-fraction
$s_x$	tangent of selectivity vs molefraction
$S_{ij}$	selectivity of reaction $i$ over reaction $j$
$SI_s$	solubility index for salt $s$
$sr_{ij}$	scaled property ratio value
$T$	temperature, K

---

$t$	time
$T_{slack}$	slack variable for keeping temperature away from its upper and lower limits
$t_{stop, P_{low}}$	the point in time where the point in time where the lower pressure limit is close to violation
$t_{stop, P_{up}}$	the point in time where the upper pressure limit is close to violation
$t_{stop, S}$	the point in time where the approximation of the end selectivity drops below the selectivity constraint
$t_{stop, T_{low}}$	the point in time where the lower temperature limit is close to violation
$t_{stop, T_{up}}$	the point in time where the upper temperature limit is close to violation
$t_{x^{reac}}$	the point in time where the molefraction objective is reached
$t_{yield}$	the point in time where the yield objective is reached
$V$	volume, $m^3$ or vapour boilup rate, $kmol/hr$
$x$	(liquid) molefraction
$x_F^{max}$	maximum binary feed composition of the most volatile compound, above which an intermediate cut needs to be distilled
$x^{reac}$	molefraction of the limiting reactant in the reaction of interest
$x_{az}$	azeotropic composition
$x_{Dav}$	assumed constant distillate composition over a batch distillation sub-task
$Y$	total relative yield according to total moles of limiting reactant consumed
$y$	vapour composition
$Y'$	total yield according to total moles of limiting reactant charged
$y_{km,i}^s$	recovery for separation task $k$ and product $m$ at the end of sub-task $i$



---

$y_{km}^s$	desired recovery for separation task $k$ and product $m$ for batch distillation
$y_{ps}^s$	recovery of solid $s$ in the $p^{th}$ precipitation for batch crystallization
$Y_i$	yield of desired product at the end of sub-task $i$

**Superscripts**

$bin$	binary
$max$	maximum
$r$	reaction
$s$	separation
$sf$	solvent free
$sim$	simulation

**Subscripts**

$B$	bottom
$D$	distillate
$F$	feed
$i$	sub-task (period) no or individual solid precipitation no
$i, j$	reaction no
$inv$	invariant point
$j$	plate no
$k$	separation task no for batch distillation or task no in batch route
$l$	liquid
$low$	lower limit
$min$	minimum
$p$	total precipitation no
$s$	solid
$up$	upper limit

# References

- Allgor, R. and Barton, P. (1999). Screening Models for Batch Process Development: Part II. Case Studies. *Chem. Eng. Sci.*, **54**, 4065–4087.
- Allgor, R.; Barrera, M.; Barton, P. and Evans, L. (1996). Optimal Batch Process Development. *Computers Chem. Engng.*, **20**(6/7), 885–896.
- Allgor, R.; Evans, L. and Barton, P. (1999). Screening Models for Batch Process Development: Part I. Design Targets for Reaction/Distillation Networks. *Chem. Eng. Sci.*, **54**, 4145–4164.
- Applequist, G.; Samikoglou, O.; Pekny, J. and Reklaitis, G. (1997). Issues in the Use, Design and Evolution of Process Scheduling and Planning Systems. *ISA Transactions*, **36**(2), 81–121.
- Aris, R. (1969). *Elementary Chemical Reactor Analysis*. Prentice-Hall Inc., Englewood Cliffs, N.J.
- Barbosa-Povoa, A. and Macchietto, S. (1993). Optimal Design of Multipurpose Batch Plants - 1. Problem Formulation. *Computers Chem. Engng.*, **17**, S33–S38.
- Bek-Pedersen, E.; Gani, R. and Levaux, O. (2000). Determination of Optimal Energy Efficient Separation Schemes Based on Driving Forces. *Computers Chem. Engng.*, **24**(2-7), 253–259.
- Benders, J. (1962). Partitioning Procedures for Solving Mixed-Variable Programming Problems. *Numerische Mathematik*, **4**, 238–252.
- Bernot, C.; Doherty, M. and Malone, M. (1990). Patterns of Composition Change in Multicomponent Batch Distillation. *Chem. Eng. Sci.*, **45**(5), 1207–1221.
- Bernot, C.; Doherty, M. and Malone, M. (1991). Feasibility and Separation Sequencing in Multicomponent Batch Distillation. *Chem. Eng. Sci.*, **46**(5), 1311–1326.
- Bernstein, G.; Carlson, E.; Felder, R. and Bokeny, R. (1992). A Simulation-Based Decision Support System for a Specialty Chemicals Production Plant. *1992 Winter Simulation Conference Proceedings, New Jersey: Institute of Electrical and Electronics Engineers*, pages 1262–1270.

- Birewar, D. and Grossmann, I. (1990). Simultaneous Synthesis, Sizing, and Scheduling of Multiproduct Batch Plants. *Ind. Eng. Chem. Res.*, **29**, 2242–2251.
- Bonné, D. and Jørgensen, S. (2004). Iterative Learning Model Predictive Control of Batch Processes. In C. Kiparissides, editor, *BatchPro - Symposium on Knowledge Driven Batch Processes*, pages 67–72, Thessaloniki, Greece. CERTH.
- Bonvin, D. (1998). Optimal Operation of Batch Reactors - a Personal View. *J. Proc. Cont.*, **8**(5-6), 355–368.
- Cesar, M. and Ng, K. (1999). Improving Product Recovery in Fractional Crystallization Processes: Retrofit of an Adipic Acid Plant. *Ind. Eng. Chem. Res.*, **38**, 823–832.
- Charalambides, M.; Shah, N. and Pantelides, C. (1995). Synthesis of Batch Reaction/Distillation Processes Using Detailed Dynamic Models. *Computers Chem. Engng.*, **19**, S167–S174.
- Cheng, R.; Gen, M. and Tsujimura, Y. (1996). A Tutorial Survey of Job-Shop Scheduling Problems Using Genetic Algorithms - I. Representation. *Computers Ind. Engng.*, **30**(4), 983–997.
- Chilton, T. and Colburn, A. (1935). Distillation and Absorption in Packed Columns - A Convenient Design and Correlation Method. *Ind. Eng. Chem.*, **27**(3), 255.
- Christensen, F. and Jørgensen, S. (1987). Optimal Control of Binary Batch Distillation with Recycled Waste Cut. *Chem. Engng. J.*, **34**, 57–64.
- Cisternas, L. and Rudd, D. (1993). Process Designs for Fractional Crystallization from Solution. *Ind. Eng. Chem. Res.*, **32**, 1993–2005.
- Constantinou, L. and Gani, R. (1994). New Group Contribution Method for Estimating Properties of Pure Compounds. *AIChE J.*, **40**(10), 1697–1709.
- Cuthrell, J. and Biegler, L. (1989). Simultaneous Optimization and Solution Methods for Batch Reactor Control Profiles. *Computers Chem. Engng.*, **13**(1-2), 49–62.
- Das, B.; Shah, N. and Chung, P. (1998). Off-Line Scheduling a Simple Chemical Batch Process Production Plan Using the ILOG Scheduler. *Computers Chem. Engng.*, **22**, S947–S950.
- Diwekar, U. (1995). *Batch Distillation: Simulation, Optimal Design and Control*. Taylor and Francis, 1101 Vermont Ave., N.W., Suite 200, Washington, DC 20005.

- Diwekar, U. and Madhavan, K. (1989). Optimization of Multicomponent Batch Distillation Columns. *Ind. Eng. Chem. Res.*, **28**, 1011–1017.
- Diwekar, U. and Madhavan, K. (1991). Multicomponent Batch Distillation Column Design. *Ind. Eng. Chem. Res.*, **30**, 713–721.
- Diwekar, U.; Malik, R. and Madhavan, K. (1987). Optimal Reflux Rate Policy Determination for Multicomponent Batch Distillation Columns. *Computers Chem. Engng.*, **11**(6), 629–637.
- Duran, M. and Grossmann, I. (1986). An Outer-Approximation Algorithm for a Class of Mixed-Integer Nonlinear Programs. *Math. Program.*, **36**, 307–339.
- Dye, S. and Ng, K. (1995). Fractional Crystallization: Design Alternatives and Tradeoffs. *AIChE J.*, **41**(11), 2427–2438.
- Eaton, J. and Rawlings, J. (1990). Feedback Control of Chemical Processes Using on-Line Optimization Techniques. *Computers Chem. Engng.*, **14**(4), 469–479.
- Farhat, S.; Czernicki, M.; Pibouleau, L. and Domenech, S. (1990). Optimization of Multiple-Fraction Batch Distillation by Nonlinear Programming. *AIChE J.*, **36**, 1349–1360.
- Fitch, B. (1970). How to Design Fractional Crystallization Processes. *Ind. Eng. Chem.*, **62**, 6–33.
- Gani, R. (2002). *ICAS Documentation*. CAPEC, Technical University of Denmark.
- Gani, R.; Hytoft, G.; Jalsland, C. and Jensen, A. (1997). An Integrated Computer Aided System for Integrated Design of Chemical Processes. *Computers Chem. Engng.*, **21**(10), 1135–1146.
- Garcia, V.; Cabassud, M.; Lann, M. L.; Pibouleau, L. and Casamatta, G. (1995). Constrained Optimization for Fine Chemical Productions in Batch Reactors. *Chem. Eng. J.*, **59**, 229–241.
- Goldman, R. and Boddy, M. (1997). A Constraint-Based Scheduler for Batch Manufacturing. *IEEE Expert*, **12**(1), 49–56.
- Goodall, W. and Roy, R. (1996). Short Term Scheduling and Control in the Batch Process Industry Using Hybrid Knowledge Based Simulation. *Int. J. Prod. Res.*, **34**(1), 33–50.
- Ha, J.-K.; Chang, H.-K.; Lee, E.; Lee, I.-B.; Lee, B. and Yi, G. (2000). Intermediate Storage Tank Operation Strategies in the Production Scheduling of Multi-Product Batch Processes. *Computers Chem. Engng.*, **24**(2-7), 1633–1640.

- Hansen, T. and Jørgensen, S. (1986). Optimal Control of Binary Batch Distillation in Tray or Packed Columns. *Chem. Engng. J.*, **33**(3), 151–155.
- Hostrup, M. (2002). *Integrated Approach to Computer Aided Process Synthesis*. Ph.D. thesis, Department of Chemical Engineering, Technical University of Denmark.
- Huang, W. and Chung, P. (2000). Scheduling of Pipeless Batch Plants Using Constraint Satisfaction Techniques. *Computers Chem. Engng.*, **24**, 377–383.
- Ierapetritou, M. and Floudas, C. (1998). Effective Continuous-Time Formulation for Short-Term Scheduling. 1. Multipurpose Batch Processes. *Ind. Eng. Chem. Res.*, **37**, 4341–4359.
- Iribarren, O.; Malone, M. and Salomone, H. (1994). Heuristic Approach for the Design of Hybrid Batch-Continuous Processes. *Trans. IChemE*, **72**(Part A), 295–306.
- Jain, A. and ElMaraghy, H. (1994). The Use of Batch Sizing to Improve Flow and Waiting Times in FMS. *Proceedings of the Fourth International Conference on Computer Integrated Manufacturing and Automation Technology*, pages 403–408.
- Jakobsen, C. (1996). *Separation Process Design and Synthesis Based on Thermodynamic Insights*. Ph.D. thesis, Department of Chemical Engineering, Technical University of Denmark.
- Jänecke, E. (1906). Über eine Neue Darstellungsform der Wässerigen Lösungen. *Z. Anorg. Chem.*, **51**, 132–157.
- Joback, K. and Reid, R. (1987). Estimation of Pure-Component Properties from Group-Contributions. *Chem. Eng. Comm.*, **57**, 233–243.
- Joglekar, G. and Reklaitis, G. (1984). A Simulator for Batch and Semi-Continuous Processes. *Computers Chem. Engng.*, **8**(6), 315–327.
- Jørgensen, S.; Bonn  , D. and Gregersen, L. (2004). chapter Monitoring and Control of Batch Processes. Elsevier Science B.V.
- Jung, J.; Lee, C. and Lee, I.-B. (1998). A Genetic Algorithm for Scheduling of Multi-Product Batch Processes. *Computers Chem. Engng.*, **22**(11), 1725–1730.
- Kim, M. and Lee, I.-B. (1997). Rule-Based Reactive Rescheduling System for Multi-Purpose Batch Processes. *Computers Chem. Engng.*, **21**, S1197–S1202.
- Kim, M.; Jung, J. and Lee, I.-B. (1996). Optimal Scheduling of Multiproduct Batch Processes for Various Intermediate Storage Policies. *Ind. Eng. Chem. Res.*, **35**(11), 4058–4066.

- Kim, S.; Lee, H.-K.; Lee, I.-B.; Lee, E. and Lee, B. (2000). Scheduling of Non-Sequential Multipurpose Batch Processes under Finite Intermediate Storage Policy. *Computers Chem. Engng.*, **24**(2-7), 1603–1610.
- Kim, Y. (1999). Optimal Design and Operation of a Multi-Product Batch Distillation Column Using Dynamic Model. *Chem. Eng. Proc.*, **38**, 61–72.
- Kondili, E.; Pantelides, C. and Sargent, R. (1993). A General Algorithm for Short-Term Scheduling of Batch Operations - I. MILP Formulation. *Computers Chem. Engng.*, **17**(2), 211–223.
- Ku, H. and Karimi, I. (1988). Scheduling in Serial Multiproduct Batch Processes with Finite Interstage Storage: A Mixed Integer Linear Program Formulation. *Ind. Eng. Chem. Res.*, **27**, 1840–1848.
- Ku, H.-M. and Karimi, I. (1991). An Evaluation of Simulated Annealing for Batch Process Scheduling. *Ind. Eng. Chem. Res.*, **30**, 163–169.
- Kudva, G.; Elkamel, A.; Pekny, J. and Reklaitis, G. (1994). Heuristic Algorithm for Scheduling Batch and Semi-Continuous Plants with Production Deadlines. Intermediate Storage Limitations and Equipment Changeover Costs. *Computers Chem. Engng.*, **18**(9), 859–875.
- Kuriyan, K. and Reklaitis, G. (1989). Scheduling Network Flowshops so as to Minimize Makespan. *Computers Chem. Engng.*, **13**(1-2), 187–200.
- Lee, J.; Lee, K. and Kim, W. (2000). Model-Based Iterative Learning Control with a Quadratic Criterion for Time-Varying Linear Systems. *Automatica*, **36**, 641–657.
- Logsdon, J.; Diwekar, U. and Biegler, L. (1990). On the Simultaneous Optimal Design and Operation of Batch Distillation Columns. *Trans. IChemE*, **68**, 434–444.
- Luus, R. (1999). Towards Practical Optimal Control of Batch Reactors. *Chem. Eng. J.*, **75**(1), 1–9.
- Marrero, J. and Gani, R. (2001). Group-Contribution Based Estimation of Pure Component Properties. *Fluid Phase Equilib.*, **183-184**, 183–208.
- Mauderli, A. and Rippin, D. (1979). Production Planning and Scheduling for Multi-Purpose Batch Chemical Plants. *Computers Chem. Engng.*, **3**, 199–206.
- Mayne, D.; Rawlings, J.; Rao, C. and Scokaert, P. (2000). Constrained Model Predictive Control: Stability and Optimality. *Automatica*, **36**, 789–814.
- McCabe, W. and Thiele, E. (1925). Graphical Design of Fractionating Columns. *Ind. Eng. Chem.*, **17**(6), 605–611.

- Mockus, L. and Reklaitis, G. (1997a). Mathematical Programming Formulation for Scheduling of Batch Operations Based on Nonuniform Time Discretization. *Computers Chem. Engng.*, **21**(10), 1147–1156.
- Mockus, L. and Reklaitis, G. (1997b). A Bayesian Approach to Batch Process Scheduling. *Int. Trans. Opl. Res.*, **4**(1), 55–65.
- Moore, K.; Dahleh, M. and Bhattacharyya, S. (1992). Iterative Learning Control: A Survey and New Results. *J. Robotics Systems*, **9**(5), 563–594.
- Morari, M. and Lee, J. (1999). Model Predictive Control: Past, Present and Future. *Computers Chem. Engng.*, **23**, 667–682.
- Mujtaba, I. and Macchietto, S. (1996). Simultaneous Optimization of Design and Operation of Multicomponent Batch Distillation Column-Single and Multiple Separation Duties. *J. Proc. Cont.*, **6**(1), 27–36.
- Musier, R. and Evans, L. (1989). An Approximate Method for the Production Scheduling of Industrial Batch Processes with Parallel Units. *Computers Chem. Engng.*, **13**, 229–238.
- Muske, K. and Rawlings, J. (1993). Model Predictive Control with Linear Models. *AIChE J.*, **39**(2), 262–287.
- Nielsen, T.; Abildskov, J.; Harper, P.; Papaiconomou, I. and Gani, R. (2001). The CAPEC Database. *J. Chem. Eng. data*, **46**, 1041–1044.
- Palanki, S.; Kravaris, C. and Wang, H. (1993). Synthesis of State Feedback Laws for End-Point Optimization in Batch Processes. *Chem. Eng. Sci.*, **48**(1), 135–152.
- Perry, R.; Green, D. and Maloney, J. (1997). *Perry's Chemical Engineers' Handbook*. McGraw-Hill Book Company, New York, N.Y.
- Peters, M. and Timmerhaus, K. (1991). *Plant Design and Economics for Chemical Engineers*. McGraw-Hill Book Company, New York, N.Y., fourth edition.
- Qian, Y. and Lien, K. (1995). Rule Based Synthesis of Separation Systems by Predictive Best First Search with Rules Represented as Trapezoidal Numbers. *Computers Chem. Engng.*, **19**(11), 1185–1205.
- Raaymakers, W. and Hoogeveen, J. (2000). Scheduling Multipurpose Batch Process Industries with No-Wait Restrictions by Simulated Annealing. *Eur. J. Opl. Res.*, **126**, 131–151.
- Rayleigh, L. (1902). On the Distillation of Binary Mixtures. *Philosophical Magazine (vi)*, **23**, 521–.
- Reklaitis, G. (1995). Scheduling Approaches for the Batch Process Industries. *ISA Transactions*, **34**, 349–358.

- Rippin, D. (1983a). Simulation of Single- and Multiproduct Batch Chemical Plants for Optimal Design and Operation. *Computers Chem. Engng.*, **7**(3), 137–156.
- Rippin, D. (1983b). Design and Operation of Multiproduct and Multipurpose Batch Chemical Plants - An Analysis of Problem Structure. *Computers Chem. Engng.*, **7**(4), 463–481.
- Rippin, D. (1993). Batch Process Systems Engineering: A Retrospective and Prospective View. *Computers Chem. Engng.*, **17**, S1–S13.
- Salomone, H.; Montagna, J. and Iribarren, O. (1994). Dynamic Simulations in the Design of Batch Processes. *Computers Chem. Engng.*, **18**(3), 191–204.
- Shah, N.; Pantelides, C. and Sargent, R. (1993). A General Algorithm for Short-Term Scheduling of Batch Operations - II. Computational Issues. *Computers Chem. Engng.*, **17**(2), 229–244.
- Shaw, K.; Nortcliffe, A.; Thompson, M.; Love, J.; Fleming, P. and Fonseca, C. (1999). Assessing the Performance of Multiobjective Genetic Algorithms for Optimization of a Batch Process Scheduling Problem. *Proceedings of the 1999 Congress on Evolutionary Computation - CEC 99*, pages 37–45.
- Smith, J. and VanNess, H. (1987). *Introduction to Chemical Engineering Thermodynamics*. McGraw-Hill Book Company, New York, N.Y., fourth edition.
- Srinivasan, B. and Bonvin, D. (2004). Dynamic Optimization under Uncertainty Via NCO Tracking: A Solution Model Approach. *BatchPro Symposium*, pages 17–35.
- Srinivasan, B.; Bonvin, D.; Visser, E. and Palanki, S. (2003a). Dynamic Optimization of Batch Processes II. Role of Measurements in Handling Uncertainty. *Computers Chem. Engng.*, **27**, 27–44.
- Srinivasan, B.; Palanki, S. and Bonvin, D. (2003b). Dynamic Optimization of Batch Processes I. Characterization of the Nominal Solution. *Computers Chem. Engng.*, **27**, 1–26.
- Stefanis, S.; Livingston, A. and Pistikopoulos, E. (1997). Environmental Impact Considerations in the Optimal Design and Scheduling of Batch Processes. *Computers Chem. Engng.*, **21**(10), 1073–1094.
- Steffen, M. and Greene, T. (1986). Hierarchies of Sub-Periods in Constraint-Directed Scheduling. *Proceedings of a Symposium on Real-Time Optimization in Automated Manufacturing Facilities.*, pages 167–183.
- Stephanopoulos, G. and Han, C. (1996). Intelligent Systems in Process Engineering: A Review. *Computers Chem. Engng.*, **20**(6/7), 743–791.



- Suhami, I. and Mah, R. (1981). An Implicit Enumeration Scheme for the Flowshop Problem with No Intermediate Storage. *Computers Chem. Engng.*, **5**, 83–91.
- Suhami, I. and Mah, R. (1982). Optimal Design of Multipurpose Batch Plants. *Ind. Eng. Chem. Proc. D. D.*, **21**(1), 94–100.
- Takano, K. (2000). *Computer Aided Design and Analysis of Separation Processes with Electrolyte Systems*. Ph.D. thesis, Department of Chemical Engineering, Technical University of Denmark.
- Tandon, M.; Cummings, P. and LeVan, M. (1995). Scheduling of Multiple Products on Parallel Units with Tardiness Penalties Using Simulated Annealing. *Computers Chem. Engng.*, **19**(10), 1069–1076.
- Ubrich, O.; Srinivasan, B.; Lerena, P.; Bonvin, D. and Stoessel, F. (1999). Optimal Feed Profile for a Second Order Reaction in a Semi-Batch Reactor under Safety Constraints. Experimental Study. *J. Loss Prevent. Proc.*, **12**, 485–493.
- Voudouris, V. and Grossmann, I. (1996). MILP Model for Scheduling and Design of a Special Class of Multipurpose Batch Plants. *Computers Chem. Engng.*, **20**(11), 1335–1360.
- Wellons, M. and Reklaitis, G. (1991a). Scheduling of Multipurpose Batch Chemical Plants - Formation of Single Product Campaigns. *Ind. Eng. Chem. Res.*, **30**(4), 671–688.
- Wellons, M. and Reklaitis, G. (1991b). Scheduling of Multipurpose Batch Chemical Plants - Multiple Product Campaign Formation and Production Planning. *Ind. Eng. Chem. Res.*, **30**(4), 688–705.
- Zentner, M.; Elkamel, A.; Pekny, J. and Reklaitis, G. (1992). An Interval Based Mathematical Model for the Scheduling of Resource-Constrained Batch Chemical Processes. In *NATO ASI, Batch Process Systems Engineering*, Antalya, Turkey.